UNIVERSIDAD COMPLUTENSE DE MADRID
FACULTAD DE CIENCIAS QUÍMICAS
Departamento de Bioquímica y Biología Molecular I

TESIS DOCTORAL

Efectos biológicos de la cardiolipina extracelular en pulmón. Acción antiviral frente a la infección por el virus respiratorio sincitial

MEMORIA PARA OPTAR AL GRADO DE DOCTOR

PRESENTADA POR

Alba de Lorenzo Avilés

Directora

Cristina Casals Carro

Madrid, 2018

UNIVERSIDAD COMPLUTENSE DE MADRID

FACULTAD DE CIENCIAS QUÍMICAS

Departamento de Bioquímica y Biología Molecular I

TESIS DOCTORAL
EFECTOS BIOLÓGICOS DE LA CARDIOLIPINA EXTRACELULAR EN PULMÓN. ACCIÓN ANTIVIRAL FRENTE A LA INFECCIÓN POR EL VIRUS RESPIRATORIO SINCITIAL.

MEMORIA PARA OPTAR AL GRADO DE DOCTOR

Presentada por

Alba de Lorenzo Avilés

Directora

Dra. Cristina Casals Carro

Madrid, 2017

COMPLUTENSE UNIVERSITY OF MADRID

CHEMISTRY FACULTY

Department of Biochemistry and Molecular Biology I

BIOLOGICAL EFFECTS OF EXTRACELLULAR CARDIOLIPIN IN THE LUNG. ANTIVIRAL ACTION AGAINST RESPIRATORY SYNCYTIAL VIRUS INFECTION.

DOCTORAL THESIS OF

ALBA DE LORENZO AVILÉS

DIRECTOR

DRA. CRISTINA CASALS CARRO

Madrid, 2017

A mi familia.
A mis amigos.

The research for this doctoral thesis has been performed at the Department of Biochemistry and Molecular Biology I of the Complutense University of Madrid, under the supervision of Professor Cristina Casals Carro.
Part of the experimental work was conducted in close collaboration with Dr. Isidoro Martínez González from the Institute of Health Carlos III and CIBER of Respiratory Diseases, at the National Center of Microbiology of Madrid.
The completion of this thesis was possible thanks to a fellowship for initiation into investigation from CIBERES, the funding of the Ministry of Science and Innovation (SAF2012-32728 and SAF2015-65307-R) and the funding of CIBER of Respiratory Diseases (Institute of Health Carlos III-CB06/06/0002).

TABLE OF CONTENTS

ABBREVIATIONS

LIST OF ABBREVIATIONS

ΔH	Enthalpy of the gel-to-liquid phase transition
T1/2	Temperature width at half-height of the DSC peak
γ	Surface tension
ABCA3	ATP-binding cassette transporter A3
AEC	Alveolar epithelial cell
ALI	Acute lung injury
AM	Alveolar macrophage
ARDS	Acute respiratory distress syndrome
ATCC	American Type Culture Collection
BCA	Bicinchoninic acid
cAMP	Cyclic adenosine monophosphate
CD	Cluster of differentiation
CD200R	Cluster of differentiation 200 receptor
cDNA	Complementary deoxyribonucleic acid
CL	Cardiolipin
COX2	Cyclooxygenase 2
Cp	Excess heat capacity
CRD	Carbohydrate recognition domain
CXCL10	C-X-C motif chemokines 10
DAMPs	Damage-associated molecular patterns
DAPI	4’,6-diamidino-2-phenylindole
DiI	1,1’-dioctadecyl-3,3,3’,3’-tetramethylindocarbocyanine perchlorate
DLS	Dynamic Light Scattering
DMEM	Dulbecco’s modified Eagle’s medium
DMSO	Dimethyl sulfoxide
DNA	Deoxyribonucleic acid
DNase I	Deoxyribonuclease I
dNTP	Deoxynucleotide triphosphate
DPPC	Dipalmitoylphosphatidylcholine
DSC	Differential scanning calorimetry
dsRNA	Double-stranded ribonucleic acid
ECL	Enhanced chemiluminescent
EDTA	Ethylenediaminetetraacetic acid
ELISA	Enzyme-linked immune sorbent assay
ERK	Extracellular signal-regulated kinase
FBS	Fetal bovine serum
FCS	Fetal calf serum
FITC	Fluorescein isothiocyanate
GAPDH	Glyceraldehyde-3-phosphate dehydrogenase
GM-CSF	Granulocyte macrophage colony stimulation factor
HRP	Horseradish peroxidase
IFN	Interferon
IL	Interleukin

iNOS	Inducible nitric oxide synthase
IRF	Interferon regulatory factor
ISG15	Interferon-stimulated gene 15
ISGF3	Interferon-stimulated gene factor 3
ISRE	Interferon-stimulated response element
JAK	Janus kinase
JNK	c-Jun N-terminal kinase
Lα	Liquid-crystalline phase
Lβ	Gel phase
LB	Lamellar body
LBP	Lipopolysaccharide-binding protein
Lo	Liquid-ordered phase
LPS	Lipopolysaccharide
MAPK	Mitogen-activated protein kinase
MCP-1	Monocyte chemoattractant protein-1
MLV	Multilamellar vesicle
moi	Multiplicity of infection
MVB	Multivesicular body
NF-AT	Nuclear factor of activated T cells
NF-kB	Nuclear factor-kB
NMR	Nuclear magnetic resonance
PA	Palmitic acid
PAMPs	Pathogen-associated molecular patterns
PBS	Phosphate buffered saline
PC	Phosphatidylcholine
PE	Phosphatidylethanolamine
pfu	Plaque-forming units
PG	Phosphatidylglycerol
PGE2	Prostaglandin E2
PI	Phosphatidylinositol
PI3K	Phosphatidylinositol-3-kinase
PKC	Protein kinase C
PMSF	Phenylmethylsulfonyl fluoride
POPC	Palmitoyloleoylphosphatidylcholine
POPG	Palmitoyloleoylphosphatidylglycerol
PRRs	Pattern recognition receptors
PVDF	Polyvinylidene difluoride
qPCR	Quantitative real-time polymerase chain reaction
RANTES	Regulated on activation normal T cell expressed and secreted
RDS	Respiratory distress syndrome
RIG-I	Retinoic acid-inducible gene I
RLRs	RIG-I-like receptors
RNA	Ribonucleic acid
RNase	Ribonuclease
ROS	Reactive oxygen species

RPMI	Roswell Park Memorial Institute
RSV	Respiratory syncytial virus
SDS	Sodium dodecyl-sulphate
SDS-PAGE	Sodium dodecyl-sulphate polyacrylamide gel electrophoresis
S.E	Standard error
SP-A, -B, -C, -D	Surfactant protein A, B, C, D
sPL	Synthetic surfactant without human recombinant SP-C
STAT	Signal transducer and activator of transcription
SUV	Small Unilamellar Vesicle
TBS	Tris buffered saline
TGF-β	Transforming growth factor beta
TH	Helper T cell
TLR	Toll-like receptor
Tm	Phase transition temperature
TM	Tubular myelin
TMB	Tetramethylbenzidine
TNF-α	Tumor necrosis factor alpha

RESUMEN

1. INTRODUCCIÓN E HIPÓTESIS

Para facilitar el intercambio gaseoso, el pulmón presenta la mayor área del cuerpo en contacto con el medio externo, lo que facilita la oxigenación pero aumenta el riesgo de infección e inflamación por patógenos y endotoxinas presentes en el aire que respiramos. El epitelio alveolar (neumocitos tipo I y II) y los macrófagos alveolares están cubiertos por un fluido acuoso que contiene membranas extracelulares, sintetizadas y secretadas por los neumocitos tipo II, denominadas surfactante pulmonar.

El surfactante pulmonar está compuesto por un 90% en peso de lípidos (mayoritariamente fosfolípidos) y un 10% en peso de proteínas, dentro de las cuales encontramos las cuatro proteínas específicas del surfactante pulmonar SP-A, SP-B, SP-C y SP-D. La principal función del surfactante pulmonar es reducir la tensión superficial en la interfase aire-líquido al final de la espiración, evitando así el colapso alveolar. Además, el surfactante pulmonar, juega un papel fundamental en la defensa inmune innata del alveolo [Cañadas and Casals, 2012]. Se ha descrito que las proteínas del surfactante SP-A y SP-D, denominadas colectinas pulmonares, actúan como opsoninas incrementando la fagocitosis de bacterias [McCormack and Whitsett, 2002] y son capaces de modular la respuesta inmune innata desencadenada por LPS [Stamme *et al.*, 2002; Yamazoe *et al.*, 2008]. Los fosfolípidos aniónicos del surfactante, principalmente POPG, presentan efecto anti-inflamatorio en macrófagos estimulados con LPS [Kuronuma *et al.*, 2009] y *Mycoplasma pneumoniae* [Kandasamy *et al.*, 2011], bloqueando la unión de LPS a TLR4 o de *M. pneumoniae* a TLR2 [Kuronuma *et al.*, 2009; Kandasamy *et al.*, 2011]. Además, se ha descrito que POPG es capaz de neutralizar los virus respiratorios, *influenza A* y virus respiratorio sincitial (VRS), *in vitro e in vivo* [Numata *et al.*, 2010; Numata *et al.*, 2012]. Sin embargo, su acción anti-inflamatoria y antiviral desaparece al estar inmersos en las estructuras membranosas que forman el surfactante pulmonar.

La cardiolipina (CL) es un fosfolípido aniónico que presenta cuatro cadenas de acilo en vez de dos, lo cual le otorga una estructura molecular voluminosa, en comparación con el resto de fosfolípidos. CL se encuentra en la membrana externa de bacterias Gram- negativas y -positivas (~ 10% y ~25%, respectivamente) [Barák y Muchová, 2013]. En células eucariotas se localiza principalmente en la membrana mitocondrial interna (~ 20 %) [Krebs *et al.*, 1979; Zinser *et al.*, 1991; Paradies *et al.*, 2013]. Sin embargo, también se encuentra en la membrana mitocondrial externa (~ 5%), especialmente en los sitios de contacto entre las membranas externa e interna [Daum 1985; Zinser *et al.*, 1991; Kroon *et al.*, 1997]. En la mitocondria, CL tiene

un papel crucial en la estructura y función mitocondrial. Durante la apoptosis, las cadenas de acilo insaturadas de CL sufren una extensiva oxidación y el contenido en CL en la membrana externa aumenta. Así, CL actúa como patrón molecular de daño específico de la muerte celular por apoptosis [Maguire *et al.*, 2017].

Se ha descrito que existen altos niveles de cardiolipina en el fluido alveolar de humanos y ratones infectados con bacterias causantes de neumonía [Ray *et al.*, 2010]. Las especies moleculares de CL encontradas en el fluido alveolar de ratones y humanos con neumonía indican que la CL es de origen mitocondrial más que bacteriano. Además, se ha detectado una alta concentración de este fosfolípido en el lavado broncoalveolar de ratones con neumonía causada por *Haemophilus influenzae* que carece de CL en su membrana. Se ha descrito que concentraciones elevadas de CL en el fluido alveolar alteran la función pulmonar y se ha sugerido que dicha alteración podría deberse a la inhibición de la actividad tensoactiva del surfactante pulmonar [Ray *et al.*, 2010].

Recientemente, se ha sugerido que la cardiolipina podría tener un papel dual en el contexto de las interacciones huésped-huésped y huésped-patógeno [Balasubramanian *et al.*, 2015]. La presencia de CL aumenta la fagocitosis de membranas que contienen CL mitocondrial o bacteriana por parte de los macrófagos (RAW 264.7, THP-1 tratadas con ésteres de forbol, macrófagos peritoneales de ratón y macrófagos humanos derivados de monocitos). La fagocitosis de membranas que contienen CL es dependiente del receptor tipo “scavenger” CD36. Por otra parte, CL atenúa la respuesta inflamatoria de macrófagos peritoneales de ratón RAW 264.7 estimulados con LPS a través del bloqueo del TLR4, receptor del LPS. Estos autores proponen que CL podría tener un efecto beneficioso para ambos, huésped y patógeno. Así, el aumento de la fagocitosis a través de CD36 favorecería la eliminación de los patógenos bacterianos sin embargo, la atenuación de la respuesta inflamatoria de las células del huésped dificultaría la lucha contra la infección [Balasubramanian *et al.*, 2015]. No obstante, los efectos biológicos de CL en el alveolo son desconocidos. No se ha investigado anteriormente el efecto de CL sobre la respuesta inmune de las células alveolares ni sobre la estructura y función de las membranas del surfactante.

Teniendo en cuenta esta información previa, nuestra **primera hipótesis** es que la liberación de CL en el fluido alveolar por parte de las células del huésped, podría ser un mecanismo protector frente a la infección y/o inflamación. La **segunda hipótesis** que nos planteamos es si la secreción de altas cantidades de CL como resultado de daño celular exacerbado podría alterar la estructura y función de las membranas del surfactante pulmonar.

2. OBJETIVOS

El **objetivo principal** de esta tesis ha sido determinar las propiedades anti-infecciosas y anti-inflamatorias de bajas concentraciones de CL utilizando células alveolares y patógenos respiratorios. Además, se ha estudiado el efecto de altas concentraciones de CL en la estructura y función de las membranas del surfactante pulmonar.

Esta tesis está compuesta por cuatro apartados con los siguientes objetivos concretos:

1. Estudiar el papel inmunomodulador de bajas concentraciones de vesículas de CL en la respuesta inflamatoria de macrófagos alveolares murinos estimulados con LPS o zymosan.

2. Determinar el papel antiviral y anti-inflamatorio de bajas dosis de vesículas de CL frente a la infección causada por el virus respiratorio sincitial en células epiteliales alveolares humanas, profundizando en el mecanismo subyacente a la acción antiviral de CL y la influencia de los componentes del surfactante pulmonar en las propiedades antivirales de CL.

3. Investigar el efecto protector de CL frente a la infección por *Haemophilus influenzae* en células epiteliales alveolares murinas.

4. Evaluar el efecto inhibitorio de altas concentraciones CL en la estructura y función biofísica del surfactante pulmonar.

3. RESULTADOS Y CONCLUSIONES

3.1. Efecto anti-inflamatorio de cardiolipina en macrófagos alveolares estimulados con patrones moleculares bacterianos y fúngicos

Para estudiar el efecto inmunomodulador de bajas concentraciones de CL (≥0.07 nmol/ml) sobre la respuesta inflamatoria de macrófagos alveolares murinos (MH-S) y aislados de rata, se emplearon dos estímulos pro-inflamatorios:

o LPS o endotoxina: componente de la membrana externa de bacterias Gram-negativas que induce daño pulmonar agudo o ARDS como consecuencia de infecciones bacterianas o sepsis [Matute-Bello *et al.*, 2008].

o Zymosan: componente particulado complejo presente en la superficie de hongos y levaduras tradicionalmente empleado como estímulo fagocítico y pro-inflamatorio tanto *in vitro como in vivo* [Pillemer and Ecker, 1941, Di Carlo and Fiore, 1958].

Para estudiar el efecto de CL sobre la respuesta inmune celular, se emplearon dos aproximaciones experimentales distintas: las vesículas de CL se añadieron simultáneamente con el estímulo pro-inflamatorio (CL extracelular) o bien las células fueron preincubadas durante 18 horas con CL antes de la estimulación (CL intracelular).

En ambos casos, CL, inhibió las rutas de señalización activadas por LPS o zymosan (MAPKs, la ruta PI3K/Akt y la activación NFkB). Como consecuencia, inhibió la producción de los mediadores pro-inflamatorios TNF-α e iNOS, tanto a nivel de mRNA como de proteína. Además, disminuyó la producción del mRNA inducida por LPS de los marcadores pro-inflamatorios IL1-β, CXCL10 y de un mediador que puede tener actividad pro- o anti-inflamatoria en función del contexto, COX2. Además, empleando macrófagos alveolares primarios de rata, observamos que CL tiene un efecto inhibitorio en la fosforilación de Akt y Erk inducida por LPS, similar a lo obtenido con macrófagos murinos.

Conclusiones: bajas dosis de vesículas de CL añadidas junto con el estímulo pro-inflamatorio y preincubadas con las células antes de la estimulación, presentan un extraordinario efecto anti-inflamatorio en la respuesta immune de macrófagos alveolares. Además, hemos comprobado que el efecto anti-inflamatorio de CL no está restringido a un único estímulo.

3.2. Efecto antiviral e inmunomodulador de vesículas de cardiolipina frente al virus respiratorio sincitial

El virus respiratorio sincitial es el principal agente causante de neumonía y bronquiolitis en niños menores de dos años, ancianos e individuos inmunodeprimidos [Collins and Mellero, 2011]. Se ha sugerido que durante la infección, la cardiolipina

podría ser liberada al fluido alveolar procedente de células alveolares dañadas [Ray *et al.*, 2010]. Nuestra hipótesis es que CL, a bajas concentraciones, podría actuar como factor de defensa para proteger al huésped frente a la infección por el virus respiratorio sincitial.

En experimentos con células epiteliales alveolares humanas, hemos observado que la coadministración de pequeñas dosis de CL con VRS, inhibe la replicación viral y la consiguiente respuesta celular inducida por VRS. Así, CL inhibió la expresión de los receptores celulares para VRS (TLR3 y RIG-I), ISG-15 y TNF-α en células epiteliales alveolares infectadas con VRS. Sin embargo, la preincubación de las células con CL previo a la infección no produjo ningún efecto en la replicación viral pero inhibió la expresión de TNF-α. A nivel mecanístico, CL bloquea la infección por RSV impidiendo la unión de las partículas virales a la superficie celular, evitando así la entrada y replicación del VRS en las células epiteliales. Además, hemos comparado las propiedades antivirales de CL con las de fosfatidilglicerol, un componente del surfactante pulmonar con actividad antiviral. A bajas concentraciones de lípido, CL tiene una actividad antiviral mucho más potente que fosfatidilglicerol.

Por último, hemos comprobado que la presencia de surfactante pulmonar nativo, que cubre el epitelio pulmonar, o de sus componentes aislados (SP-A y la fracción hidrofóbica del surfactante, formada por lípidos y las proteínas hidrofóbicas SP-B y SP-C) no reduce el efecto antiviral de CL.

Conclusiones: nuestros resultados indican que CL podría tener un papel importante durante la infección por VRS, previniendo la interacción huésped-VRS y atenuando la replicación viral y respuesta inflamatoria. Estos hallazgos sugieren que CL podría ser un agente antiviral prometedor frente a VRS.

3.3. Efecto protector de cardiolipina frente a la infección por *Haemophilus influenzae* no tipable

Haemophilus influenzae no tipable es una bacteria Gram-negativa que carece de CL en la composición de su membrana [Ray *et al.*, 2010]. NTHi se encuentra en la nasofaringe de la mayoría de individuos sanos como comensal pero cuando alcanza las vías respiratorias inferiores actúa como agente patógeno [Murphy, 2005]. NTHi es la principal causa de exacerbación en pacientes con enfermedades pulmonares subyacentes como enfermedad pulmonar obstructiva crónica (EPOC) [Sethi and Murphy, 2008].

NTHi es capaz de causar infecciones crónicas debido a su capacidad de internarse en el epitelio alveolar y sobrevivir en estado no replicativo [Clementi and Murphy, 2011]. El mecanismo de internación requiere la integridad de las balsas lipídicas y del citoesqueleto de actina, así como la fosforilación de Akt mediada por PI3K [Morey *et al.*, 2011].

Nuestros resultados indicaron, que la coadministración de vesículas de CL con NTHi, disminuye la invasión pero no la adhesión en células epiteliales alveolares de ratón (línea MLE-12). Los resultados fueron similares para las dos cepas bacterianas clínicas estudiadas, aisladas de individuos con EPOC y otitis. Estos resultados sugieren que CL actúa bloqueando rutas de señalización implicadas en la invasión bacteriana. Como se ha indicado antes, la fosforilación de Akt inducida por NTHi es esencial para la internación de NTHi, y hemos observado que la presencia de CL drásticamente disminuye la fosforilación de Akt inducida por NTHi.

Conclusiones: muchos patógenos se refugian en el interior de las células del huésped durante la infección. Una terapia basada en CL podría suponer un beneficio clínico en infecciones persistentes debido a la capacidad de CL para inhibir la internación de la bacteria en el epitelio.

3.4. Efecto de la cardiolipina en la estructura y función del surfactante pulmonar

Para determinar el efecto de CL en la estructura y función del surfactante pulmonar, se empleó surfactante pulmonar nativo (SPN) de rata que contiene las proteínas hidrofóbicas SP-B y SP-C y la colectina pulmonar SP-A, así como vesículas de extracto lipídico de surfactante pulmonar de rata (ELS), que carece de SP-A.

Para evaluar el efecto de CL en la función del surfactante, se determinó su capacidad para adsorberse a una interfase aire-liquido empleando una balanza de Langmuir que consta de una subfase acuosa acoplada a un sensor de presión. Los experimentos se realizaron empleando tres aproximaciones experimentales distintas: A) las vesículas de CL se inyectaron en la subfase acuosa simultáneamente o 10 minutos antes de la inyección de SPN o ELS; B) CL se encontraba presente en la composición de las vesículas de ELS a distintos porcentajes molares (3,6 y 12 %), y se determinó su capacidad de adsorberse a la interfase aire-líquido. Los resultados indicaron que CL inhibe la función tensoactiva del surfactante tanto si se encuentra libre en la subfase acuosa como formando parte de la composición de las vesículas de surfactante.

El efecto inhibitorio de las vesículas de CL es mucho mayor si se inyectan 10 minutos antes que ELS comparado con la inyección simultánea de ELS. Esta inhibición es debida a adsorción competitiva, ya que las vesículas de CL presentan actividad interfacial. Sin embargo, la adsorción de CL a la interfase es más lenta que la de LES. A destacar, la co-inyección de CL con SPN no afecta a la adsorción interfacial de NPS, mientras que la pre-inyección de CL inhibe la adsorción de NPS. Hemos demostrado que SP-A se une a CL (Kd=2.2 ± 0.4 nM) y sugerimos que la SP-A presente en NPS podría unir vesículas de CL libres protegiendo a las membranas del surfactante frente a la inhibición cuando SPN y las vesículas de CL se coinyectan.

Por otra parte, hemos observado que CL es capaz de insertarse en las membranas de ELS y afecta a las propiedades físicas de las membranas de surfactante, tanto en ausencia como en presencia de SP-A. En presencia de CL, las membranas del surfactante son más fluidas y menos ordenadas. Observamos un aumento de fluidez y disminución del orden lipídico de las membranas de ELS a medida que aumentaba la cantidad de CL incorporada en las membranas ELS. Este efecto podría deberse a la estructura molecular voluminosa de CL que dificulta el correcto empaquetamiento de las moléculas de dipalmitoilfosfatidilcolina, un fosfolípido esencial para la función biofísica del surfactante.

Conclusiones: Nuestros resultados demuestran la acción inhibitoria de altas dosis de CL sobre la función surfactante pulmonar. CL actúa a través de dos mecanismos distintos: (i) adsorción competitiva, en la cual CL compite con el surfactante por la adsorción a la interfase aire-líquido; (ii) un efecto fluidificante sobre las membranas del surfactante. Por otra parte, SP-A es capaz de contrarrestar el ligero efecto inhibitorio de vesículas de CL libres en la subfase acuosa en la función del surfactante. Sin embargo, si CL se encuentra formando parte de la composición del LES, SP-A no es capaz de revertir el efecto de CL en las propiedades físicas del LES.

SUMMARY

1. INTRODUCTION AND HYPOTHESIS

To facilitate gas exchange, the lung has the largest area of the body in contact with the external environment. This extensive surface in contact with the external medium aids oxygenation but increases the risk of infection and inflammation by pathogens and endotoxins present in the air we breathe. The alveolar epithelium (type I and type II pneumocytes) and alveolar macrophages are covered by an aqueous fluid containing extracellular membranes called pulmonary surfactant that are synthesized and secreted by type II pneumocytes.

Pulmonary surfactant is composed of approximately 90 wt.% lipids (mainly phospholipids) and 10 wt.% proteins, among which are four specific surfactant proteins: SP-A, SP-B, SP-C, and SP-D. The main function of pulmonary surfactant is to reduce the surface tension at the air-liquid interface at the end of exhalation, preventing alveolar collapse. In addition, pulmonary surfactant plays a key role in innate immune defense in the alveolus [Cañadas and Casals, 2012]. Pulmonary collectins (SP-A and SP-D) act as opsonins, increasing the phagocytosis of bacteria [McCormack and Whitsett, 2002], and are able to modulate the LPS-triggered innate immune response [Stamme *et al.*, 2002; Yamazoe *et al.*, 2008]. Anionic surfactant phospholipids, mainly POPG, have anti-inflammatory actions on macrophages stimulated with bacterial lipopolysaccharide (LPS) [Kuronuma *et al.*, 2009] and *Mycoplasma pneumoniae* [Kandasamy *et al.*, 2011], blocking the binding of either LPS to TLR4 or *M. pneumoniae* to TLR2 [Kuronuma *et al.*, 2009; Kandasamy *et al.*, 2011]. Moreover, POPG is capable of neutralizing respiratory viruses such as influenza and respiratory syncytial virus, *in vitro* and *in vivo* [Numata *et al.*, 2010; Numata *et al.*, 2012]. However, its anti-inflammatory and antiviral actions disappear when POPG forms part of pulmonary surfactant membranes.

Cardiolipin (CL) is an anionic phospholipid carrying four acyl chains instead of two, which gives it a bulky molecular structure, compared with other phospholipids. CL is found in the inner membrane of Gram-negative and –positive bacteria (~ 10% and ~25%, respectively) [Barák and Muchová, 2013]. In eukaryotic cells, CL is mainly located in the inner mitochondrial membrane (~ 20 %) [Krebs *et al.*, 1979; Zinser *et al.*, 1991; Paradies *et al.*, 2013]. However, CL is also found in the outer mitochondrial membrane (~ 5%), preferably in the contact sites between the outer and the inner membrane [Daum 1985; Zinser *et al.*, 1991; Kroon *et al.*, 1997]. In the mitocondria, CL plays a key role in the structure and function of mitochondrial membranes. During apoptosis, the unsaturated acyl chains of CL suffer extensive oxidation and CL levels in the outer mitochondrial membrane increase. Thus, CL acts as molecular pattern of specific damage of cell death by apoptosis [Maguire *et al.*, 2017].

High levels of CL have been found in the bronchoalveolar lavage (BAL) of humans and mice infected with bacteria causing pneumonia [Ray *et al.*, 2010]. These molecular species of CL appear to be from human rather than bacterial origin. Furthermore, high levels of this phospholipid have been detected in the BAL of mice with pneumonia caused by *Haemophilus influenzae*, which lacks CL on its membrane. High levels of CL in the alveolar fluid alter lung function; it has been suggested that this alteration might be due to impairment of the surfactant function [Ray *et al.*, 2010].

Recently, it has been suggested that CL might have a dual role in the context of host-host and host-pathogen interactions [Balasubramanian *et al.*, 2015]. The presence of CL increases the phagocytosis of membranes containing mitochondrial or bacterial CL by macrophages (RAW 264.7, THP1 treated with phorbol esters, mouse peritoneal macrophages, and human macrophages derived from monocytes). Phagocytosis of CL containing membranes is dependent on the scavenger receptor CD36. On the other hand, CL attenuates the inflammatory response of mouse peritoneal RAW 264.7 macrophages stimulated with LPS by blocking the LPS receptor TLR4. These authors propose that CL could have beneficial effects for both host and pathogen. Thus, increased phagocytosis through CD36 would favor bacterial clearance; however, an attenuated inflammatory response by host cells would hamper the fight against infection [Balasubramanian *et al.*, 2015]. However, the biological role of CL in the alveolus is unknown. Its effect on the immune response of alveolar cells or on the structure and function of surfactant membranes still remains unknown.

Taking all this into consideration, our **first hypothesis** is that the release of low amounts of CL in the alveolar fluid by host cells could be a protective mechanism against infection and/or inflammation. Our **second hypothesis** is that the secretion of high amounts of CL as a result of exacerbated cellular damage could alter the structure and function of pulmonary surfactant membranes.

2. OBJECTIVES

The main objective of this thesis was to determine the anti-infectious and anti-inflammatory properties of low concentrations of CL using alveolar cells and respiratory pathogens. In addition, to study the effect of high concentrations of CL on the structure and function of pulmonary surfactant membranes was an objective of this thesis.

This doctoral thesis consists of four sections with the following specific objectives:

1. To investigate the immunomodulatory role of CL on the immune innate response of alveolar macrophages stimulated with LPS or zymosan.

2. To determine the antiviral and anti-inflammatory effect of CL against respiratory syncytial virus infection on human alveolar epithelial cells, as well as to obtain deeper insight into the mechanism underlying CL antiviral action and the influence of lung surfactant components on CL antiviral properties.

3. To study CL protective action against alveolar epithelial cell infection with *Haemophilus influenzae*.

4. To evaluate the inhibitory effect of high amounts of CL on lung surfactant structure and biophysical function.

3. RESULTS AND CONCLUSIONS

3.1. Anti-inflammatory effects of cardiolipin on alveolar macrophages stimulated with bacterial and fungal molecular patterns

To study the immunomodulatory effects of low concentrations of CL (≥0.07 nmol/ ml) on the inflammatory response of murine alveolar macrophages (MH-S) and isolated alveolar macrophages from rats, we employed two proinflammatory stimuli:

o LPS or endotoxin: component of the outer membrane of Gram-negative bacteria that induces acute lung injury or ARDS [Matute-Bello *et al.*, 2008].

o Zymosan: complex particulate component present on the surface of fungi and yeasts traditionally used as phagocytic and proinflammatory stimulus both *in vitro* and *in vivo* [Pillemer and Ecker, 1941; Di Carlo and Fiore, 1958].

To study the effect of CL on the immune response of alveolar macrophages, two different experimental approaches were employed: CL vesicles were added simultaneously with the proinflammatory stimulus (extracellular CL) or cells were preincubated with CL for 18 hours previous to stimulation (intracellular CL).

In both cases, CL inhibited LPS- or zymosan-elicited signaling pathways (MAPK cascade, the PI3K/Akt pathway, and NF-κB activation). As a consequence, CL inhibited the production of the proinflammatory markers TNF-α and iNOS at both mRNA and protein level. Moreover, CL reduced mRNA production of proinflammatory cytokines IL1-β and CXCL10, as well as COX2, a mediator that can have pro- or anti-inflammatory activity depending on the environment. Furthermore, employing primary rat AMs, we found that CL have an inhibitory effect on LPS-elicited Akt and Erk phosphorylation, similar to that obtained with murine AMs.

CONCLUSIONS: CL vesicles simultaneously added with the proinflammatory stimulus and preincubated with cells before stimulation present a strong immunomodulatory effect at low doses on the inflammatory response of AMs. Moreover, we have proved that the anti-inflammatory action of CL is not restricted to a particular stimulus.

3.2. Antiviral and immunomodulatory effects of cardiolipin against respiratory syncytial virus

Respiratory syncytial virus is the main causal agent of pneumonia and bronchilitis in children under the age of two, the elderly, and immunocompromised individuals [Collins and Mellero, 2011]. It has been suggested that during infection, CL could be released to the alveolar fluid from damaged host cells [Ray *et al.*, 2010]. We propose that CL, at low concentrations, could act as a defensive factor against RSV infection.

In experiments with human alveolar epithelial cells, we found that the coadministration of low amounts of CL with RSV inhibited viral replication and the subsequent RSV-elicited cellular responses such as expression of RSV cellular receptors (TLR3 and RIG-I), ISG-15, and TNF-α by RSV-infected alveolar epithelial cells (AECs). However, preincubation of the cells with CL previous infection did not inhibit viral replication but inhibited TNF-α expression. Mechanistically, CL blocks RSV infection by inhibition of RSV attachment to the cell surface, preventing RSV entry and replication inside the epithelial cells. We have further compared the antiviral properties of Cl with that of phosphatidylglycerol (PG), a component of lung surfactant with reported

antiviral activity. At low lipid concentrations, CL had much stronger antiviral activity than PG. Finally, we found that the presence of native lung surfactant or its isolated components (SP-A and the hydrophobic fraction of lung surfactant, composed by lipids and the hydrophobic proteins SP-B and SP-C) did not diminish CL antiviral effects.

CONCLUSIONS: Our results indicate that CL might play a significant role during RSV infection, preventing host-RSV interaction and attenuating virus replication and inflammatory responses. These findings raise CL as a promising antiviral agent against RSV.

3.3. Cardiolipin protective effects against non-typeable *Haemophilus influenzae* (NTHi) infection

Non-typeable *Haemophilus influenzae* is a Gram-negative bacteria lacking CL in the composition of its membrane [Ray *et al.*, 2010]. NTHi is present in the nasopharynx of the vast majority of healthy individuals as a commensal, but when it reaches the lower airways, it acts as a pathogen [Murphy, 2005]. NTHi is the leading cause of exacerbation in patients with underlying lung diseases such as COPD [Sethi and Murphy, 2008].

NTHi is capable of causing chronic infections due to their ability to penetrate into the alveolar epithelium and survive in a non-replicative state [Clementi and Murphy, 2011]. The mechanism requires the integrity of the lipid rafts and actin cytoskeleton, as well as Akt phosphorylation mediated by PI3K [Morey *et al.*, 2011].

Our results indicated that CL addition simultaneous with NTHi infection reduces the internalization of NTHi by murine AECs (cell line MLE-12) without affecting NTHi adhesion to the epithelium surface. Results were similar for two clinical bacterial strains studied, isolated from individuals with COPD and otitis. These results suggest that CL acts by blocking signaling pathways involved in bacterial internalization. As noted above, Akt phosphorylation induced by NTHi is essential for NTHi internalization, and we found that the presence of CL drastically decreased NTHi-induced Akt phosphorylation.

CONCLUSIONS: Many pathogens seek refuge inside host cells during infection. A therapy based on CL might be beneficial in persistent infections due to the ability of CL to inhibit bacterial internalization by the epithelium.

3.4 Cardiolipin effects on pulmonary surfactant structure and function

To determine the effect of CL on surfactant structure and function, we employed rat native pulmonary surfactant (NPS) containing the hydrophobic proteins SP-B and SP-C and the lung collectin SP-A as well as vesicles prepared from the lipid extract of surfactant (LES) that lacks SP-A.

To evaluate the effect of CL on surfactant function, we determined its capacity to adsorb and spread onto an air-liquid interface using a Langmuir balance consisting of an aqueous subphase coupled to a pressure sensor. Experiments were performed using different experimental approaches: A) CL vesicles were injected into the aqueous subphase simultaneously or 10 minutes before NPS or LES injection; B) CL was present in LES vesicles at different molar percentages (3, 6, and 12%), and the ability of CL-containing LES vesicles to adsorb to the air-liquid interface was determined. The results indicated that CL was able to inhibit surfactant function if CL vesicles were free in the aqueous subphase or CL was forming part of the composition of surfactant vesicles.

The inhibitory effect of CL vesicles was much greater if CL vesicles were injected in the subphase 10 minutes before LES injection compared to simultaneous LES injection. This inhibition was due to competitive adsorption since CL vesicles showed interfacial activity, but CL adsorption to the interface was slower than that of LES. Interestingly, co-injection of CL with NPS did not affect the interfacial adsorption of NPS, whereas preinjection of CL strongly hampered the adsorption of NPS. We found that SP-A bound to CL (Kd = 2.2 ± 0.4 nM) and suggest that SP-A present in NPS would bind to CL free vesicles protecting surfactant membranes from inhibition when NPS and CL vesicles were co-inyected.

On the other hand, we found that CL was capable of inserting into LES membranes and affected the physical properties of surfactant membranes both in the absence and presence of SP-A. The presence of CL rendered surfactant membranes more fluid and less ordered. There was an increase of fluidity and decrease of lipid order of LES membranes as the amount of CL incorporated into LES membranes increased. This effect might be due to the bulky molecular structure of CL that impairs the correct packing of DPPC molecules, an essential phospholipid for surfactant biophysical function.

CONCLUSIONS: In summary, our results highlight an inhibitory action for CL at high doses on lung surfactant function. CL action takes place by two different mechanisms: (i) competitive adsorption, in which CL competes with surfactant for the air-liquid interface, (ii) a fluidizing effect of CL on surfactant membranes. Furthermore, we proved that SP-A is able to counteract the slight inhibitory effect caused by free CL vesicles in the aqueous subphase but did not show any effect when CL forms part of the composition of LES vesicles.

I. INTRODUCTION

1.1. THE RESPIRATORY SYSTEM

Respiration is the act of breathing, namely inhaling (inspiration) oxygen (O_2) from the atmosphere into the lungs and exhaling (expiration) into the atmosphere the waste product, carbon dioxide (CO_2).

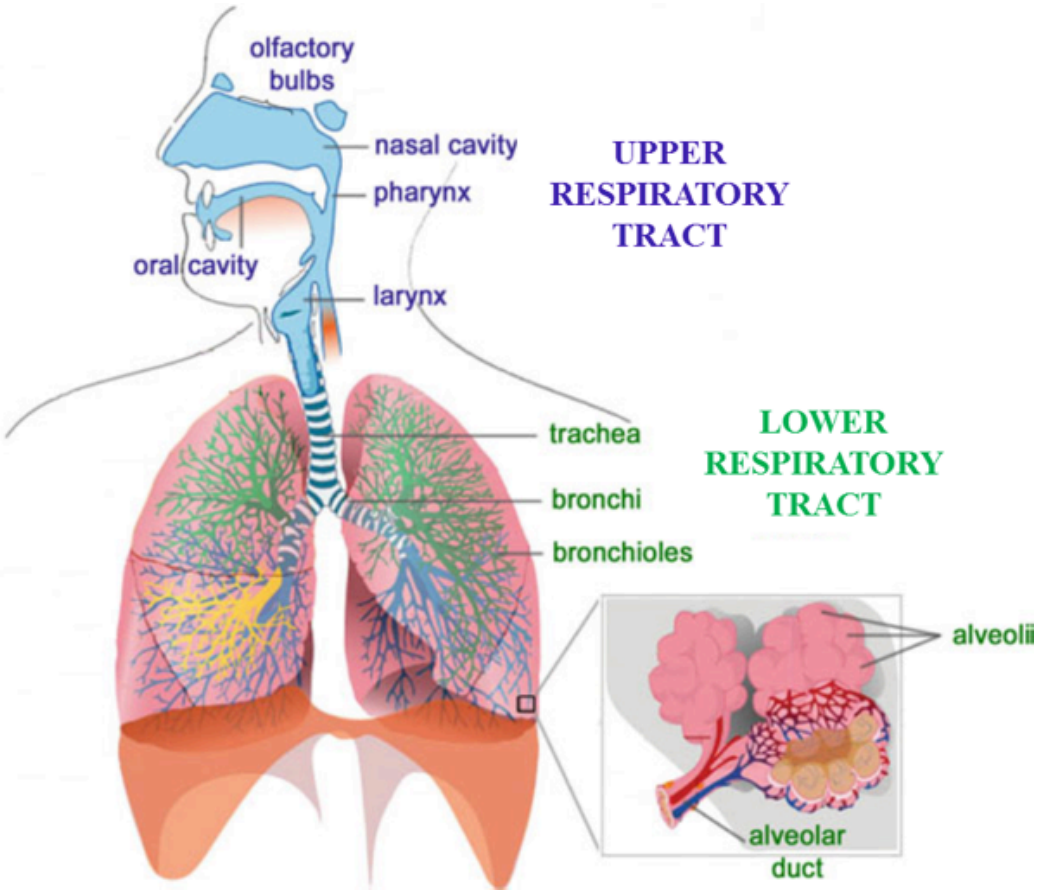

Figure 1.1. Diagram of the upper and lower respiratory airways.

The respiratory system can be divided into main parts: the upper and lower airways (Figure 1.1). The upper respiratory tract includes the oral cavity, the nasal cavity, the pharynx and the larynx. Its primary function consists in trapping larger dust particles, warming and humidifying the inhaled air before it reaches the conducting airways of the lower respiratory tract, which is composed of the tracheo-bronchial tree and the lungs. Over the course of 23 divisions, the bronchial tree descends from the trachea to the alveolar sacs (Figure 1.2). The first 16 branches form the **conducting zone** of the airways which transport the air to and from the outside (bronchi and bronchioles). The remaining seven branches form the **transition zone** (respiratory bronchioles and alveolar ducts) and the **respiratory zone**, where are found the alveoli. There are approximately 300 million of alveoli in the lung and their alveolar-capillary membrane provides a large surface area (130 cm^2) for gas

exchange [Weibel, 1984].

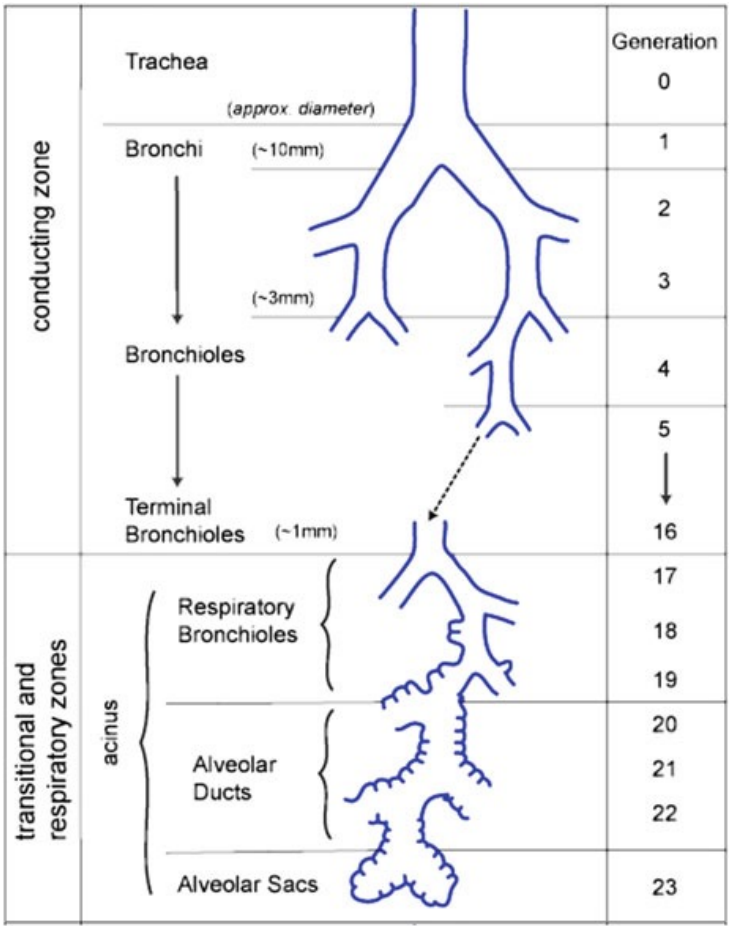

Figure 1.2. Schematic representation of the human adult airways (re-drawn from Weibel, 1984).

1.1.1.Lung parenchyma

The alveolar-capillary unit consists of three layers: epithelial, interstitial and endothelial (Figure 1.3).

The alveolar epithelium is composed by two different cell types:

-**Alveolar type I pneumocytes** cover over 95% of the alveolar surface while comprising only 8% of the total cells in the normal adult human lung [Crapo *et al.*, 1982]. These cells are derived from the type II pneumocytes during alveolar repair [Evans and Hackney, 1972]. They are able to stretch into flattened cells with very little depth (approximately 0.1 μm), but with a large surface area which minimizes the distance between the alveolar air space and pulmonary capillaries, thus maximizing

gas exchange [Castranova *et al.*, 1988].

-**Alveolar type II pneumocytes** are typically secretory cells and present polarized morphology, with cuboid appearance and microvilli on the apical side [Whitsett *et al.*, 1985]. They only comprise 4% of the alveolar surface, however, they constitute 60% of alveolar epithelial cells and 10-15% of all lung cells. These cells play several roles on the alveolar unit. Therefore, they are responsible for regeneration of damaged alveolar epithelium, metabolism of toxic compounds and the trans-epithelial movement of water. Nevertheless, their most important function is to synthesize and secrete lung surfactant, which is a unique feature of these cells [Castranova *et al.*, 1988, Herzog *et al.*, 2008].

Above the alveolar surface, there is a thin film of liquid which is secreted and absorbed by antagonistic processes: absorption is due to an osmotic process that requires active sodium transport, whereas fluid secretion requires active chlorine transport outward of alveolar epithelial cells. This alveolar fluid needs of the presence of lung surfactant, a lipoprotein complex that reduces the surface tension into the air-liquid interface, thus avoiding alveolar collapse.

In the alveolus there are also found the **alveolar macrophages (AMs)**. They are tissue-resident cells found in the inner epithelial surface close to the epithelium. AMs are professional phagocytes that contribute to the clearance of infectious agents such as bacteria, viruses and pollutants that reach the alveolar space. AMs need further specialization than other types of macrophages because lungs suffer marked environmental fluctuations. Thus, the partial oxygen pressure in the alveoli in normal conditions is 100–110 mm Hg, but this value will vary after the exposure to environmental agents, lung infection or chronic inflammatory diseases. AMs activation is tightly controlled by interacting with epithelial, stromal and other immune cells and soluble mediators that creates a regulatory environment to limit unwanted inflammatory responses. This cell-cell contact will be lost when AMs receptors interact with their respective ligands [Hussel and Bell, 2014]. Another important function of AMs is to internalize and tdegrade altered surfactant, thus helping to maintain surfactant homeostasis [Trapnell and Whitsett, 2002].

Beneath the epithelium it is found the interstitial layer which is constituted of connective tissue composed of elastic and collagen fibers, where are present mesenchymal cells and fibroblasts which support the alveolar structure through the secretion of extracellular matrix proteins and immune cells (lymphocytes, interstitial macrophages and mast cells) [Herzog *et al.*, 2008].

Finally, under the interstitial layer it is found the alveolar endothelium, which forms a barrier between the blood and the air. It is composed of a single continuous layer of squamous epithelial cells of mesenchymal origin called endothelial cells, which in human lungs occupy a surface area of 130 m2. This extensive area allows filtering the blood before it enters in the systemic circulation [Simionescu *et al.*, 1991].

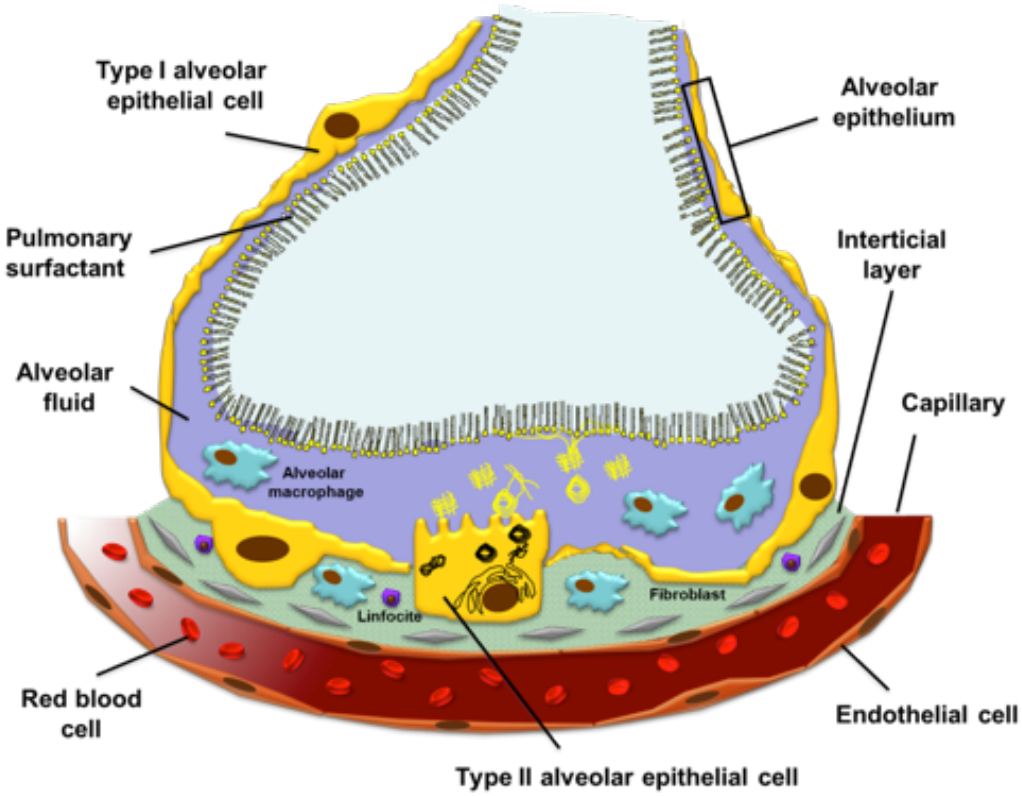

Figure 1.3. Schematic diagram of the alveolar-capillary unit. The three layers and their components are represented: alveolar epithelium, interstitial layer and alveolar endothelium.

1.1.2. The respiratory tract and its role as a defensive barrier

The first lines of defense in the respiratory system are structural and mechanical barriers which hamper the entry of pathogens, allergens and foreign particles into the lung. Physical defenses mainly comprise the upper airways filtering system, the airway epithelium and the mucociliary system.

The upper airway filtering system is constituted by the nose and the nasopharynx. Particles with a diameter > 10μm are found within these structures. They are able to remove airborne particles and water soluble gases from inspired air. This anatomical

mechanism of defense is augmented by sneezing and coughing reflexes which remove unwanted particles from the nose, pharynx and large airways [Nishino *et al.*, 2000].

The airway epithelium is another physical barrier between the external environment and the internal milieu [Ganesan *et al.*, 2013]. This barrier presents three components that contribute significantly to the defense of the respiratory tract: the **mucociliary escalator** which traps and clear foreign particles from airways, intercellular tight and adherent junctions which regulate epithelial paracellular permeability, and secreted antimicrobial peptides which aid to kill inhaled pathogens. The mucus is secreted by globet cells and submucosal glands present in the upper and lower airways. It contains micromolecules such as electrolytes and amino acids as well as macromolecules including lipids, carbohydrates, nucleic acids, mucins, immunoglobulins, enzymes and albumin. The function of the mucus is to trap particles, absorb gases and facilitate their removal by the cilia which sweeps the trapped material from the lungs towards the pharynx [Knowles *et al.*, 2002].

1.1.3. Lung surfactant

Pulmonary surfactant is a lipoprotein complex of extracellular membranes placed in the alveoli aqueous layer covering alveolar cells. Its main function is to reduce the surface tension at the air water interface that exerts a collapsing pressure, thus avoiding alveolar collapse [Perez-Gil, 2008; Casals and Cañadas, 2012]. Moreover, surfactant plays a key role in the innate immune defense in the lung, forming together with AMs the first barrier against inhaled pathogens or pollutants. Both surfactant properties-lowering surface tension and immune innate defense- depend on its lipid and proteic components [Whitsett and Weaver, 2002; Wright, 2005].

Pulmonary surfactant is crucial for lung physiology, given that deficiency or dysfunction of surfactant components causes impaired lung performance which leads to develop respiratory diseases [Ballard *et al.*, 1995; Skelton *et al.*, 1999; Gower and Nogee, 2011]. The first described and commonest cause of morbidity in neonates is respiratory distress syndrome, pathology due to surfactant deficiency in which preterm newborns are not able to synthesize enough lung surfactant. They can be treated with exogenous surfactant replacement [Avery and Mead, 1959; Robertson and Halliday, 1998; Jobe, 2006].

1.1.3.1. Lung surfactant composition

Pulmonary surfactant is a highly conserved complex mixture of lipids (90 wt.%), and proteins (10 wt.%). The lipid fraction consists mainly of phospholipids (PL) (~90-95 wt.%) with a small amount of neutral lipids (~5-10 wt.%), mainly cholesterol. The proteic fraction mainly consists of surfactant specific apolipoproteins: SP-A, SP-B, SP-C and SP-D, as well as non-specific surfactant proteins, mainly serum-derived proteins.

Phospholipids are amphipathic molecules that form bilayers in aqueous environment and monolayers at the air-water interface. At the air-water interface, phospholipids polar head group is toward the water and the acyl chains are facing to the air. Phosphatidylcholine (PC), which is the major phospholipid (70-80%) is primarily disaturated, being the predominant molecular species of PC, dipalmitoylphosphatidylcholine (DPPC) (16:0/16:0-PC) accounting for ~55 mol% (in human, rat, pig, and mouse) to ~40 mol % (in goat, caw, and rabbit). DPPC provides tightly membrane packing due to its saturated acyl chains being, by this reason, responsible of lowering the surface tension at the air-liquid interface during compression. The remaining forms of PC are unsaturated being 1-palmitoyl-2-oleoyl phosphatidylcholine (POPC) (16:0/18:1-PC) the most abundant among them. Primarily unsaturated forms of anionic phospholipids, mainly phosphatidylglycerol (PG) and phosphatidylinositol (PI) (~8–15 wt. %) are also found in mammals. Other phospholipids are present in surfactant at very low levels such as unsaturated phosphatidylethanolamine (PE), sphingomyelin (SM), lyso-PC, and choline plasmalogens [Goerke, 1988; Veldhuizen *et al.*, 1998; Casals and Cañadas, 2012].

Apart of the lipid component, there are four specific surfactant proteins (SP-) designated as SP-A, SP-B, SP-C and SP-D according to the nomenclature proposed by Possmayer [Possmayer, 1988], which have a distribution in mass of 5.0, 0.7, 0.8 and 0.5%, respectively, and are classified in two groups: hydrophobic (SP-B and SP-C) and hydrophilic (SP-A and SP-D). The small hydrophobic proteins, SP-B and SP-C, together with DPPC, are responsible of surfactant tensoactive properties. The large hydrophilic surfactant proteins, SP-A and SP-D, participate in pulmonary host defense and modulate immune responses. SP-A, SP-B and SP-C are obtained together with surfactant membranes by ultracentrifigation of BAL, whereas SP-D is not associated with membranes [Casals and Cañadas, 2012].

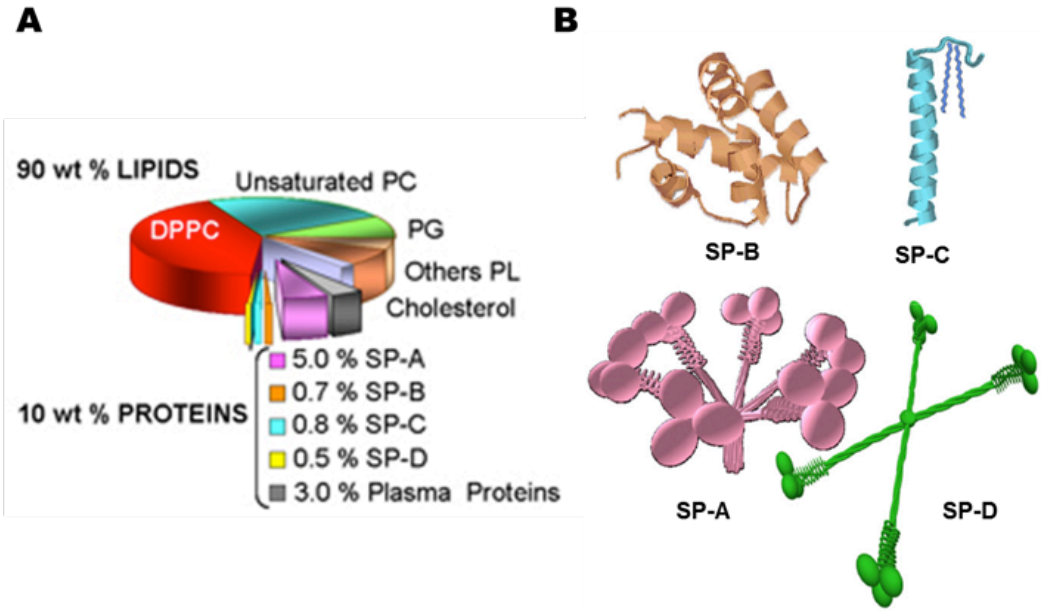

Figure 1.4. Cartoon illustrating the composition of pulmonary surfactant in percentages by weight (A). Three-dimensional models of hydrophobic (SP-B and SP-C) and hydrophilic (SP-A and SP-D) specific surfactant proteins (B) (adapted from Cañadas and Casals, 2012). PL: Phospholipid; DPPC: dipalmitoylphosphatidylcholine; PC: phosphatidylcholine; PG: phosphatidylglicerol; SP-: surfactant protein-.

1.1.3.2. Lung surfactant biological cycle

Pulmonary surfactant is synthesized in the endoplasmic reticulum of type II pneumocytes [Agassandian and Mallampali, 2013]. Life cycle of pulmonary surfactant comprises the following established steps (Figure 1.5):

1. Synthesis of pulmonary surfactant components by type II pneumocytes.

2. Assembly and storage of surfactant and regulated surfactant secretion into the alveolar fluid.

3. Rapid adsorption of surfactant into air-liquid interface, forming a monolayer. The monolayer will be compressed to reach low surface tension in order to prevent alveolar collapse.

4. Degradation and/or retrieval of surfactant components by alveolar macrophages and/or type II pneumocytes.

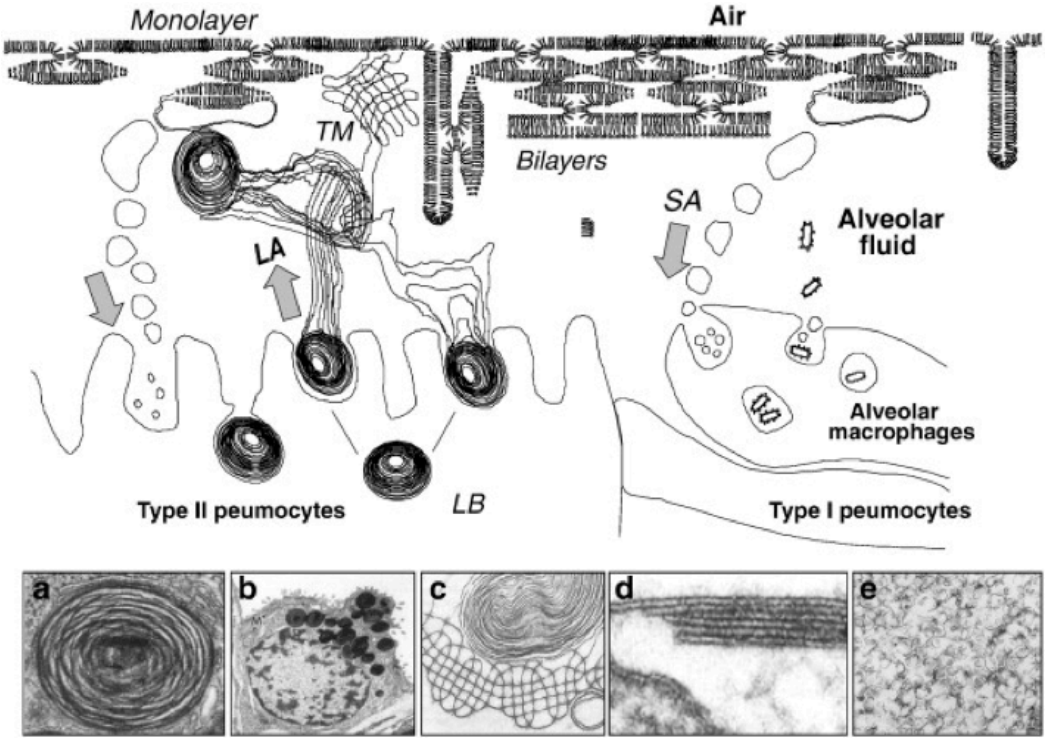

Figure 1.5. Schematic representation of pulmonary surfactant biological cycle. Pulmonary surfactant is synthesized by type II epithelial cells and then stored as closely packed bilayer membranes called lamellar bodies (LB) (a) which will be secreted into alveolar fluid by exocytosis forming a highly organized lattice-like membrane structure termed tubular myelin (TM) (c). These large extracellular membranes, called large surfactant aggregates (LA), adsorb quickly to the air-liquid interface thereby allowing to reduce surface tension values along the alveolar epithelium at the end of expiration thus avoiding alveolar collapse. These surface-active monolayer presents bilayer structures attached to it (d). Upon several surface compression and expansion cycles, small surfactant aggregates (SA) are generated (E) and present poor surface activity. Small aggregates are taken up and degraded by alveolar macrophages and type II cells. Taken from Cañadas and Casals, 2012.

1.2. RESPIRATORY INFECTIONS AND PULMONARY PATHOGENS

During breathing, respiratory airways are continuously exposed to contaminated air. In spite of the lung defense barriers cited above, many respiratory pathogens have evolved to successfully colonize and grow on or within lung epithelial cells, occasionally causing life-threatening diseases.

Respiratory infections are usually classified as upper and lower tract respiratory infections. Upper respiratory tract infections comprise common cold, sinusitis,

pharyngitis, epiglottitis and laryngotracheitis. The causative agents are mainly viruses but also bacteria, *mycoplasma* and fungi. Organisms gain entry into the respiratory tract by inhalation and invade the mucosa. Lower respiratory tract infections include bronchitis, bronchiolitis and pneumonia and are usually more severe than the upper ones. The etiological agents are usually viruses or bacteria but also *mycoplasma* and fungi. The pathogens reach the lower respiratory airways by inhalation or aspiration. They grow in the epithelium causing inflammation, increased mucus secretion and impared mucociliary function. In severe bronchiolitis, inflammation and necrosis of the epithelium may block small airways leading to airway obstruction [Dasaraju and Liu, 1966].

Pneumonia is a common and serious illness and represents the major cause of morbility and mortality in humans. Pneumonia may manifest as a wide range of possible outcomes because of different disease severities and pathogenic features. For critically ill patients, community-acquired pneumonia and ventilator-associated pneumonia are associated with high mortality [Mizgerd, 2008]. Moreover, in immunocompromised individuals, pneumonia might derive in sepsis, thus pathogen enters into the bloodstream and rapidly disseminates to and infect other organs.

Bacteria are the most common cause of pneumonia, however it also can be produced by viruses, such as respiratory syncytial virus (RSV) and fungi. Bacterial pathogens causing pneumonia include Gram-negative bacteria, such as *Pseudomonas aeruginosa*, *Escherichia coli*, *Klebsiella pneumoniae* and *Haemophilus influenzae* and Gram-positive bacteria, mainly *Staphylococcus aureus* and *Streptococcus pneumoniae* [Woodhead, 2011].

When pathogens reach the lungs, the innate immune system is crucial to eliminate them. As stated above, the first step is the recognition of PAMPs by phagocytic cells, mainly AMs. One of the best known bacterial PAMPs is endotoxin (LPS), which is the major component of the outer membrane of Gram negative bacteria and a potent stimulator of inflammatory processes [O´Brien *et al.* 1980, Ulevitch and Tobias, 1995].

LPS is a complex glycolipid consisting of a polysaccharide fraction covalently bound to a hydrophobic moiety designated as lipid A, which gives its character of endotoxin [Lüderitz *et al.*, 1978].

LPS recognition by AMs requires the intervention of extracellular and plasma

membrane proteins, including serum LPS-binding protein (LBP) [Tobias *et al.*, 1986]. LBP monomerizes LPS and transfers LPS molecules to cluster of differentiation 14 (CD14) [Wright *et al.*, 1990, Tobias *et al.*, 1993], a GPI-anchored protein which is found in lipid rafts, membrane microdomains with a lower degree of fluidity [Pugin *et al.*, 1998]. CD14 activation triggers the mobilization of myeloid differentiation protein 2 (MD-2), Toll-like receptor 4 (TLR4) and other molecules into lipid rafts, thereby forming the LPS receptor complex that results in the presentation of the endotoxin to TLR4 [Triantafilou *et al.*, 2002]. Following to the recognition of LPS by its receptor, intracellular signaling pathways are activated. TLR4 activation triggers the activation of phosphatidylinositol-3-kinase (PI3K) [O'Toole and Peppelenbosch 2007] and the two major downstream signaling pathways, one that depends on the adaptor protein myeloid differentiation factor 88 (MyD88) and the other that requires recruitment of Toll-interleukin-1 (IL-1) receptor (TIR)-domain–containing adaptor inducing interferon-β (TRIF) [Kawai and Akira, 2005] (Figure 1.7). Activation of the MyD88-dependent signaling pathway requires of the recruitment of the adaptor proteins TIRAP and MyD88. The clustering of the interleukin-1 receptor-associated (IRAK) 4 on MyD88 facilitates IRAK1 phosphorylation and activation, recruitment of TNF receptor-associated factor (TRAF) 6 and engagement of Transforming growth factor beta-activated kinase (TAK) 1 [Commane *et al.*, 2001]. TAK1 activates extracellular signal-regulated kinase (ERK), c-Jun N-terminal kinase (JNK) and p38 mitogen-activated protein kinases (MAPKs) and the transcription factor activator protein (AP)-1 as well as nuclear factor- κB (NF-κB). AP-1 and NF-κB translocate to the nucleus to facilitate transcription of proinflammatory cytokines such as tumor necrosis factor α (TNFα) and interleukin-12 (IL-12), chemokines (CCL2, CXCL10, and CXCL11), inducible nitric oxide synthase (iNOS), among others [Akira and Sato, 2003].

After activation of the MyD88-associated pathway, the LPS/MD-2/TLR4 complex translocates to endosomes and associates with the adaptor proteins TRIF and TRAF3 (Figure 1.6). TRIF facilitates the delayed activation of the MAPKs/AP-1 and NF-κB signaling pathways through engagement of TRAF-6 and Receptor-interacting protein (RIP) 1, respectively [Kagan *et al.*, 2008]. The tank-binding kinase (TBK)/ interferon regulatory factor 3 (IRF3) pathway is activated by TRAF3 and results in the production of type I interferons (IFNα/β), which are important for generating an effective host response to viral and bacterial [Jiang *et al.*, 2004]. Finally, the endotoxin receptor complex is sorted to late endosomes/lysosomes for degradation and signal termination [Husebye *et al.*, 2006].

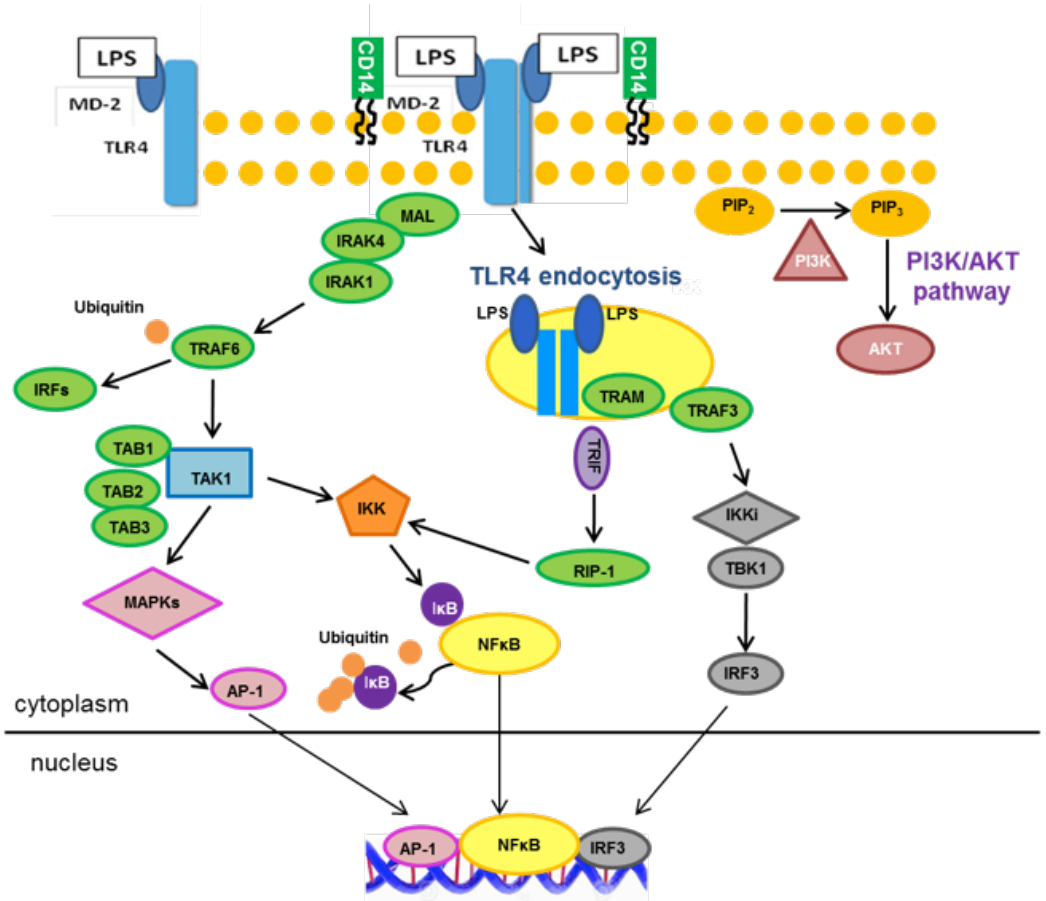

Figure 1.6. Schematized LPS signaling pathway. Activation of the LPS receptor complex induces TLR4 dimerization/oligomerization with rapid activation of the MyD88-depedent signaling pathways. Activated TLR4 is then endocytosed and the TRIF-dependent signaling pathway is induced. Re-drawn from Bohannon *et al.*, 2013.

LPS-elicited inflammatory response activates host defense mechanisms to fight infection. However, an exacerbated inflammatory response can contribute to the development of respiratory diseases such as pneumonia, acute lung injury, acute respiratory distress syndrome or multiple organ failure associated with severe sepsis [Hardaway, 2000; Cohen, 2002; Piantadosi and Schwartz, 2004].

Concerning to **fungal pathogens**, *Aspergillus fumigatus* is considered as one of the most common airborne fungal pathogens able to produce severe to fatal invasive infections in immunocompromised individuals [Dixon *et al.*, 1996; Lehrnbecher *et al.*, 2010]. Immunosuppressed individuals infected with *A.fumigatus* lead to develop respiratory diseases, such as community-acquired pneumonia or allergic bronchopulmonary aspergillosis. Furthermore, sensitivity to *A.fumigatus* has been

associated with severe persistent asthma in adults [Knutsen *et al.*, 2012].

The small conidia of *A.fumigatus* enter into the terminal respiratory airways by inhalation and reach the alveoli [Ben-Ami *et al.*, 2010]. In healthy individuals, inhaled conidia are efficiently cleared by the lung innate immune system [Margalit and Kavanagh, 2015]. If not, they will germinate into hyphal structures, which could damage lung tissue [Dagenais and Keller, 2009].

Fungal cell wall presents several PAMPs that allow the immune cells to recognize them and mount the inflammatory response to fight infection. Zymosan is a complex fungal cell wall particle which contains multiple PAMPs and has been traditionally used as a phagocytic and inflammatory stimulus *in vivo* and *in vitro* [Pillemer and Ecker, 1941, Di Carlo and Fiore, 1958]. Zymosan is mainly composed by polysaccharides, of which β-glucan and mannan are the major constituents. Zymosan triggers immune response in AMs through TLR2, eliciting similar pathways to those described above for LPS. TLR2 could form heteromers with TLR1 or TLR6 in order to expand the spectrum of ligand recognition [Farhat *et al.*, 2008]. TLR2 cooperates with TLR6 and CD14 in response to zymosan [Ozinsky *et al.*, 2000; Lee *et al.*, 2012], however CD14 participate to a lesser extent in signaling mediated by the TLR2-TLR6 complex than in signaling mediated by TLR4, because the TLR2-TLR6 complex was also shown to associate with the scavenger receptor B (CD36) [Hoebe *et al.*, 2004], which is also implicated in atherosclerosis by its ability to bind oxidized lipoproteins [Silverstein *et al.*, 2010].Moreover, it is known that TLR2 alone, in contrast to TLR4, can interact with bacterial peptidoglycan regardless or whether CD14 is present, nonetheless CD14 enhances peptidoglycan signaling [Sato *et al.,* 2003]. During phagocytosis processes, zymosan is recognized by another receptor, Dectin-1, that cooperates with TLR2 to trigger the appropriate inflammatory response against the pathogen [Goodridge and Underhill, 2008].

Finally, viral infections of the lower respiratory tract cause an enormous disease burden in children, and the role of respiratory viruses in serious lower respiratory tract infections in older adults is increasingly appreciated. A variety of viruses have been associated with clinical syndromes ranging from mild illnesses, such as the common cold, to more severe devastating conditions, such as pneumonia [Hamelin *et al.*, 2004]. Most viruses that infect humans enter into the body through the respiratory tract as in aerosols produced by coughing or sneezing of other infected hosts. Large particles are usually trapped in the sinuses and could cause upper respiratory infections. Smaller particles can reach the alveolar spaces and cause infections in the lower respiratory tract. After virus entrance, they could cause local respiratory infections as with most respiratory viruses such as influenza, rhinovirus,

respiratory syncytial virus, parainfluenza virus, coronavirus and metapneumovirus, occasionally causing lower respiratory infections [Flint *et al.*, 2000].

1.2.1. Respiratory Syncytial Virus

Respiratory syncytial virus is a member of the *Paramyxoviridae* family, subfamily *Pneumovirinae*. Discovered in 1956 [Morris *et al.*, 1956], RSV was quickly identified as a human virus and shown to be the leading cause of pediatric lower respiratory tract infections, mainly bronchiolitis and pneumonia, as well as an important cause of lower respiratory tract infections in adults underlying cardiopulmonary disease or immunosuppressed individuals. Most children are infected by RSV during the first year of life and virtually all are infected by the age of two. Re-infection is frequent during the first years of life and can occur multiple times throughout life, seriously impacting adults with chronic pulmonary diseases. Furthermore, severe RSV infection early in life is commonly associated with persistent abnormalities in airway function, such as recurrent wheezing, allergic sensitization and asthma. There is still no licensed vaccine against RSV infection and the therapeutic options are not effective or controversial [Collins and Mellero, 2011].

1.2.1.1. Morphology

RSV is a non-segmented negative-sense RNA virus consisting of 15,2 kb [Collins and Crowe, 2007]. The virion of the RSV is enveloped with a lipid bilayer, which is obtained from the host plasma membrane [Collins *et al.*, 2013]. The genome is found in the helical nucleocapsid. Ten genes encode for eleven proteins named non-structural protein 1 (NS1), non-structural protein 2 (NS2), nucleoprotein (N), phosphoprotein (P), matrix protein (M), SH, glycoprotein (G), fusion protein (F), matrix protein 1 (M2-1), matrix protein 2 (M2-2) and polymerase (L) [Collins and Graham, 2013]. The virion is relatively large, of about 150-300 nm in diameter [Collins *et al.*, 2013]. (Figure 1.7).

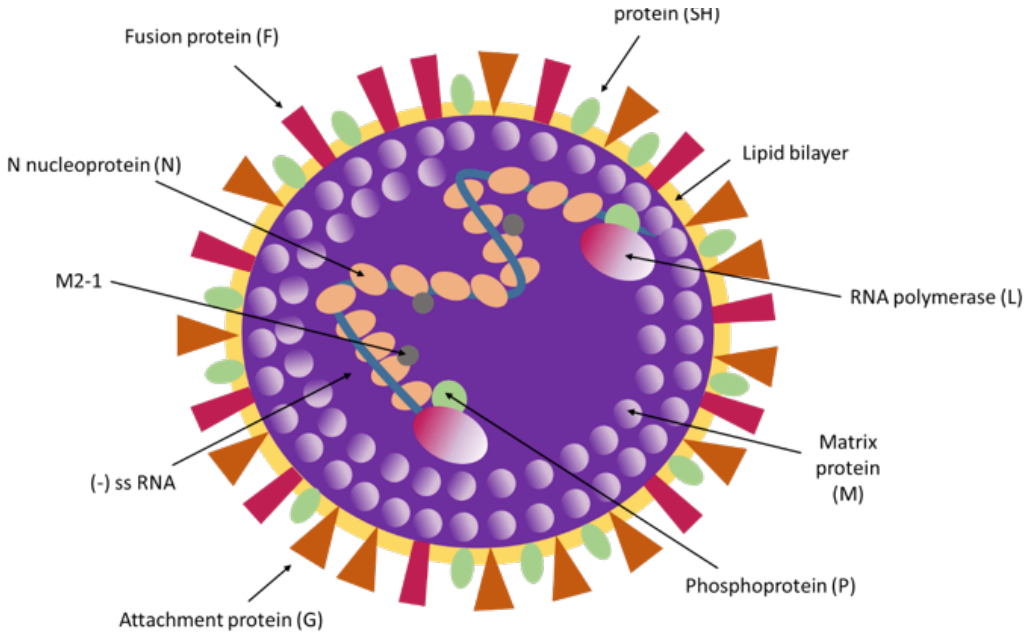

Figure 1.7. Particle of RSV.

1.2.1.2. Viral proteins

Five of the eleven RSV proteins are involved in nucleocapsid structure and/or RNA synthesis [Collins and Crowe, 2007]. In RSV-infected cells, the viral RNA with the L, N, P and M2-1 proteins form the polymerase complex in which the transcription of mRNA and genomic RNA occurs [Li *et al.*, 2008].

The **nucleocapsid protein (N)** tightly encapsidates genomic RNA as well as it positive-sense replicative intermediate, called the antigenome [Collins and Crowe, 2007]. This probably reduces detection of viral RNAs by host cell toll-like receptors (TLRs) and intracellular RNA recognition helicases that initiate innate immune responses through IFN regulatory factors and NF-κB [Akira *et al.*, 2006; Liu *et al.*, 2007].

The **Large subunit of the polymerase complex (L)** is the RNA-dependent RNA polymerase which replicates the viral RNA genome and transcribe mRNAs, the capping enzyme to cap the mRNA 5′ end, and the methylase to methylate the cap [Dochow *et al.*, 2012]. Given that the enzymatic activities of the polymerase complex are primarily associated with L, this protein is an attarctive drug target [Morin *et al.*, 2012].

The **phosphoprotein (P**) is an essential cofactor in RNA synthesis and also is thought to associate with free N and L to maintain them in soluble form for assembly of and interaction with nucleocapsids [Dupuy *et al.*, 1999].

The **Matrix protein 1 (M2-1)** and **matrix protein 2 (M2-2)** are found only in close relatives of RSV [Collins and Graham, 2008]. M2-1 protein is necessary for processive transcription and is essential for viral viability [Fearns and Collins, 1999]. In its absence, transcription terminates nonspecifically within several hundred nucleotides and results in reduced expression of NS1 and NS2 alone [Fearns and Collins, 1999]. The other product of the M2 gene, the M2-2 protein, is not essential but appears to downregulate transcription in favor of RNA replication as infection progresses [Bermingham and Collins, 1999; Beyer *et al.*, 2004].

The four other RSV proteins associate with the lipid bilayer to form the viral envelope [Collins and Crowe, 2007]. The M matrix protein lines the inner envelope surface and is important in virion morphogenesis [Teng and Collins, 1998]. The heavily glycosylated G, fusion F, and small hydrophobic SH proteins are transmembrane surface glycoproteins. G and F are the only virus neutralization antigens and are the two major protective antigens [Collins and Crowe, 2007].

The **M matrix protein** is a non-glycosylated inner virion protein, plays a central role in infection [Collins and Crowe, 2007]. M protein is mainly located in the cytoplasm where RSV replication occurs, but M also is present in the nucleus at particular stages of infection. RSV M plays a crucial role in virus assembly, budding and the formation of virus particles. The assotiation of this protein with the ribonucleoprotein complex inhibits viral transcription [Ghildyal *et al.*, 2002]. The M protein has also been implicated in viral protein trafficking. This protein is also capable of associating with the plasma membrane, F and G proteins at the cell surface. This probably contributes to the transport of the ribonucleoprotein complex to the cell surface [Mitra *et al.*, 2012; Shaikh and Crowe, 2013].

The **G glycoprotein** is produced, both, as a type II transmembrane protein that is incorporated into virions and as a soluble form lacking the signal/membrane-anchor region that is secreted from infected cells [Hendricks *et al.*, 1988]. G protein plays a crutial role in RSV binding to the cell surface through interaction with glycosaminoglycans, C-X3-C motif chemokine receptor 1 (CX3CR1) and the C type lectins, L-SIGN and DC-SIGN, on the cell surface [Bourgeois *et al.*, 1998; Malhotra *et al.*, 2003; Tripp R *et al.*, 2001; Johnson *et al.*, 2012]. The G protein also modulates the host immune response via the CX3C motif that mimics fractalkine/C-X3-C motif

ligand 1. The G protein containing CX3C motif binds to CX3CR1 and has leukocyte chemoattractant activity, thereby inducing disease pathogenesis [Fong *et al.*, 1998; Tripp *et al.*, 2001; Chirkova *et al.*, 2013].

The **F protein** is a transmembrane protein of the surface of the viral envelope. The F protein has two cleavage sites, however, activation seems to be readily achieved by ubiquitous celular proteases [Collins and Graham, 2008]. F protein binds to the host cell membranes through GAGs and fuses irreversibly the viral and host cell membranes through changes in its conformation [Techaarpornkul *et al.*, 2002]. In later stages of the infective cycle, F protein is involved in the dissemination of the virus by fusion of an infected cells with neighboring cells leading to the formation of syncytia [Walsh and Hruska, 1983].

During infection, the **SH protein** has been shown to exist in several forms as full-length truncated protein (4.5 kDa), and post-translationally modified by glycosylation and phosphorylation [Olmsted and Collins, 1989; Rixon *et al.*, 2005], although the full-length unmodified form are the major species [Collins and Mottet, 1993]. SH permeabilizes membranes [Carter *et al.,* 2010]. SH absence leads to viral attenuation in the context of whole organisms and it prevents apoptosis in infected cells [Gan *et al.*, 2012]. SH does not seem to play a key role role in RSV replication and pathogenesis. Thus, deletion of SH from recombinant RSV had little effect on virus production *in vitro* and resulted in only a small decrease in replication in chimpanzees [Collins and Graham, 2008].

The remaining two RSV proteins, **NS1** and **NS2**, are nonessential proteins solely found in the pneumovirus genus [Buchholz *et al.*, 1999]. Both interfere with the induction and signaling of IFNI and IFNIII, thus suppressing one of the main pathways of the immune innate response [Elliott *et al.*, 2007; Barik, 2013]. They are not necessary for virus replication *in vitro* whereas deletion of either NS gene severely attenuates RSV *in vivo*, indicating important defects in virus-host interplay [Bossert *et al.*, 2003].

1.2.1.3. Replication cycle

The infection cycle begins with the interaction of RSV with receptor at the cell surface and the fusion of its envelope with the plasma membrane [Collins *et al.*, 2013]. Subsequently, the viral nucleocapsid is released into the cytoplasm of the cell. The nucleocapsid consists of the viral RNA, encapsidated along its length with the N nucleoprotein to form a helical structure [Bakker *et al.*, 2013; Maclellan *et al.*, 2007; Tawar *et al.*, 2009], and associated with the viral RNA-dependent polymerase,

a complex comprising proteins L, P and M2-1 [Garcia *et al.*, 1993]. In the cytoplasm, the polymerase complex transcribes the viral mRNAs and replicates the genome by generating a positive-sense RNA intermediate, named antigenome, which acts as a template for further viral RNA synthesis [Collins *et al.*, 1984; Collins and Wertz, 1983]. Genomes and antigenomes are encapsidated with N nucleoprotein as they are synthesized and associate with the polymerase proteins to form nucleocapsids. Nucleocapsids are transported to the plasma membrane where they associate with other viral structural proteins. The virions will be released by budding [Fearns and Dewal, 2016]. (Figure 1.8).

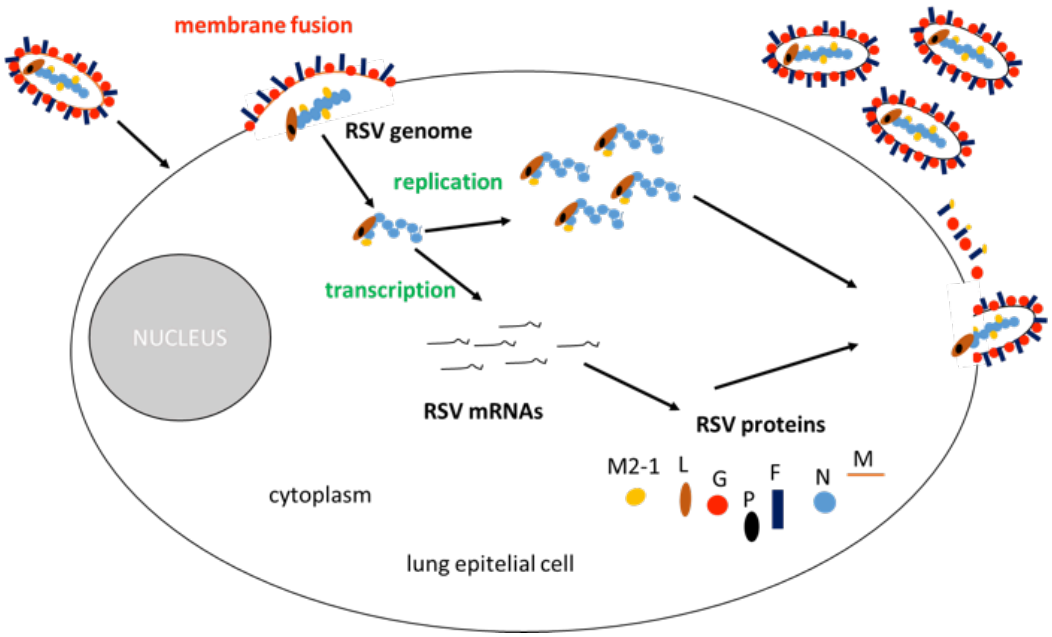

Figure 1.8. Schema of RSV replication cycle. Re-drawn from Fearns and Dewal, 2016. The attachment glycoprotein (G protein, red circle) binds to the chemokine receptor, CX3CR1, on the apical surface of epithelial cells and the fusion protein (F) (blue cylinder) mediates entry of the nucleocapsid into the cytoplasm. The complex consists of N nucleoprotein and viral RNA (chain of blue circles) serves as a template for the RSV polymerase complex, consisting of the L and P proteins (brown and black ovals, respectively), to synthesize viral mRNAs. The transcription process also requires the M2-1 protein (yellow circle). The surface glycoproteins are synthesized, post-translationally modified, and transported through the endoplasmic reticulum and exocytic pathway. The M matrix protein (orange rod) associates with replication complexes in the cytoplasm and interacts with the cytoplasmic tail of the F protein to elicit formation of viral filaments. This allows nucleocapsids to be packaged into filamentous virus particles, which are released by budding from the cell plasma membrane.

1.2.1.4. Immune innate response against RSV

Airway epithelial cells are the prime targets for RSV replication, thus these cells play a key role in regulating the respiratory tract inflammation that occurs upon viral infection [Lotz and Peebles, 2012]. The initial sensor for RSV infection is retinoic acid-inducible gene I (RIG-I), an intracellular RNA helicase that recognizes viral double-stranded RNA (dsRNA) [Liu *et al.* 2007]. Cells also sense RSV through toll-like receptors. RSV commonly activates TLR2 and TLR6 [Murawski *et al.*, 2009], TLR3 [Groskreutz *et al.*, 2006], TLR4 [Haynes *et al.*, 2001] and TLR7 [Lukacs *et al.*, 2010]. Nevertheless, RIG-I and TLR3 are the main receptors for RSV [Liu *et al.*, 2007]. RIG-I mediates RSV-induced early signaling events whereas TLR3, which is also a viral dsRNA sensor, acts later in the course of the viral infection [Alexopolou *et al.*, 2001, Liu *et al.*, 2007]. The activation of these receptors triggers the phosphorylation and degradation of IκB, thereby allowing nuclear translocation of transcription factors NFκB, IRF3 or IRF7 for the induction of type-I IFNs and proinflammatory cytokines [Kubota *et al.*, 2008]. IFN-I (IFN-α and β) is produced by most nucleated cells whereas IFN-II is produced mainly by T cells and natural killer cells as IFN-ɣ [Katze *et al.*, 2002]. IFN-I plays an important defensive role in many respiratory virus infections by limiting viral replication until the host develops its own defense mechanisms [Le Bon and Tough, 2002]. IFN-I bind to their extracellular receptors activating JAK-STAT pathway, which promotes the expression of IFN-stimulated gene (ISG) [Horvath *et al.* 1996, Kong *et al.*, 2003, Ramaswamy *et al.*, 2004]. (Figure 1.9).

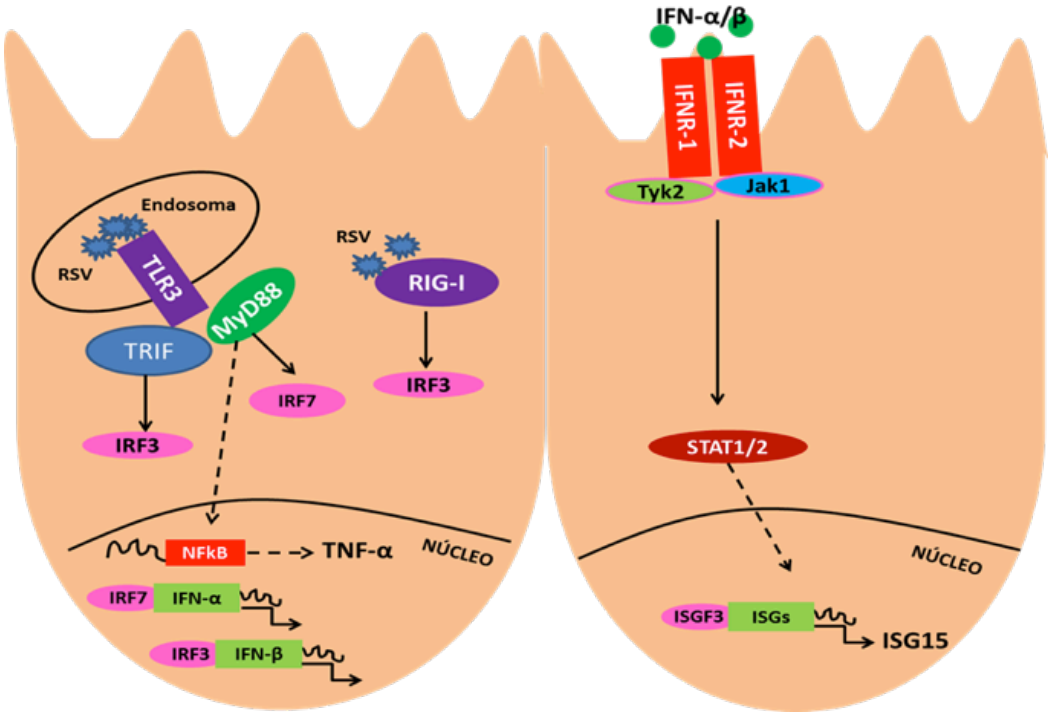

(legend continued on next page

Figure 1.9. Major signaling pathways activated in alveolar epithelial cells after RSV infection. TLR3 is expressed in intracellular endosomes and recognizes viral ssRNAs, such as those of rhinovirus, RSV, and influenza virus. TLR3 activates IRF-3 via the Toll/IL-1 receptor domain-containing adaptor (TRIF), resulting in IFN-β production. TLR3 also activates IRF-7 and NFκB through MyD88 activation. Activation of NFκB and IRF-7 leads to the production of proinflammatory cytokines such as TNF-α and the production of IFN-α, respectively. The RNA helicases RIG-I detect viral replication products in the cytosol to activate IRF-3. IFNs-α/-β bind to their receptor on the epithelial cell surface and promote the phosphorylation and activation of STAT1/2 that lead to the transcription of IFN-stimulated gene such as ISG15.

ISG15 is one of the earliest and most important ISG induced by type I IFN after viral infection. This gene encodes an ubiquitin-like protein that exerts its antiviral action by conjugation with host and viral proteins [Kunzi *et al.*, 2003]. ISG15 promotes an antiviral state by subverting proteosome-mediated degradation of IRF3 in infected cells [Pitha-Rowe and Pitha, 2007]. ISG15 can also be released to the extracellular medium by lysis of infected cells where activates the production and secretion of IFN-ɣ from B-cell-depleted lymphocytes, thus acting also as a proinflammatory mediator [Recht *et al.*, 1991; Jeon *et al.*, 2010]. It has been reported that TLR3 expression in the context of RSV infection, depends on RIG-I-induced IFN-β secretion [Liu *et al.*, 2007]

It has been postulated that RSV-elicited TLR3 activation leads to the production of chemokines, mainly CXCL8 and CCL5 [Rudd *et al.*, 2005], which recruit and activate immune cells that produce high levels of proinflammatory cytokines including TNF-α and IFN-I that triggers inflammatory processes [Tian *et al.*, 2002]. TNF-α secretion is necessary to develop the innate immune response against the virus. In this way, TNF-α was shown to promote neutrophil activation and migration to the lungs [Noah *et al.*, 2002, Abraham, 2003] that will help to kill RSV. Nevertheless, TNF-α can induce lung injury due to an exacerbated proinflammatory response through excessive recruitment of inflammatory cells or direct cytotoxic effects on alveolar epithelial cells [Zhao *et al.*, 2000].

1.3. INNATE IMMUNE SYSTEM IN THE ALVEOLAR SPACE

The innate immune system in respiratory mucosa acts as first line of lung defense against inhaled microbes. Once pattern recognition receptors sense the microbes, inflammatory responses are triggered immediately. These inflammatory responses must be regulated to prevent tissue damage caused by an exacerbated inflammation. The innate immune system consists of an array of soluble components which bind

microbial products and phagocytic cells which travel through the blood and migrate into the sites of inflammation in the lung, or reside in the lung waiting to fight infection [Martin and Frevert, 2005].

1.3.1. Soluble immune components

The presence of soluble components in the alveolar space is very important to fight infection and clear inhaled pathogens from the lung. In the conducting airways, aqueous fluids contain lysozyme, which present lytic activity against several bacterial membranes, lactoferrin which is an iron binding protein that reduce the availability of iron (essential for bacterial grow) and defensins, which are antimicrobial peptides released from leukocytes and respiratory epithelial cells [Becker *et al.*, 2000]. IgG, the most abundant immunoglobulin in alveolar fluids, complement proteins and surfactant-associated proteins act as additional microbial opsonins. In particular, SP-A and SP-D, members of the collectin family, promote phagocytosis by AMs. Lung collectins bind LPS and hamper their interaction with LBP in alveolar fluid and the TLR4 complex on alveolar macrophages [Borron *et al.*, 2000; Sano *et al.*, 2000]. Alveolar fluid contains high levels of LBP and soluble CD14 (sCD14), which are key molecules in the recognition of LPS by AMs and other immune cells [Martin and Frevert, 2005]. sCD14 is released from the surface of AMs by proteases, and this is augmented by IL-6, which is abundant in the BAL of patients with lung injury [Park *et al.*, 2001; Lin *et al.*, 2004]. AMs produce inflammatory cytokines and orchestrate a local inflammatory response by recruiting neutrophils from the blood into the alveolar space.

1.3.2. Alveolar epithelial cells

The pulmonary epithelium is involved in lung defense in different ways. Firstly, it acts as a structural barrier and contributes to the clearance of foreign inhaled particles and pathogens by the muco-ciliary escalator. Lung epithelial cells are attached to their neighbouring cells by intercellular junctions that divide the epithelium into apical and basal surfaces and restrict the passive movement of particles across the epithelium. In addition, alveolar epithelial cells participate in the immune innate response in the lung. Type II cells appear to be the primary alveolar epithelial cells (AECs) responsible for this part of innate immunity, but it is highly probable that type I cells are also involved. AECs are able to recruit inflammatory cells by releasing arachidonic acid derivates [Holtzman, 1992], chemokines in response to diverse stimuli such as bacterial and viral products [Lin *et al.*, 1998; Vareille M *et al.*, 2011]. AECs up-regulate adhesion molecules in response to inflammatory stimuli, allowing the adhesion of neutrophils and mononuclear cells to an inflamed area. AECs are also able to secrete antimicrobial substances, such as SP-A and SP-D, antimicrobial

proteins such as lysozyme, β-defensins, lactoferrins, cathelicidins, lipocalins and antioxidants such as reduced glutathione, which contribute to host defense. AECs II express toll-like receptors (TLR), mainly TLR2 and TLR4. Hence, they can recognize Gram-positive and Gram-negative bacteria. AECs II also express TLR3 to recognize some viruses such as Respiratory Syncytial Virus (RSV). In response to a viral infection, AECs secrete IL-6, IL-8, and RANTES as well as type I interferons (IFN-α, IFN-β). These interferons in turn will increase the production of chemokines and surface expression of ICAM-1, which is crucial to induce the migration of inflammatory cells [Mason, 2006].

1.3.3. Alveolar macrophages

Alveolar macrophages are the primary resident macrophages in the alveolar space. These cells constitute the major cell type recovered by bronchoalveolar lavage (BAL). AMs account approximately for 95% of the cell burden in BAL, with the remainder being lymphocytes (1-4%) and only about 1% of neutrophils [Gordon and Read, 2002].

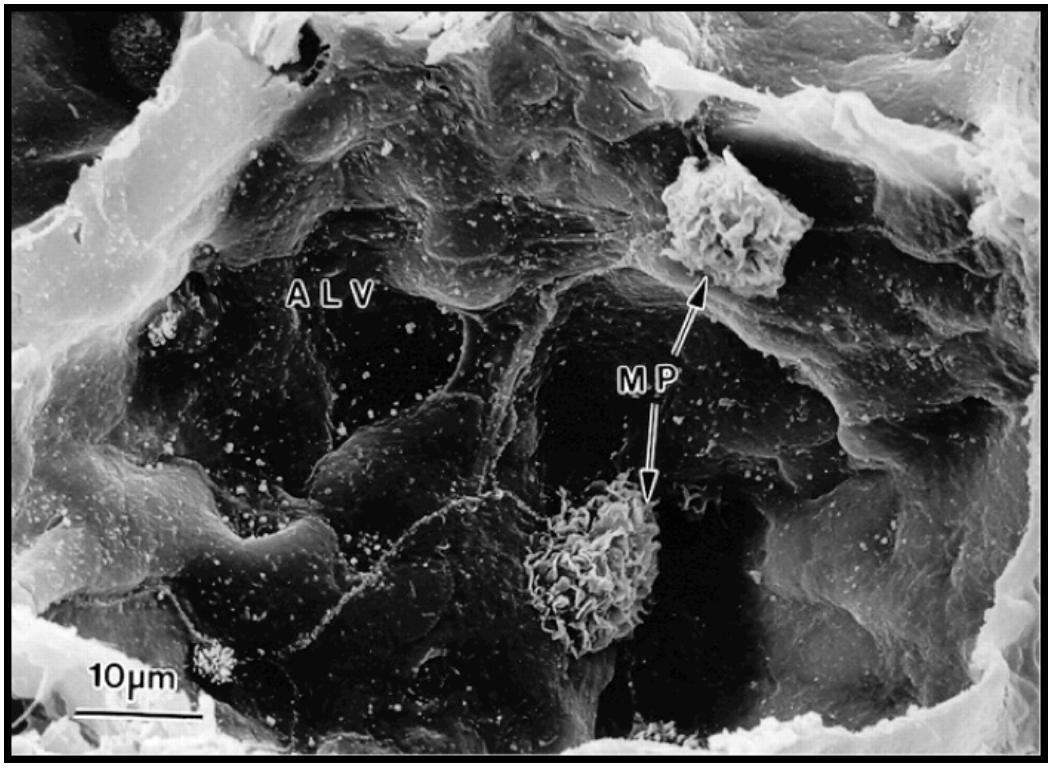

Figure 1.10. Scanning electron micrograph of a rat lung showing the images of erythrocytes in the alveolar wall capillaries and two ruffled alveolar macrophages (MP) in the alveolar space (ALV). Taken from Martin and Frevert, 2005.

AMs are derived from hematopoietic precursors and then specialized in the lungs into AMs. They are distributed in different tissues where they develop a key role in homeostasis, tissue remodeling and host defense [Lambretch *et al.*, 2006]. AMs, typically exhibit a lobulated nucleus surrounded by vacuolated cytoplasm containing abundant mitochondria and electron-dense secondary lysosomes. They are usually observed protruding from the alveolar epithelial walls into the lumen of the lungs [Laskin *et al.*, 2001].

In the lung, AMs are exposed to high oxygen levels and are also bathed in high concentrations of Granulocyte Macrophage Colony-Stimulating Factor (GM-CSF) and surfactant proteins (SP-A and SP-D) which present immunomodulatory actions. This particular environment made them to show certain unique features. The high levels of GM-CSF in the alveolar space favor the increase of CD11c expression, which is the most important difference between AMs and the rest of macrophage populations [Guth *et al.*, 2009].

In the steady state, AMs produce little amounts of proinflammatory cytokines and exhibit poor phagocytic activity. They are responsible of maintaining an immunological tolerant environment in order to prevent an exacerbated immune response against the vast repertoire of environmental antigens at which are continuously exposed. This fact avoids T-cell mediated lung damage by lymphocytostatic signals released by AMs such as immunosuppressive prostaglandins, TGF-β and IL-1 receptor antagonist [Roth and Golub, 1993]. It has also been described that AMs abrogate immune responses through the inhibition of dendritic cell-mediated activation of T cells [Holt, 1993].

Interestingly, under homeostatic conditions, AMs are in close contact with the alveolar epithelium. This mechanism aids to limit unwanted inflammatory responses. AMs express high levels of CD200 receptor (CD200R), a type I transmembrane glycoprotein of the immunoglobulin superfamily and the alveolar epithelium express its ligand (CD200). The interaction between CD200R and CD200 inhibits the activation of MAPK pathways elicited by TLRs in AMs [Hussel and Bell, 2014]. Additionally, in the healthy lung, AMs are in close contact with type AECs II and induce the expression of the integrin αvβ6 on the surface of these cells. This integrin activates TGF-β which restricts the inflammatory response of AMs [Lambretch, 2006].

Despite their quiescent state in healthy lungs, following antigenic challenge, AMs lose their contact with the alveolar epithelium and trigger an inflammatory response to fight infection. AMs present several pattern recognition receptors, such

as TLRs, nucleotide-binding oligomerization domain-like receptors, and retinoic acid-inducible gene-I-like receptors. These PRRs allow them to sense pathogen-associated molecular patterns (PAMPs) such as bacterial LPS, viral nucleic acids and components of the fungal cell wall, among others, or host-derived damage-associated molecular patterns (DAMPs) by triggering activation of NF-kB, AP1, CREB, c/EBP, and IRF transcription factors which in turn activates the expression of proinflammatory mediators [Newton and Dixit, 2012].

Moreover, the proinflammatory cytokines produced by AMs, mainly IL-8 and related C-X-C chemokines trigger an inflammatory response by recruiting neutrophils into the alveolar space. AMs also produce and secrete CC chemokines, such as MCP-1 and RANTES, which recruits monocytes and lymphocytes into the inflamed regions of the lung [Martin and Frevert, 2005].

In spite of an appropriate inflammatory response is necessary to combat inhaled pathogens, an aberrant proinflammatory response could induce lung injury through excessive recruitment of inflammatory cells or direct cytotoxic effects on AECs. For this reason, it is necessary the development of new therapies that aid to limit AMs responses during disease.

1.3.4. ROLE OF SURFACTANT COMPONENTS IN THE INNATE IMMUNE DEFENSE

Pulmonary surfactant has been proved to play a pivotal role in the immune innate system in the lung, helping to clear inhaled pathogens and to modulate inflammatory responses [Wright, 2005].

Firstly, pulmonary surfactant acts as a structural barrier hampering the entrance of pathogens in the lung. Moreover, there is mounting evidence indicating that both, surfactant phospholipids and proteins, play an indispensable role in lung defense [Chroneos *et al.*, 2010].

Several evidences have linked disorders in surfactant levels or composition with inflammation in acute lung injury, pulmonary fibrosis, emphysema, cystic fibrosis and chronic obstructive pulmonary disease, among others [Gunther *et al.*, 1999; Lewis and Veldhuizen, 2003; Chroneos *et al.*, 2010].

Results from *in vivo* experiments support the concept that genetic polymorphisms in one or more surfactant proteins genes are correlated with increased susceptibility to pulmonary inflammatory disease in humans [Chroneos *et al.*, 2010].

1.3.4.1 Surfactant phospholipids

There is growing evidence that support an important function for surfactant phospholipids in modulating innate immune response in the alveoli. This may represent a control mechanism to limit prolonged inflammation that could damage lung tissue.

Dipalmitoylphosphatidylcholine

DPPC is the most predominant phospholipid in the composition of pulmonary surfactant and has been demonstrated to be crucial to reduce surface tension to low levels at the end of expiration, thereby preventing alveolar collapse [Cañadas and Casals, 2012]. Interestingly, it has been described immunomodulatory properties for DPPC in the lung [Chroneos *et al.*, 2010].

Firstly, it has been described that DPPC inhibits platelet-activating factor (PAF) biosynthesis, which has a major role in the inflammatory response in the lung. The proposed mechanism is via perturbation of the cell membrane, which becomes more rigid, thereby inhibiting the action of the enzymes involved in PAF biosynthesis [Tonks *et al.*, 2003]. Moreover, it has been reported that preincubation of cells with DPPC inhibited the respiratory burst in response to LPS and zymosan through inhibition of protein kinase (PKC) δ [Tonks *et al.*, 2005]. In addition, it has been described that DPPC is able to up-regulate COX2 via CREB transcription factor, which in turn implies an increased expression of the anti-inflammatory prostaglandin PGE2 [Morris *et al.*, 2008]. All these experiments where performed using human monocytic cell lines.

Finally, it has been proved that DPPC is able to reduce IL-8 secretion in the human A549 AECs by impairing TLR4 translocation into specific membrane domains designated as lipid rafts [Abate *et al.*, 2010].

Anionic phospholipids

Several studies have postulated a potentially important role for anionic phospholipids in modulating the immune response with special emphasis on POPG.

POPG has been reported to compete with LPS for the positively charged LPS-binding site on LBP through electrostatic interactions [Hashimoto *et al.*, 2003]. Furthermore, POPG has been demonstrated to bind to CD14 and MD-2 thus inhibiting LPS-elicited NO and TNF-α production from rat and human AMs and U937 cells [Kuronuma *et al.*, 2009]. In addition, POPG is able inhibit the production of inflammatory mediators through TLR2 activation by *Micoplasma pneumoniae* [Kandasamy *et al.*, 2011].

Interestingly, it has been described that anionic phospholipids carrying acyl chains with a higher degree of unsaturated bonds exhibit stronger immunomodulatory properties. Thus, DPPG did not show inhibitory effect on TLR4-elicited NFκB activation, whereas POPG and DOPG, did. It is plausible that the transfer of a phospholipid to LBP or CD14 from fluid phospholipid vesicles occurs more readily than the transference from those more rigid [Hashimoto *et al.*, 2003].

In addition, anionic phospholipids have been proved to exhibit antiviral properties. It has been described that anionic pulmonary surfactant phospholipids such as POPG and PI, are able to bind RSV and block viral attachment to the epithelium, thereby suppressing RSV-induced replication and inflammation *in vitro* and *in vivo* and to provide short-term prophylaxis against RSV infection in mice [Numata *et al.*, 2010; Numata *et al.*, 2013a; Numata *et al.*, 2013b, Numata *et al.*, 2015]. POPG also has been proved to protect against Influenza A virus infection by suppressing viral attachment to the plasma membrane and subsequent replication and inflammation [Numata *et al.*, 2012].

1.3.4.2 Surfactant proteins

Among surfactant proteins, lung collectins (SP-A and SP-D) have been proved to play a significant role in lung defense. On the other hand, hydrophobic proteins (SP-B and SP-C) are mainly involved in respiratory dynamics. Nevertheless, increasing evidence indicate that SP-B and SP-C present immunomodulatory function [Glasser and Mallampali, 2012].

Lung collectins

Hydrophilic surfactant proteins SP-A and SP-D, belong to the C-type collectin superfamily and are called lung surfactant collectins. Concerning to their structure, they present four domains that consist of an N-terminus involved in interchain disulfide bonding, a collagen-like domain, a coiled coil neck domain and a lectin

or carbohydrate recognition domain (CRD). Each monomeric protein is assembled to form a triple helix at the collagenous domain. These trimers are oligomerized to form a bouquet-like octadecamer for SP-A and a cruciform dodecamer for SP-D [Ariki *et al.*, 2012].

Lung collectins are able to recognize a wide range of pathogens by PAMPs on their surface. For example, LPS on Gram-negative bacteria, lipoteichoic acid on Gram-positive bacteria, glycoprotein on fungi, lipoarabinomannan on mycobacteria, phospholipids on *mycoplasma*, and viral surface glycoproteins have been identified as ligands for pulmonary collectins [Hogenkamp *et al.*, 2007].

Upon recognition, they can act as opsonins agglutinating microorganisms [Sano and Kuroki, 2005] or directly inhibit the growth of microbes such as *Histoplasma capsulatum* yeast and some strains of Gram-negative bacteria, by increasing the permeability of the microbial cell membrane [McCormack *et al.*, 2003; Wu *et al.*, 2003].

Genetic elimination of lung collectins in mice has provided compelling evidence of its important role against infectious agents of the respiratory tract. These knockout mice show slower clearance of microbes including *Haemophilus influenzae* [Levine *et al.*, 2000] and respiratory syncytial virus [Levine *et al.*, 1999; Levine *et al.*, 2004], among others. Moreover, deficiency of these lectins has been associated with increased inflammation after infection with certain pathogens such as group B *Streptococcus*, *Haemophilus influenzae* and influenza A virus [Levine *et al.*, 2000; Levine *et al.*, 2002].

Lung collectins could augment the uptake of particles and infectious agents by different mechanisms. One mechanism described is opsonization. In this way, C1q receptor mediates the phagocytosis of SP-A-opsonized *Staphylococcus aureus* by monocytes [Geertsma *et al.*, 1994]. SP-A opsonizes Bacillus Calmette-Guerin and *Staphylococcus aureus* enhancing their phagocytosis by alveolar macrophages via SP-R210, which is a specific receptor for SP-A [Weikert *et al.*, 1997; Sever-Chroneos *et al.* 2011].

Another mechanism by which lung collectins promote uptake of pathogens is by increasing the expression of cell surface receptors. SP-A up-regulates the expression of scavenger receptor A and mannose receptor on the surface of alveolar macrophages, thereby favoring the phagocytosis of *Streptococcus* pneumoniae

and Mycobacterium avium, respectively [Kuronuma *et al.*, 2004; Kudo *et al.*, 2004].

In the context of inflammation, lung collectins have been shown to modulate the inflammatory response elicited by different infectious agents. Thus, SP-A interacts with CD14 on alveolar macrophages and avoids smooth LPS (s-LPS) binding to CD14 and inhibiting as a consequence s-LPS-induced TNF-α expression [Sano *et al.*, 1999]. In agree with this finding, it has been proved that intratracheal instillation of s-LPS into SP-A-deficient mice leads to an increased lung inflammation in comparison to wild-type mice and that co-instillation of s-LPS with SP-A attenuates inflammation in SP-A knockout mice [Borron *et al.*, 2000]. Similarly, by binding to TLR2, SP-A inhibits the interactions of peptidoglycan and zymosan with TLR2 [Murakami *et al.*, 2002; Sato *et al.*, 2003].

Surfactant protein B

SP-B is a small hydrophobic peptide crucial for sustaining respiratory physiology. Newborns with mutations that lead to deficiency of SP-B develop respiratory distress syndrome and die after birth due to the impossibility of inflate their lungs [Nogee *et al.*, 1994; Perez-Gil, 2008]. Despite of its main function on surfactant physiology, increasing data indicate that an immunomodulatory role for SP-B cannot be ruled out [Chroneos *et al.*, 2010]. Experiments with conditional knockout mice of SP-B indicate that SP-B deficiency was associated with increased levels of proinflammatory markers such as IL-6, IL1-β and MIP-2 in AMs and AECs. Restoration of SP-B levels decreased lung inflammation. This fact highlights a role for SP-B in the control of the inflammatory response in the lung [Ikegami *et al.*, 2005].

Moreover, it has been reported that SP-B reduces nitric oxide production by rat AMs by decreasing iNOS levels [Miles *et al.*, 1999]. Furthermore, *in vivo* experiments have proved that SP-B protects against lung injury induced by intratracheal administration of endotoxin.

In addition, SP-B has been proved to exhibit antimicrobial properties. Thus, a synthetic SP-B peptide is capable of inhibiting E. Coli growth *in vitro* [Kaser *et al.*, 1997]. Interestingly, it has been demonstrated that SP-B is able to aggregate and kill *Klebsiella pneumonia*, *Pseudomonas aeruginosa*, *Staphylococcus aureus* and group B *streptococcus* by increasing bacterial membrane permeability [Ryan *et al.*, 2006].

Surfactant protein C

The surface-tension reducing properties of SP-C have been exhaustively studied. Recently, it has been described that in addition to lung collectins, SP-C presents immunomodulatory properties. SP-C interacts with lipid A and CD14 [Augusto *et al.*, 2001; Augusto *et al.*, 2002; Chaby *et al.*, 2005]. These findings imply that SP-C neutralizes LPS to induce inflammatory stimuli in the alveoli.

Interestingly, it has been demonstrated that SP-C-deficient mice are more susceptible to bacterial and viral infections. In fact, it has been demonstrated that SP-C knockout mice are more vulnerable to pulmonary infection caused by *Pseudomonas aeruginosa*. Lower bacterial clearance and increased pulmonary inflammation were reported in mice lacking SP-C [Glasser *et al.*, 2008]. Moreover, in the absence of SP-C, RSV infection augmented lung inflammation due at least in part by SP-C-mediated inhibitory effect on TLR3 signaling [Glasser *et al.*, 2009]..

1.4. CARDIOLIPIN

Cardiolipin (1,3-diphosphatidyl-sn-glycerol, CL) is present in the outer membrane of Gram-negative bacteria and the membrane of Gram-positive bacteria (~ 10 and ~25%, respectively) [Barák and Muchová, 2013]. In eukaryotic cells, CL is mainly located in the inner mitochondrial membrane (~20 %), where fits perfectly due to its molecular structure [Krebs *et al.*, 1979; Zinser *et al.*, 1991 Paradies *et al.*, 2013; Mayr, 2015]. Nevertheless, CL is also present in the outer mitochondrial membrane (~5%) and is enriched at contact sites between the inner and outer membrane [Daum, 1985; Zinser *et al.*, 1991; Kroon *et al.*, 1997]. Cardiolipin is a dimeric phosphatidic acid with a glycerol backbone containing two phosphates and four acyl chains, thus differing from the rest of phospholipids (Figure 1.11) [Lecocq and Ballou, 1964]. CL belongs to non-bilayer forming phospholipids since the head group is significantly smaller than the tail

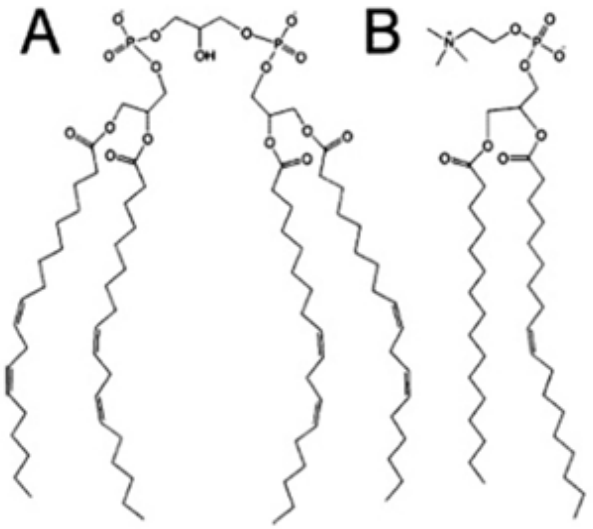

Figure 1.11. (A) Structure of the main molecular specie of CL in humans [$(18:2)_4$, CL] (B) in comparison with 1-palmitoyl-2-oleoyl-phosphatidylcholine.

that is formed by four fatty acids [Mayr, 2015]. The two phosphates are ionized at physiological pH resulting in CL being a doubly-negatively charged amphiphilic lipid [Few *et al.*, 1960].

In bacteria, CL is synthesized from two molecules of phosphatidylglicerol whereas in the mitochondria is synthesized from phosphatidylglicerol and cytidine diphosphate diacilglycerol (CDP-DAG) [Tian *et al.*, 2012]. In the mitochondria, two molecules of CDP-DAG are required to attach the two phosphatidyl groups to the positions 1 and 3 of the glycerol backbone.Two enzymes are required in CL synthesis: phosphatidyl-glycerol-phosphate synthetase and CL synthetase [Schlame *et al.*, 2005].

Interestingly, molecular species of CL found in eukaryotic and prokaryotes organisms are different: shorter acyl chains and saturated or mono-unsaturated CL species are typical of bacteria whereas longer chain polyunsaturated CL are mainly found in the mitochondria [Schlame, 2008]. Furthermore, bacterial CLs undergo limited acyl chain modifications, including formation of plasmalogen acyl chains which contain an alk-1´-enyl ether linkage as described in *Clostridium difficile* [Guan *et al.*, 2014]. Nevertheless, mitochondrial CLs undergo an extensive acyl chain remodeling to generate cell and tissue-especfific CL molecular species. The enzymes involved in these post-translational modifications are: (i) a CL specific phospholipase which produces monolyso-CL [Baile *et al.*, 2013]; (ii) An acyl transferase (tafazzin) that is located in the intermembrane space of the mitochondria and reversibly exchange acyl chains between phospholipids and monolyso-CL [Schlame, 2008; Claypool and Koehler 2012; Lu *et al.*, 2016]; (iii) A monolyso-CL acyltransferase-1 that is located in the mitochondrial matrix [Lu and Claypool, 2015] and (iv) An acyl-CoA:lyso-CL-acyltransferase-1 which is beyond the outer side of the mitochondrial outer membrane, in the mitochondria associated membranes of the endoplasmic reticulum [Zhao *et al.*, 2009; Lu and Claypool, 2015].

In the mitochondria, CL is essential for its function and structural integrity. After remodeling, CL is mainly concentrated in the inner leaftet of the inner mitochondrial membrane where CL bind to several mitochondrial proteins and, among them, the respiratory super-complexes [Bazan *et al.*, 2013; Mejia *et al.*, 2014]. Thus, this phospholipid is essential for ATP production by oxidative phosphorylation and also participates in mitochondrial fusion and fission processes [Claypool and Koehler, 2012; Mayr, 2015].

Moreover, CL acts as a DAMP in damaged mitochondria changing its localization from the inner to the outer membrane thus promoting mitophagy [Chu *et al.*, 2013;

Kagan *et al.*, 2017]. Externalized CL binds to microtubule-associated protein 1 light chain 3 which forms part of the autophagy machinery [Hsu and Shi, 2017; Maguire *et al.*, 2017]. CL is also involved in apoptosis. To trigger apoptosis, CL should be externalized but also undergo peroxidation of its polyunsaturated acylchains by cytochrome c [Kuwana *et al.*, 2002; Kagan *et al.*, 2017; Maguire *et al.*, 2017]. CL enables tBid recruitment to the mitochondrial membrane and Bax activation, a pore-forming pro-apoptotic protein involved in mitochondrial membrane permeabilization [Claypool and Koehler, 2012].

The relevance of CL on cell function has been demonstrated by the existence of several diseases (heart failure, diabetes or Barth syndrome) associated with deficiency in CL biosynthesis and/or alteration in the remodeling mechanisms of CL acyl chains [Claypool and Koehler 2012; Acehan *et al.*, 2011; Chatfield *et al.*, 2014]. Nevertheless, outside of the mitochondrial scenario, the effect of CL on cell function remains poorly understood. The role of secreted CL into the extracellular medium on the immune response of alveolar cells or molecular effects of CL on membrane structure and dynamics have been poorly investigated.

It has been reported that in humans with pneumonia or mice infected with bacterial pathogens, CL is released into the alveolar fluid. CL could be released into the alveolar fluid from either dying host lung cells or from bacterial membranes. The molecular characteristics of the CL found in the alveolar fluid of patients or mice with pneumonia suggest a mitochondrial rather than bacterial origin. In fact, in pneumonias caused by *Haemophilus influenzae*, which lacks CL on its membrane composition, high levels of CL have been detected in BAL of infected mice. High concentrations of CL in the alveolar fluid impair lung function as it might damage the surface activity of pulmonary surfactant, a lipoprotein complex that prevents alveolar collapse and is involved in the innate immune defense of the lung [Ray *et al.*, 2010].

Recently, it has been described a dual role for CL in the context of host-host and host-pathogens interactions. Balasubramanian and co-workers found that the presence of CL increases the phagocytosis of membranes with externalized mitochondrial or bacterial CLs by macrophages (RAW 264.7, THP1 treated with phorbol esters, mouse peritoneal macrophages and human macrophages derived from monocytes) in a CD36 scavenger receptor dependent manner. On the other hand, CL attenuates the inflammatory response of mouse peritoneal RAW 264.7 macrophages stimulated with LPS by blocking the LPS receptor, TLR4. Given that bacteria externalize CL during host encounter, these investigators propose that externalization of CL might be an evasion strategy to avoid its recognition by the

innate immune system. Nevertheless, the presence of CL on the bacterial surface favors the pathogen clearance mediated by macrophages dependent on CD36. Therefore, these investigators propose that extracellular CL could be used by both, host and pathogen, for their own benefit [Balasubramanian *et al.*, 2015].

II. HYPOTHESIS AND OBJECTIVES

Cardiolipin is an unusual anionic tetra-acylated phospholipid [Lecocq and Ballou, 1964] which is mainly located in the mitochondrial membranes of eukaryotic cells and in Gram-negative and Gram-positive bacteria [Paradies *et al.*, 2013; Barak and Muchová, 2013]. In the mitochondria, CL develops a crucial role in membrane structure and function [Mayr, 2015]. Moreover, its implication in apoptosis is well-known [Kagan *et al.*, 2017; Maguire *et al.*, 2017]. However, little is known about the biological function of CL outside the cellular environment.

It has been reported that in mice and humans infected with bacteria that cause pneumonia, cardiolipin, presumably from the host, is released to the alveolar fluid. High levels of CL in the alveolar fluid impair lung function [Ray *et al.*, 2010]. It has been suggested that damaged lung function might be a consequence of CL-dependent inhibition of the tensoactive properties of pulmonary surfactant [Ray *et al.*, 2010]. On the other hand, it was recently postulated that extracellular CL could be beneficial for the host since membranes presenting mitochondrial or bacterial CLs on their surface are avidly phagocytosed by macrophages, which could facilitate clearance of host damaged membranes [Balasubramanian *et al.*, 2015]. At the same time CL, as well as other anionic lipids, can block LPS binding to TLR4 [Kuronuma *et al.*, 2009; Balasubramanian *et al.*, 2015], which limits inflammation. However, the potential anti-inflammatory action of CL could also be beneficial for pathogens in evading the host immune response.

We hypothesize that CL actions must depend on the CL concentrations in the extracellular medium. We aim to understand the biological actions of extracellular CL in the alveolar microenvironment in which these particles can interact with surfactant membranes, the alveolar epithelium, alveolar macrophages, and invading microorganisms (virus and bacteria).

The focus of this doctoral thesis is to understand how extracellular CL exerts its action in the alveolus during infection. To this end, we have studied whether low doses of cardiolipins are able to control inflammation and/or infection using cell culture models of inflammation and infection with respiratory pathogens. On the other hand, we studied whether high doses of CL might have any impact on the structure and function of pulmonary surfactant, and the mechanism by which this might occur.

Accordingly, this thesis comprises four sections of results with the following **specific objectives:**

1. To investigate the immunomodulatory role of CL on the immune innate response of alveolar macrophages stimulated with LPS or zymosan.

2. To determine the antiviral and anti-inflammatory effect of CL against respiratory syncytial virus infection on human alveolar epithelial cells, as well as to obtain deeper insight into the mechanism underlying CL antiviral action and the influence of lung surfactant components on CL antiviral properties.

3. To study CL protective action against non-typeable *Haemophilus influenzae* (NTHi) infection on alveolar epithelial cells.

4. To evaluate the inhibitory effect of high amounts of CL on lung surfactant structure and biophysical function.

III. MATERIALS AND METHODS

3.1. BIOCHEMICAL AND BIOPHYSICAL METHODS

3.1.1. Isolation of native rat pulmonary surfactant.

Male Sprague Dawley rats (Charles River, USA) were anesthetized with an intraperitoneal injection of Ketamine (80 mg/kg) and Xylazine (10 mg/kg). BALs were performed with 40 ml of NaCl 0.9% (p/v), instilling into the trachea 10 ml each time. The BAL recovered was centrifuged for 7 min at 250 g to obtain cell-free BAL, which was stored at -80ºC in order to isolate pulmonary surfactant.

BALs from five rats were pooled and centrifuged at 48000g for 1h at 4ºC in a centrifuge XL-90 model (Beckman Coulter, Fullerton, USA) to separate LA from SA which remain in the pellet and supernatant, respectively. LA presents high surface activity and consists of surfactant lipids and apolipoproteins SP-A, SP-B, and SP-C, but not SP-D. SA represents the non-functional surfactant fraction that is generated due to respiratory dynamics. Given that SP-D is not able to bind to surfactant membranes, remains in the SA fraction [Casals and Cañadas, 2012]. After the centrifugation step, supernatant (SA) was discarded. The pellet (LA) was recovered and homogenized in 1ml of NaCl (0.9% p/v) using a potter and stored at -80ºC until its use.

3.1.2. Isolation of lipid extract from native surfactant

A lipid extraction from the LA fraction of pulmonary surfactant using organic solvents was performed according to the method described by Bligh and Dyer [Bligh and Dyer, 1959]. For this purpose, 1 ml of LA was transferred into conical tubes previously delipidized with CHCl3:CH3OH (2:1, v/v). Then, 2 ml of CH3OH and 1 ml of CHCl3 were added and the mixture was stirred using vortex for 30 seconds to form a monophasic system CHCl3:CH3OH:H2O (1:2:1, v/v). Subsequently, samples were incubated for 30 minutes at 37 ºC in a 320 Unitronic OR bath with continuous stirring to produce protein flocculation. After that, 1 ml of CHCl3 and 1 ml of H2O were added and samples were shaken for 30 seconds and centrifuged at 3000 rpm for 5 minutes to form a biphasic system CHCl3:CH3OH: H2O (2:2:2). After that, the organic layer was separated and transferred into a delipidized B20 tubes (Afora, Spain). Then, 2 ml of CHCl3 were added to the remaining aqueous phase. After shaking and centrifugation as explained above, the organic layer was transferred into a B20 tube. This last step was repeated once, in order to recover as much possible hydrophobic material.

Finally, the organic phase contained into the B20 tube was evaporated with a rotary evaporator (Buchi, Flawil, Switzerland) and resuspended in 1ml of CHCl3:CH3OH (3:1, v/v). The samples were kept at -20 until use.

3.1.3. Quantification of total amount of phospholipid

Total phospholipid amount in the lipid extract of the LA fraction was performed by the phosphorus method described by Rouser and co-workers [Rouser *et al.*, 1966]. Samples (2µl) and standards (calibration curve of KH2PO4 0.05 mg/ml) each in duplicate, were taken to complete evaporation. Phosphorus present in phospholipids was mineralized by adding 0.45 ml of 70% HClO4 into each tube and incubated covered with glass ampoules in a sand bath at 260ºC for 30 minutes. After hydrolysis, the phosphorus liberated was quantitated by a colorimetric reaction by adding to each tube 3.5 ml of H2O, 0.5 ml of ammonium molybdate (2.5% w/v) and 0.5 ml ascorbic acid (10% w/v). Molybdate forms a complex with phosphorus which is reduced by ascorbic acid and that results in a colored compound. The reaction was developed for 7 minutes in boiling water and stopped by immersing the tubes in ice. The amount of phosphorus was determined by measuring absorbances at 820 nm in a DU.800 spectrophotometer (Beckman Coulter, Fullerton, USA).

3.1.4. Preparation of liposomes of lipid extract of pulmonary surfactant

Multilamellar vesicles (MLVs) of lipid extract of rat pulmonary surfactant (LES) in the absence or presence of CL, were formed upon hydration in HEPES 25 mM pH 7.0, NaCl 150 mM (buffer A) for interfacial adsorption experiments, or in Tris-HCl 5mM pH=7.4, NaCl 150 mM (buffer B) for Differential Scanning Calorimetry (DSC) and emission anisotropy of DPH experiments. MLVs were prepared by hydrating the dry proteolipid film, with or without the fluorescent probe DPH, in the suitable buffer, and allowing it to swell for 1 h at 55°C. After that, MLVs were used directly or sonicated at the same hydration temperature for 4 min at 390 W/cm2 (burst of 0.6 s, with 0.4 s between bursts) in a UP 200S sonifier with a 2 mm microtip [Canadas O *et al.*, 2004] to perform fluorescence experiments. Vesicles were prepared freshly each day, just before the experiment was started.

3.1.5. Preparation of cardiolipin vesicles.

Cardiolipin (1',3'-Bis-(1,2-dilinolenil-sn-glycero-3-phospho)-sn-glycerol)) was dissolved in HPLC grade chloroform/methanol (Scharlau, Spain) (2:1 v/v) and was carried first to total evaporation under a nitrogen stream and subsequently, in a

vacuum centrifuge to remove any traces of organic solvent. Then, the dry lipid film was hydrated in 1 ml of 20 mM Tris pH = 7.4 containing 150 mM NaCl, for 1 h at 10°C in a Thermomixer (Eppendorf, Hamburg, Germany) with constant stirring. Afterthat, the vesicles formed upon hydration were sonicated to obtain small unilamellar vesicles (SUVs) at the same temperature of hydration for 3 minutes at 390 W/cm2 (burst of 0.6 s, with 0.4 s between bursts) in a UP 200S sonifier with a 2 mm microtip (Hielscher Ultrasonics, Teltow, Germany).

3.1.6. Dynamic Light Scattering analysis

CL was prepared as described in section 3.1.5 at a final concentration of 1mg/ml. The size of the vesicles obtained upon sonication and its stability over time were determined at 37°C in a Zetasizer Nano S (Malvern Instruments, Malvern, UK) equipped with a 633-nm HeNe laser. Three scans were performed for each sample. The hydrodynamic diameter was calculated using the general purpose algorithm available from the Malvern software for dynamic light scattering (DLS) analysis, which correlates the diffusion coefficient to the hydrodynamic diameter through the Stokes-Einstein equation, Eq.3.1:

$$d_H = \frac{k_B T}{3\pi\eta D}$$

where kB is the Boltzmann constant, T is the temperature, η is the viscosity, and D is the translational diffusion coefficient [Sáenz *et al.*, 2010].

3.1.7. Monolayer experiments

Monolayer experiments were performed as described previously [Cañadas *et al.*, 2011]. Studies were carried out at 25°C using a thermostatted Langmuir-Blodgett trough (102M micro Film Balance; NIMA Technologies, Coventry, UK) equipped with an injection port and magnetically stirred. The trough is equipped with two symmetrical movable barriers controlled by an electronic device. A concentrated solution (1 mg/ml) of rat LES dissolved in CHCl3:CH3OH 3:1 (v/v) was used for monolayer experiments. The subphase employed was buffer B. For insertion studies, monolayers were formed by spreading increasing amounts of LES (1mg/mL) at the air-water interface to reach initial surface pressures from 0 to 13 mN/m. After organic solvent evaporation, the monolayer was allowed to stabilize for a few minutes before injection into the subphase a CL amount equivalent to 12mol % with

respect to LES, without disturbing the lipid monolayer. Then, CL-induced changes in the monolayer surface pressure at constant surface area were measured.

3.1.8. Interfacial adsorption

The effect of CL on the ability of either rat LES or rat NPS to adsorb and spread onto at an air-water interface was analyzed with a Wilhelmy-like highly sensitive surface microbalance coupled to a small teflon dish. MLVs of rat LES or NPS (266 nmol) were injected into the hypophase chamber of the Teflon dish, which contained 1.5ml of buffer A containing 2.5 mM CaCl2 (Figure 3.1). Interfacial adsorption was measured following the change in surface pressure (π) as a function of time. The surface pressure (π) is a parameter that represents the ability of pulmonary surfactant to adsorb and spread onto an air-liquid interface and is related to the surface tension (γ) by the following expression: $\pi = \gamma_0 - \gamma$, where γ_0 is the surface tension of the clean air-water interface and γ that of the surface covered by the lipid monolayer. Thus, when surfactant spreads and adsorbs onto the air-water interface, the surface tension reaches the equilibrium value (25mN/m), which corresponds to a surface pressure value of 47mN/m ($\pi = \gamma_0 - \gamma = 72 - 25 = 47$mN/m) [Zuo *et al.*, 2008; Cañadas and Casals, 2012].

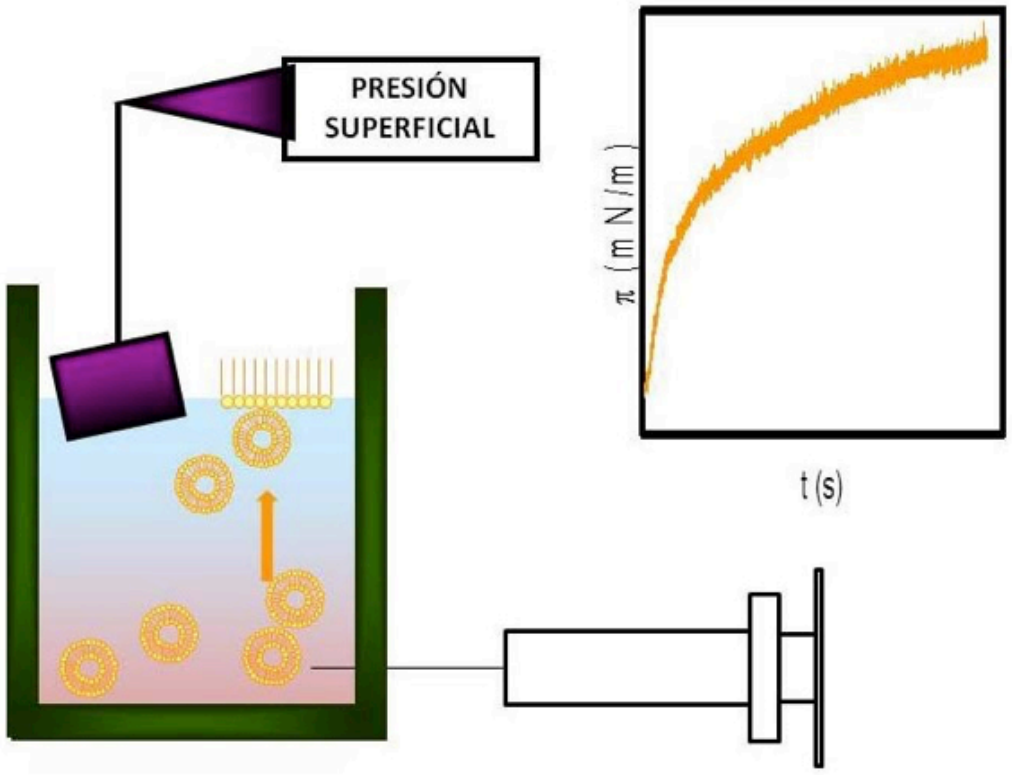

Figure 3.1. Adsorption of MLVs composed of surfactant membranes onto an air-water interface. This results in the formation of an interfacial monolayer which lowers the surface tension of water molecules located at the interface, which is reflected in an increase in the surface pressure, π. The surface pressure

is defined as: π= γ0-γ, where γ0 is the surface tension of water at the air-liquid interface (72 mN/m) and γ is the surface tension in the presence of the phospholipid monolayer.

3.1.9. Differential Scanning Calorimetry (DSC)

Differential scanning calorimetry (DSC) is a technique which allows to determine the thermodynamic properties of temperature-induced phase transitions. In DSC experiments, the sample to study and a reference material (a material which does not undergo a phase transition within the desired temperature range, usually the buffer in which the sample is reconstituted) are simultaneously heated or cooled at identical and predetermined rates. If the sample undergoes a temperature-induced phase transition, the sample will release or absorb heat. This fact results in a difference of temperature between the sample and the reference cell. To correct this, the instrumental control system will supply more (or less) heat.

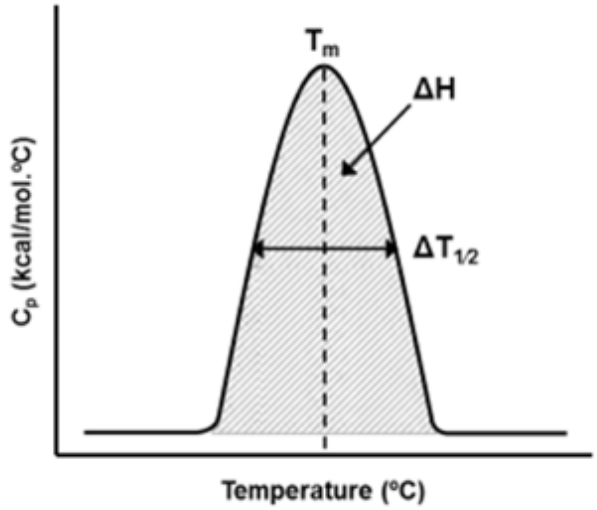

Figure 3.2. DSC thermogram for a two-state endothermic process. Tm is the phase transition temperature, ΔT1/2 is the temperature width at half-height of the peak, and ΔH is the enthalpy of the thermodynamic event

Biological membranes undergo a temperature-induced phase transition from a relatively ordered crystalline-like state (gel phase (Lβ)) to a relatively disordered fluid-like state (liquid-crystalline phase (Lα)). The properties of the gel-to-liquid phase transition of different lipid mixtures can be therefore studied by DSC.

The registered parameter in a DSC scan is the excess heat capacity (Cp) of a sample according to the reference cell as a function of temperature. Endothermic transitions are represented as positive peaks. Three thermodynamic parameters can be directly determined from the thermogram (Figure 3.2). Firstly, the phase transition temperature, Tm, represents the temperature at which the gel-to-liquid crystalline phase transition is half complete. Secondly, the relative cooperativity of

a phase transition is related to the sharpness of the transition peak, which is given by the temperature width at half-height, ΔT1/2. Finally, the enthalpy of the transition (ΔH) can be calculated by integrating the area below the thermogram [Cañadas and Casals, 2013].

Calorimetric measurements were performed in a Microcal VP differential scanning calorimeter (Microcal Inc., Northampton, MA, USA) at a heating rate of 0.5°C/min. MLVs of lipid extract of pulmonary surfactant (1 mM), containing or not different molar percentages of CL (3, 6, 12 mol %) and hydrated in buffer B, were loaded in the sample cell of the microcalorimeter with 0.7 ml of buffer B in the reference cell. Three calorimetric scans were recorded from each sample between 15 and 65°C. The standard Microcal Origin software was used for data acquisition and analysis. The excess heat capacity functions were obtained after subtraction of the buffer-buffer base line.

3.1.10. Fluorescence emission anisotropy measurements

Steady-state fluorescence emission anisotropy measurements were carried out as described previously [Sáenz *et al.*, 2007] in a SLM-Aminco AB2 spectrofluorimeter equipped with Glam prism polarizers and a thermostated cuvette holder (Thermo Spectronic, Waltham, MA, USA) (± 0.1 °C), using 5x5 mm path-length quartz cuvettes. MLVs of LES containing or not increasing molar percentages of CL (3, 6, 12 mol %) were mixed with 1,6-diphenyl-1,3,5-hexatriene (DPH) (Molecular Probes Inc, Eugene, OR, USA) at a probe/phospholipid molar ratio of 1:200 (final phospholipid concentration of 1 mg·ml–1). DPH concentration was determined measuring its absorbance at 350 nm, using a molar extinction coefficient in methanol of 88000 M-1.cm-1. Excitation and emission wavelengths were set at 360 and 430 nm, respectively. For each sample, fluorescence emission intensity data in parallel and perpendicular orientations, with respect to the exciting beam, were collected 10 times each and then averaged. Background intensities in DPH-free samples as a result of the vesicles were subtracted from each recording of fluorescence intensity. Anisotropy, r, was calculated according to Eq.3.2:

$$r = \frac{I_{\parallel} - G \cdot I_{\perp}}{I_{\parallel} + 2G \cdot I_{\perp}}$$

where I_{II} and I are the parallel and perpendicular polarized intensities measured with the vertically polarized excitation light and G is the monochromator grating correction factor.

3.1.11. Binding studies

Tryptophan fluorescence emission spectra of SP-A were measured in the absence or the presence of increasing amounts of CL in buffer B plus CaCl2 150μM. SP-A samples (with and without CL) and blank samples (CL alone) were excited at 295 nm and emission spectra recorded from 300 to 400 nm.

The apparent dissociation constant, Kd, for the SP-A/CL complex was obtained by analyzing the tryptophan fluorescence change when 10 μg/ml (15 nM) of SP-A reacted with various concentrations of CL. Each titration data point was performed in separated samples, and tryptophan fluorescence emission was monitored 10 minutes after CL addition.

The change in the fluorescence of SP-A at 337 nm and 25 ºC was monitored as a function of CL concentration and the titration data were analyzed by nonlinear least-squares fitting to the Hill equation 3.3:

$$\Delta F / \Delta F_{\max} = [L]^n \Big/ \left([L]^n + K_d \right) \quad (3.3)$$

where ΔF is the change in fluorescence intensity at 337 nm relative to the intensity of free SP-A; ΔFmax is change in fluorescence intensity at saturating CL concentrations; Kd is the apparent equilibrium dissociation constant; [CL] is the molar concentration of free CL; and n is the Hill coefficient.

3.2. EXPERIMENTS WITH MOUSE AND RAT ALVEOLAR MACROPHAGES

3.2.1. Isolation of rat alveolar macrophages by bronchoalveolar lavage and culturing.

Bronchoalveolar lavages (BALs) of lungs obtained from male Sprague Dawley rats (Charles River, USA) were performed with 40 ml of phosphate buffered saline (PBS, pH 7.4) containing 0.2 mM EDTA to obtain AMs. Rats were anesthetized with an intraperitoneal injection of ketamine (80 mg/kg) and xylazine (10 mg/kg). BALs from three rats were pooled and collected by centrifugation for 7 min at 250 g. After washing twice with sterile PBS, cells were resuspended in RPMI supplemented with

FBS (10% v/v), 100 U/ml penicillin, 100 µg/ml streptomycin and glutamine 2 mM. Then, cells were poured into 100 cm2 culture plates and allowed to adhere for 90 min at 37ºC in a humidified atmosphere of 5% CO2 in air. After that, supernatants were discarded and cells were washed with PBS to remove non-adherent cells. Cell purity was assessed by staining of CD11c to carry out the analysis by flow cytometry. Cellular population consisted of >88% alveolar macrophages.

3.2.2. Culture conditions of mouse alveolar macrophage cell line.

Two different types of alveolar macrophages were employed to study the anti-inflammatory action of CL: murine MH-S AMs [Mbawuike and Herscowitz, 1989] (Figure 3.3), acquired from the American Type Culture Collection (ATCC) (Manassas, VA, USA), and primary rat AMs isolated and cultured as described before. MH-S cells were cultured in RPMI 1640 with HEPES and glutamine (Gibco, Invitrogen, Auckland, NZ) and supplemented with fetal bovine serum (FBS) (10% v/v) (decomplemented at 56°C for 30 minutes) (Biochrom) antibiotic (penicillin/streptomycin) at 1% v/v (Lonza, Basel, Switzerland). Cell growth was performed in 100 mm dishes (TPP, Switzerland) maintaining the cells at a concentration of 1.105 and 2.105 cells/ml in an incubator at 37º C and in a humidified atmosphere of 5 % CO2. MH-S cells were scraped every 2-3 days. In any case 35 cellular passes were exceeded.

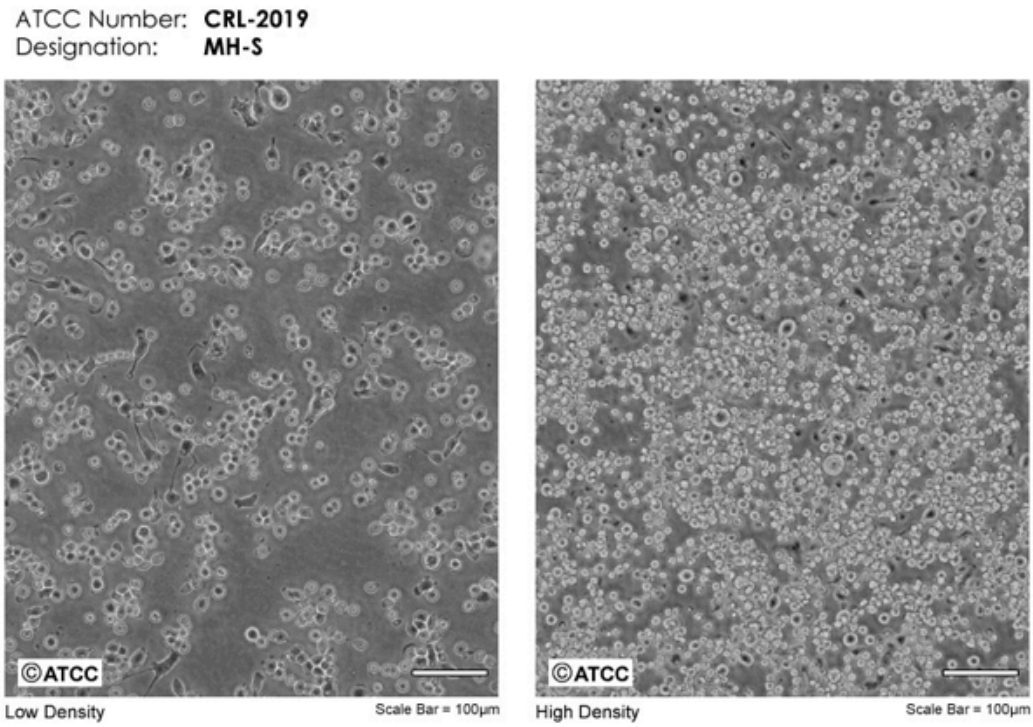

Figure 3.3. Morphology of MH-S cells by light microscopy.

3.2.3. Stimulation of MH-S or rat alveolar macrophages.

MH-S cells (3.10^5 per well) or rat AMs (1.105 per well) in RPMI containing FBS (5 % v/v) were seeded on 24-well plates or 96-well plastic dishes respectively. Cells were incubated O/N at 37º C in a humidified atmosphere of 5% CO_2 in air.

AMs were preincubated with CL vesicles for 18 hours and subsequently, stimulated with s-LPS extracted from E. coli serotype (B5:O55) (Sigma-Aldrich, St. Louis, MO) or zymosan A (Sigma-Aldrich, St. Louis, MO), in order to determine the anti-inflammatory effect of endocytosed CL vesicles. Moreover, we studied the effect of the co-administration of CL with the proinflammatory stimulus (LPS or zymosan).

To measure proinflammatory markers in the supernatants of cell cultures (TNF-α secretion) and protein levels of iNOS in cell lysates, cells were incubated for 6h at 37ºC, 5% CO2 whereas 10-30 minutes to determine phosphorylation of proteins involved in TLR4- or TLR2-elicited signaling events.

To determine the role of CL vesicles on the expression of certain genes induced by LPS, MH-S cells (5x105 cells per well) were seeded in 6-well plates (TPP) in 2 ml of RPMI medium containing FBS (5% v/v). Macrophages were then stimulated with 1 µg/ml of s-LPS for 1h.

3.2.4. Cell viability assays

The effect of CL vesicles on MH-S AMs viability was determined by propidium iodide exclusion assay:

Propidium iodide exclusion assay

AMs were maintained in the absence or presence of different amounts of CL vesicles for 24 hours. AMs were scrapped, centrifuged (200g, 10 min, 4°C) to remove the cell culture medium, resuspended in 0.5 ml of PBS and treated for 5 minutes with 50 µg/ml propidium iodide (Sigma Aldrich, St. Louis, MO). Propidium iodide is a waterproof dye which is excluded from viable cells. However, it is able to penetrate the non-viable cells with damaged plasma membrane and to intercalate into DNA bases, thereby increasing its fluorescence. The permeability of the plasma membrane to propidium iodide (was determined by flow cytometry (BD Biosciences FACScalibur). The fluorescence of propidium iodide was determined in the FL-2 channel using

Cell Quest Pro software.

3.2.5. Immunofluorescence microscopy

MH-S cells were seeded as described in section 3.2.3, in wells containing a round cover slide previously irradiated with UV light to allow sterilization. CL vesicles were fluorescently labeled with 1,1'-dioctadecyl-3,3,3',3'-tetramethylindocarbocyanine perchlorate (DiIC18) (Invitrogen, Carlsbad, CA), in a molar ratio of 200:1 phopholipid:probe. CL (dissolved in chloroform/methanol 2:1 (v/v)) was mixed with DiIC18 (dissolved in methanol) and dried as described in section 8. The dry lipid film was hydrated in 1 ml PBS for 1 h at 10°C in a Thermomixer (Eppendorf, Hamburg, Germany) with constant stirring. Then, CL was sonicated as explained in section 3.1.5 and added to the cells at a final concentration of 7 nmol/ml for increasing preincubation times (see Figure 4.1.3 in section 1 of results). Cells were washed with PBS and fixed in paraformaldehyde (PFA) (3.8% p/v) for 30 minutes. After that, wells were blocked with PBS containing FBS (10%v/v) for one hour and incubated with anti-mouse CD14 antibody developed in rat (1:100) (eBioscience, San Diego, CA) for one hour. Cells were washed with PBS and incubated for 30 minutes with a secondary anti-rat FITC-conjugated antibody (AbD Serotec). After a final washing step, cover slides were mounted on slides with Mowiol containing 1 µg/ml 4',6-diamidino-2-phenylindole (DAPI) to stain cell nuclei. Micrographs were taken on a Leica TCS SP2 Confocal system (Leica Camera AG, Solms, Germany).

3.2.6. Quantification of TNF-α release.

Secretion of TNF-α was determined in culture supernatants of AMs by enzyme-linked immune sorbent assay (ELISA) kits (BD Biosciences, NJ, USA). Firstly, wells of a Maxisorp® polystyrene plate (Nunc, Rochester, NY, USA) were coated overnight at 4ºC with a primary antibody against TNF-α. After washing with PBS-Tween-20 0.05% (v/v), the plate was blocked with PBS-FBS 10% (v/v) for one hour at room temperature to prevent non-specific binding. Then, wells were washed and incubated with the samples or TNF-α standards for two hours. After washing, the plate was incubated with a biotinylated detection antibody against TNF-α and streptavidin-horseradish peroxidase conjugate for one hour. Subsequently, wells were washed to remove unbound antibody and tetramethylbenzidine (TMB) was used as substrate. The reaction was stopped with H2SO4 and the absorbance of the plate at 450 nm was read on a plate reader ELISA DIGISCAN (Asys Hitech GmbH, Eugendorf, Austria).

3.2.7. Cell lysates and Western-Blot.

Once the time of phosphorylation (Akt, MAPKs, IkBα) or induction of protein levels (iNOS) has elapsed, the culture medium was removed and the plate containing the cells was rapidly frozen in liquid nitrogen. Then, a lysis buffer with the following composition was added: 10 mM HEPES pH 7.9, 1.5 mM MgCl2, 10 mM KCl, 0.5 mM EDTA, Triton X-100 0.2% , 1 mM benzamidine , aprotinin, 200 µg/ml leupeptin 200 µg/ml and 1 mM PMSF. For experiments in which phosphorylated proteins were analyzed, the buffer employed to perform cells lysates also contained the following phosphatase inhibitors: 20 mM β-glycerophosphate, 10 mM NaF, 10 mM sodium pyrophosphate and 2 mM orthovanadate. Cells were gently scraped and the content was transferred into an eppendorf. Samples were centrifuged (10000g, 10 min, 4°C) to remove genomic DNA. Finally, the supernatants were collected and the amount of protein was quantified using the bicinchoninic acid (BCA) assay. Subsequently, a loading buffer with the following composition was added to samples: 80 mM Tris HCl pH 6.8, 10% glycerol, 2% SDS, 0.1 % bromophenol blue and 5 % β-mercaptoethanol.

An amount of total protein present in the cell lysate of 6µg was loaded on polyacrylamide gels at 10%. Proteins were transferred to a PVDF membrane. Once the transfer was completed, membranes were blocked with PBS-Tween 0.1 % and skim milk (2.5% p/v) for 1 hour at room temperature with continuous stirring. All primary antibodies used were obtained from cell signaling: anti-iNOS (1:1000), GAPDH (1:10000), P-Erk (1:1000), Total Erk (1:2000), P-p38 (1:1000), total p38 (1:2000) P-Akt (1: 1000), total Akt (1:2000) and P-ikBα (1:1000). The secondary antibody used was anti-rabbit Ig-G coupled SIGMA peroxidase (1:5000). Bands corresponding to the protein of interest were detected using ECL substrate (Millipore) and quantified using Quantity One software program (Biorad).

3.2.8. Determination of total protein amount by Bicinchoninic acid (BCA) assay

The principle of BCA assay relies on the formation of a Cu2+-protein complex under basic conditions, followed by reduction of the Cu2+ to Cu1+ by cysteine, tryptophan, tyrosine and peptide bonds [Wiechelman *et al.*, 1988]. The extent of reduction is correlated with protein content. BCA forms a purple-blue complex with Cu1+ in alkaline environments, thus providing a basis to monitor the reduction of alkaline Cu2+ by proteins [Smith *et al.*, 1985]. To develop this assay, 10 µl of each cell lysate were mixed with 80 µl of the working reagent supplied in the BCA Kit for Protein Determination (Sigma) in 96-well polystyrene microplates (Nunc). The working reagent was prepared mixing 50 parts of BCA basic solution (reagent A)

with 1 part of 4% (w/v) copper (II) sulfate pentahydrate solution (reagent B). The plate was incubated for 30 minutes at 37ºC, and absorbance was read at 570 nm in a microplate reader (Asys Hitech). The protein concentration in each cell lysate was calculated from a bovine serum albumin standard curve.

3.2.9. Gene expression analysis by quantitative real-time polymerase chain reaction (qPCR)

MH-S AMs were seeded as described in section 3.2.3. CL vesicles were co-administered with LPS or preincubated with cells for 18 hours before the stimulation with LPS. Afterthat, culture medium was removed, cells were washed and trypsinized. Samples were centrifuged at 200g for 10 minutes. Subsequently, supernatants were discarded and pellets were washed with PBS. Cell pellets were stored at -80ºC until RNA extraction.

RNA extraction was performed employing High Pure RNA Isolation kit (Roche Diagnostics, Basel, Switzerland), according to the manufacturer's instructions. Briefly, cell pellets were resuspended in 200µl of PBS, then 400 µl of lysis/binding buffer were added to each sample and mixed by vortexing. Samples were transferred to a high pure filter tube coupled to a collection tube, which retain RNA into membrane. Residual DNA contaminations were removed adding to the samples 1.8 U/µl deoxyribonuclease I (DNase I) and incubating for 15 minutes at room temperature. Bound RNA was washed several times with different buffers given in the kit to eliminate salts, proteins, cellular impurities and inhibitory contaminants. RNA was finally recovered in 50 µl of elution buffer, quantified in a Spectrophotometer ND-1000 (NanoDrop Technologies, Wilmington, DE, USA) and stored at -80ºC.

cDNA synthesis was performed with the High-Capacity cDNA Archive Kit (Applied Biosystems) following the supplier's instructions. The reaction was developed in 50 µl of volume containing 1.25 µg RNA as input, random primers, deoxynucleotide triphosphate (dNTP) mix, 1.25U/µl MultiScribeTM reverse transcriptase, reverse transcription buffer and nuclease-free water. Samples were mixed with reagents by pipetting and incubated for 10 minutes at 25ºC (primers annealing), for 2 hours at 37ºC (cDNA synthesis) and for 5 minutes at 85ºC (enzyme inactivation) in a thermomixer (Eppendorf, Hamburg, Germany). Finally, cDNA was stored at -20ºC until PCR was performed.

Quantitative RT-PCRs were performed using PCR primers and Taqman MGB probes (FAM dye-labeled) for the genes cited in Table 3.1 which are products acquired from

Assays-on-demand (Aplied Biosystems, Life Technologies, USA).

Target gene	Gene name	Gene expression assay
GAPDH	glyceraldehyde-3-phosphate dehydrogenase	Mm99999915_g1
CXCL10	C-X-C motif chemokine 10	Mm01345163_g1
IL1-β	Interleukin 1-β	Mm00434228_m1
IL1-β	Tumor Necrosis Factor α	Mm00443258_m1
NOS2	Nitric Oxide Synthase 2	Mm00440502_m1
COX2	cyclooxygenase 2	Mm00478474_m1

Table 3.1. Gene expression assays used in qPCRs performed using predesigned primers.

Reactions were developed in 10 µl of final volume using 0.5 µl of gene expression assay, 2 µl of 1:10 diluted cDNA, TaqMan Gene Expression master mix (Applied Biosystems) and nuclease-free water. Reactions were carried out in an ABI PRISM 7900 HT-Fast (Applied Biosystems). The amplification program was: 10 minutes at 95ºC, followed by 40 cycles of denaturation for 15 seconds at 95ºC and primer annealing and extension for 1 minute at 60ºC. Assays were performed in triplicates. Data were analyzed using the 2-ΔΔCT method [Livak and Schmittgen, 2001], and results were normalized to the expression levels of glyceraldehyde-3-phosphate dehydrogenase (GAPDH).

3.3. EXPERIMENTS WITH HUMAN EPITHELIAL CELLS AND RESPIRATORY SYNCYTYAL VIRUS (RSV).

3.3.1. Culture conditions of human epithelial cells (A549 and HEp2 cell line)

We employed two epithelial human cell lines: A549 alveolar epithelial cells (Figure 3.4) [Giard *et al.*, 1973] and HEp-2 epithelial cells (Figure 3.5) [Moore *et al.*, 1955]. Both cell lines were acquired from the ATCC and cultured in Dulbecco's modified Eagle's medium (DMEM) supplemented with 4 mM glutamine, 100 U/ml penicillin, 100 U/ml streptomycin (Lonza Group Ltd, Basel, Switzerland) and FBS (10% v/v) (Linus, Madrid, Spain) at 37ºC and 5% CO2.

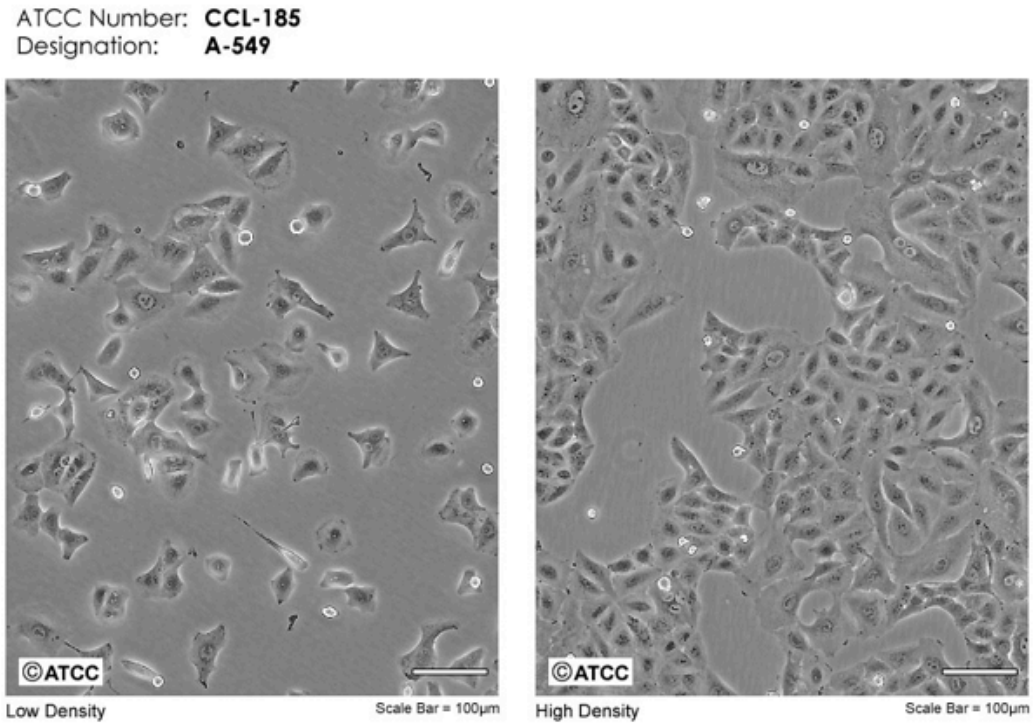

Figure 3.4. Morphology of A549 AECs by light microscopy.

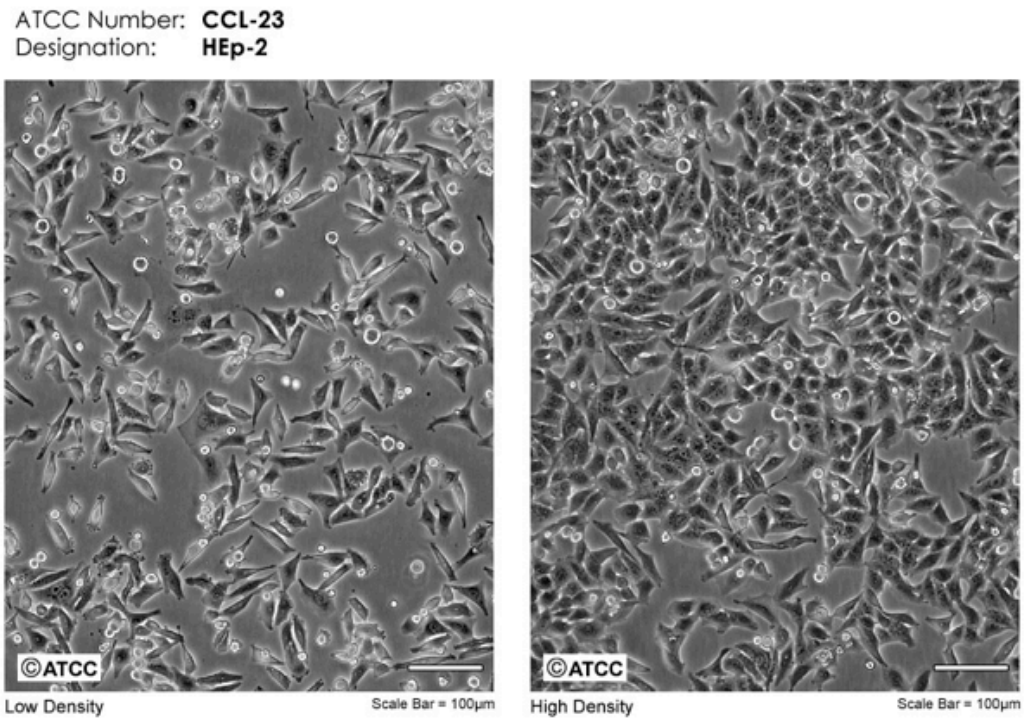

Figure 3.5. Morphology of HEp-2 cells by light microscopy.

3.3.2. Cell viability assays.

We analyzed the effect of increasing amounts of CL vesicles on the viability of A549 AECs employing wst-1 reagent:

Wst-1 reagent

WST-1 assay is based on the cleavage of the tetrazolium salt WST-1 in viable cells only, leading to the formation of a soluble formazan salt, which absorbance can be read at 450 nm. A549 AECs were maintained in the absence or presence of different amounts of CL vesicles for 24 hours. Five minutes before the end of the experiment, WST-1 diluted 1:40 was added to the cell culture. Finally, the supernatants were transferred into a 96-well microplate and the absorbance was measured at 450/600 nm using microplate reader (Asys Hitech GmbH, Eugendorf, Austria).

3.3.3. RSV propagation and purification.

The Long strain of human RSV was grown in HEp-2 cells seeded in DMEN containing FBS (2% v/v). RSV was purified from cell culture supernatants employing polyethylene glycol to allow precipitation and then, were centrifugated in a 30-45% discontinuous sucrose gradient in TNE buffer (10 mM Tris-HCl, pH 7.5, 100 mM NaCl, 1 mM EDTA) [Mbiguino and Menezes, 1991].

For this purpose, HEp-2 cells were plated at a cellular density of 5.106 cells in P100 plate (TPP) in DMEN-FBS (10% v/v) and grown overnight at 37ºC. Then, cells were infected at a multiplicity of infection (moi) of 0.5 plaque-forming units (pfu) per cell in DMEM-FBS (2%v/v). After 48 hours of infection, cells were scrapped and homogenized three times using a syringe coupled to a needle. Subsequently, ten P150 plates of HEp-2 cells were infected with the virus obtained from the first plate diluted in DMEM-FBS (2% v/v). After 48 hours of infection, supernatants were collected and cells were gently scrapped. Both were mixed and homogenized three times with a syringe coupled to a needle. After that, a centrifugation step was performed (4000g, 20 min, 4ºC) to clarify the mix. In the following step, 50% polyethylene glycol 6000 was added to the supernatant to a final concentration of 10%. The mix was maintained for 90 minutes at 4ºC with soft swelling. Then, it was centrifuged (4000g, 20 min, 4ºC). The pellets obtained were resuspended in TNE buffer and homogenized five times with a syringe coupled to a needle and sonicated three times for 10 seconds. Samples were added into a 30-45% discontinuous sucrose gradient in TNE buffer and centrifuged (150000g, 90 min, 4ºC). We observed a white band corresponding to RSV, placed between the 30%

and 45% sucrose solutions, which was recovered. Finally, RSV was aliquoted and stored in liquid N2. Viral titers were determined by plaque assay in layered HEp-2 cells, as it is described in the following section.

3.3.4. Determination of viral titers.

A549 AECs were seeded at 5.105 cells per well in 6-well plates (TPP) in 2 ml of DMEM-FBS (10% v/v) and grown overnight at 37ºC. In experiments aiming to determine the effect of the coadministration of CL with RSV, cells were mock-infected (with sucrose) or infected with RSV (moi=3) in DMEM-FBS (2% v/v) in the absence or presence of varying amounts of CL vesicles and/or pulmonary surfactant components for 90 minutes. Then, cells were maintained in the absence or presence of CL for 24 hours (post-infection period) at 37ºC in a humidified atmosphere containing 5% CO2 in air. In order to analyze the intracellular effect of CL on viral replication, cells were preincubated for 18h with CL and then, cells were washed with PBS and infected with RSV for 24 hours. Afterthat, supernatants were collected to infect HEp-2 monolayers.

HEp-2 cells were seeded the day before at 1.2.106 cells per well in 6-well plates (TPP) in 2 ml of DMEM-FBS (10% v/v) and maintained overnight at 37ºC in a humidified atmosphere containing 5% CO2 in air. A549 AECs culture supernatants were diluted in DMEM-FBS (2% v/v) (10-1 to 10-3) to infect HEp-2 monolayers. A549 AECs were incubated at 37ºC for 90 minutes to allow virus adsorption. After that, 3 ml of 0.7% low melting-point agarose (Conda, Madrid, Spain) in DMEM-FBS (2% v/v) were added into each well. Plates were maintained at 4ºC for 30 minutes to allow agarose solidification. Afterthat, plates were incubated at 37ºC for 5 days to allow RSV replication.

To visualize viral plaques, HEp-2 monolayers were firstly fixed with PBS-PFA (4% p/v) for 45 minutes. Then, the agarose blocks were removed, cell monolayers were also fixed with methanol, washed twice and blocked with PBS-BSA 1% (p/v) for 30 minutes at room temperature to avoid non-specific binding. Subsequently, wells were washed, and incubated for 1 hour with a pool of monoclonal antibodies (dilution 1:50) which recognize the two major RSV glycoproteins (2F, 47F, 56F, 021/1G, 021/2G) [Martínez *et al.*, 1997]. Then, wells were washed three times and incubated with an anti-mouse IgG HRP-linked whole antibody (1:500) (Amersham Biosciences, Buckinghamshire, UK) for one hour. Finally, RSV-forming plaques were revealed using 3-amino-9-ethylcarbazole (Sigma). Viral titer was calculated employing the next equation, Eq 3.4:

$$T = \frac{N.D}{V}$$

where T is the viral titer (pfu/ml), N corresponds to the number of viral plaques obtained, D is the dilution factor of the assayed infected-supernatant, and V represents the volume of culture supernatant used to infect cells expressed in ml.

3.3.5. Gene expression analysis by quantitative real-time polymerase chain reaction (qPCR)

A549 AECs were seeded at a cellular density of 5.105 cells per well in 6-well plates in 2 ml of DMEM-FBS 10% (v/v) and maintained overnight at 37ºC. Next day, the culture medium was removed, cells were washed and then, mock-infected (with sucrose) or infected with RSV (moi=3) in the presence or absence of CL (7nmol/ml) for 90 minutes. In experiments aiming to elucidate the anti-inflammatory action of endocytosed CL vesicles, cells were preincubated with CL for 24h and then, washed with PBS and then infected with RSV. Afterthat, fresh medium was added and cells were maintained at 37ºC for 24 hours. Then cells were trypsinized, washed with PBS and stored at -80ºC.

RNA was isolated from cellular pellets using ReliaPrep RNA Cell Miniprep System (Promega, Madison, WI, USA) according to the manufacturer´s instructions. Briefly, 250 µl of lysis buffer (BL+TG) were added to each cellular pellet and mixed well by vortexing and pipetting. Then, isopropanol was added to the samples and mixed by vortexing for 5 seconds. After that, samples were transferred to a minicolumn coupled to a collection tube and centrifugated (30 seconds, 14000 g, 25ºC). The resulting eluate was discarded. Total RNA will be retained into the minicolumn membrane. After a washing step, the membrane of the minicolumns was treated with DNAse I (Promega, Madison, WI, USA) for 15 minutes to remove potential contaminations with DNA.

After several washing steps, RNA was eluted in 40µl of RNase-free water by centrifugation (2min, 14000g, 25ºC). Total RNA extracted was measured at 260 nm in a spectrophotometer Biophotometer Plus (Eppendorf, Hamburg, Germany) and stored at -80ºC.

cDNA synthesis was performed as described in section 3.2.9.

To perform Quantitative RT-PCRs we used PCR primers and Taqman MGB probes (FAM dye-labeled) for the genes cited in Table 3.2 which were acquired from Assays-on-demand (Aplied Biosystems, Life Technologies, USA). A Custom Taqman Gene Expression Assay (Aplied Biosystems, Life Technologies, USA) was employed for amplification and quantification of the RSV Nucleoprotein N (forward primer: 5´CATGATTCTCCGATTGTGGGATGA 3´; reverse primer: 5´ TCACGGCTGTAAGACCAGATCTAT 3´; probe: 5´ CCCCTGCTGCCAATTT 3´.

Target gene	Gene name	Gene expression assay
ACTB	β-actin	Hs99999903_m1
DDX58 (RIG-I)	Dead (Asp-Glu-Ala-Asp) box polypeptide 58	Hs00204833_m1
TLR3	Toll-like receptor 3	Hs01551078_m1
TNF-α	Tumor Necrosis Factor α	Hs01113624_g1
ISG15	Interferon stimulated Gene 15	Hs01921425_s1

Table 3.2. Primers and probes used to carry out qPCR assays.

To develop PCR reaction, a mix of a total volume of 50µl for each sample containing the following components was prepared: Gene expression assay (2.5µl), cDNA (3µl) and 5x Pyrotaq probe qPCR mix plus (Cultek) (15µl) and nuclease free PCR water (29.5µl) (Promega, Madison, WI, USA). PCR reactions were performed in triplicate (15µl/PCR tube) on a StepOne sequence detection system (Aplied Biosystems, Life Technologies, USA). Samples were subjected to the following amplification program: 94ºC for 3 minutes, followed by 35 cycles 94ºC for 30 seconds (DNA denaturation), 45 seconds at 65ºC (primer annealing) and 45 seconds at 72ºC (DNA chains extension). Finally, samples were maintained at 72ºC for 2 minutes. ACTB was used as an endogenous control. Experiments were analyzed using the comparative CT (ΔCCT) method for relative quantifications.

3.3.6. Flow cytometric analysis of RSV binding to A549 cells.

A549 cells were cultured in plastic Petri dishes with DMEN-FBS 10% (v/v). The day on which the experiment will be performed, the culture medium was removed, cells were washed once with PBS plus EDTA 1 mM and then, cells were incubated with 10ml of PBS-EDTA for 10 min at 37ºC and 5% CO2 to allow cells detachment from the Petri dish. Subsequently, PBS-EDTA was removed and cells were recovered

using 5ml of PBS- FBS 2% (v/v). After cell counting, 5.105 cells were placed into each eppendorf and centrifuged at 3000 rpm for 5 minutes in a minifuge. From here, the whole process was carried out at 4ºC. Then, supernatant was discarded and celular pellet was resuspended in 2 ml of DMEN-FBS 2% (v/v) in the presence or absence of RSV (moi 3) containing or not CL (7 and 25 nmol/ml). Cells were incubated on a rotating wheel for 45 min. Afterthat, cells were incubated with primary mouse antibody against G glycoprotein of RSV for 30 min and, successively, anti-mouse Ig labeled with FITC. Finally, cells were fixed with PFA 1% in PBS. The Fluorescence of cells was determined in a Becton Dickinson FASCalibur cytometer using CellQuest software. PBS-FBS 2% (v/v) was used for washes carried out between steps and for dilutions of antibodies. This protocol is based on [Martínez and Melero, 2000].

3.4. EXPERIMENTS WITH MURINE EPITHELIAL CELLS AND *HAEMOPHILUS INFLUENZAE* (NTHi).

3.4.1. Culture conditions of murine epithelial cells (MLE-12 cell line)

We used the murine cell line MLE-12 which expresses some features of normal type II alveolar epithelial cells [Wikenheiser *et al.*, 1993]. MLE-12 cells were cultured under the same conditions described for A549 cell line (section 3.3.1).

3.4.2. Adhesion experiments of NTHi to pneumocytes MLE-12

Murine pneumocytes MLE-12 were infected with NTHi (108 c.f.u per well) in the absence or the presence of different concentrations of CL (7 and 27 mol/ml) for 30 minutes at 37ºC and 5% CO2. Infection was carried out in Hank´s medium (0.137 M NaCl, 5.4 mM KCl, 0.25 mM Na2HPO4, 0.44 mM KH2PO4, 1.3 mM CaCl2, 1 mM MgSO4, 4.2 mM NaHCO3). After infection, culture medium was removed and washed 5 times with PBS, lysed with 300 µl of PBS-saponin 0.025% for 10 min at room temperature, and serial dilutions were plated on Brain heart infusion (BHI)-agar. Next day, we proceed to c.f.u counting [López-Gómez *et al.*, 2012].

3.4.3. Experiments of internalization of NTHi into pneumocytes MLE-12

A similar protocol to that described above for adhesion experiments was performed. However, cells were infected with NTHi for 2h and then, they were incubated with RPMI-FBS 10% (v/v) containing gentamicin (200µg/ml) in order to kill extracellular bacteria. After three washing steps, pneumocytes were lysed according to the

protocol described for adhesion experiments. Then, cellular lysates were serial diluted for c.f.u counting on BHI-agar plates [López-Gómez *et al.*, 2012].

3.4.4. Analysis of Akt phosphorylation by western-blot

Pneumocytes were infected with NTHi (108 c.f.u per well) in the absence or the presence of CL (7 and 27 nmol/mL) for 1h at 37ºC and 5% CO2. Then, cells were lysed in a buffer with the following composition: 10 mM HEPES pH 7.9, 1.5 mM MgCl, 10 mM KCl, 0.5 mM EDTA, Triton X-100 0.2%, 1 mM benzamidine, aprotinin, 200 µg/ml leupeptin 200 µg/ml and 1 mM PMSF. To determine phosphorylated Akt, we carried out a western blot of cellular lysates according to the protocol described in section 3.2.7. Specific anti-bodies were used in order to detect P-Akt and GAPDH. Finally, membranes were incubated with a rabbit secondary antibody coupled to SIGMA peroxidase. Bands were detected using ECL substrate (Millipore) and quantified using Quantity One software program (Biorad).

3.5. STATISTICS

Data are shown as means ± SE. Statistical comparisons were made using one-way ANOVA followed by Bonferroni test. p values <0.001 or <0.05 were considered statistically significant. All statistical calculations were performed using SIGMAPLOT.

IV. RESULTS AND DISCUSSION

4.1. ANTI-INFLAMMATORY EFFECT OF CARDIOLIPIN IN ALVEOLAR MACROPHAGES STIMULATED WITH BACTERIAL AND FUNGAL MOLECULAR PATTERNS

4.1.1. INTRODUCTION

Cardiolipin is an anionic phospholipid having a head group (glycerol) that is esterified to two phosphatidylglyceride backbone fragments rather than one. This structure, combined with its four acyl chains makes CL unique among phospholipids [Paradies *et al.*, 2014]. CL is present in the outer membrane of Gram-negative bacteria and the membrane of Gram-positive bacteria (~10 and ~25%, respectively) [Barák and Muchová, 2013]. In eukaryotic cells, CL is preferably found in the inner mitochondrial membrane (~20 %) [Krebs *et al.*, 1979; Zinser *et al.*, 1991 Paradies *et al.*, 2014]. Nevertheless, CL is also present in the outer mitochondrial membrane (~5%) and is enriched at contact sites between the inner and outer membrane [Daum 1985; Zinser *et al.*, 1991; Kroon *et al.*, 1997]. Nevertheless, high levels of CL have been found in the bronchoalveolar lavage of human and mice with pneumonia. CL found in BAL could proceed from dying host cells as well as from bacterial membranes. The analysis of the acyl chain composition of these CLs (longer and unsaturated) suggest that they are presumably from the host [Ray *et al.*, 2010]. The biological function of CL in the alveolar fluid is unknown. It has been previously reported that POPG, an anionic surfactant phospholipid, plays a key role in the alveolar space modulating inflammation induced by respiratory pathogens (*Mycoplasma pneumoniae*) [Kandasamy *et al.*, 2011] or pathogen-associated molecular patterns such as [bacterial lypopolisaccharide (LPS)] [Kuronuma *et al.* 2009] or TLR2 ligands such as Pam3Cys [Kandasamy *et al.*, 2011; Kuronuma *et al.*, 2009].

We hypothesize that the secretion of low amounts of CL might modulate the inflammatory response of AMs and protect the host from the inflammatory response elicited as a consequence of the infection, that when it turns into aberrant, could damage lung tissues. However, high amounts of CL might be harmful for lung surfactant. Upon its secretion, CL could act in the extracellular medium and also be internalized by AMs and type II pneumocytes.

Therefore, the proposal of the present study was to determine the effect of extracellular and intracellular low concentrations of CL vesicles (≥0.07 nmol/ml) on the immune response of AMs stimulated with two pathogen-associated molecular patterns, to elucidate whether the action of CL is specific or not for a particular proinflammatory stimulus.

4.1.2. EXPERIMENTAL DESIGN

To study the potential immunoregulatory role of CL vesicles on the LPS or zymosan-elicited immune response, CL small unilamellar vesicles were coadministered with smooth bacterial LPS from E.Coli (1µg/ml) or zymosan A from *S.Cerevisiae* (50µg/ml) to MH-S murine AMs or rat AMs (Figure 4.1.1, t=0, co-addition CL-LPS). Alternatively, cells were previously incubated with CL vesicles for 18h and subsequently, washed with PBS and then stimulated with LPS (1µg/ml) or zymosan (50µg/ml) (Figure 4.1.1, t=18h, preincubation with CL). This preincubation time was long enough to ensure CL endocytosis by AMs, demonstrated with confocal microscopy experiments shown bellow (Figure 4.1.3).

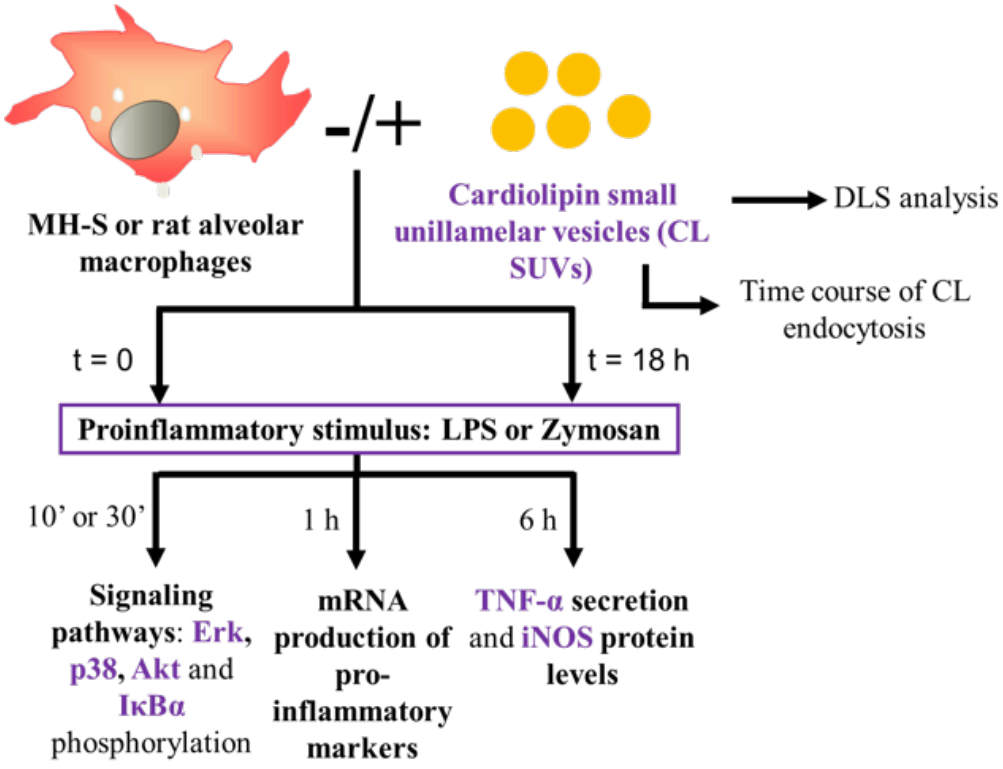

Figure 4.1.1. Experimental design.

4.1.3. RESULTS

4.1.3.1. Determination of the size and stability of cardiolipin vesicles.

We determined the hydrodynamic diameter of CL vesicles obtained upon sonication and analyzed the stability of these vesicles at 25ºC by Dynamic Light Scattering (DLS) technique after 30 min, 1h, 2h, 4h and 24h. Figure 4.1.2 shows DLS analysis of CL vesicles in buffer Tris 20 mM pH= 7.4 containing NaCl 150 mM. Two minutes of

sonication were enough to obtain a homogeneous population of CL small unillamelar vesicles (SUVs) with 50 nm of hydrodynamic dyameter (volume adjustment). The size of the vesicles was maintained at least for 24h.

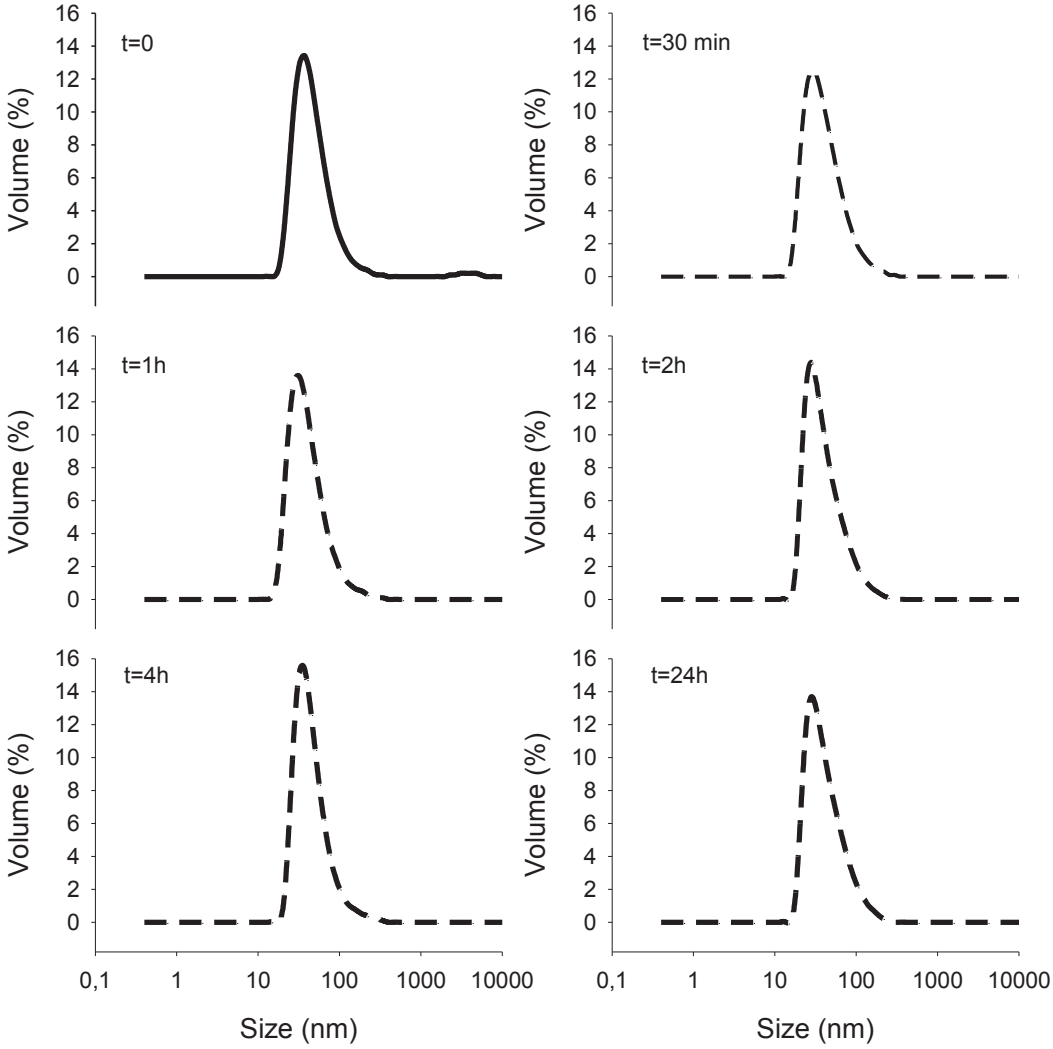

Figure 4.1.2. DLS analysis of the hydrodynamic diameter of CL vesicles obtained after 2 minutes of sonication (50nm,volume adjustement). CL SUVs were stable for 24h. The Y axis represents the relative volume of scattered light and the X axis shows the hydrodynamic diameter of the particles present in the solution.

4.1.3.2. Alveolar macrophages are able to internalize cardiolipin SUVs.

CL is secreted to the alveolar fluid from dying host cells during infection [Ray *et al.*, 2010]. Once there, CL could modify the activation state of AMs acting in the extracellular medium but also at the intracellular level if AMs were able to internalize

this phospholipid as it has been described for lung surfactant membranes [Agassandian and Mallampalli, 2013]. Therefore, we conducted confocal microscopy experiments in order to determine wheter CL is endocytosed by MH-S AMs. Then, cells were incubated for different times (10min, 30 min, 4h and 18h) in the presence of CL SUVs labeled with DiIC18 probe (200:1 phospholipid: probe molar ratio). Cells were fixed with paraformaldehyde, plasma membranes were labeled with anti-CD14 and FITC-conjugated secondary antibody whereas cell nuclei were stained with DAPI. Figure 4.1.3 indicates that after 10 minutes of CL addition, most of CL SUVs were located in the plasma membrane because they co-localized with the macrophage membrane receptor, CD14. After 30 minutes of preincubation, CL SUVs are beginning to be endocytosed by AMs and after 18 hours, the endocytosis of CL SUVs was maximal. From Figure 4.1.3, we can conclude that AMs are able to internalize CL SUVs.

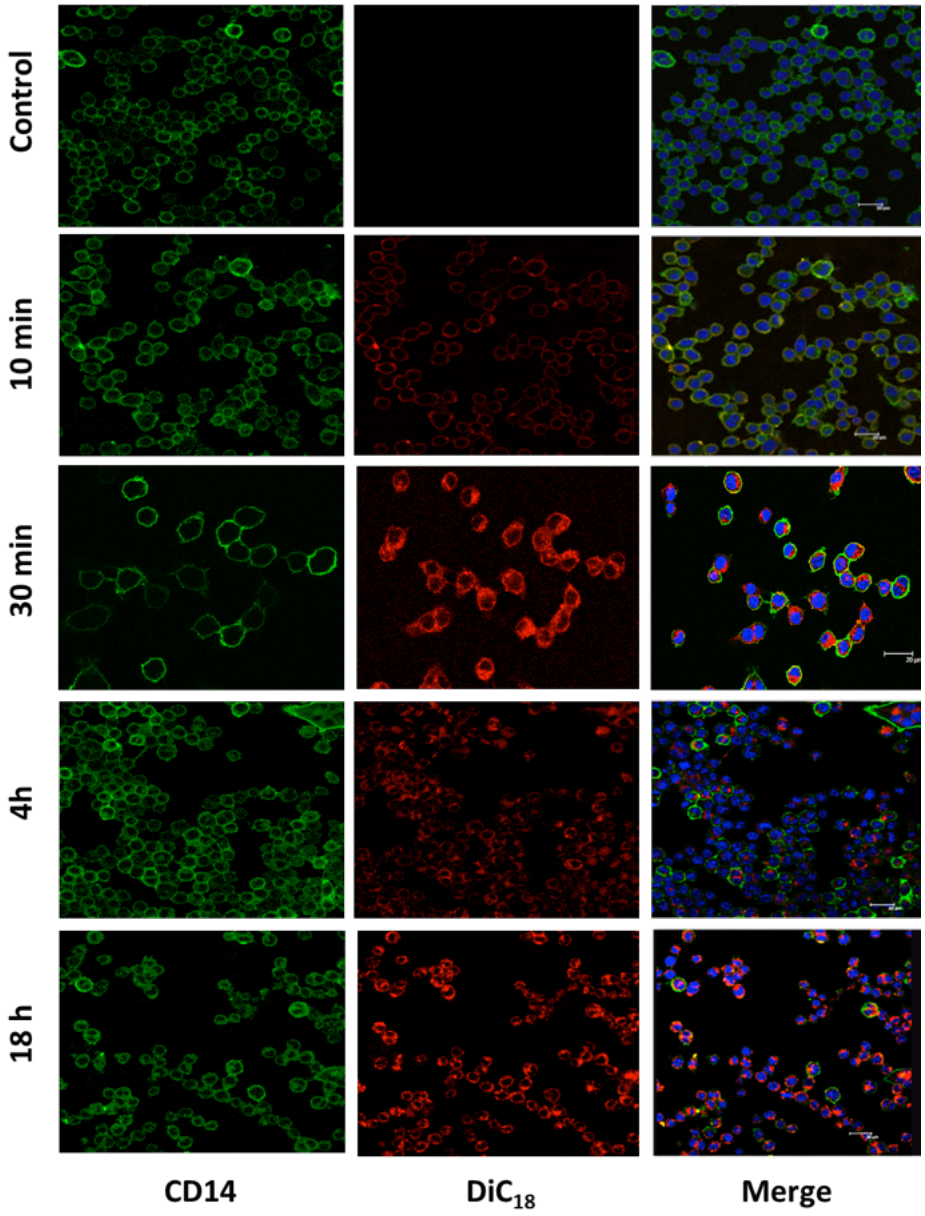

(legend continued on next page

Figure 4.1.3. Cardiolipin internalization by MH-S AMs. Images taken by confocal microscopy of MH-S cells incubated with CL SUVs (7nmol/ml) labeled with DiIC18 (in a 200:1 phospholipid: probe molar ratio) (in red) for 10 minutes to 18 hours, fixed, labeled with anti-CD14 antibody (in green) and stained with DAPI (1µg/ml) (in blue). After 10 minutes of incubation with CL, CL co-localized with CD14 at the cellular membrane. Nevertheless, note that after 30 minutes of incubation, CL SUVs were being endocytosed by the cells. CL endocytosis increased over time, being maximal at 18 hours.

4.1.3.3. Cardiolipin vesicles do not impair cell viability at the concentrations tested.

MH-S cells were incubated in the absence or presence of different doses of CL (7, 27 and 70 nmol/ml) for 24 hours. Cell viability was assessed by propidium iodide exclusion assay by flow citometry. We assessed that cell viability was not impaired at the concentrations of 7-70 nmol/ml of CL and these concentrations were used in the following experiments.

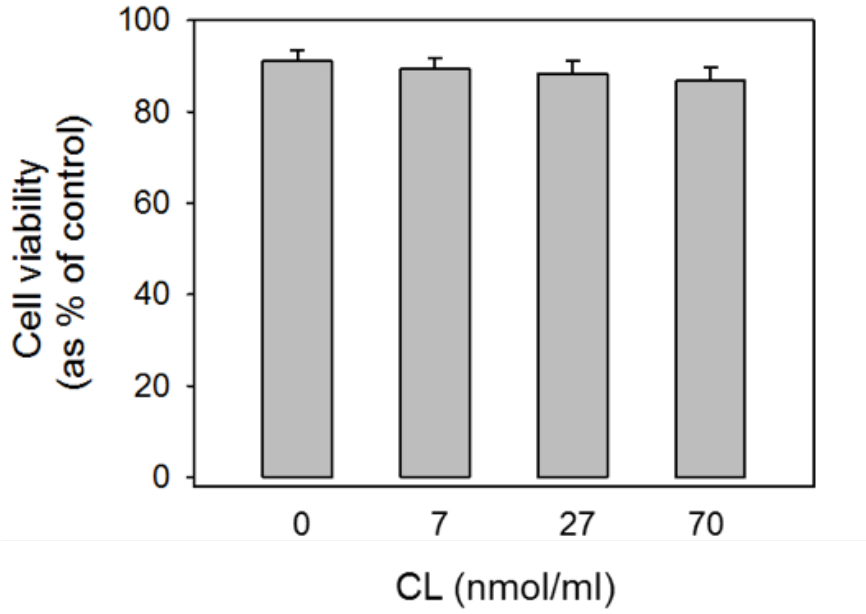

Figure 4.1.4. Cardiolipin vesicles do not affect viability of MH-S cells at 7-70 nmol/ml concentrations as determined by propidium iodide exclusion assay. Dose-dependent effect of CL vesicles on cell viability was evaluated after 24 hours of incubation with CL vesicles. Results are represented as means ± S.E from three different cell cultures with at least three biological replicates.

4.1.3.4. Cardiolipin inhibits LPS-elicited proinflammatory markers.

During Gram-negative sepsis, AMs produce large quantities of proinflammatory cytokines in response to LPS. One of the most important is TNF-α, that triggers an array of immune responses against invading pathogens [Lin and Yeh, 2005]. To examine whether extracellular, endocytosed CL vesicles or both, were capable of modulating the activation state of AMs stimulated with LPS, we first studied the effect of CL on LPS-induced TNF-α release. In Figure 4.1.5A, CL vesicles were co-administered with LPS to MH-S cells. In Figure 4.1.5B, cells were incubated in the absence or presence of different amounts of CL for 18h to ensure its endocytosis and then, cells were stimulated or not with bacterial LPS. As it is shown in Figure 4.1.5, basal TNF-α levels were almost undetectable, and were not affected by CL vesicles. Co-addition of CL vesicles with LPS (Figure 4.1.5A) as well as the preincubation with CL before the addition of LPS (Figure 4.1.5B), diminished LPS-induced TNF-α secretion by AMs in cell culture supernatants, in a dose-dependent manner.

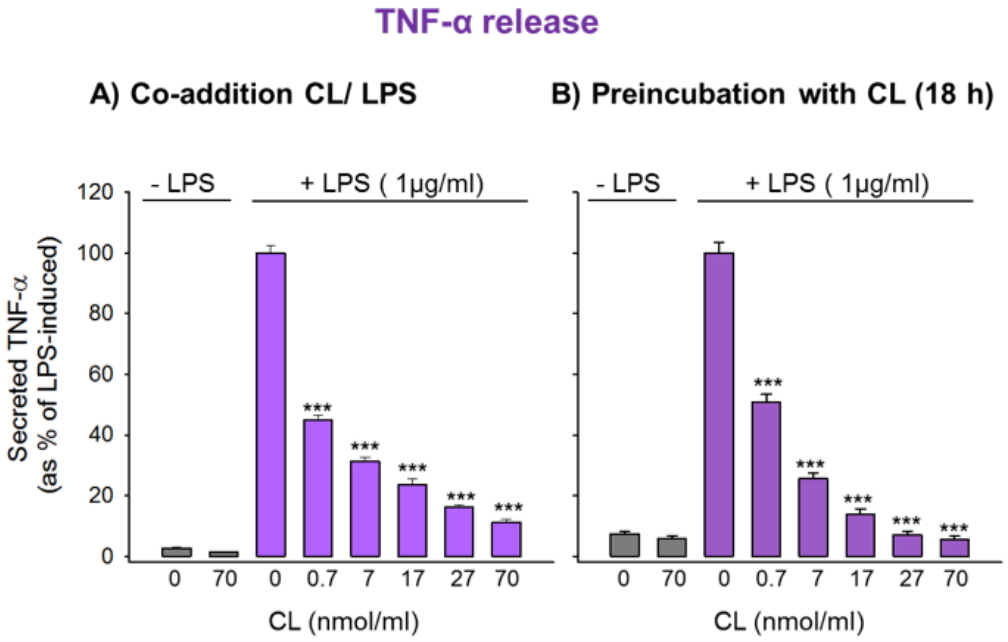

Figure 4.1.5. Low amounts of CL inhibited LPS-induced TNF-α release in a dose-dependent manner. LPS and CL were simultaneously added to MH-S cells (n=6) (A). MH-S cells were preincubated with CL for 18h and then, treated with LPS (1 µg/ml) for 6h (n=9) (B). TNF-α levels were measured by ELISA. Data are expressed as percentages of LPS-induced TNF-α release ± S.E in the absence of CL. Basal TNF-α secretion was 8 ± 1 pg/ml, and the average LPS-induced TNF-α secretion in the absence of CL was 483 ± 26 pg/ml (*** $p<0.001$ vs LPS).

The next step was to study whether CL vesicles were able to inhibit the production of another relevant proinflammatory marker, inducible nitric oxide synthase. The expression of this enzyme is activated in rodent macrophages in response to an appropriate stimulus such as LPS or proinflammatory cytokines. iNOS produce nitric oxide (NO) which contributes to pathogen killing [Jorens *et al.*, 1995]. We observed, as expected, that LPS increased iNOS protein levels. Concerning to the effect of CL, similarly to what we have observed for TNF-α, co-administration of CL vesicles and LPS (Figure 4.1.6A) or endocytosis of CL vesicles before LPS addition (Figure 4.1.6B), diminished iNOS protein expression induced by LPS in a dose-dependent manner. Nevertheless, we noticed that inhibitory effect of CL was less pronunciated when CL vesicles had been endocytosed. The co-administration of CL with LPS significantly reduced iNOS protein levels at lower concentrations of CL (≥ 0.07nmol/ml) than CL vesicles preincubated with cells before LPS addition, when a concentration of 7 nmol/ml was necessary to diminish iNOS production.

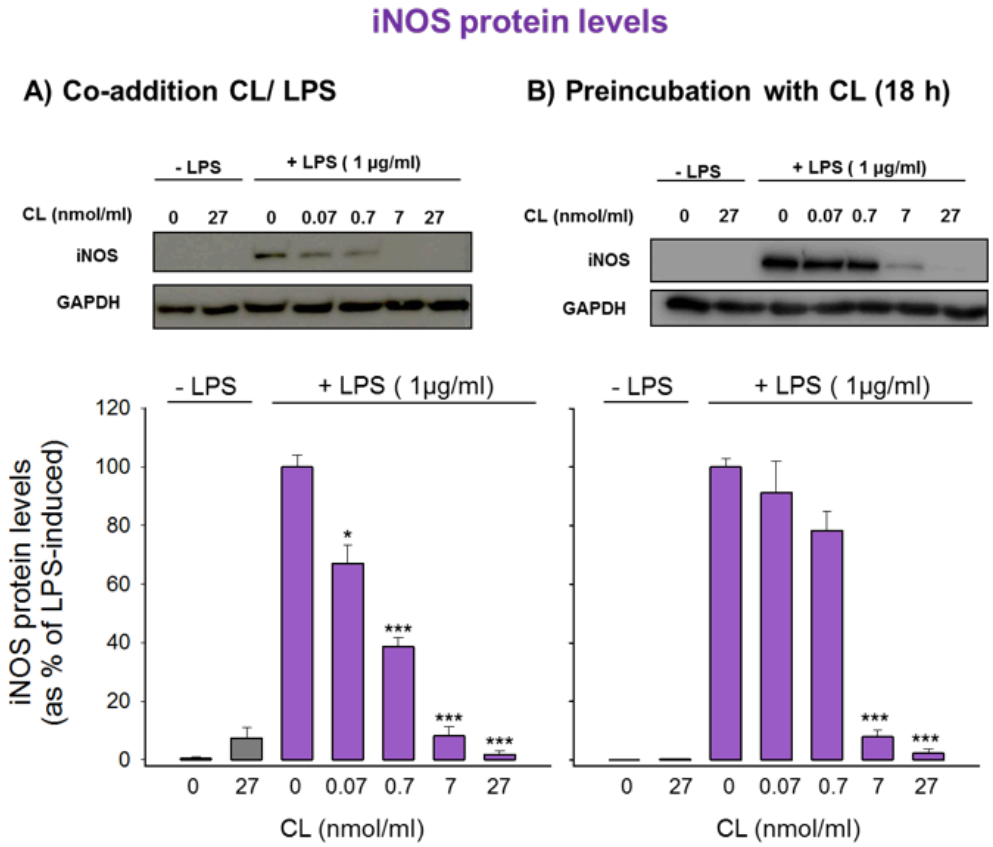

Figure 4.1.6. Low amounts of CL vesicles inhibited LPS-induced iNOS expression in a dose-dependent manner. LPS and CL were co-administered to MH-S cells and maintained at 37°C for 6h (n=6) (A). MH-S cells were preincubated with CL for 18h and subsequently, stimulated with LPS (1 µg/ml) and maintained at 37°C for 6h (n=9) (B). iNOS protein levels were measured by western-blot and quantified by densitometry. Data are expressed as percentages of LPS-induced iNOS protein levels ± S.E in the absence of CL. (*p<0.050; *** p<0.001 vs LPS).

We then investigated if CL vesicles were able to modify the expression of another LPS-induced proinflammatory genes. To that end, we studied by qPCR the mRNA expression of nitric oxide synthase 2 (NOS2), cyclo-oxygenase 2 (COX2), C-X-C motif chemokine 10 (CXCL10), interleukin 1 beta (IL1-β) and TNF-α in MH-S AMs. CL and LPS were co-administered to the cells or incubated with CL for 18 hours before the stimulation with LPS.

All these proteins encoded by these genes are important mediators of the inflammatory response. NOS2 is the gene that encodes iNOS protein, which is the responsible of NO production, as described above [Jorens *et al.*, 1995]. COX-2 is the enzyme responsible of the synthesis of the proinflammatory mediators called prostaglandins. COX2 is expressed at very low levels in basal conditions and strongly induced by proinflammatory stimuli such as LPS [Barrios-Rodiles *et al.*, 1999]. CXCL10 is a chemokine that plays an important role in the recruitment of immune cells to the site of inflammation [Liu *et al.*, 2011]. IL1-β and TNF-α are proinflammatory cytokines commonly produced by LPS-activated macrophages [Meng and Lowell, 1997].

As we can observe in Figures 4.1.7 to 4.1.11, LPS-elicited the expression of all these proinflammatory genes in MH-S AMs after 1 hour of treatment. Basal mRNA production was not affected by CL vesicles. Nevertheless, we demonstrated that CL vesicles in both cases (co-addition with LPS or incubation previous to LPS addition) diminished the mRNA expression of these proteins after LPS exposure. Interestingly, in this case, the inhibitory effect of CL vesicles was greater when they had been endocytosed by AMs before LPS treatment.

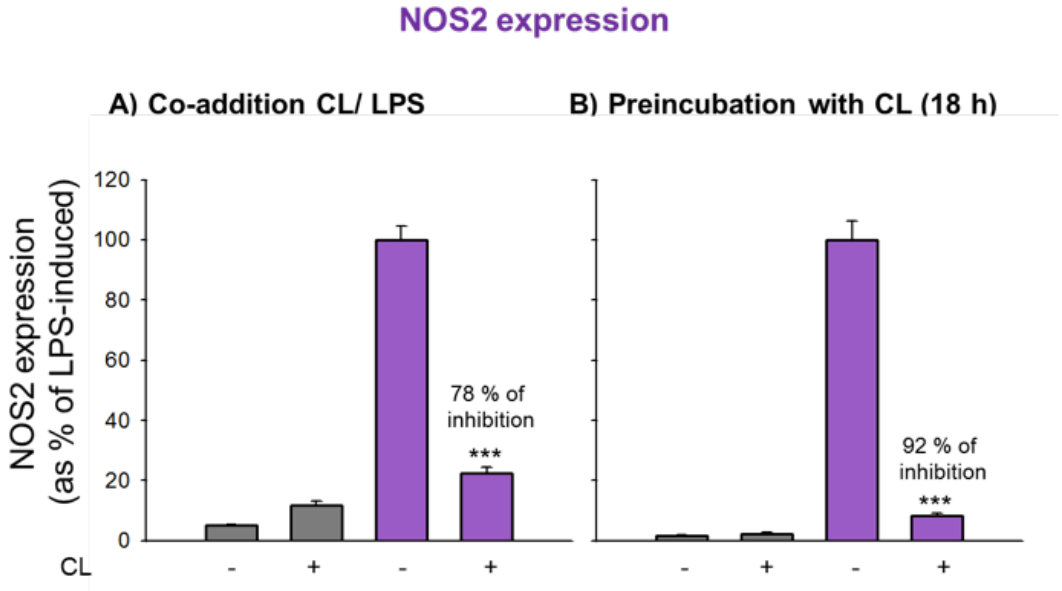

(legend continued on next page

Figure 4.1.7. CL vesicles (7nmol/ml) reduced LPS-induced NOS2 mRNA expression in MH-S AMs. LPS and CL vesicles were co-administered to MH-S cells (A) or cells were incubated with CL (18h) before LPS exposure (B). NOS2 mRNA levels were detected by q-PCR and normalized to GAPDH levels. Data are expressed as percentages of LPS-induced NOS2 expression ± S.E in the absence of CL. (*** p<0.001 vs LPS).

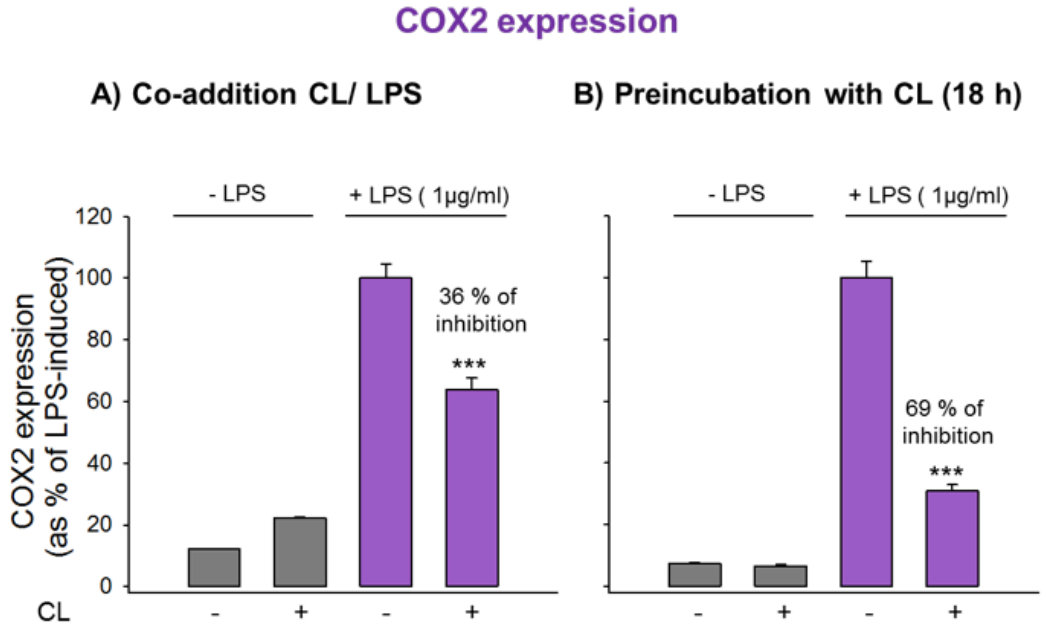

Figure 4.1.8. CL vesicles (7nmol/ml) reduced LPS-induced COX2 mRNA expression in MH-S AMs. LPS and CL vesicles were co-administered to MH-S cells (A) or cells were incubated with CL (18h) before LPS exposure (B). COX2 mRNA levels were detected by q-PCR and normalized to GAPDH levels. Data are expressed as percentages of LPS-induced COX2 expression ± S.E in the absence of CL. (*** p<0.001 vs LPS).

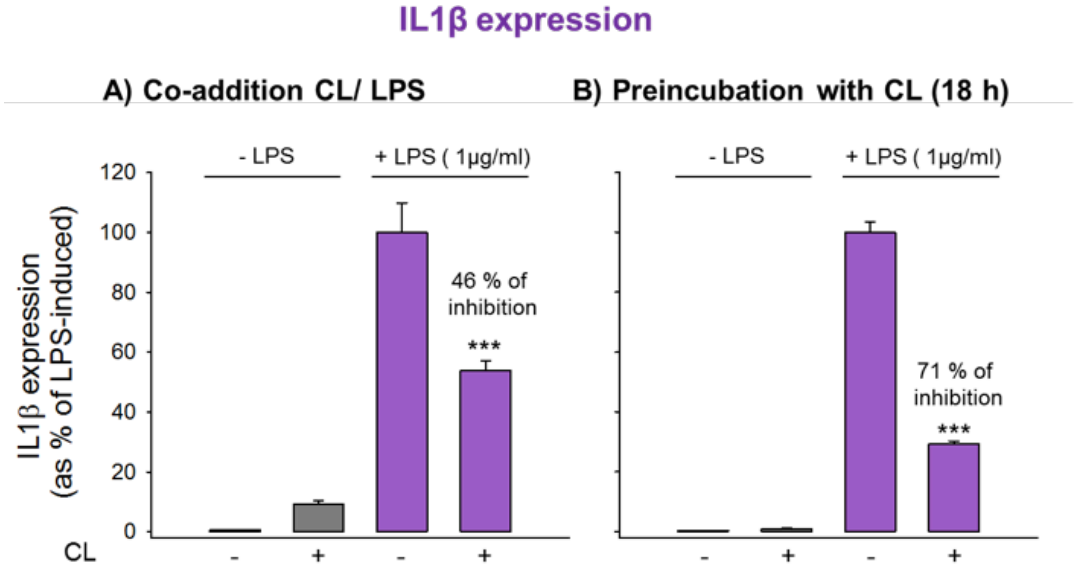

(legend continued on next page

Figure 4.1.9. CL vesicles (7nmol/ml) reduced LPS-induced IL1-β mRNA expression in MH-S AMs. LPS and CL vesicles were co-administered to MH-S cells (A) or cells were incubated with CL (18h) before LPS exposure (B). IL1-α mRNA levels were detected by q-PCR and normalized to GAPDH levels. Data are expressed as percentages of LPS-induced IL1-β expression ± S.E in the absence of CL. (*** p<0.001 vs LPS)

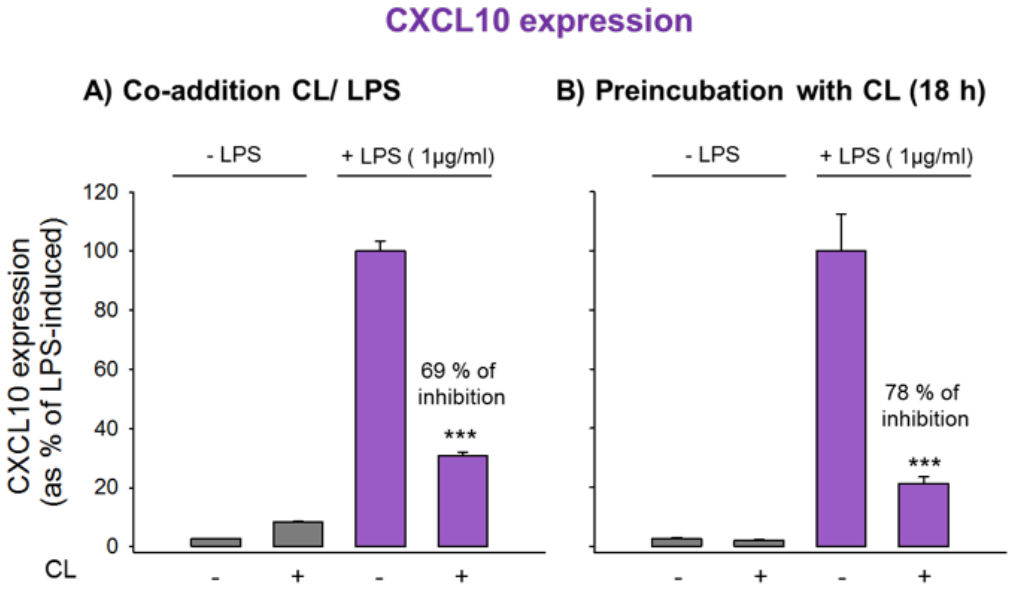

Figure 4.1.10. CL vesicles (7nmol/ml) reduced LPS-induced CXCL10 mRNA expression in in MH-S AMs. LPS and CL vesicles were co-administered to MH-S cells (A) or cells were incubated with CL (18h) before LPS exposure (B). CXCL10 mRNA levels were detected by q-PCR and normalized to GAPDH levels. Data are expressed as percentages of LPS-induced CXCL10 expression ± S.E in the absence of CL. (*** p<0.001 vs LPS).

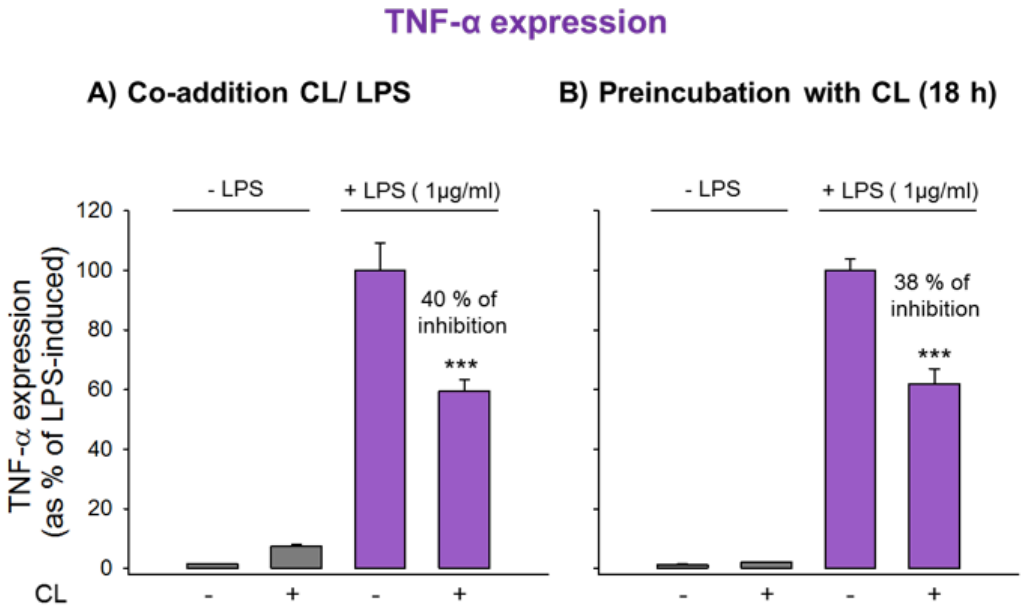

(legend continued on next page

Figure 4.1.11. CL vesicles (7nmol/ml) reduced LPS-induced TNF-α mRNA expression in MH-S AMs. LPS and CL vesicles were co-administered to MH-S cells (A) or cells were incubated with CL (18h) before LPS exposure (B). TNF-α mRNA levels were detected by q-PCR and normalized to GAPDH levels. Data are expressed as percentages of LPS-induced TNF-α expression ± S.E in the absence of CL. (*** $p<0.001$ vs LPS).

4.1.3.5. Cardiolipin inhibits LPS-elicited signaling pathways

LPS recognition by TLR4 elicits signal transduction pathways that leads to the transcription of genes encoding several proinflammatory mediators such as those that we have studied above (NOS2, COX2, TNF-α, IL1-β and CXCL10). Several studies have identified signal transduction pathways that are activated by LPS, including activation of NF-kB and activation of MAPKs, including Erk, c-Jun N-terminal kinase and p38 [Medzhitov and Janeway, 2000].

Therefore, we next investigated the influence of CL in signaling pathways triggered by LPS. In experiments shown in Figures 4.1.12A, 4.1.13A and 4.1.14A, CL and LPS were co-administered to the cells. In Figures 4.1.12B, 4.1.13B and 4.1.14B, AMs were incubated 18h in the absence or presence of increasing doses of CL vesicles and were then stimulated with LPS. Then, cell lysates were electrophoresed and immunoblotted. After 10 (Akt and MAPKs) or 30 (ikB-α) minutes of the addition of LPS, we could appreciate an increment of the

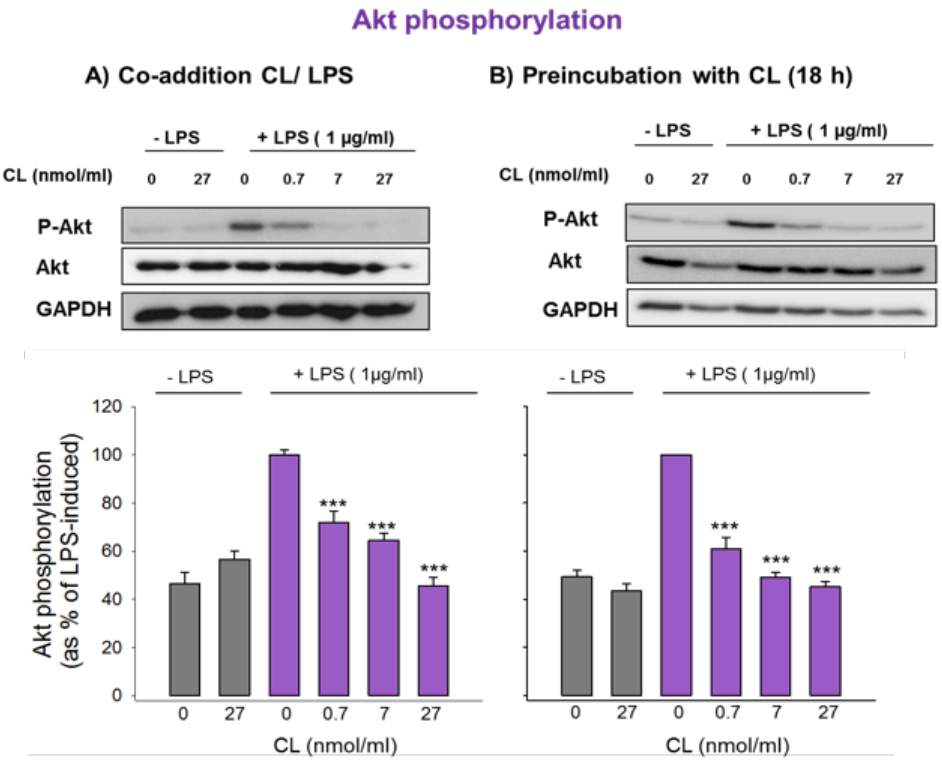

(legend continued on next page

Figure 4.1.12. Low amounts of CL inhibit LPS-elicited Akt phosphorylation in a dose-dependent manner. MH-S cells were stimulated with LPS for 10 minutes in the presence and absence of extracellular (n=18) (A) or endocytosed CL (n=12) (B). Phosphorylated Akt was detected by western blot, quantified by densitometry and normalized to total Akt. LPS-induced Akt phosphorylation in the absence of CL was considered as 100%. Data are expressed as mean percentages ± S.E. (***p<0.001 vs LPS).

Phosphorylated forms of the proteins Akt (Figure 4.1.12), Erk (Figure 4.1.13), p38 (Figure 4.1.14) and ikB-α, which is a NF-kB inhibitor, and whose phosphorylation promotes its proteasome degradation, activating NF-kB (Figure 4.1.15). As it is shown in Figures 4.1.7 to 4.1.10, CL reduced LPS-elicited phosphorylation of all these proteins. Thus, these results agreed with the reduction that we have observed in the expression of the proinflammatory mediators studied above.

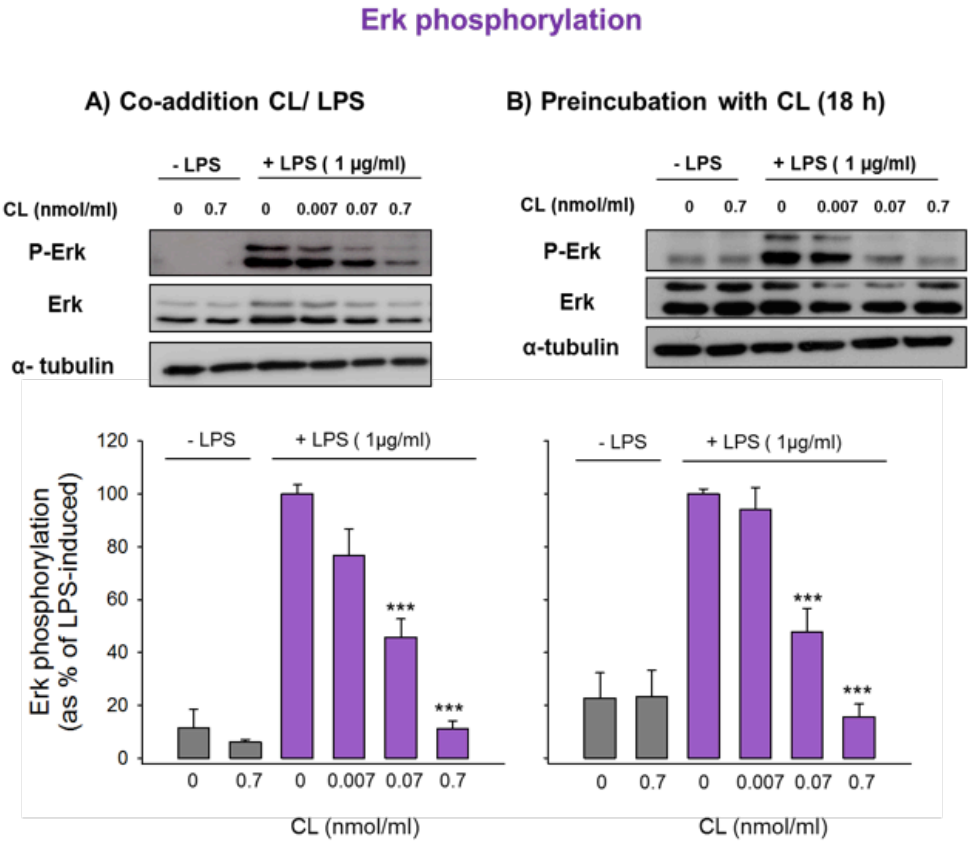

Figure 4.1.13. Low amounts of CL vesicles inhibited LPS-elicited Erk phosphorylation in a dose-dependent manner. MH-S cells were stimulated with LPS for 10 minutes in the absence or presence of extracellular (n=8) (A) or endocytosed (n=8) CL vesicles (B). Phosphorylated Erk was detected by western blot, quantified by densitometry and normalized to total Erk. LPS-induced phosphorylation in the absence of CL was set at 100%. Data are expressed as mean percentages ± S.E. (**p<0.001 vs LPS).

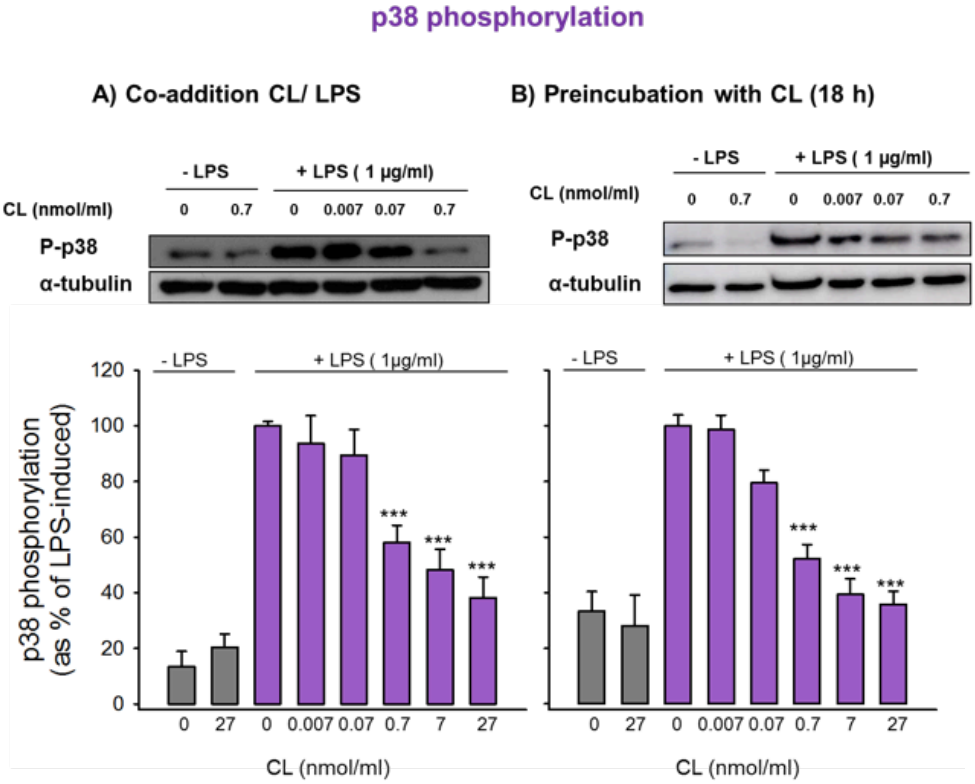

Figure 4.1.14. Low amounts of CL vesicles inhibited LPS-elicited p38 phosphorylation in a dose-dependent manner. MH-S cells were stimulated with LPS for 10 minutes in the absence or presence of extracellular (n=9) (A) or endocytosed (n=8) (B) CL. Phosphorylated p38 was detected by western blot and quantified by densitometry. LPS-induced p38 phosphorylation in the absence of CL was set at 100%. Data are expressed as mean percentages ± S.E. (***p<0.001 vs LPS).

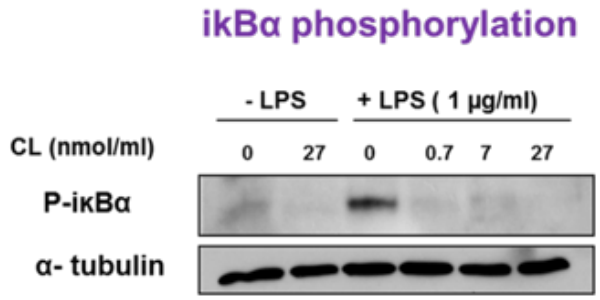

Figure 4.1.15. Cardiolipin inhibited LPS-induced IκBα phosphorylation. MH-S cells were preincubated with different amounts of CL vesicles for 18h and then, stimulated or not with LPS (1µg/ml) for 30 minutes. After that time, cells were lysed and cellular lysates were analyzed by western-blot. One representative experiment is shown.

4.1.3.6. Cardiolipin inhibits LPS-elicited signaling in primary rat alveolar macrophages.

To verify that the anti-inflammatory action of CL was not specific of the cell line MH-S, we conducted some experiments using AMs isolated from the lungs of male Sprague-Dawley rats. Vesicles of CL and LPS (1µg/ml) were co-administered to rat AMs. We obtained similar results to those obtained with MH-S macrophages. In Figure 4.1.16, we could observe that LPS-elicited Akt and Erk phosphorylation were strongly diminished in the presence of increasing amounts of CL vesicles (≥ 0.7nmol/ml). Thus, this allow us to conclude that the anti-inflammatory action of CL is not restricted to the MH-S cell line.

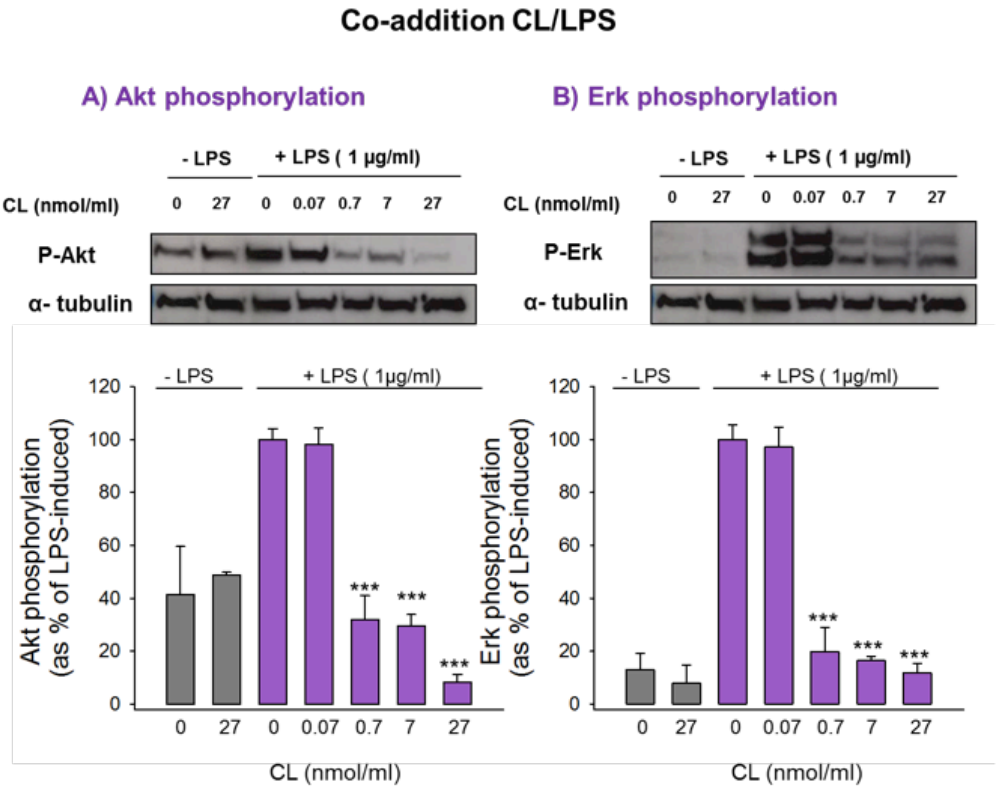

Figure 4.1.16. Cardiolipin inhibits LPS-induced signaling in primary rat AMs. Rat alveolar macrophages were stimulated with LPS (1µg/ml) in the absence or presence of the indicated doses of CL vesicles. Akt (A) and Erk (B) phosphorylation levels were detected by western-blot. LPS-induced phosphorylation in the absence of CL was set at 100%. Data are expressed as mean percentages ± S.E. (n=3) (*** $p<0.001$ vs LPS).

4.1.3.7. Cardiolipin immunomodulatory effect is not restricted to the LPS response.

In order to elucidate whether the immunomodulatory effect of CL was specific or

not of the LPS-elicited inflammatory response through TLR4 receptor, we decided to investigate the anti-inflammatory action of CL in zymosan-stimulated MH-S AMs. Zymosan is an insoluble preparation of *Saccharomyces cerevisiae* cell wall which is known to activate macrophages via TLR2. TLR2 cooperates with TLR6 and CD14 to orchestrate the innate immune response against zymosan [Ozinsky *et al.*, 2000]. Zymosan is also recognized by Dectin-1, a phagocytic receptor expressed on macrophages and dendritic cells, which collaborates with TLR2 and TLR6 enhancing the immune responses triggered by the recognition of zymosan by each receptor [Gantner *et al.*, 2003].

With the aim of analyzing the effect of CL on zymosan-stimulated MH-S AMs, we incubated the cells in the absence or presence of increasing doses of CL vesicles for 18 hours. Then, cells were washed and fresh culture medium was added. AMs were stimulated or not with zymosan (50µg/ml) for 6h to determine production of proinflammatory markers (TNF-α secretion and iNOS protein levels).

As we could appreciate in Figure 4.1.17, the preincubation of the cells with vesicles of CL before stimulation with zymosan, reduced zymosan-induced production of TNF-α and iNOS.

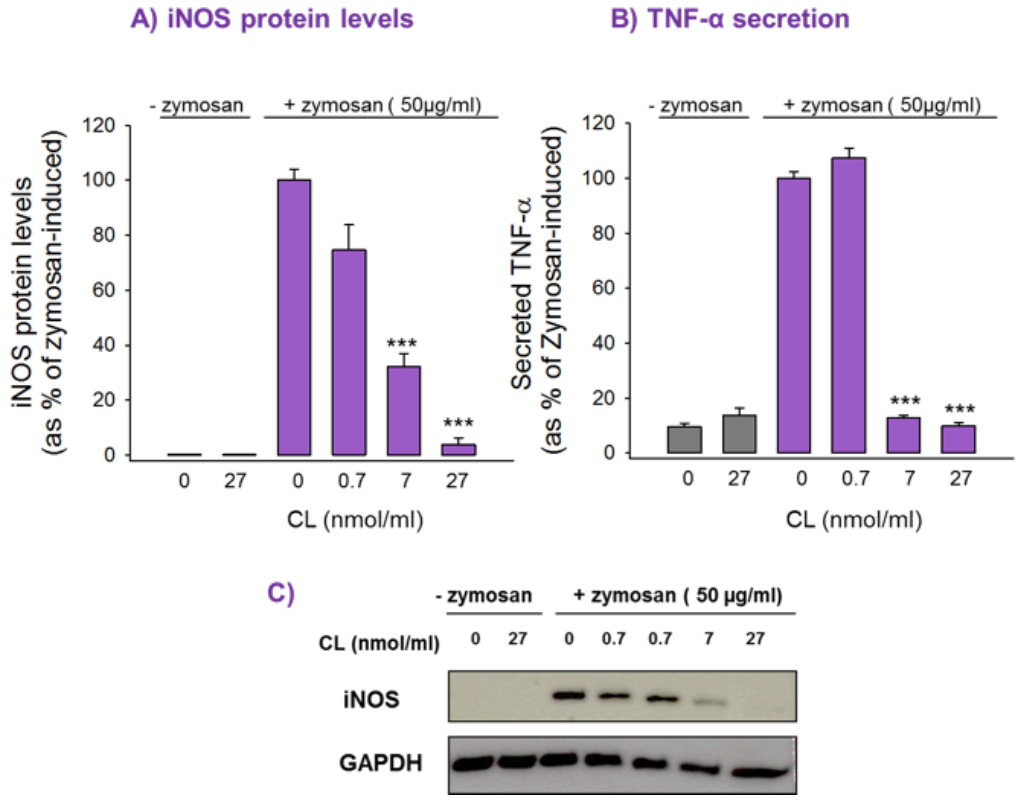

(legend continued on next page

Figure 4.1.17. Endocytosis of cardiolipin vesicles inhibited TNF-α release and iNOS protein expression. MH-S cells were preincubated with CL at the indicated concentrations for 18h. After that time, cells were stimulated with zymosan (50μg/ml) for 6h (A, B). iNOS protein levels were detected by western blot, quantified by densitometry and normalized to GAPDH levels (n=4) (A). TNF-α levels in culture supernatants were assessed by ELISA (n=4) (B). Data are expressed as mean percentages of iNOS protein levels (A) or zymosan-induced TNF-α release (B) ± SE. One representative image of iNOS is shown (C). (***p<0.001 vs zymosan).

We then analyzed the effect of CL vesicles on zymosan-elicited Erk phosphorylation. CL and zymosan were co-administered to AMs (Figure 4.1.18A) and alternatively CL for 18 hours before zymosan addition (Figure 4.1.18B). As it is shown in Figure 4.1.18, in MH-S cells, stimulation with zymosan (50μg/ml) for 10 minutes led to a significant increase in Erk phosphorylation levels, whereas the presence of CL vesicles reduced their phosphorylation.

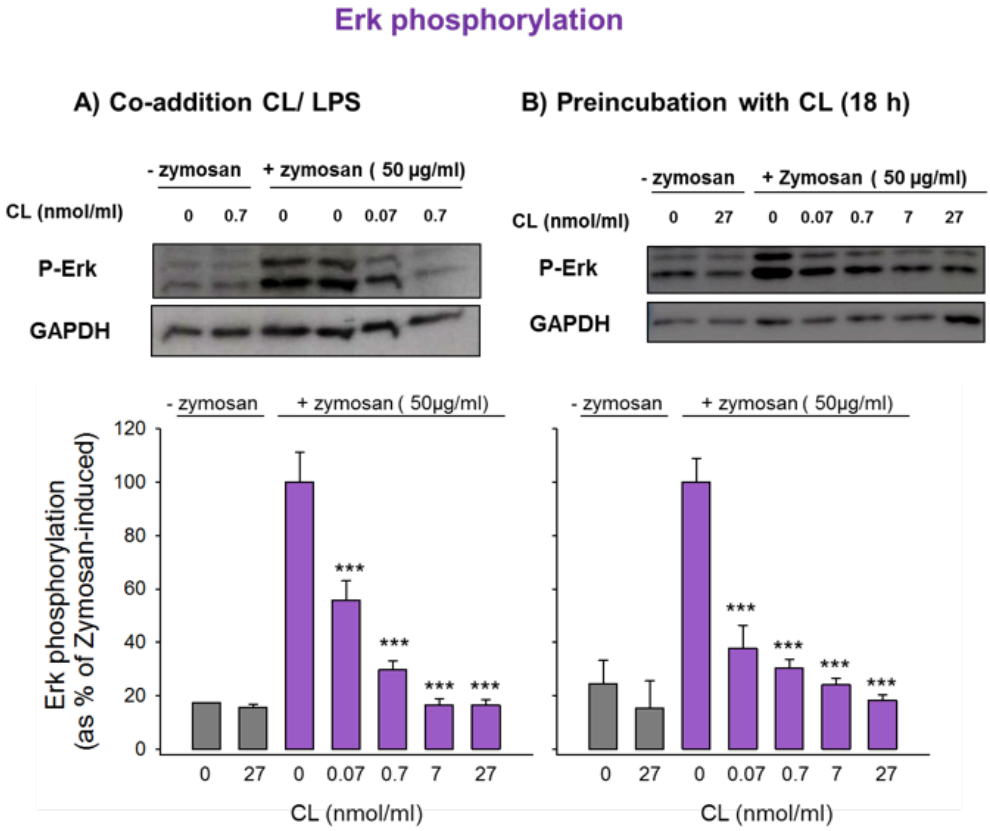

Figure 4.1.18. CL vesicles reduced zymosan-induced Erk-phosphorylation in a dose-dependent manner in MH-S AMs. Zymosan and CL vesicles were simultaneously added to MH-S cells (A) or incubated with CL (18h) before zymosan addition (B). Erk phosphorylation was detected by western-blot after ten minutes of zymosan exposure. Zymosan-induced phosphorylation in the absence of CL was set at 100%. Data are expressed as mean percentages ± S.E. (n=3). (*p< 0.050,*** p< 0.001 vs zymosan).

We next studied CL effect on zymosan-induced Akt phosphorylation. CL was added to AMs simultaneously to zymosan (50µg/ml). As we could appreciate in Figure 4.1.19, CL inhibited zymosan-elicited Akt phosphorylation.

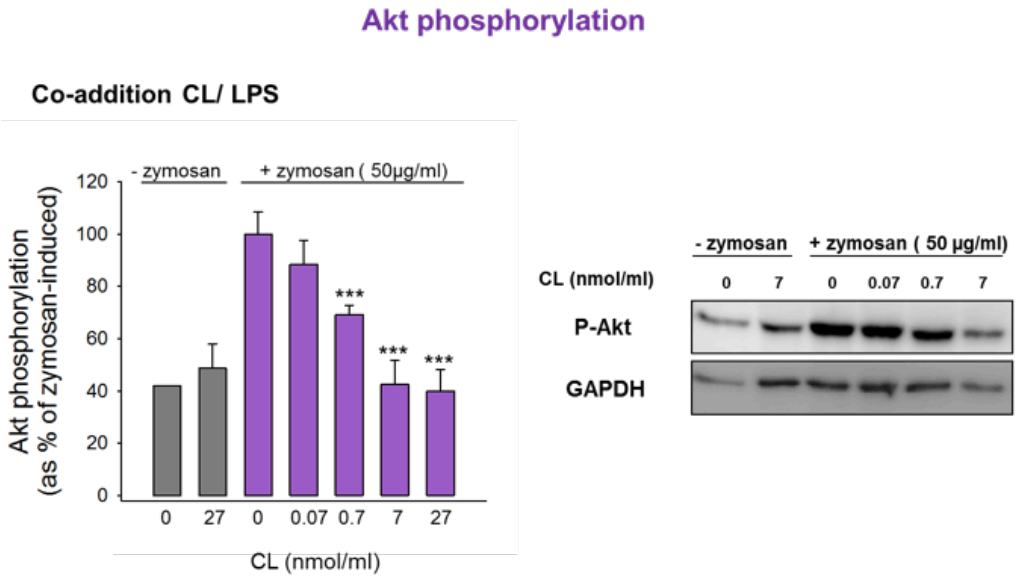

Figure 4.1.19. Low amounts of CL vesicles inhibited zymosan-elicited Akt phosphorylation. CL vesicles were added to MH-S cells simultaneously to zymosan (50 µg/ml). Akt phosphorylation was detected by western-blot after ten minutes of zymosan exposure. Zymosan-induced phosphorylation in the absence of CL was set at 100%. Data are expressed as mean percentages ± SE, (n=3). (***p<0.001 vs zymosan).

Altogether, the results described in section 4.1.3.7, allow us to conclude that CL vesicles were able to inhibit zymosan-elicited innate immune response in AMs as it happened when LPS is used as stimulus. Therefore, the anti-inflammatory action of CL vesicles is not specific of a particular proinflammatory stimulus (LPS), suggesting that CL could act as a potential broad spectrum treatment to counteract inflammatory processes caused by bacterial and fungal pathogens.

4.1.4. DISCUSSION

In the present part of results, we examined the anti-inflammatory effect of low amounts of CL on the activation state of MH-S AMs stimulated with LPS or zymosan. We have studied the immunomodulatory action of CL by two different experimental approaches: CL was co-administered with the proinflammatory stimuli or preincubated with AMs for 18 hours before stimulation in order to allow CL endocytosis.

First, we conducted confocal microscopy experiments to determine whether AMs could endocyte the CL vesicles obtained after sonication which present a hydrodynamic diameter of 50 nm (Figure 4.1.2). In Figure 4.1.3, we could appreciate that the endocytosis process began almost 30 minutes after the addition of CL SUVs and increased with preincubation time, being maximal at 18 hours (Figure 4.1.3). This result is consistent with previous information about CL internalization by alveolar cells. In this line, Ray and co-workers cultured mouse type II lung epithelial cells in the presence of CL for 2 hours and they found that these cells are able to internalize CL through the P-type ATPase transmembrane lipid pump, ATP8B1. ATP8B1 binds and internalizes CL from extracellular fluid employing a basic residue-enriched motive [Ray *et al.*, 2010]. Interestingly, it has been described in several cellular models [mouse peritoneal macrophages RAW 264.7, human monocytes THP1 treated with phorbol 12-myristate 13-acetate, primary human monocyte derived macrophages and mouse peritoneal macrophages] that internalization of liposomes composed of CL and dioleoylphosphatidylcholine (DOPC) occurs through phagocytosis after 1 hour of incubation. Otherwise, they proved that RAW 264.7 cells engulfed two- to fourfold more CL-presenting mitochondria than control mitochondria. They found that the enhanced phagocytosis in the presence of CL was dependent on a member of the subclass B of scavenger receptors, CD36 [Balasubramanian *et al.*, 2015].

Either, when CL was co-administered with or preincubated with cells 18 hours before LPS-driven stimulation, CL was proved to block LPS-induced signaling pathways (PI3K, MAPK, NF-κB) as it inhibited phosphorylation of Akt (Figure 4.1.12), Erk (Figure 4.1.13), p38 (Figure 4.1.14) and IκB-α phosphorylation (Figure 4.1.15). Moreover, CL was also effective in attenuating LPS-induced TNF-α release (Figure 4.1.5) and TNF-α mRNA expression (Figure 4.1.11) as well as iNOS protein levels (Figure 4.1.6) and its mRNA expression (Figure 4.1.7). Finally, CL was able to diminish the mRNA expression of several proinflammatory markers induced by LPS such as COX2 (Figure 4.1.8), IL1-β (Figure 4.1.9) and CXCL10 (Figure 4.1.10) in MH-S AMs. This strong immunomodulatory action of CL was not restricted to a single cell type, since the addition of CL vesicles simultaneously to LPS was also capable of attenuating ERK and Akt phosphorylation in rat primary AMs (Figure 4.1.16).

We also have also demonstrated that CL vesicles (co-administered or preincubated for 18 hours), inhibited zymosan-induced Akt (Figure 4.1.19) and Erk phosphorylation (Figure 4.1.18A). Internalized CL vesicles diminished Erk phosphorylation (Figure 4.1.18B), iNOS protein levels and TNF-α secretion elicited by zymosan (Figure 4.1.17). These results provide evidence that CL is also capable of modulating innate immune responses triggered by proinflammatory stimuli distinct to LPS and

mediated by different types of TLR.

The mechanism underlying the anti-inflammatory action of CL is unknown and subject of ongoing research. We hypothesize that in the extracellular medium, CL could bind to and block one or more receptors involved in the cellular response to LPS or zymosan. Intracellular immunomodulatory effect is assured because AMs were preincubated with CL for 18h to ensure CL endocytosis. After preincubation, cells were washed. Then, fresh medium was added and cells were stimulated. Thus, intracellularly, we hypothesize that CL modifies the expression of cellular receptors involved in AMs response to the proinflammatory stimuli cited above, promotes the endocytosis of TLR4 and/or TLR2 receptors or its accessory molecules or maybe disrupts lipids rafts, that were found to be essential for LPS-signaling [Olsson and Sundler, 2006]. It is likely to be involved more than one of the proposed mechanisms.

In the literature there are few data about the role of CL on the immune response. Nevertheless, Balasubramanian and co-workers, according to our results, reported that CL attenuates inflammatory response in macrophages stimulated with LPS. However, they described that CL action occurs exclusively through an extracellular mechanism.

The binding of LPS to MD-2 at the cell surface is necessary for TLR4 activation [Park *et al.*, 2009]. Therefore, due to the similar molecular structure of CL and the lipid A of LPS, Balasubramanian and co-workers decided to carry out competitive binding experiments. They proved that CL, but not phosphatidylcholine or phosphatidylserine, was capable of inhibiting LPS binding to MD-2 [Balasubramanian *et al.*, 2015].

Thus, according to the experiments cited above, these investigators ruled out that the anti-inflammatory effect of CL would occur at the intracellular level.

LPS-binding protein is required for LPS recognition by AMs. In this way, LBP monomerizes LPS and transfers LPS molecules to CD14 [Wright *et al.*, 1990, Tobias *et al.*, 1993].

Mueller and co-workers reported that LBP binds CL, thereby blocking LPS-binding site [Mueller *et al.*, 2005]. These authors previously found that a synthetic compound structurally related to lipid A and CL, failed to induce an inflammatory response on immune cells but it possessed a strong antagonistic activity against the LPS

response. Furthermore, they found that the addition of CL to the cells 15 minutes before LPS exposure, potently inhibited TNF-α secretion by human mononuclear cells and macrophages *in vitro*. This time of preincubation is short and most of the CL vesicles were probably outside the cells, as we have determined by confocal microscopy for the cells we used (Figure 4.1.3). This finding is consistent with our results, in which we observed that the co-administration of CL with LPS reduced LPS-elicited inflammation. These investigators postulated that CL binds to LBP and compete with LPS for the same binding site inhibiting LPS-elicited inflammatory response. The proposed mechanism is reasonable because the LPS-binding region of LBP contains several positive charged amino acids [Lamping *et al.*, 1996], which are a good target for anionic phospholipids such as CL.

According to the action mechanism proposed by Mueller and colleagues for CL, Bochkov and co-workers showed that 1-palmytoil-2-arachnidonoyil-sn-glycerol-3-phosphorylcholine oxidation products (oxPAPC), phospholipid that is not found in healthy humans and is produced only at the sites of inflammation, inhibits LPS signaling by blocking the binding of LPS to LBP and CD14 in endothelial cells. In addition, they demonstrated that oxPAPC is capable of protecting mice challenged with a lethal dose of LPS [Bochkov *et al.*, 2002]. We further proved the effect of CL vesicles once endocytosed by AMs. Under such circumstances, it was not possible that CL competes with LPS for LBP on AMs surface because CL vesicles were inside the cells.

Taking into account the information obtained from our experiments, we cannot assume that CL inhibitory action is based exclusively on the CL-LBP interaction because we have also stimulated AMs with zymosan, a TLR2 ligand independent of LBP to trigger the inflammatory response and we have found that CL inhibited inflammation.

Given that the integrity of lipid rafts is a requisite for the activation of the LPS-response [Triantafilou *et al.*, 2002, Finberg and Kurt-Jones, 2006; Ruysschaert *et al.*, 2015], we hypothesize that CL could bind to CD14 as described for POPG [Kuronuma *et al.* 2009], impairing the recruitment directed by CD14 of TLR4 and/or TLR2 and/or its associated molecules into lipid rafts [Finberg and Kurt-Jones, 2006; Ruysschaert *et al.*, 2015]. Thus, this could be another possible mechanism involved in the anti-inflammatory effect of CL.

Previous studies demonstrated the immunomodulatory action of POPG, an anionic phospholipid present in the composition of pulmonary surfactant. POPG has been

demonstrated to bind to CD14 and MD-2 thus inhibiting LPS-elicited NO and TNF-α production from rat and human AMs and U937 cells [Kuronuma *et al.*, 2009]. POPG impairs LPS response by disrupting LBP-CD14 function [Hashimoto *et al.*, 2003]. In addition, POPG inhibits the production of inflammatory mediators triggered by TLR2 activation by *Micoplasma pneumoniae* [Kandasamy *et al.*, 2011]. As CL is another anionic phospholipid, it might be blocking TLR4 and TLR2 responses through similar mechanisms of those described for POPG. However, our work describes a strong immunomodulatory action of CL that occurs to a much lower relation phospholipid: LPS to that described for POPG [Hashimoto *et al.*, 2003; Kuronuma *et al.*, 2009].

Interestingly, Hashimoto and co-workers found that the acyl chain structure of phospholipids was determinant for a phospholipid to present or not anti-inflammatory properties on LPS-elicited response. Thus, they studied the anti-inflammatory effect of different molecular species of phosphatidylglycerol on NF-κB activation using murine bone marrow immortalized cells expressing TLR4 and MD-2. DPPG did not show an inhibitory effect, while POPG and DOPG did. Thus, they concluded that the presence of unsaturated bonds on the acyl chain structure is mandatory for a phospholipid to display anti-inflammatory action. The transfer of a phospholipid to LBP or CD14 from fluid phospholipid vesicles occurs more readily than the transference from those with a lower degree of fluidity. CL vesicles as well as POPG and DOPG vesicles are very fluid and we propose that this could be an additional reason to justify their strong anti-inflammatory properties [Hashimoto *et al.*, 2003].

Balasubramanian and co-workers discarded an intracellular immunomodulatory action of CL. They studied CL internalization in wild type primary and knockout mouse peritoneal macrophages for CD36. They observed that in CD36-deficient cells, CL internalization was minimal referred to wild type cells. Interestingly, CL inhibited LPS-elicited production of cytokines in wild type and CD36-deficient cells. This suggests that CD36 and CD36-mediated internalization are not required for CL anti-inflammatory action [Balasubramanian *et al.*, 2015]. Nevertheless, in our experiments to study the intracellular action of CL, AMs were incubated in the presence or absence of CL for 18 hours and then, the culture medium was removed. After washing and adding fresh culture medium, cells were stimulated with LPS or zymosan. We observed the inhibitory action of CL at very low amounts of phospholipid (≤ 0.07 nmol/ml). Therefore, we suggest that the small amount of CL internalized in CD36-deficient cells [Balasubramanian *et al.*, 2015], could be enough for CL to exert its intracellular anti-inflammatory action.

On the other hand, as we cited above, Ray and co-workers demonstrated that ATP8B1 is a CL import protein which regulates CL levels in the lung fluid. Therefore,

ATP8B1 could be another receptor mediating CL internalization. Nevertheless, they performed their experiments using AECs, in which ATP8B1 expression is higher compared to macrophages or fibroblasts [Ray *et al.*, 2010].

Recently, it has been described that P4-ATPases, among which it is found ATP8B1, attenuate LPS-induced TLR4 signaling by mediating endocytic retrieval of TLR4 [van der Mark *et al.*, 2017]. P4-ATPases are integral membrane proteins which translocate phospholipids from the exoplasmic leaflet to the cytoplasmic leaflet to create phospholipid asymmetry [Sebastian *et al.*, 2012] and to initiate the biogenesis of transport vesicles [Sebastian *et al.*, 2012; van der Mark *et al.*, 2013; Lopez-Marques *et al.*, 2014]. These proteins function as a heterodimer with a member of CDC50 family (β-subunit) and the P4-ATPase (α-subunit) [Katoh Y and Katoh M, 2004; van der Mark *et al.*, 2013].

When LPS bind to TLR4 receptor complex on the cell surface, induces an early response dependent on MyD88 that results in the production of proinflammatory cytokines (TNF-α, IL-1β and IL-6) [Lee *et al.*, 2012]. Consequently, TLR4 is internalized and signals from the endosomal compartment in a MyD88-independent manner. This develops type I IFN response, which dampens the inflammatory reaction and is critical to counteract an ongoing infection [Kagan *et al.*, 2008; Zanoni *et al.*, 2011]. These investigators found that depletion of CDC50A in THP1 cells leads to a hyperactivation of the early LPS response as demonstrated by high levels of TNF-α, IL-1β and IL-6 release, increased MAPK signaling and sustained NFκB-activation. On the other hand, they observed that in CDC50A-depleted cells TLR4 internalization is impaired, leading to a defective IFN response. Similar results were obtained when they used depleted cells of P4-ATPases ATP8B1 and ATP11A [van der Mark *et al.* 2017].

CDC50A was detected in intracellular vesicles whereas ATP8B1 and ATP11A are mainly located in the plasma membrane of THP1 cells. The preferred substrate of these P4-ATPases is phosphatidylserine [Paulusma *et al.*, 2008; Lopez-Marques *et al.*, 2014; Takatsu *et al.*, 2014]. Interestingly, Ray and co-workers proved that ATP8B1 bound CL through a basic residue enriched-motive [Ray *et al.*, 2010]. Nevertheless, recently it has been described that ATP8B1 could bind PC, a non-anionic PL [Takatsu *et al.*, 2014].

Van der Mark and co-workers propose that ATP8B1 and ATP11A mediate local clustering at the plasma membrane of PS or another PLs which are prone to induce curvature which enhances the binding of proteins involved in the generation of

vesicles which are involved in TLR4 endocytosis [Van der Mark *et al.*, 2017].

On the other hand, Cighetti and co-workers described the ability of a synthetic bacterial lipid A mimetic, structurally related to CL, to induce specifically CD14 internalization without changes in cell surface expression of TLR4-MD2 complex. Therefore, CD14 internalization would lead to the disruption of the cellular response to LPS [Cighetti *et al.*, 2014].

We hypothesize that CL could promote TLR4 and/or CD14 internalization through the P4-ATPase complex, thus promoting signaling through endosomal TLR4 which counteract the inflammatory response of MyD88-dependent signaling.

Scavenger receptors are classified as subclass A (SR-AI and SR-AII) or subclass B which includes CD36 and SR-BI/SR-BII [Thorne *et al.*, 2007]. SR-A, expressed on the surface of AMs, is well known in the context of atherosclerosis by its capability to bind and internalize modified low density lipoproteins [Winther *et al.*, 2000; Michael *et al.*, 2015]. In addition, it has been described that SR-A recognizes several PAMPs among which are found LPS and zymosan [Mukhopadhyay and Gordon, 2004, Hollifield *et al.*, 2007]. Recent studies have postulated that LPS stimulation promotes an association between TLR4 and SR-A which is required for optimal LPS-induced activation of the TLR4-mediated NF-κB pathway [Yu *et al.*, 2012]. Given that SR-A bind lipids, we thought that CL could form an inactive complex with SR-A impairing the development of the immune response following LPS or zymosan exposure.

Otherwise, Balasubramanian and co-workers incubated serial dilutions of PC or CL with the extracellular domain of CD36 and CD204 (SR-A). They found that neither CD36 nor CD204 recognize PC, whereas CD36 but not CD204, recognizes CL. In addition, using blocking antibodies, they discarded SRBI/II and proposed CD36 as the putative receptor that mediates the phagocytosis of CL liposomes [Balasubramanian *et al.*, 2015].

The peroxisome proliferator-activated receptor γ (PPARγ) is known to be highly expressed in AMs [Ricote *et al.*, 1998]. PPARγ ligands are unsaturated fatty acids, 15-deoxy-delta-12,14-prostaglandin J2, 15-Hydroxyeicosatetraenoic acid, acid components of oxidized low-density lipoprotein, 9- and 13-hydroxyoctadecadienoic [Varga *et al.*, 2011]. PPARs activate gene expression by binding to specific DNA response elements in target genes as heterodimers with the retinoid X receptors [IJpenberg *et al.*, 1997]. PPARs activated by appropriate ligands, release the

corepressor and binds to coactivator molecules [Glass and Ogawa, 2006].

It has been described that mice with deficiency in lysosomal acid lipase, and as a consequence, low levels of fatty acid, exhibited an inflammatory phenotype which was counteracted by PPAR-γ agonists [Lian *et al.*, 2005]. In macrophages/monocytes, PPARγ ligands suppressed the upregulation of iNOS, TNF-α, IL-1β, IL-12, and matrix metallopeptidase 9 [Ricote *et al.*, 1997; Jiang *et al.*, 1998; Welch *et al.*, 2003]. Several reports have suggested that PPARs inhibit the expression of proinflammatory genes by interference with signal-dependent activation of NF-κB, AP-1, C/EBP, STAT and NF-AT. PPARs can inhibit inflammatory gene expression through different mechanisms such as competition for a limiting pool of coactivators, direct interaction with the subunits of NF-κB (p65 and p50) and c-Jun or modulation of p38 MAPK activity [reviewed in Ricote *et al.*, 2007]. We hypothesize that CL could act as a ligand for PPARγ inhibiting LPS or zymosan-elicited inflammatory response.

Yui and Yamazaki studied the effect of CL on peritoneal macrophages growth and activation state [Yui and Yamazaki, 1991]. They first examined the effect of increasing doses of CL on cell viability after 3 days of preincubation with CL. They found that ≤ 40μg/ml (27nmol/ml) had no toxic effects on macrophages and that 40μg/ml of CL was the optimal concentration to induce growth. Nevertheless, they observed that 80μg/ml (54 nmol/ml) impaired cell viability. We also conducted experiments to determine AMs viability one day after preincubation with different doses of CL (7, 27 and 70 nmol/ml) (Figure 4.1.4). In our case, we did not detect loss of cell viability, even at the highest concentration tested, probably due to a shorter time of incubation or the cellular type. In discrepancy with our results, Yui and Yamazaki observed that pretreatment of macrophages with low amounts of CL (7 to 14 nmol/ml) for one to three days, enhanced macrophage TNF-α release induced by LPS *in vitro*. Nevertheless, they found that higher amounts of CL (27 nmol/ml) completely suppressed TNF-α release. These investigators failed to elucidate the mechanism underlying CL action. In agree with us, Yui and Yamazaki proposed that the inhibitory action of CL is not specific of a single PAMP since they obtained similar results in macrophages treated with a whole pathogen, *Enterococus faecalis*.

In summary, data shown in this part of results demonstrates that small amounts of CL have an extracellular and also intracellular anti-inflammatory effect. The intracellular effect was demonstrated by incubating CL with cells for 18 hours followed by washing and adding fresh culture medium, where cells were stimulated with LPS or zymosan. Furthermore, we have found that all signaling pathways activated after exposure to these PAMPs were inhibited in the presence of CL. This fact suggests that the molecular target for the inhibition exerted by CL is TLR itself and/or one

or more of its associated proteins, but not molecules involved in downstream pathways. Moreover, we have found that the anti-inflammatory effect of CL occurs in murine MH-S AMs and also in primary rat AMs.

It has been proposed that recognition of oxidized phospholipids by the host could be an endogenous feedback mechanism that helps to limit the damage caused by inflammation in the context of severe Gram-negative bacterial infection [Bochkov *et al.*, 2002]. Since CL is released, probably from host membranes, to the alveolar fluid during infection [Ray *et al.*, 2010], we hypothesize that this might be a protective mechanism developed by the host to control bacterial- and fungal-induced inflammatory responses. Furthermore, the anti-inflammatory action of CL should be considered in order to design new antibacterial and antifungal therapies based on CL.

4.2. ANTIVIRAL AND IMMUNOMODULATORY EFFECTS OF CARDIOLIPIN VESICLES AGAINST RESPIRATORY SYNCYTIAL VIRUS

4.2.1 INTRODUCTION

Respiratory syncytial virus (RSV) is the main cause of lower respiratory tract infections such as pneumonia and bronchiolitis in the elderly, immunocompromised individuals and children under the age of two [Collins and Mellero, 2011].

In the bronchoalveolar lavage of mice and humans with pneumonia high levels of cardiolipin were found [Ray *et al.*, 2010]. CL could be released to the alveolar fluid by dying host cells. There, lung surfactant components, viral particles and vesicles of CL could interact among them.

In this thesis, we have previously demonstrated the strong anti-inflammatory action of low doses of CL vesicles (≥ 0.7nmol/ml) on alveolar macrophages in response to LPS or zymosan. Moreover, it was recently published that anionic phospholipids, such as POPG and PI, present in lung surfactant, inhibit RSV replication and the subsequent cytokine production [Numata *et al.*, 2010; Numata *et al.*, 2013a; Numata *et al.*, 2013b, Numata M *et al.*, 2015]. Taking into account this prior information, we hypothesized that CL could act as a defense factor at low concentrations, protecting the host from RSV infection.

Therefore, the purpose of this study was to examine the effect of low doses of cardiolipins on viral replication and immune response of human AECs infected with RSV. In addition, we also studied the mechanism underlying CL action on RSV infection and the potential effects of the presence of native pulmonary surfactant on CL antiviral action.

4.2.2 EXPERIMENTAL DESIGN

To study the effect of CL on viral replication and the inflammatory response, AECs were mock-infected (with sucrose) or infected with human RSV (Long strain) at a multiplicity of infection (moi) of 3 plaque forming units (pfu) per cell in the absence or presence of CL vesicles. CL vesicles were added simultaneously to RSV infection (t=0) or were preincubated with cells for 18h before RSV infection (t=18h) to allow endocytosis of CL vesicles and evaluate the intracellular effect of CL.

RSV replication was evaluated determining 1) virus titers by plaque assay of infected supernatants in layered HEp-2 cells and 2) mRNA levels of the N nucleoprotein of RSV by qPCR. Expression of RSV-induced inflammatory markers was also evaluated by qPCR

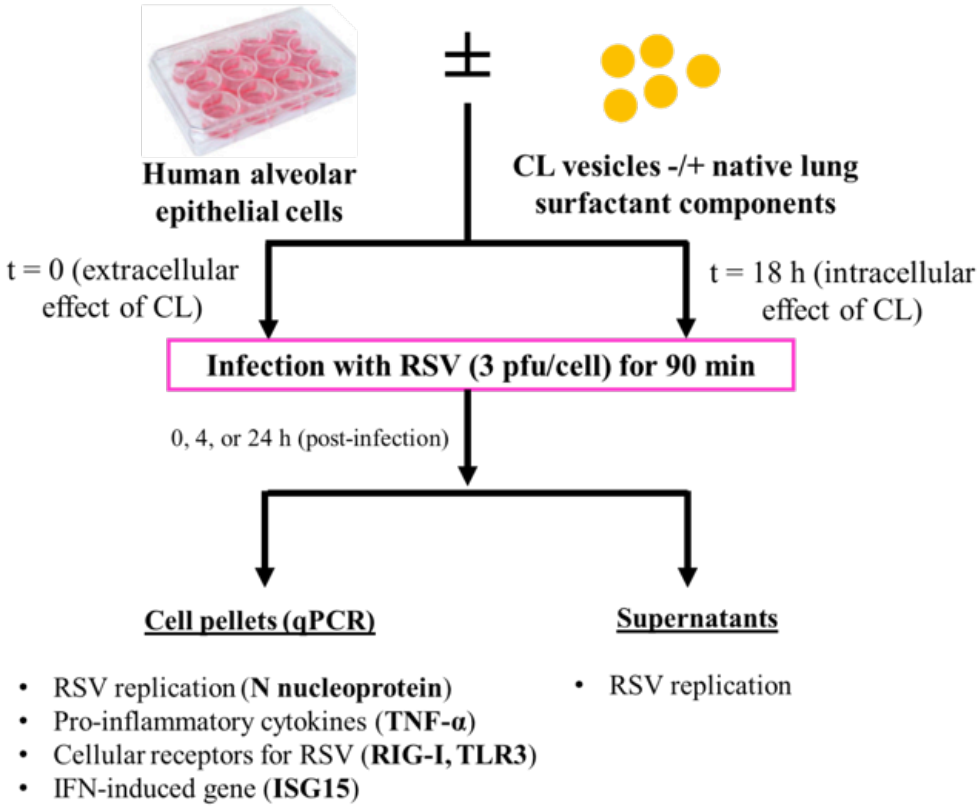

Figure 4.2.1. Experimental design.

4.2.3. RESULTS

4.2.3.1. Cardiolipin does not impair cell viability at the tested concentrations.

Human AECs (A549 cell line) were seeded as described in the materials and methods section. Next day, cells were preincubated in the presence or absence of increasing amounts of CL (0.7, 7, 14 and 27 nmol/ml) for 24 hours. To determine cell viability, we performed a colorimetric assay using the compound WST-1 as described in the materials and methods section. This reagent is a tetrazolium salt which is reduced to formazan in the presence of mitochondrial dehydrogenases. The absorbance of reduced tetrazolium could be read at 450 nm. The higher activity of mitochondrial enzymes is correlated with increased cell viability. We assessed that cell viability was not impaired at the concentrations of CL used (7 to 27 nmol/ml) (Figure 4.2.2).

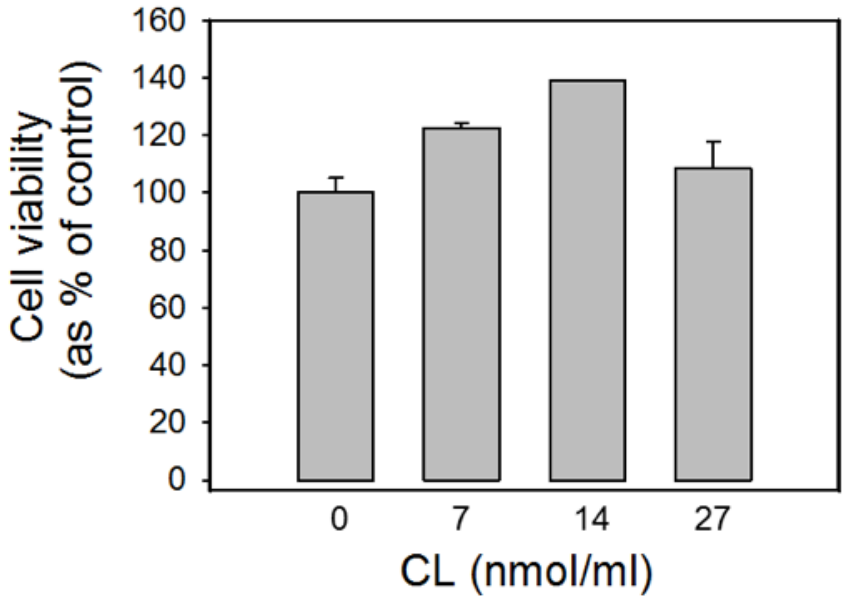

Figure 4.2.2. Cardiolipin does not affect AECs viability at the tested concentrations. AECs (5.105 per well) were seeded and maintained at 37ºC O/N. Then, cells were treated with different amounts of CL (0, 7, 14, and 27 nmol/ml) for 24 hours. Cell viability was determined by WST-1 assay. Cell viability in the absence of CL was set at 100%. Data are expressed as the mean ± S.E (n=2).

4.2.3.2. Cardiolipin inhibits viral replication.

To study CL action on RSV replication, cells were infected with RSV (moi 3 pfu/cell) in the absence or presence of increasing amounts of CL (0.7, 3.5, 7 nmol/ml) for 90 minutes at 37ºC. Subsequently, fresh medium was added and cells were maintained at 37ºC for 24 hours, in the absence or presence of CL. Viral titer in culture supernatants was determined by plaque assay in layered HEp-2 cells. As it is depicted in Figure 4.2.3 and Table 4.2.1, CL vesicles were able to reduce viral titer in culture supernatants of RSV-infected AECs.

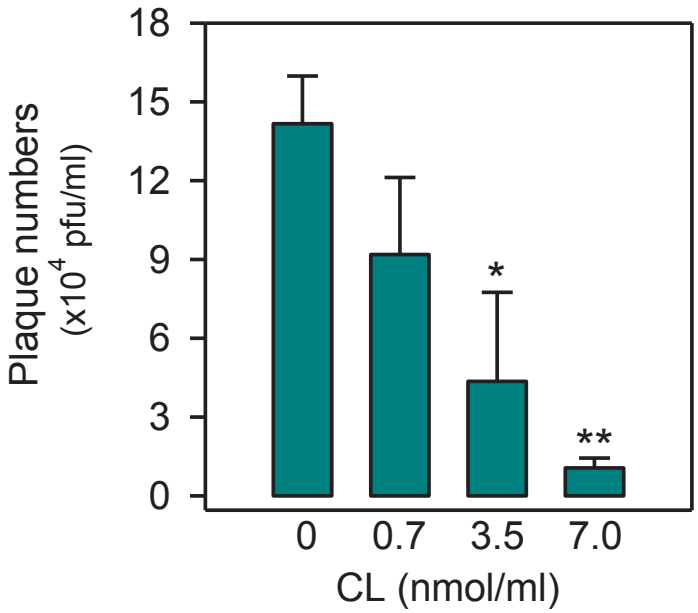

CL (nmol/ml)	0	0.7	3.5	7
RSV (pfu/ml)	$1.4x10^5 \pm 1.8$	$9.2x10^4 \pm 2.9$	$4.4x10^4 \pm 3.4$	$1.1x10^4 \pm 0.4$

Figure 4.2.3 and table 4.2.1. Cardiolipin reduces viral titer in supernatants of AECs. HEp2 cells (1.2x106) were seeded in 6-well plates and infected for 90 minutes at 37ºC with a series of dilutions (10-1 to 10-3) of supernatants from RSV-infected AECs that have been treated with or without CL (0.7, 3.5 or 7 nmol/ml). After infection, 3 ml of 0.7% agarose in 2% FBS DMEN were added to each well. Plates were maintained at 4ºC for 30 minutes to allow agarose solidification. Then, cells were incubated at 37ºC for 5 days to perform plaque quantification. The results are presented as means (± SEM) from three different RSV-infected AEC cultures. (* $p<0.050$ vs RSV; ** $p<0.010$ vs RSV).

We further analyzed the CL effect on viral replication by quantifying mRNA levels of the N nucleoprotein of RSV by qPCR. N nucleoprotein is essential for RSV encapsidation by coating the entire viral RNA genome to form the ribonucleoprotein complex [Collins *et al.*, 2013]. N nucleoprotein expression was quantified by qPCR in AECs infected with RSV (moi 3 pfu/cell) in the absence or presence of CL (7 nmol/ml) for 90 minutes and maintained at 37ºC for 0, 4, and 24 h post-infection. Figure 4.2.4 shows that CL was able to reduce N nucleoprotein expression after 90 minutes of infection. This inhibitory effect was maintained in the post-infection period (4h or 24h). These results suggest that CL action takes place in the early stages of infection. We hypothesized that CL vesicles might inhibit RSV uptake by AECs. CL vesicles might block RSV attachment to the epithelium surface and/or inhibit the endocytosis of RSV.

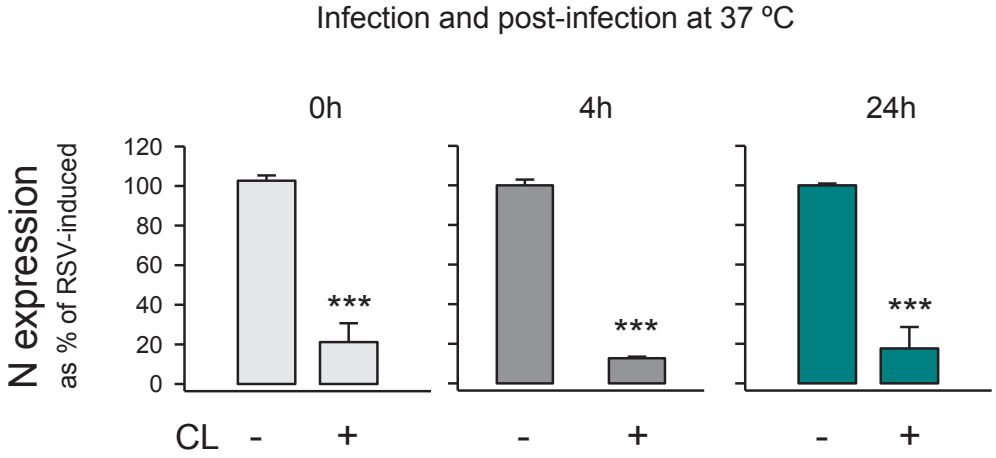

Figure 4.2.4. Cardiolipin vesicles inhibit RSV N nucleoprotein expression in AECs infected with RSV. CL vesicles (7 nmol/ml) were added to AECs and simultaneously infected with RSV (moi of 3 pfu/cell) in 2% FBS DMEN for 90 min at 37ºC. After that, cells were maintained in the absence or presence of CL vesicles (7 nmol/ml) for 0, 4 or 24 hours at 37ºC. Then, RNA was then extracted from cellular pellets for qPCR analysis. The results are presented as means (± SEM) from three different RSV-infected AEC cultures. (*** $p<0.001$).

4.2.3.3. Cardiolipin inhibits RSV attachment to the epithelium surface. Cardiolipin acts at lower dose than POPG.

RSV uptake by epithelial cells is a two-step process that firstly involves the binding of viral G and F proteins by electrostatic interaction with glycosaminoglycans (GAGs) of the cell surface. The second step, directed by F protein, implies the fusion of viral envelope with the cellular plasma membrane [Krusat and Streckert, 1997; Hallak *et al.*, 2000]. There is also evidence of entry by clathrin-mediated endocytosis although endosomal acidification is not required [Collins *et al.*, 2013]. Therefore, endocytosis involves the same fushion mechanism with the endosomal membrane than with the plasma membrane. In the cytoplasm, genome transcription occurs and it is encapsidated with N nucleoprotein and associated with the polymerase complex to form nucleocapsides. Finally, nucleocapsides are transported to the plasma membrane and virions will be released by budding (see Figure 1.8 of the introduction) [Fearns and Dewal, 2016].

In order to understand how the vesicles of CL inhibit viral replication, we investigated the ability of CL to inhibit RSV attachment to the cell surface. AECs in suspension were infected with RSV in the presence and absence of CL, and cells were analyzed for attached virus by FACScan, using a mouse antibody against G glycoprotein and subsequently with fluorescent phycoerythrin-conjugated antibody directed against

mouse IgG. Binding experiments were performed at 4ºC. The results presented in Figures 4.2.5A and 4.2.5B demonstrate significant binding of the RSV to the cell surface in the absence of CL. The addition of CL markedly inhibited the adhesion of viral particles to the cell surface, being almost completely suppressed at 25 nmol/ml of CL (fluorescence intensity similar to mock samples). We conclude that CL exerts its antiviral action by inhibiting viral particles attachment to the cell surface. As a result, RSV fusion to the cell membrane and replication will be impaired.

Figure 4.2.5. Cardiolipin inhibits RSV binding to AECs. (A) CL effects upon cell

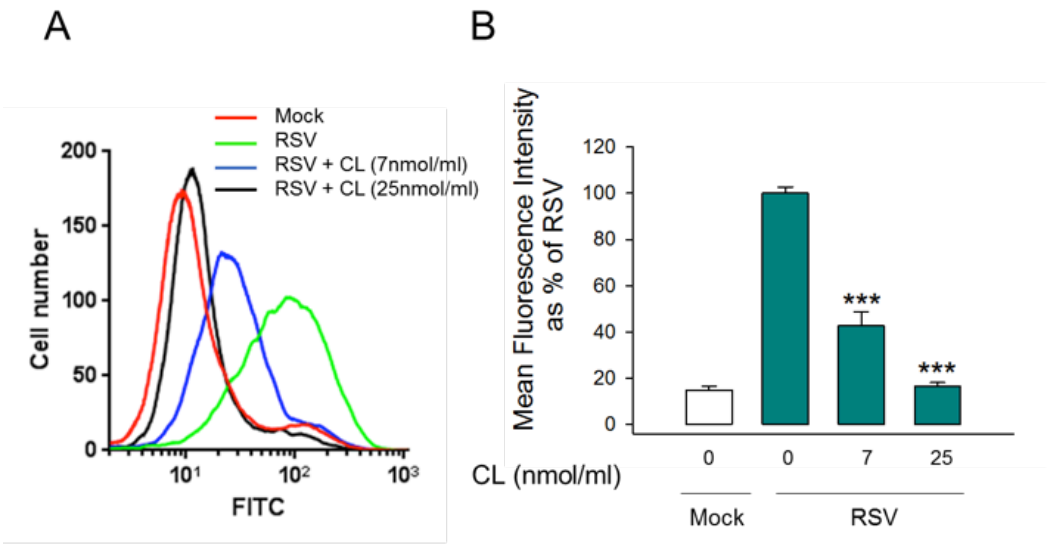

surface binding of RSV. Suspensions of AECs were incubated with RSV (moi of 3 pfu/cell) for 1 hour in the presence and absence of CL. Then, the cells were treated with a mouse antibody against RSV G glycoprotein and subsequently with a phycoerythrin-conjugated antibody directed against mouse IgG. All incubations were performed at 4ºC. Finally, the cells were fixed with PBS-PFA 1% and analyzed by flow citometry. A representative FACScan is shown in which cells were not infected with virus (mock), infected with virus alone (RSV) or infected with virus and CL (RSV + CL). (B) Summary of FACScan data from three independent experiments. (***p<0.001 vs RSV infection in the absence of CL).

4.2.3.4. Cardiolipin acts at lower dose than POPG.

We next determined viral particles adhesion to the cell surface in comparison with POPG, an anionic surfactant phospholipid which is capable of disrupting viral attachment to epithelial cells surface [Numata *et al.*, 2013a, Numata *et al.*, 2013b]. AECs were infected at 4ºC for 90 minutes and then RNA was extracted from cellular pellets. RNA of N nucleoprotein from viral particles attached to AECs surface was analyzed by qPCR. As we could see in Figure 4.2.6, CL vesicles from a concentration of 7 nmol/ml markedly suppressed N nucleoprotein RNA detection in AECs, whereas in the case of POPG occurs at 25 nmol/ml. We can conclude that CL inhibits RSV attachment to the epithelium surface at lower dosis than POPG.

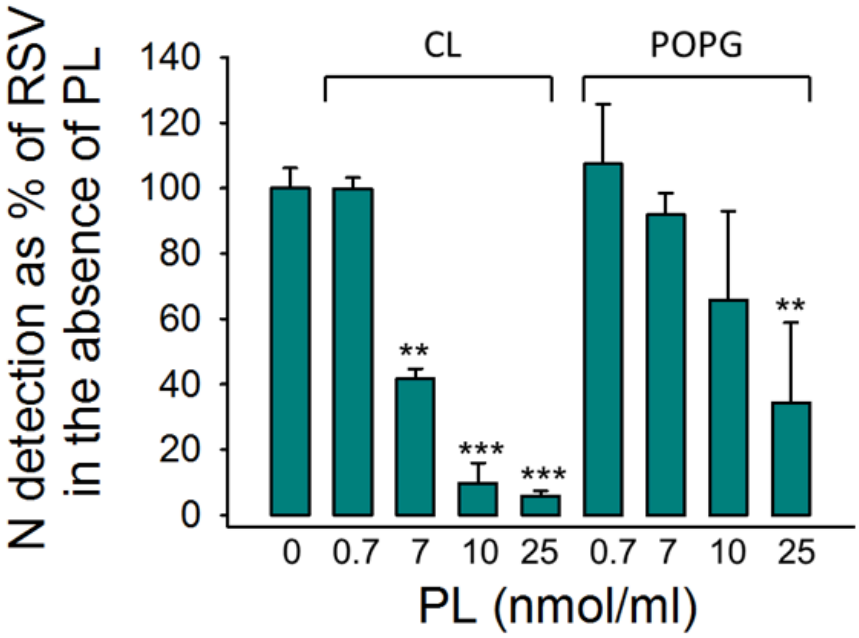

Figure 4.2.6. Cardiolipin inhibits RSV adhesion to AECs to a higher extent than POPG. Different amounts of CL or POPG vesicles were added to AECs and simultaneously infected with RSV (moi of 3 pfu/cell) for 90 min at 4ºC. After that, cells were washed and cellular pellets were collected (0h post-infection). The results are presented as means (± SEM) from three different RSV-infected AEC cultures. (**p<0.010; *** p<0.001 vs RSV).

4.2.3.5. Cardiolipin vesicles inhibit the expression of RSV-induced infection markers in alveolar epithelial cells.

We have demonstrated the strong inhibitory action of low amounts of CL on RSV replication in AECs. We would expect that if less viral particles are able to bind and enter cells in the presence of CL, the inflammatory response induced by RSV will be reduced. Moreover, we have previously described in part 1 of results that CL is able to inhibit LPS and zymosan-elicited signaling and the production by AMs of several proinflammatory markers (TNF-α, IL1-β, CXCL10, iNOS (NOS2) and COX2). Thus the role of low amounts of CL vesicles on the inflammatory response of AECs after RSV infection was investigated. AECs were mock-infected (with sucrose) or infected with RSV (moi 3 pfu/cell) in the absence or presence of CL vesicles (7 nmol/ml) for 90 minutes at 37 ºC. After that, cells were maintained 24 hours at 37 ºC in the absence or presence of CL vesicles (7 nmol/ml).

Then, we quantified by q-PCR the mRNA expression of certain molecules that are upregulated during RSV infection. These are the main cellular receptors for RSV (RIG-I and TLR3), IFN-induced gene 15 (ISG15) and TNF-α.

RIG-I and TLR3 are the main RSV-receptors and sense double-stranded RNA (dsRNA). RIG-I is a cytosolic RNA helicase, whereas TLR3 is transmembrane protein found in the cell surface or in endosomal compartments [Yu and Levine, 2011]. ISG15 is the earliest IFN-induced gene after RSV infection and encodes an ubiquitin-like protein that promotes an antiviral state [Kunzi *et al.*, 2003]. TNF-α is a proinflammatory cytokine that contributes to RSV clearance but an excessive TNF-α secretion exacerbates illness by causing lung damage [Rutigliano and Graham, 2004]. The expression of all of these molecules have been demonstrated to be up-regulated during RSV infection in human A549 or murine MLE-15 epithelial cells [Liu *et al.*, 2007; Martínez *et al.*, 2007; Moore *et al.*, 2008]. ISG15 and TNF-α play a key role in the development of an inflammatory response against RSV. Despite of a controlled inflammatory response is necessary for virus clearance, an exacerbated inflammation results in tissue injury.

Figure 4.2.7 shows that RIG-I, TLR3, ISG15 and TNF-α expression were up-regulated in RSV-infected AECs. The presence of CL vesicles drastically decreased RSV-elicited expression of all these markers.

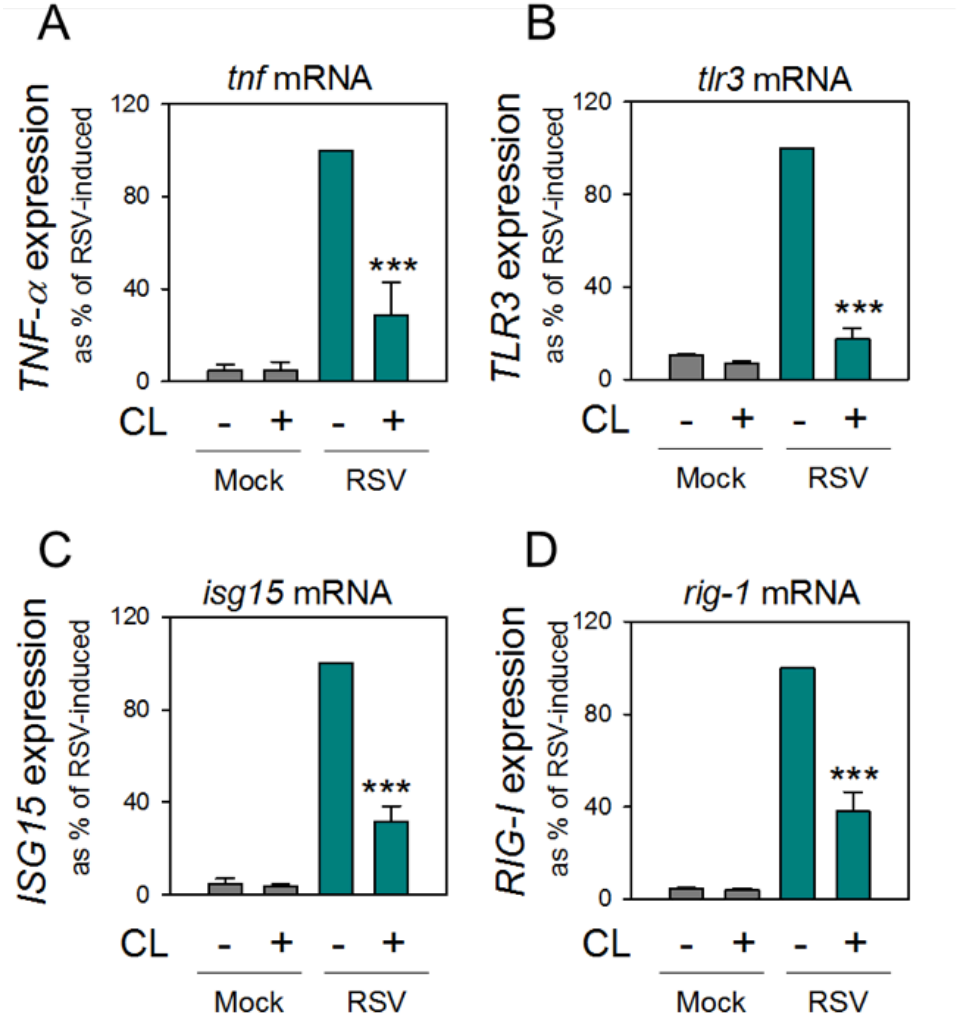

(legend continued on next page

Figure 4.2.7. CL vesicles inhibited RSV-induced TNF-α (A), TLR3 (B), ISG15 (C) and RIG-I (D) expressions. Vesicles of CL (7 nmol/ml) were added to A549 AECs and simultaneously infected with RSV (moi of 3 pfu/cell) for 90 min at 37ºC. After a post-infection period of 24 hours in the presence or absence of CL, RNA was extracted from cellular pellets for qPCR. The results are presented as means (± SEM) from three different RSV-infected AEC cultures and expressed as percentages of RSV-induced expression in the absence of CL. (***$p<0.001$ vs RSV).

4.2.3.6. Cardiolipin antiviral action is preserved regardless of the presence of pulmonary surfactant components.

Given that the alveolar epithelium is covered by surfactant membranes and that the main surfactant protein, SP-A, binds CL vesicles (section 4 of results), we decided to study whether the inhibitory effect of CL could be blocked by the presence of surfactant components. To this end, we studied CL antiviral action in the presence or absence of either rat native pulmonary surfactant (NPS), purified surfactant protein SP-A, or MLVs prepared from the lipid extract of NPS (LES), a fraction containing phospholipids, cholesterol and the hydrophobic surfactant proteins SP-B and SP-C. Note that NPS contains both LES components and SP-A, which is attached to surfactant membranes. Cells were infected with RSV (moi 3 pfu/cell) in the absence or presence of CL (7 nmol/ml), NPS (250µg/ml), LES (250µg/ml), SP-A (100µg/ml) and combinations thereof for 90 minutes at 37ºC. Then, 2ml of 2% FBS DMEN and a new dose of the components mentioned above were added. Cells were maintained for 24 hours at 37ºC. Finally, viral replication was evaluated determining viral titers in culture supernatants of infected AECs by plaque assay in layered HEp-2 cells. Figure 4.2.8 shows that either NPS, LES nor SP-A exhibited any effect on RSV replication. Importantly, NPS, LES and SP-A did not block the antiviral action of CL vesicles.

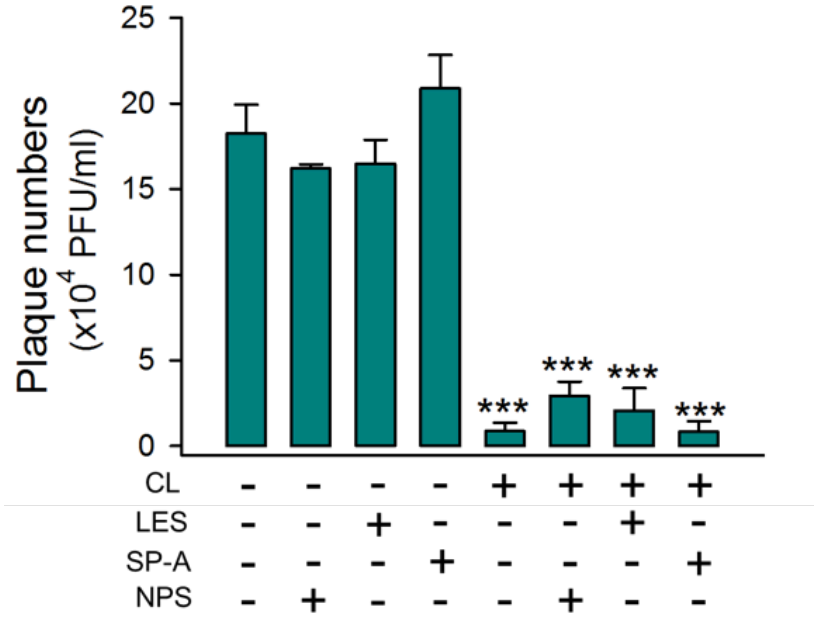

Figure 4.2.8. Rat native pulmonary surfactant (NPS) nor the hydrophobic fraction of lung surfactant (LES) or SP-A inhibited viral titer in supernatants of RSV-infected A549 AECs. The presence of NPS nor SP-A or LES did not impair or ameliorate CL antiviral action. HEp2 cells (1.2x106 per well) were seeded in 6-well plates and infected for 90 minutes at 37ºC with a series of dilutions (10-1 to 10-3) of RSV-infected supernatants from A549 AECs that have been treated or not with CL (7 nmol/ml), NPS (250 µg/ml), LES (250 µg/ml), SP-A (100 µg/ml) or combinations thereof. After infection, 3 ml of 0.7% agarose in 2% FBS DMEN were added to each well. Plates were maintained at 4ºC for 30 minutes to allow agarose solidification. Then cells were incubated at 37ºC for 5 days to perform plaque quantification. The results are presented as means (± SEM) from three different RSV-infected AEC cultures. (***p<0.001 vs RSV).

4.2.3.7. Internalized vesicles did not affect viral replication but inhibit TNF-α production in RSV-infected A549 AECs.

We next investigated whether internalized CL vesicles were capable of inhibiting viral replication in AECs in order to determine whether intracellular CL is capable of modulating host inflammatory responses elicited by RSV infection. The cells were incubated in the presence or absence of CL (3.5, 7.0 and 28 nmol/ml) for 18h at 37ºC and then infected with RSV for 24h. We evaluated viral replication in culture supernatants by plaque assay in layered HEp-2 cells (Figure 4.2.9A) and by quantifying mRNA levels of RSV N nucleoprotein expression (Figure 4.2.9B). As it is shown in Figure 4.2.9, internalized CL vesicles did not reduce viral titers in culture supernatants of infected-AECs (A) nor inhibited mRNA production of the N nucleoprotein (B). Altogether, these results indicate that CL, once internalized into the cells, was not able to inhibit viral replication.

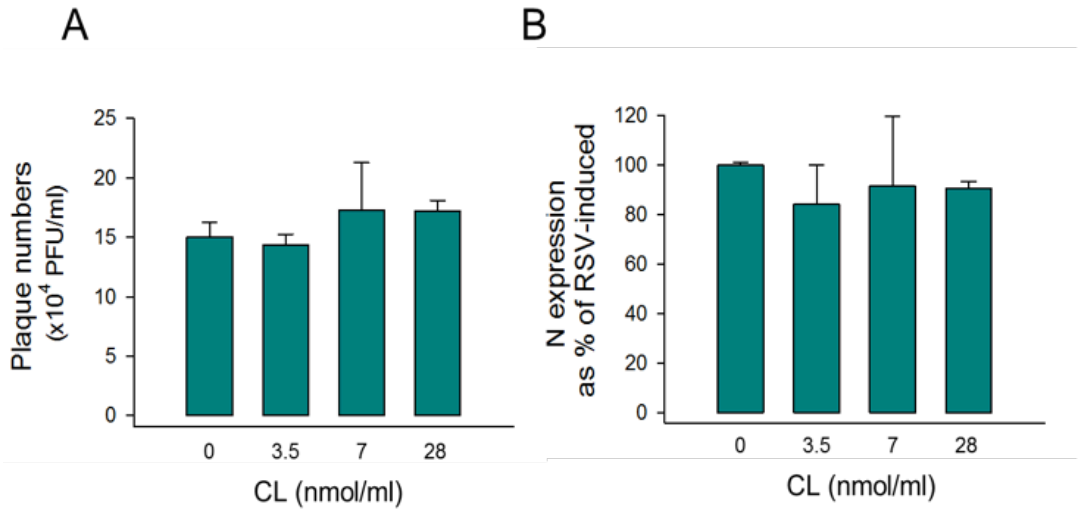

Figure 4.2.9. Internalized CL vesicles failed to inhibit RSV replication in A549 AECs. A549 cells were preincubated with CL SUVs (3.5, 7 or 28 nmol/ml) for 18 hours, and then infected with RSV (moi of 3 pfu/cell) for 24 hours. (A) Internalized CL vesicles did not decrease RSV titers in culture supernatants of infected cells (n=3). (B) Internalized CL vesicles did not reduce the expression of the mRNA of RSV N nucleoprotein. The results are presented as means (± SEM) from three different RSV-infected AEC cultures and expressed as percentages of RSV-induced expression in the absence of CL.

We have previously demonstrated in this thesis that endocytosed CL vesicles inhibit the production of several proinflammatory markers by AMs stimulated with either LPS or zymosan (part 1 of results). Thus, we investigated whether internalized vesicles of CL (7 and 28 nmol/ml) were also capable of modulating RSV-induced expression of TNF-α in AECs. TNF-α is the principal mediator of RSV-induced inflammation [Rutigliano and Graham, 2004]. AECs were preincubated with 7 or 28 nmol/ml of CL vesicles for 18 hours. Subsequently, the culture medium was removed, cells were washed and mock-infected or infected with RSV for 24 hours. After that, the mRNA expression of TNF-α was quantified by qPCR. Figure 4.2.9 shows that the effect of endocytosed CL vesicles was dependent on the dose because CL exhibited an anti-inflammatory effect at 28 but not at 7nmol/ml. Note that, CL when was co-added with RSV was able to decrease TNF-α expression at a lower amount of phospholipid (7 nmol/ml) due to the ability of extracellular CL vesicles to block virus binding to the cell surface and therefore, virus entry and cellular responses to RSV infection (Figure 4.2.7A).

Therefore, the results presented in this section indicate that intracellular CL is not able to inhibit RSV replication but is capable of modulating the proinflammatory response of AECs infected with RSV.

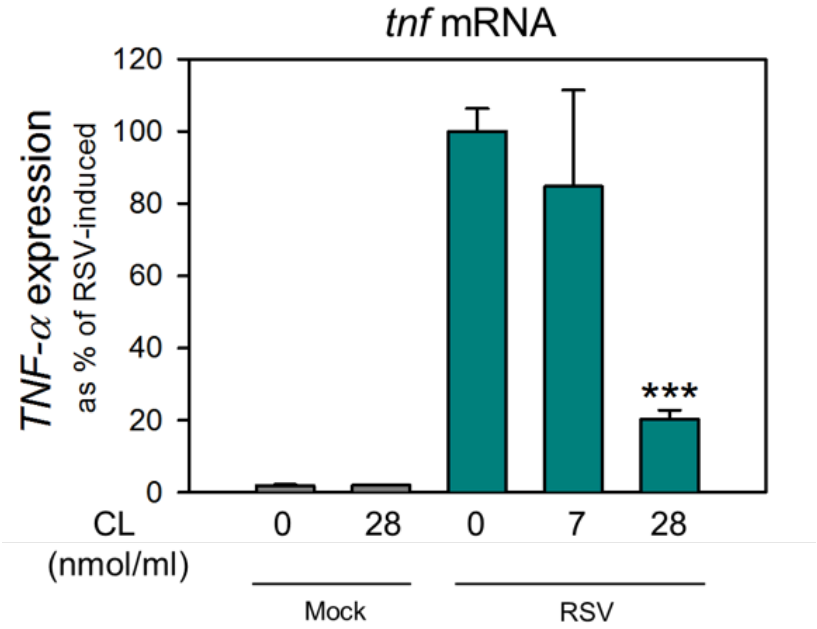

Figure 4.2.10. Internalized vesicles of CL inhibited RSV-induced TNF-α mRNA but dependent on the dose. AECs were preincubated or not with CL vesicles (7 or 28 nmol/ml) for 18h and then, they were mock-infected (with sucrose) or infected with RSV (moi of 3 pfu/cell) for 90 min at 37ºC. After 24 hours, RNA was extracted from cellular pellets for qPCR. The results are presented as means (± SEM) from three different RSV-infected AEC cultures and expressed as percentages of RSV-induced TNF-α expression in the absence of CL. (***$p<0.001$ vs RSV).

4.2.4. DISCUSSION

The role of CL on the immune response has been poorly studied. Our recent data shown in part 1 of results, provide strong evidence that low doses of this phospholipid (≥0.7nmol/ml) play a key role in modulating the innate immune response of alveolar macrophages stimulated with bacterial LPS or fungal zymosan. The purpose of the present study was to investigate the action of CL on RSV replication in AECs and the inflammatory response as a consequence of the infection. We analyzed the action of extracellular CL vesicles by addition of CL simultaneously with RSV, and the action of intracellular CL vesicles, which were endocytosed by AECs previously to RSV infection.

Our results highlight the strong antiviral action of extracellular vesicles of CL at low doses of phospholipid (7nmol/ml). When was present in the extracellular medium, CL inhibited RSV replication in a dose-dependent manner (Figures 4.2.3 and 4.2.4) and the RSV-elicited immune innate response (Figure 4.2.7). The fact that mRNA levels of N nucleoprotein were reduced immediately after 90 minutes of infection (0h post-infection) in the presence of CL (7nmol/ml) and that this inhibitory effect

was maintained over time (4 and 24h post-infection) (Figure 4.2.4), suggests that CL action occurs in an early stage of infection.

It is known that RSV uptake by epithelial cells consists of a two-step process that involves firstly, the attachment of viral G and F protein to the cell and secondly, it is required the fusion of RSV membrane with the plasma membrane directed by F protein of RSV. After fusion, RSV replicates in the cytosol of the host cells surface [Krusat and Streckert, 1997; Hallak *et al.*, 2000]. First, we investigated whether CL action takes place by blocking the binding of viral particles adhesion to the cell surface.

We first conducted flow cytometry assays to examine the direct binding of RSV to AECs and its inhibition by CL (7 and 25 nmol/ml) at 4°C (Figures 4.2.5A and 4.2.5B). In these experiments, we observed a dose-dependent CL inhibition of RSV binding to the surface of epithelial cells. At 7 and 25 nmol/ml, CL inhibited the binding of RSV to cells by greater than 50% and 80 %, respectively.

We further compared the effect of CL with POPG on RSV adhesion to the AECs surface. To that end, we determined the presence of N nucleoprotein in AECs incubated with RSV at 4ºC for 90 minutes in the presence or absence of different amounts of CL or POPG vesicles (0, 0.7,7,10, and 25 nmol/ml) (Figure 4.2.6). At this temperature, is only detected RSV adhesion because the fusion process required a physiological temperature (37ºC). We found that CL was more effective than POPG in blocking RSV adhesion to the cell surface. CL inhibitory effect occured in a dose-dependent fashion from a CL concentration of 7 nmol/ml, whereas the inhibitory effect of POPG start to be detected at 25 nmol/ml. At this concentration, CL showed 80% of inhibition. Numata and co-workers used saturating concentrations of PI and POPG (260 and 130 nmol/ml), respectively. At saturating concentrations, PI and POPG produce almost the same degree of inhibition [Numata *et al.*, 2013a]. Experiments reported by Numata and co-workers were performed at a moi of 1, however, our experiments were performed at a moi of 3. Under these experimental conditions we found a CL saturating effect at around 10 nmol/ml indicating that CL is more efficient than other acidic phospholipids such as POPG and PI.

In order to elucidate whether CL could act once endocytosed by the cells as an antiviral agent, we performed experiments to determine the effect of intracellular CL on viral replication. To that end, CL vesicles were preincubated with the cells for 18 hours before infection. After that, culture medium was removed and cells were washed. Then, fresh culture medium was added and cells were infected with

RSV. Results obtained by determining viral titer of infected culture supernatants and mRNA expression of N nucleoprotein of RSV, indicated that once endocytosed, CL was not able to inhibit RSV replication inside AECs (Figure 4.2.9).

Thereby, altogether, results depicted in Figures 4.2.5, 4.2.6 and 4.2.9 allow us to conclude that CL acts exclusively in the extracellular medium by blocking viral particles attachment to the cell surface. CL vesicles could be able to directly bind to RSV particles or well to bind and block receptors involved in RSV binding to the cell surface. Our results are in agree with those reported in the literature for other anionic phospholipids such as POPG and PI [Numata *et al.*, 2010; Numata *et al.*, 2013a; Numata *et al.*, 2013b; Numata el al., 2015].

Glycosaminoglycans are negatively charged linear polymers of repeating disaccharide units produced by mammalian cells and some bacteria [Yamada and Kawasaki, 2005], most of them linked to transmembrane proteins. In the cellular surface, GAGs act as viral receptors, and GAGs deficiency impairs RSV uptake by epithelial cells. RSV F and G proteins seem to bind to the cell surface through electrostatic interactions with negatively charged GAGs and subsequently, fusion occurs and the enter of ribonucleoprotein complex [Krusat and Streckert, 1997; Hallak *et al.*, 2007]. CL as well as POPG and PI are negatively charged phospholipids that could compete with GAGs for RSV binding, trapping RSV and blocking its entry into the cells.

In the alveolar fluid, CL vesicles might be in contact with lung surfactant components, thereby, we analyzed the effect of native pulmonary surfactant (NPS) and its isolated components on CL antiviral action.

We found that neither NPS (250 µg/ml), nor LES (250 µg/ml) nor SP-A (100 µg/ml) showed any antiviral effect at the concentrations tested (Figure 4.2.8). NPS and LES contain acidic phospholipids (PI and PG) but their distribution in surfactant membranes might impede effective binding of RSV particles. PI and POPG present in the composition of NPS are probably masked by other surfactant components and maybe, due to this reason, was not able to exert its antiviral properties [Numata *et al.*, 2010; Numata *et al.*, 2013a; Numata *et al.*, 2013b].

Importantly, we found that, the antiviral action of CL was not affected by the presence of NPS, LES or SP-A (Figure 4.2.8). We found that SP-A is able to bind to CL with high affinity (section 4 of the results). However, our data indicate that SP-A binding

to CL did not interfere with CL antiviral action. Of note, it has been reported that co-administration of RSV and SP-A reduced viral titers in the lung of SP-A deficient mice [Levine *et al.*, 1999]. However, there are controversial results with respect the activiral actions of SP-A [Hickling *et al.*, 2000].

Finally, we analyzed the action of intracellular or extracellular CL on RSV-elicited inflammatory response in AECs. As we expected, if less viral particles are able to replicate inside the cells in the presence of extracellular CL vesicles, the immune innate response will be reduced. Figure 4.2.7 shows that extracellular CL vesicles (7 nmol/ml) reduced RSV-induced expression of RIG-I, TLR3, ISG15 and TNF-α. With respect to endocytosed CL, we found that intracellular CL is able to reduce RSV-elicited TNF-α expression but at a higher phospholipid concentration (28nmol/ml) than extracellular CL vesicles (7nmol/ml). The mechanism that underlies the anti-inflammatory action of endocytosed CL vesicles is different of that described for extracellular CL vesicles, whose anti-inflammatory action is a consequence of a decreased replication of the virus inside AECs [Figure 4.2.10].

When RSV is recognized by TLR3, this receptor induces downstream signaling through its adaptor protein, MyD88. MyD88 elicits signaling pathways such as IRAK (IL-1 receptor-associated kinase)-1/4, TRAF6 (TNF receptor associated factor 6), IRF (interferon regulatory factor), and/or NF-κB [Yamamoto *et al.*, 2003; Takeda and Akira, 2015]. These signals may lead to the production of various cytokines such as type I IFN (IFN-α and -1β) and proinflammatory cytokines such as TNF-α, IL-1, IL-6, and IL-8 [Yamamoto *et al.*, 2003; McGettrick and O'Neill, 2004; Takeda and Akira, 2015]. We hypothesize that endocytosed CL vesicles could act regulating transcription factors that block some steps of the signaling pathways cited above thus producing a decrease in the RSV-elicited inflammatory response.

In summary, our results highlight the antiviral and anti-inflammatory action of low amounts CL vesicles on RSV infection. Interestingly, we found that CL is more effective than acidic phospholipids such as POPG in inhibiting viral docking to the cell surface. CL antiviral properties have not been demonstrated before and suggest that low dose of CL could be used as a promising therapy against RSV, which causes serious illness in children, elderly individuals and people with chronic cardiopulmonary diseases.

4.3. CARDIOLIPIN PROTECTS AGAINST NON-TYPABLE *HAEMOPHILUS INFLUENZAE* INFECTION OF MLE-12 MURINE ALVEOLAR EPITHELIAL CELLS.

4.3.1. INTRODUCTION

Non-typable *Haemophilus influenzae* is a non-capsulated Gram-negative present as a commensal in the nasopharynx of the vast majority of healthy individuals. However, when it moves in to the lower respiratory tract it causes disease. NTHi is the main cause of exacerbations in patients with underlying inflammatory diseases, such as chronic obstructive pulmonary disease (COPD) [Murphy *et al.*, 2004; Moghaddam *et al.*, 2011]. NTHi is also a leading cause of otitis media, sinusitis and pneumonia, often following viral respiratory infection [Murphy, 2003]. A proposed mechanism through which NTHi causes chronical infections is due to its ability to be internalized and survive inside airway epithelial cells. NTHi is able to survive into late endosomes in a non-replicative state but maintaining an active metabolism. The internalization mechanism requires lipid rafts and citoskeleton integrity, as well as Akt phosphorylation mediated PI3K [Morey *et al.*, 2011; López-Gómez *et al.*, 2012].

Cardiolipin is present in the outer membrane of Gram-negative bacteria and the membrane of Gram-positive bacteria (around 10 and 25%, respectively) [Barák and Muchová., 2013]. Nevertheless, NTHi lacks of CL in the composition of its membrane [Ray *et al.*, 2010]. In eukaryotic cells, CL is mainly located in the inner mitochondrial membrane (around 20 %) [Krebs *et al.*, 1979; Zinser *et al.*, 1991 Paradies *et al.*, 2013]

Recently, it has been described that in mice and humans with pneumonia, CL is released to the alveolar fluid presumably from the host [Ray *et al.*, 2010]. It has been shown that anionic phospholipids, such as phosphatidylglycerol, limit the immune response and infection in the alveoli [Kuronuma *et al.*, 2009; Kandasamy *et al.*, 2011]. Moreover, in the present doctoral dissertation we have proved the anti-inflammatory action of CL against bacterial and fungal molecular patterns on murine AMs and its antiviral and anti-inflammatory properties on human AECs infected with RSV.

Taking into account this prior information, the purpose of this study was to investigate whether CL protects against bacterial infection of AECs by NTHi.

4.3.2. EXPERIMENTAL DESIGN

We infected murine AEC cell line MLE-12 with two different strains of NTHi: one isolated from otitis media (NTHi 375) and the other from COPD (NTHi 86-028NP) patients. Murine MLE-12 AECs were mock-infected or infected with NTHi (108 c.f.u/ml) in the presence or absence of CL (7 and 27 nmol/ml) at 37ºC and 5% CO2.

We first evaluated adhesion of NTHi to AECs. With this purpose, cells were infected for 30 minutes, lysed with PBS-saponin and serial dilutions were plated on agar-BHI for colony counting. We then evaluated invasion of AECs by NTHi. With this aim, AECs were infected for 2h, followed by treatment with gentamicin in order to kill extracelullar bacteria. Then, cells were lysed and serial dilutions were plated on agar-BHI for colony counting.

To detect Akt phosphorylation, after incubation with NTHi for 1h, cell culture medium was discarded, wells were washed and cell lysates were obtained for western-blot.

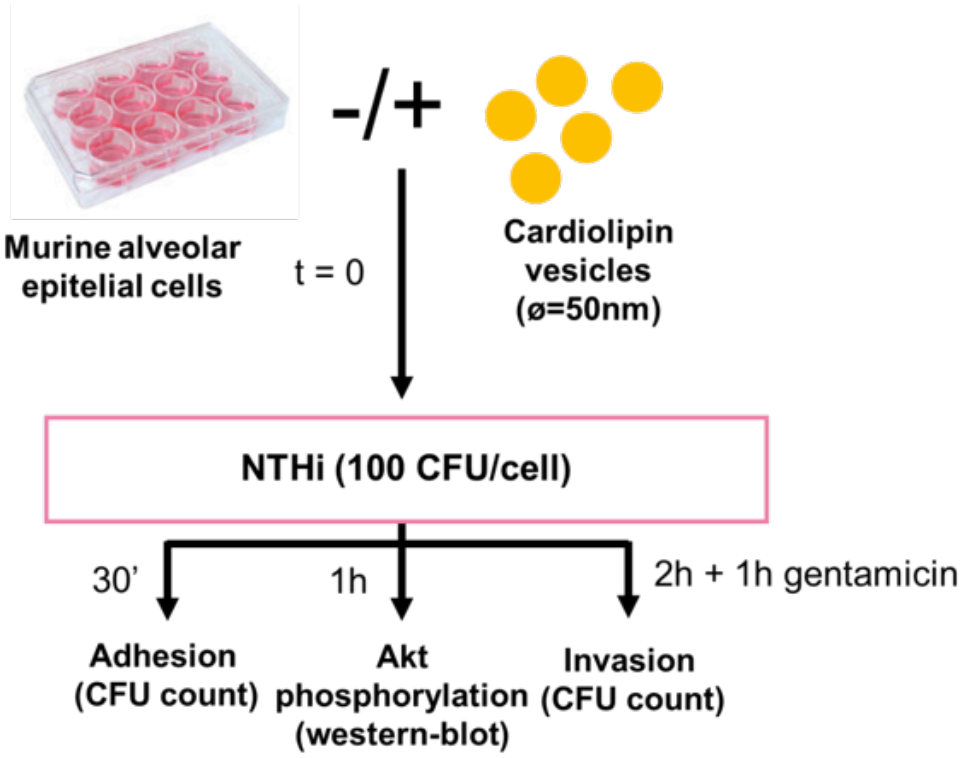

All these procedures are detailed in the materials and methods section.

Figure 4.3.1. Experimental design.

4.3.3. RESULTS

4.3.3.1. Cardiolipin inhibits NTHi internalization into epithelial cells without affecting bacterial adhesion to the cell surface.

First, we analyzed the potential effect of CL on bacterial adhesion and invasion in murine MLE-12 AECs (Figure 4.3.2). Our results indicated that the co-administration of CL with NTHi reduced bacterial invasion whereas we did not observe changes in adhesion. In both bacterial strains (otitis and COPD), the inhibitory effect on invasion was dose-dependent. From these experiments we can conclude that CL action might take place at the intracellular level because CL did not interfere with NTHi docking to the cell surface. Thereby, the next step was to analyze the effect of CL on NTHi-elicited Akt phosphorylation, a signal needed for NTHi internalization into the epithelium [López-Gómez *et al.*, 2012].

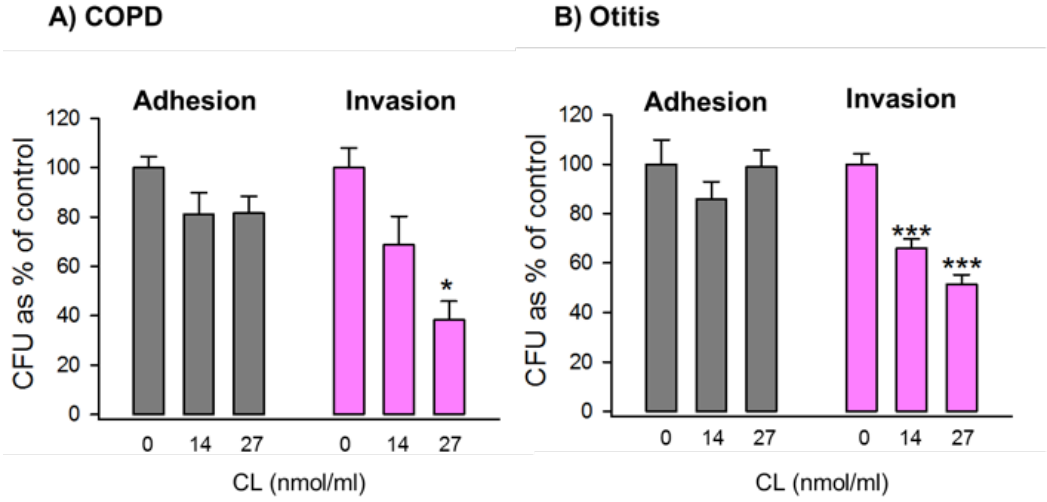

Figure 4.3.2. Cardiolipin inhibited invasion (pink bars) but not adhesion (grey bars) of NTHi COPD (A) or otitis (B) in MLE-12 cells. CL was added simultaneously with NTHi to the cells. To carry out adhesion and invasion experiments cells were infected with NTHi for 30 minutes or 2 hours respectively. Data show the percentage of viable bacteria referred to control (infected cells in the absence of CL). Data are expressed as mean percentages ± S.E. (*** $p<0.001$ vs control; *$p<0.050$ vs control).

4.3.3.2. Cardiolipin inhibits NTHi-induced Akt-phosphorylation

Results depicted in Figure 4.3.2 suggest an effect of CL on intracellular signaling. Since, we have demonstrated that CL strongly inhibited LPS- and zymosan-elicited Akt phosphorylation in murine and rat AMs (part 1 of results), we decided to investigate the effect of CL on NTHi-induced Akt phosphorylation. We analyzed NTHi-induced Akt phosphorylation in the presence or absence of CL vesicles (7 or 27 nmol/ml). Results shown in Figure 4.3.3 proved that CL is able to inhibit basal as well as NTHi-elicited Akt phosphorylation.

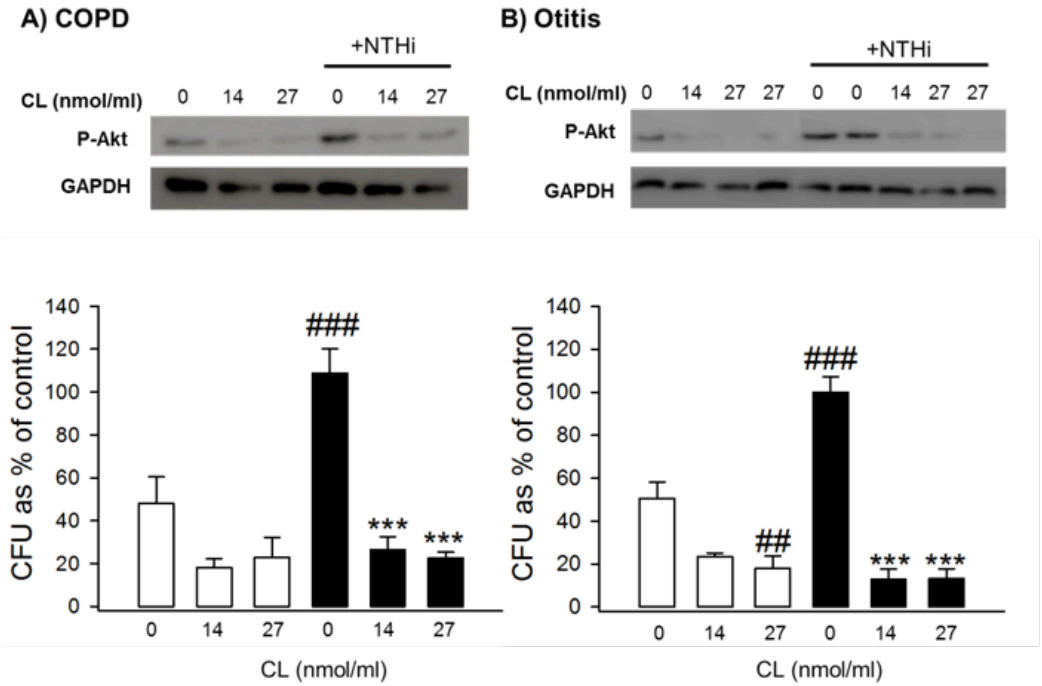

Figure 4.3.3. Low amounts of CL vesicles inhibit NTHi-elicited Akt phosphorylation. Cardiolipin vesicles were coadministrated with NTHi COPD (A) or otitis (B) to the cells for 1 hour. Phosphorylated Akt was detected by western blot and quantified by densitometry. NTHi-induced Akt phosphorylation in the absence of CL was considered as 100%. Data are expressed as mean percentages ± S.E. (### $p<0.001$ vs control; ## $p<0.010$ vs control; ***$p<0.001$ vs NTHi).

4.3.4. DISCUSSION

Non-typable *Haemophilus influenzae* is a Gram-negative bacteria which exists as a commensal of the nasopharynx but it can cause opportunistic infections in immunocompromised individuals. NTHi has been considered an extracellular pathogen but there is compelling evidence indicating that NTHi is able to invade epithelial cells [Virji *et al.*, 1991; Swords *et al.*, 2000]. Considering that intracellular

localization of NTHi favors its persistence [López-Gómez *et al.*, 2012], finding a molecule able to inhibit NTHi invasion of the epithelium would be crucial to counteract NTHi persistent or chronic infection. As depicted in Figure 4.3.2, the co-administration of CL vesicles with NTHi, inhibited NTHi internalization into murine pneumocytes without affecting bacterial adhesion to the cell surface. This fact reveals that the mechanism underlying to the protective effect of CL on NTHi infection compared to RSV infection is different. We have proved in the present thesis that CL inhibits viral replication through an extracellular mechanism by impairing viral particles docking to the cell surface (part 2 of results). In the case of NTHi infection, CL may be acting inside the cell blocking a key step of the intracellular signaling required for NTHi invasion. In fact, in this thesis, we proved that incubation of the cells in the presence of CL vesicles for 18 hours before LPS addition was as effective as coadministration of CL with LPS, which indicates that CL anti-inflammatory action takes place in the extracellular medium and also after its endocytosis as it is demonstrated in part 1 of results, Figure 4.1.3.

Given that NTHi internalization requires the phosphorylation of the serine-threonine kinase Akt mediated by PI3K [López-Gómez *et al.* 2012], we decided to analyzed CL action on NTHi-induced Akt phosphorylation. For both NTHi strains used isolated from patients suffering otitis and COPD, we found that CL inhibited NTHi-elicited Akt phosphorylation [Figure 4.3.3]. As we hypothesized in part 1 of Results, CL maybe directly blocking PI3K, another protein needed for Akt phosphorylation or some receptors upstream of these molecules.

NTHI binds to a variety of receptors on the host cell membrane. Among them, are found, Platelet-activating factor receptor (PAF-R), the betaglucan receptor and integrins α5 and β1. NTHi adhere to and enter to human epithelial cells via an interaction of lipooligosaccharide (LOS), a molecule similar to LPS, with PAF-R [Ketterer *et al.*, 1999; Swords *et al.*, 2000]. In fact, it was demonstrated that PAFR expression is upregulated in the respiratory epithelium of smokers and COPD patients. This enhaces NTHi and *Streptococcus* pneumoniae adherence to the surface of bronchial epithelium [Swords *et al.*, 2001]. In addition to PAFR, the β-glucan receptor (Dectin-1) also mediates NTHi internalization into the cells. Ahrén *et al.* found that adherence and phagocytosis of NTHI by monocytes, eosinophils and A549 AECs were both inhibited by the Dectin-1 antagonist laminarin [Ahrén *et al.*, 2001]. However, our results indicated that NTHi adhesion to the cell surface is not affected by CL. Therefore, it is unlikely that PAF-R and Dectin-1 are potential targets for CL.

López-Gómez and co-workers demonstrated that integrin α5 is needed both for

NTHi adhesion to and internalization into the host epithelial cells. However, β1 integrin inactivation, by gene silencing or blocking antibodies, leads to intact NTHi adhesion but impairs NTHi invasion [López-Gómez *et al.*, 2012]. Moreover, integrin activation elicits several signaling pathways including src, Rac1, PI3K-Akt and microtubules stabilization and polymerization [Caswell *et al.*, 2009; Huveneers and Danen., 2009]. Pharmacological inhibition of these pathways results in a diminished NTHi internalization [Morey *et al.*, 2011; López-Gómez *et al.*, 2012]. Since our results show that CL inhibits NTHi invasion but not adhesion to the epithelium surface and NTHi-induced Akt phosphorylation is inhibited by CL, it is possible that CL might target β1 integrin or its downstream signaling patways.

Many pathogens seek refuge inside host cells during infection. CL, due to its ability to inhibit bacterial internalization into pneumocytes, may lead to clinical benefits in persistent infections by NTHi or another bacteria that manipulate PI3K, Akt and/or microtubules reorganization to invade pneumocytes.

4.4. CARDIOLIPIN EFFECTS ON PULMONARY SURFACTANT

4.4.1. INTRODUCTION

Cardiolipin is present in the outer membrane of Gram-negative bacteria and the membrane of Gram-positive bacteria (around 10 and 25%, respectively) [Barák and Muchová, 2013]. In eukaryotic cells, CL is mainly located in the inner mitochondrial membrane (~ 20 %) [Krebs *et al.*, 1979; Zinser *et al.*, 1991; Paradies *et al.*, 2013]. Nevertheless, CL is also present in the outer mitochondrial membrane (~ 5%) and is enriched at contact sites between the inner and outer membrane [Daum 1985; Zinser *et al.*, 1991; Kroon *et al.*, 1997]. Unlike most naturally occurring phospholipids, CL is composed of two 1,2-diacylphosphatidate moieties esterified to the 1- and 3-hydroxyl groups of a glycerol. This results in a phospholipid with a small anionic headgroup and a large hydrophobic moiety formed by four acyl chains [Lewis and McElhaney, 2009; Unsay *et al.*, 2013] (Figure 4.4.1).

The chemical structure of CL confers this phospholipid the tendency to form nonlamellar structures involved in membrane processes [Dahlberg, 2007; Unsay *et al.*, 2013]. In fact, in the mitochondria, CL is essential for the production of ATP by oxidative phosphorylation. In addition, it participates in apoptosis and mitochondrial fusion and fission processes [Claypool and Koehler, 2012; Mayr, 2015; Kagan *et al.*, 2017; Maguire *et al.*, 2017]. The relevance of CL in cellular function is demonstrated by the existence of several pathologies associated with deficiency in CL biosynthesis and/or remodeling of their acyl chains [Acehan *et al.*, 2012; Claypool and Koehler, 2012; Lu *et al.*, 2016]. Despite its key role on cell function, molecular effects of CL on pulmonary surfactant membranes properties and function remains largely unknown.

Recently, it has been described that patients and mice with pneumonia present high levels of CL in the alveolar fluid. The chemical structure of CLs found in the bronchoalveolar fluid of these individuals is typical mammalian CL. This fact led to virtually rule out a bacterial origin. These investigators have also proved that high concentrations of CL impaired lung function, decreasing

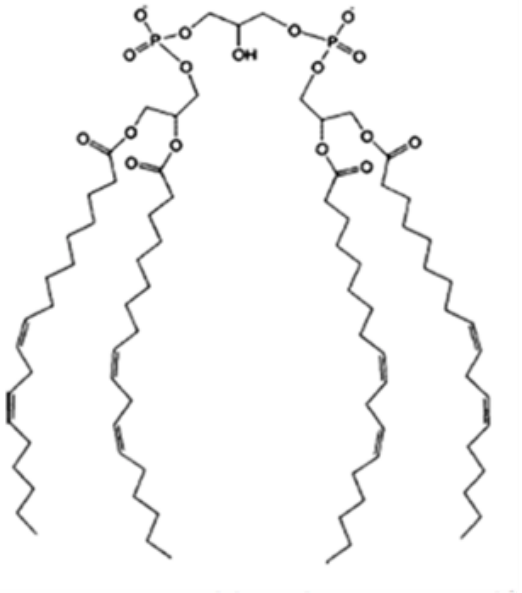

4.4.1. Cardiolipin molecular structure. Taken from Unsay *et al.*, 2013.

compliance and increasing lung elastance and resistance [Ray *et al.*, 2010].

Considering this prior information, the aim of this study was to investigate whether CL released from dying host cells to the alveolar fluid during infection could damage pulmonary surfactant membranes hampering its surface activity function.

4.4.2. EXPERIMENTAL DESIGN

We investigated the effect of CL on the function and physical properties of surfactant membranes employing different biophysical techniques (Figure 4.4.2). To determine CL action on surfactant function. To that end, we performed different experimental approaches: 1) CL was incorporated into lipid preparations of surfactant containing SP-B and SP-C (LES) at increasing molar ratios (0, 3, 6 and 12%) and mixed LES/CL multilamellar vesicles (MLVs) were prepared; 2) Small unilamellar vesicles of CL (SUVs) were prepared as described in materials and methods, and injected ten minutes before or co-inyected with MLVs of LES or NPS.

Moreover, we characterized the effect of CL incorporated into LES on the physical properties of LES by two different experimental techniques: DPH anisotropy and differential scanning calorimetry which provide information about lipid membrane order and membrane fluidity, respectively. Finally, we evaluated the ability of CL to insert into LES monolayers.

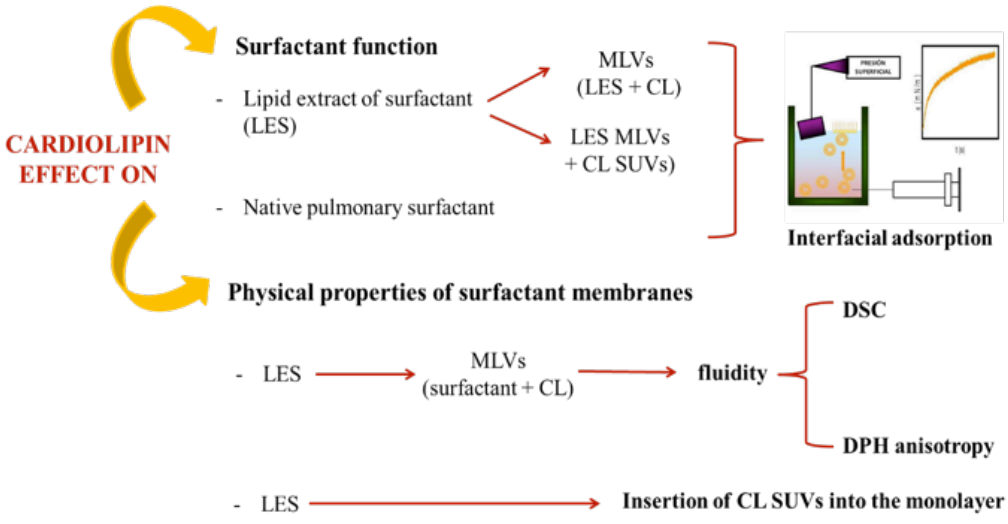

Figure 4.4.2. Experimental design used in this work. (MLVs: Multilamellamelar Vesicles; SUVs: Small Unilamellamelar Vesicles; DSC: Diferential Scanning Calorimetry; DPH: 1, 6-Diphenyl-1, 3, 5-hexatriene).

4.4.3. RESULTS

4.4.3.1. Surfactant inhibition by cardiolipin

To study CL effect on the ability of pulmonary surfactant to adsorb onto and spread at the air/liquid interface, we recorded the interfacial adsorption kinetics of NPS or LES in the absence or presence of CL injected simultaneously to surfactant (Figure 4.4.3A and 4.4.3B, blue symbols) or before surfactant injection into the aqueous subphase (1.5ml) (Figure 4.4.3A and 4.4.3B, pink symbols). LES MLVs quickly adsorbed to the air/liquid interface increasing the surface pressure up to an equilibrium value of 47 mN/m (Figure 4.4.3A, black symbols) as previously shown [Sáenz *et al.*, 2007; Sáenz *et al.*, 2010]. When CL and LES were simultaneously injected into the aqueous subphase, the maximum surface pressure and the adsorption rate decreased (Figure 4.4.3A, blue symbols), indicative of a CL-induced slight inhibition of the ability of surfactant membranes to adsorb onto and spread at an air/liquid interface. Nevertheless, when CL vesicles were injected into the aqueous subphase before LES injection, CL strongly inhibited surfactant adsorption (Figure 4.4.3, pink symbols). This inhibition must be due to competitive adsorption since CL vesicles showed interfacial activity (Figures 4.4.3A and 4.4.3B, purple symbols). On the other hand, co-injection of CL did not affect the interfacial adsorption of NPS (Figure 4.4.3B, blue symbols), whereas preinjection of CL strongly hampered the adsorption of NPS (Figure 4.4.3B, pink symbols).

In Figure 4.4.3C, we can appreciate that NPS (white bar) as well as LES (gray bar) in the absence of CL reached the equilibrium surface pressure after 30 minutes. CL co-inyected into the aqueous subphase prevented LES (gray zig-zag pattern bar) but not NPS (white zig-zag pattern bar) to attain the equilibrium surface pressure. However, when CL was inyected into the aqueous subphase10 minutes before prevent both, NPS (white balls pattern bar) and LES (white balls pattern bar) to reach the equilibrium surface pressure. This indicate that SP-A present in NPS protects NPS membranes from inhibition when NPS and CL vesicles were co-inyected. Nevertheless, SP-A was not able to avoid NPS inhibition when CL was inyected previously in the aqueous subphase.

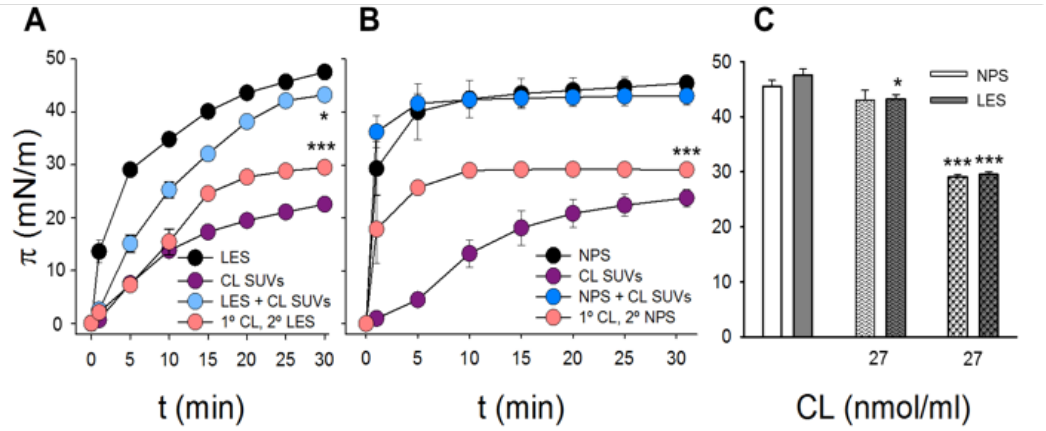

Figure 4.4.3. Inhibitory effect of CL on the interfacial adsorption of (A) LES or (B) NPS. Surface adsorption was assayed at a phospholipid concentration of 180 nmol/ml in the absence (•) and presence of CL (27 nmol/ml) simultaneously injected in the subphase with surfactant (•) or injected in the aqueous subphase before surfactant injection (•). Pure CL vesicles adsorbed onto the clean air-liquid interface (•). Data are expressed as means ± SE of three experiments. (C) Comparison of the equilibrium surface pressure attained after 30 min by NPS (white bar) and LES MLVs (gray bar), in the absence and presence of CL co-inyected with NPS or LES (zig-zag pattern) or CL injected into the subphase before NPS or LES injection (balls pattern). *** ($p<0.001$); * ($p < 0.050$) with respect to the control without CL.

Given that CL is miscible with DPPC [Sennato *et al.*, 2015], the major surfactant phospholipid [Casals and Cañadas, 2012], and DPPE [Sennato *et al.*, 2005], we next evaluated whether CL incorporation in surfactant membranes would alter their ability to adsorb onto an air/liquid interface at different molar percentages (6 and 12 %). The presence of increasing molar percentages of CL decreased the maximum surface pressure in a dose-dependent manner (Figure 4.4.4A and 4.4.4B), which indicates that the presence of CL in the composition of LES membranes inhibited the ability of surfactant membranes to adsorb onto and spread at an air/liquid interface. This effect may be due to a disturbing effect of CL on the structure of surfactant membranes.

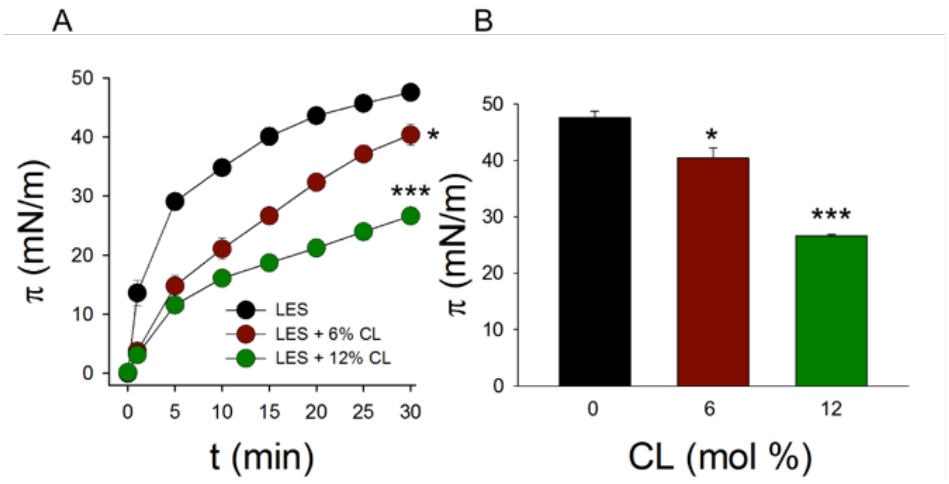

Figure 4.4.4. Incorporation of CL into LES vesicles inhibited their ability to adsorb onto and spread at an air/liquid interface. (A) Effect of the amount of CL incorporated into surfactant membranes on the adsorption kinetics of LES MLVs (180 μM PL): (•) 0 mol %; (•) 6 mol % ; and 12 mol % (•). Data are expressed as means ± SE of three experiments. (B) Effect of the amount of CL incorporated in LES MLVs on the maximum surface pressure attained after 30 min. *** ($p<0.001$); * ($p < 0.050$) with respect to the control without CL.

4.4.3.2. SP-A binds cardiolipin

SP-A is able to bind to a broad spectrum of ligands existing on the surface of microbes, such as LPS on Gram-negative bacteria, glycoprotein on fungi, lipoarabinomannan on mycobacteria, phospholipids on *Mycoplasma*, and glycoproteins on viral surface [Wright, 2005]. Since SP-A prevents surfactant inhibition by co-inyected CL [Figure 4.4.3B], it is conceivable that SP-A could bind free CL vesicles in the aqueous subphase preventing their interaction with surfactant membranes or their adsorption to the air- liquid interface. To test this hypothesis, we studied the ability of SP-A to bind CL employing fluorescence spectroscopy.

To that end, we recorded the intrinsic fluorescence emission spectrum of 15 nM SP-A in Tris-HCl 5mM buffer pH=7.4, containing NaCl 150 mM and CaCl2 150 μM using 295 nm excitation, before and after addition of increasing amounts of CL (Figure 4.4.5A). The emission spectrum of SP-A was characterized by a maximum at 338 nm (Figure 4.4.5A), due to the contribution of two conserved tryptophan residues located at positions 191 and 213 of the globular C-terminal domain [Casals *et al.*, 1993]. The addition of increasing amounts of CL resulted in a significant decrease in the amplitude of the emission spectrum of SP-A, without changes in its maximum emission wavelength (Figures 4.4.5A and 4.4.5B). This indicates that SP-A binds to CL. Figure 4.4.5B shows the intensity data from titration of 15 nM SP-A with CL at

338 nm. By fitting the titration data to equation 3.3, a Kd value of 2.2 ± 0.4 nM was obtained. These results allow us to suggest that SP-A present in NPS would bind to CL free vesicles protecting surfactant membranes from inhibition.

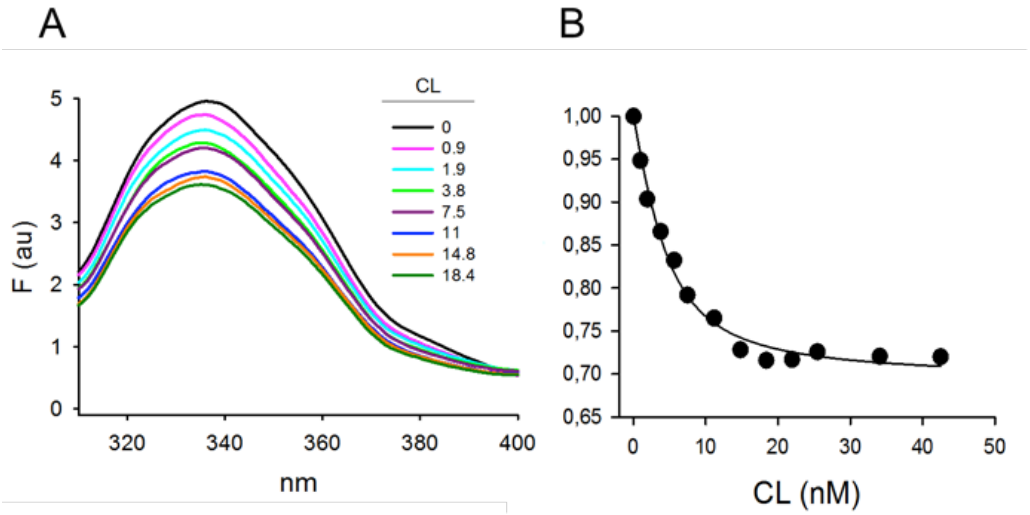

Figure 4.4.5. SP-A is able to bind cardiolipin vesicles. (A) Fluorescence emission spectra of SP-A (15 nM) recorded in the absence (black line) or the presence increasing amounts of CL (0 to 20 nM, colored lines) at 25 °C in 5 mM Tris-HCl buffer (pH 7.4) containing 150 mM NaCl and 150μM of CaCl2. (B) Fitting of the equilibrium binding titration data expressed as F/F0, where F0 is the observed intensity of pure SP-A and F, the intensity of SP-A in the presence of increasing amounts of CL. Results are means ± SE of three independent experiments (B).

4.4.3.3. Cardiolipin is able to insert into surfactant monolayers

Next, we determined whether CL is capable of inserting into LES monolayers by measuring the increase in the lipid monolayer surface pressure at a given initial pressure (Figure 4.4.6). An increase in pressure (π) indicates that CL is able to insert into the monolayer. Given that CL incorporation into LES membranes impairs their proper interfacial adsorption, we determined whether CL present in the alveolar fluid could be incorporated into surfactant membranes.

To carry out these experiments, the monolayer of LES was formed by spreading LES dissolved in chloroform:methanol (2:1) and allowing its total evaporation. Once the monolayer was formed, the pressure increases due to the presence of lipids at the interface. A certain amount of lipid was deposited (different each time), therefore different pressure values were reached for each amount of lipid. Then, CL was injected into the subphase and the variation of the surface pressure as a function of time was monitored. As we can observe, the surface pressure increased in the

presence of CL. When the monolayer is formed, CL was injected into the aqueous subphase. This increase is lower as the amount of LES deposited in the subphase increased. That is why, as the amount of LES increased, less CL molecules fit in the interface until no more could be incorporated. By plotting the surface pressure increase induced by the insertion as a function of initial surface pressure ($\Delta\pi = \pi e - \pi i$), the maximum insertion pressure (MIP) for CL could be obtained by extrapolation of the regression line to a surface pressure increase equal to zero. This pressure indicates the maximum πi above which no more CL molecules were able to penetrate into a LES membranes and increase surface pressure.

We have obtained a MIP value of 28 mN/m for CL insertion into LES monolayers. Considering that the estimated lateral pressure for a biological membrane is around 30 mN/m [Marsh, 1996]. Our data suggest that CL could be capable of inserting into LES membranes.

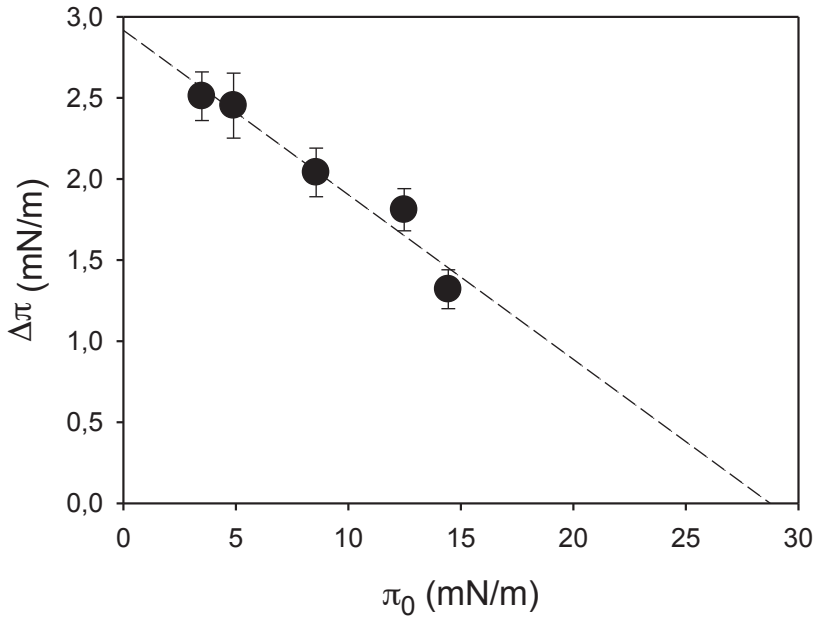

Figure 4.4.6. CL is capable of inserting into LES monolayers. LES monolayers were formed by spreading different amounts of a concentrated solution of LES (1 mg/ml) at the air-water interface of the subphase buffer (5 mM Tris buffer, pH 7.4, 150 mM NaCl and 0.175 mM CaCl2) to give the indicated initial surface pressures (0 to 13 mN/m). Then, CL was injected into the subphase and CL-induced changes in the monolayer surface pressure at constant surface area were measured using a thermostated Langmuir-Blodgett trough. Straight line was obtained by linear regression of the experimental data. Results are means ± SE of three independent experiments.

4.4.3.4. Cardiolipin effect on the physical properties of surfactant membranes in the absence and presence of SP-A.

Given that the incorporation of CL into LES membranes strongly inhibited their interfacial adsorption (Figure 4.4.4), we evaluated the effect of CL on the physical properties of LES membranes. To that end, we studied the thermotropic properties of LES membranes. LES MLVs exhibited an endothermic transition with a gel/liquid crystalline transition temperature, Tm, of approximately 44.4 ± 0.2ºC and a transition enthalpy of 2.7 ± 0.1 kcal/mol (Figure 4.4.7A and Table 4.4.1). As the amount of CL incorporated into LES MLVs increased, both the Tm and the transition enthalpy decreased (Table 4.4.1). This indicates that CL fluidizes surfactant membranes and decreases van der Waals interactions among adjacent surfactant lipid molecules. Figure 4.4.7B shows that, in the presence of CL, the emission anisotropy of DPH decreases. The lack of changes in the fluorescence of the probe in the presence of CL (data not shown) allows us to infer that CL decreases the lipid order of LES. Given that SP-A prevents surfactant inhibition by co-inyected CL vesicles as described above, we evaluated the potential protective effect of SP-A against CL incorporation in LES membranes. Figure 4.4.7 shows that SP-A (2.5 wt % SP-A) did not counteract the effect of CL 6 mol % on either the thermotropic properties (Figure 4.4.7A) or the lipid order (Figure 4.4.7B) of LES membranes.

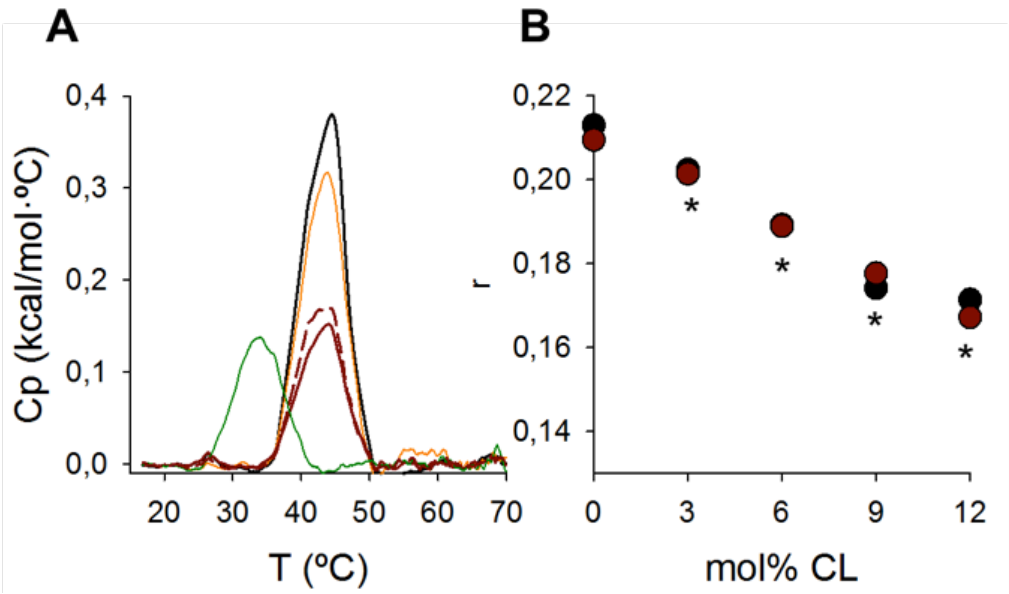

Figure 4.4.7. Cardiolipin effect on the surfactant membranes thermotropic behavior (A) and lipid order (B) in the absence or presence of SP-A. (A) DSC scans of mixed MLVs of LES containing increasing molar percentages of CL were recorded : 0 mol % (—), 3% mol (—), 6 mol % (—), 12 mol % (—) and 6 mol %. Dashed line shows that addition of 2.5 % SP-A (w/w) to the samples containing 6 mol % CL did not alter DSC trace. Calorimetric scans were performed at a scanning rate of 0.5ºC/min. Data shown are the means of three thermograms

± S.E. (B) CL in the absence (•) diminished the lipid order of LES membranes. This effect was not reverted by SP-A (•) The emission anisotropy of DPH was measured with excitation at 360 nm and emission at 430 nm. Data shown are the means of three independent measurements. All measurements were performed at 25 ± 0.1ºC. * ($p < 0.05$) between LES in the absence and presence of CL.

	ΔH (kcal/mol ºC)	Tm (ºC)
LES	2.7 ± 0.1	44.4 ± 0.2
+ CL (3% mol)	2.40 ± 0.02	43.4 ± 0.1
+ CL (6% mol)	1.3 ± 0.1	43.8 ± 0.2
+ CL (12% mol)	1.18 ± 0.09	34 ± 2
+ CL (6% mol) + SP-A	1.4 ± 0.1	44.4 ± 0.3

4.4.5. DISCUSSION

Cardiolipin is a unique phospholipid with a dimeric structure, having four acyl chains and potentially carrying two negative charges [Haines, 2009]. CL is present in bacterial membranes [Barák and Muchová, 2013] and in eukaryotic organisms, where it is mainly found in the inner [Krebs *et al.*, 1979; Zinser *et al.*, 1991 Paradies *et al.*, 2013] but also in the outer mitochondrial membrane [Daum 1985; Zinser *et al.*, 1991; Kroon *et al.*, 1997]. CL is typically a minor component of pulmonary lavage fluid and comprises only ~1–2% of surfactant [Ray *et al.*, 2010; Agassandian and Mallampali, 2013]. Ray and Co-workers determined that in human and mice with pneumonia, CL levels were increased in the bronchoalveolar lavage. CL acyl chain composition appeared to be from human rather than bacterial origin. They have also demonstrated that in a mouse model of bacteria-induced lung injury, high concentrations of CL impaired lung function, decreasing compliance and increasing lung elastance and resistance. Moreover, these investigators have demonstrated that incorporation of CL into infasurf, a commercial apoprotein-containing surfactant, hampered the surface tension-lowering ability of this surfactant *in vitro* [Ray *et al.*, 2010].

Therefore, the aim of this work was to characterize the mechanism by which CL inhibits surfactant function and to evaluate the protective role of SP-A against CL-induced surfactant inactivation.

In this work, we determined that CL vesicles slightly inhibit the surface adsorption of surfactant preparations lacking SP-A (LES) by competitive adsorption (Figure 4.4.3A) and by fluidization of surfactant membranes (Figure 4.4.4). CL vesicles

(Figures 4.4.3A) as many biologic molecules, including tissue and blood proteins, inflammation specific proteins and fatty acids among others, adsorb to the air-water interface and compete with lung surfactant for the interface [Wang and Notter, 1998; Taeusch *et al.*, 2005; Zasadzinski *et al.*, 2005; Zuo *et al.*, 2008]. As we could see in Figure 4.3A, free CL vesicles in the aqueous subphase delayed the adsorption of LES at the air-water interface (Figure 4.4.3A). This effect is similar to that observed for fibrinogen and albumin via competitive adsorption by Gunasekara and co-workers [Gunasekara *et al.*, 2007].

In addition to competitive adsorption, CL molecules could be incorporated into LES membranes inhibiting their function in a similar way to that determined for C-reactive protein [Sáenz *et al.*, 2010].

Results shown in Figure 4.4.4 demonstrate that incorporation of CL molecules in LES vesicles (Figure 4.4.5) hampers their ability to adsorb onto and spread at an air-liquid interface. When CL is incorporated in LES MLVs, its bulky structure impeded DPPC packing [Ray *et al.*, 2010].

Sennato and co-workers studied the interaction of PC, PE and CL using mixed monolayers of saturated DPPC or DPPE in the presence or absence of fully unsaturated CL. They found that DPPC, the main surfactant phospholipid [Cañadas and Casals, 2012], was miscible with CL whereas DPPE did not. Moreover, they pointed that the different behavior is due to the polar head, because they proved that unsaturated egg PC is also miscible with CL [Sennato *et al.*, 2005]. CL is also miscible with POPG and DPPG [Wydro, 2013].

Given that CL is miscible with DPPC and repulsions occur between DPPC and CL molecules [Sennato *et al.*, 2005], van der Walls interactions between phospholipids decrease. This fact agrees with the increase of fluidity and decrease of lipid order of LES membranes as amount of CL incorporated into LES membranes increased (Figure 4.4.7 and Table 4.4.1). By containing a high proportion of unsaturated acyl chains (more than 95%) [Niemelä *et al.* 2006] or maybe by establishing interactions with surfactant components, CL may render the membranes more fluid and less ordered.

In agreement with the results shown in Figure 4.4.7 and Table 4.4.1, it has been described that the fluidity of pure L-α-phosphatidylcholine from egg (EPC) membranes increased with the CL concentration. Moreover, they proved that CL also

increased the fluidity of membranes mimicking the mitochondrial outer membrane composition and decreased their mechanical stability, indicating that CL decreases the packing of the membranes [Unsay *et al.* 2013].

Our data suggest that CL could be incorporated into LES membranes (Figure 4.4.6). Nevertheless, further experiments should be conducted to insure it. We propose that CL might be incorporated into surfactant membranes during surfactant recycling by type II pneumocytes [Agassandian and Mallampali, 2013] or directly, due to the fusion of CL vesicles with those of surfactant, since CL vesicles fuse in the presence of calcium [Ortiz *et al.*, 1999].

Another focus of this study was to investigate SP-A´s effect on surfactant inhibition by CL. SP-A is able to bind a broad spectrum of ligands and is mainly involved in the immune innate defense in the alveoli [Wright, 2005]. We proved that NPS, which contains SP-A, is not inhibited when co-inyected with CL SUVs in the air/liquid subphase (Figure 4.4.3B). These data allow us to hypothesize that SP-A could counteract the slight inhibitory effect observed in the case of LES, probably due to the ability of SP-A to accelerate surfactant adsorption [Schürch *et al.*, 1992; Casals, 2001]. It is well known that adding non-surface active hydrophilic polymers to the subphase provides a depletion attraction between surfactant aggregates and the interface, which can overcome the steric and electrostatic resistance to adsorption induced by serum and albumin among other substances [Zasadzinski *et al.*, 2005; Lu *et al.*, 2000; Taeusch *et al.*, 1999]. SP-A is a natural hydrophilic polymer which can enhance adsorption to eliminate surfactant inactivation by CL as it is described for serum [Zasadzinski *et al.*, 2005].

In addition, SP-A binding to CL (Figure 4.4.5) might block CL interaction with surfactant membranes as it has been described in our research group for beta-glucan (unpublished data) or impairs CL incorporation into LES as it has been reported for CRP [Sáenz *et al.*, 2010].

On the other hand, we proved that when CL is incorporated into LES membranes, SP-A did not revert effect on CL´s effects on LES physical properties (Figure 4.4.7). It has been described that SP-A promotes solid/fluid phase coexistence in model surfactant membranes lacking colesterol (DPPC/POPG/PA) which ameliorates membranes physical properties and their surfactant activity. Nevertheless, phase coexistence is characteristic of LES both in the presence as in the absence of SP-A [Sáenz *et al.*, 2007].

In summary, our results highlight an inhibitory action for CL at high doses on lung surfactant function. CL action takes place by two different mechanisms: (i) competitive adsorption, in which CL competes with surfactant for the air-liquid interface, (ii) a fluidizing effect of CL on surfactant membranes. Furthermore, we proved that SP-A is able to counteract the slight inhibitory effect caused by free CL vesicles in the aqueous subphase but if CL forms part of the composition of LES, SP-A did not revert CL effect on LES physical properties

V. CONCLUSIONS

The research presented in this doctoral thesis highlights the dual effect of cardiolipin (CL) in the alveolus in function of the dose. Low amounts of CL are beneficial for the host, acting as an anti-infectious and anti-inflammatory agent, whereas higher doses are harmful, affecting lung surfactant function and cell viability. The results compiled in this thesis allow us to conclude that:

1. CL vesicles either simultaneously added with the proinflammatory stimulus or preincubated with cells before stimulation present a strong immunomodulatory effect at low doses on the inflammatory response of alveolar macrophages. We have proved that the anti-inflammatory action of CL is not restricted to a particular stimulus, and occurs both extra- and intracellularly likely by different mechanisms. On the surface of alveolar macrophages, CL might impair LPS or zymosan binding to their respective receptors. Once internalized by cells, CL might modify the expression of cellular receptors and molecules involved in cell response.

2. Extracellular CL vesicles exert antiviral and anti-inflammatory properties against RSV infection of human alveolar epithelial cells (AECs). CL antiviral action is carried out exclusively in the extracellular medium, whereas its anti-inflammatory properties were preserved once endocytosed by AECs. In the extracellular medium, CL inhibits RSV replication and the subsequent inflammatory response by interfering with viral particles docking to the cell surface. Moreover, we proved that CL antiviral action is maintained in the presence of lung surfactant components.

3. The co-administration of CL vesicles with non-typable *Haemophilus influenzae* (NTHi) inhibits NTHi internalization by murine AECs without affecting bacterial adhesion to the cell surface. CL action occurs via inhibition of Akt phosphorylation, a mechanism necessary for bacterial invasion of the epithelium.

4. Higher doses of CL than those used in experiments with cells exert an inhibitory action on lung surfactant function. CL action takes place by two different mechanisms: (i) competitive adsorption, in which CL competes with surfactant for the air-liquid interface; and (ii) a fluidizing effect of CL on surfactant membranes. Furthermore, we proved that surfactant protein Ç A is able to counteract the slight inhibitory effect caused by free CL vesicles in the aqueous subphase but did not show any effect when CL forms part of the composition of surfactant vesicles.

VI. REFERENCES

Abate W, Alghaithy AA, Parton J, Jones KP, Jackson SK. (2010). Surfactant lipids regulate

LPS-induced interleukin-8 production in A549 lung epithelial cells by inhibiting translocation of TLR4 into lipid raft domains. J Lipid Res. 51(2):334-344.

Abraham E. (2003) Neutrophils and acute lung injury. Crit Care Med. 31(Suppl 4): S195-S199.

Acehan D, Vaz F, Houtkooper RH, James J, Moore V, Tokunaga C, Kulik W, Wansapura J, Toth MJ, Strauss A, Khuchua Z. (2011) Cardiac and skeletal muscle defects in a mouse model of human Barth syndrome. J Biol Chem. 286(2):899-908.

Agassandian M and Mallampalli RK. (2013) Surfactant phospholipid metabolism. Biochim Biophys Acta, 1831(3):612-625.

Ahrén IL, Williams DL, Rice PJ, Forsgren A, Riesbeck K. (2001) The importance of a beta-glucan receptor in the nonopsonic entry of nontypeable *Haemophilus influenzae* into human monocytic and epithelial cells. J Infect Dis. 184(2):150-158.

Akira S and Sato S. (2003) Toll-like receptors and their signaling mechanisms. Scand J Infect Dis. 35(9):555-562.

Alexopoulou LA, Holt C, Medzhitov R, Flavell RA. (2001) Recognition of double-stranded RNA and activation of NF-kappaB by Toll-like receptor 3. Nature. 413(6857):732-738.

Ariki S, Nishitani C, Kuroki Y. (2012) Diverse functions of pulmonary collectins in host defense of the lung. J Biomed Biotechnol. 2012:532071.

Augusto L, Le Blay K, Auger G, Blanot D, Chaby R. (2001) Interaction of bacterial lipopolysaccharide with mouse surfactant protein C inserted into lipid vesicles. Am J Physiol Lung Cell Mol Physiol. 281(4): L776-785.

Augusto LA, Li J, Synguelakis M, Johansson J, Chaby R. (2002) Structural basis for interactions between lung surfactant protein C and bacterial lipopolysaccharide. J Biol Chem, 277(26):23484-23492.

Avery ME and Mead J. (1959) Surface properties in relation to atelectasis and hyaline membrane disease. AMA J Dis Child. 97(5, Part 1):517-523.

Baile MG, Whited K, Claypool SM. (2013) Deacylation on the matrix side of the mitochondrial inner membrane regulates cardiolipin remodeling. Mol Biol Cell. 24(12):2008-20.

Bakker SE, Duquerroy S, Galloux M, Loney C, Conner E, Eléouët JF, Rey FA, Bhella D. (2013) The respiratory syncytial virus nucleoprotein-RNA complex forms a left-handed helical nucleocapsid. J Gen Virol. 94, 1734-1738.

Balasubramanian K, Maeda A, Lee JS, Mohammadyani D,……, Mallampalli RK, Bayir H, Fadeel B, Kagan VE. 2015 Dichotomous roles for externalized cardiolipin in extracellular signaling: Promotion of phagocytosis and attenuation of innate immunity. Sci Signal. 8(395):ra95.

Ballard PL, Nogee LM, Beers MF, Ballard RA, Planer BC, Polk L, deMello DE, Moxley MA, Longmore WJ. (1995) Partial deficiency of surfactant protein B in an infant with chronic lung disease. Pediatrics. 96(6):1046-1052.

Barák I and Muchová K. (2013) The Role of Lipid Domains in Bacterial Cell Processes. Int J Mol Sci .14(2):4050-4065.

Barik, S. (2013) Respiratory syncytial virus mechanisms to interfere with type 1 interferons. Curr Top Microbiol Immunol. 372:173-191.

Barrios-Rodiles M, Tiraloche G, Chadee K. (1999) Lipopolysaccharide modulates cyclooxygenase-2 transcriptionally and posttranscriptionally in human macrophages independently from endogenous IL-1 beta and TNF-alpha. J Immunol. 163(2):963-969.

Bazan S, Mileykovskaya E, Mallampalli VK, Heacock P, Sparagna GC, Dowhan W. (2013) Cardiolipin-dependent reconstitution of respiratory supercomplexes from purified *Saccharomyces cerevisiae* complexes III and IV, J. Biol. Chem. 288(1): 401-411.

Becker MN, Diamond G, Verghese MW, Randell SH. (2000) CD14-dependent lipopolysaccharide-induced beta-defensin-2 expression in human tracheobronchial epithelium. J Biol Chem. 275(38):29731-29736.

Ben-Ami R, Lewis RE, Kontoyiannis DP. (2010) Enemy of the (immunosuppressed) state: an update on the pathogenesis of Aspergillus fumigatus infection. Br J Haematol. 150(4):406-417.

Bermingham A and Collins PL. (1999) The M2-2 protein of human respiratory syncytial virus is a regulatory factor involved in the balance between RNA replication and transcription. Proc Natl Acad Sci USA. 96(20):11259-11264.

Beyer M, Bartz H, Horner K, Doths S, Koerner-Rettberg C, Schwarze J (2004). Sustained increases in numbers of pulmonary dendritic cells after respiratory syncytial virus infection. J Allergy Clin Immunol. 113(1):127–133.

Bligh EG and Dyer WJ. (1959) A rapid method of total lipid extraction and purification. J Biochem Physiol. 37(8): 911-917.

Bochkov, VN, Kadl A, Huber J, Gruber F, Binder BR, Leitinger N. (2002) Protective role of phospholipid oxidation products in endotoxin-induced tissue damage. Nature. 419(6902):77-81.

Bohannon JK, Hernandez A, Enkhbaatar P, Adams WL, Sherwood ER. (2013) The Immunobiology of TLR4 Agonists: From Endotoxin Tolerance to Immunoadjuvants. Shock (Augusta, Ga). 40(6):451-462.

Borron P, McIntosh JC, Korfhagen TR, Whitsett JA, Taylor J, Wright JR (2000). Surfactant-associated protein A inhibits LPS-induced cytokine and nitric oxide production *in vivo*. Am J Physiol Lung Cell Mol Physiol. 278(4): L840-L847.

Bossert B, Marozin S, Conzelmann KK. (2003) Nonstructural proteins NS1 and NS2 of bovine respiratory syncytial virus block activation of interferon regulatory factor 3. J Virol. 77(16):8661-8668.

Bourgeois C, Bour JB, Lidholt K, Gauthray C, Pothier P. (1998) Heparin-like structures on respiratory syncytial virus are involved in its infectivity *in vitro*. J Virol. 72(9):7221-7227.

Buchholz UJ, Finke S, Conzelmann KK. (1999) Generation of bovine respiratory syncytial virus (BRSV) from cDNA: BRSV NS2 is not essential for virus replication in tissue culture, and the human RSV leader region acts as a functional BRSV genome promoter. J Virol.73(1):251-259.

Cañadas O and Casals C. (2013) Differential scanning calorimetry of protein-lipid interactions. Methods Mol Biol. 974:55-71.

Cañadas O, Guerrero R, Garcia-Canero R, Orellana G, Menendez M, Casals C. (2004) Characterization of liposomal tacrolimus in lung surfactant-like phospholipids and evaluation of its immunosuppressive activity. Biochemistry. 43(30):9926-9938.

Carter SD, Dent KC, Atkins E, Foster TL, Verow M, Gorny P, Harris M, Hiscox JA, Ranson NA, Griffin S, Barr JN. (2010) Direct visualization of the small hydrophobic protein of human respiratory syncytial virus reveals the structural basis for membrane permeability. FEBS Lett. 584(13):2786-2790.

Casals C. (2001) Role of surfactant protein A (SP-A)/lipid interactions for SP-A functions in the lung. Pediatr Pathol Mol Med. 20(4):249-268.

Casals C and Cañadas O. (2012) Role of lipid ordered/disordered phase coexistence in pulmonary surfactant function. Biochim Biophys Acta. 1818(11):2550-2562.

Casals C, Miguel E, and Perez-Gil J. (1993) Tryptophan fluorescence study on the interaction of pulmonary surfactant protein A with phospholipid vesicles. The Biochemical journal. 296 (Pt 3): 585-593.

Castranova V, Rabovsky J, Tucker JH, Miles PR. (1988) The alveolar type II epithelial cell: a multifunctional pneumocyte. Toxicol Appl Pharmacol. 93(3):472-83.

Caswell PT, Vadrevu S, Norman JC. (2009) Integrins: masters and slaves of endocytic transport. Nat Rev Mol Cell Biol. 10(12):843-853.

Chaby R, Garcia-Verdugo I, Espinassous Q, Augusto LA. (2005) Interactions between LPS and lung surfactant proteins. J Endotoxin Res. 11(3):181-185.

Chatfield KC, Sparagna GC, Sucharov CC, Miyamoto SD, Grudis JE, Sobus RD, Hijmans J, Stauffer BL. (2014) Dysregulation of cardiolipin biosynthesis in pediatric heart failure. J Mol Cell Cardiol. 74:251-259.

Chirkova T, Boyoglu-Barnum S, Gaston KA, Malik FM, Trau SP, Oomens AG, Anderson JL. (2013) Respiratory syncytial virus G protein CX3C motif impairs human airway epithelial and immune cell responses. J Virol. 87(24):13466-13479.

Chroneos ZC, Sever-Chroneos Z, Shepherd VL (2010). Pulmonary surfactant: an immunological perspective. Cell Physiol Biochem. 25(1):13-26.

Chu CT, Ji J, Dagda RK, Jiang JF,……,Bahar I, Bayır H, Kagan VE. (2013) Cardiolipin externalization to the outer mitochondrial membrane acts as an elimination signal for mitophagy in neuronal cells. Nat Cell Biol. 15(10):1197-1205.

Cighetti R, Ciaramelli C, Sestito SE, Zanoni I, Kubik Ł, Ardá-Freire A, Calabrese V, Granucci F, Jerala R, Martín-Santamaría S, Jiménez-Barbero J, Peri F. (2014) Modulation of CD14 and TLR4-MD-2 activities by a synthetic lipid A mimetic. Chembiochem. 15(2):250-258.

Claypool SM and Koehler CM. (2012) The complexity of cardiolipin in health and disease. Trends Biochem Sci. 37(1):32-41.

Cohen J. (2002) The immunopathogenesis of sepsis. Nature. 420(6917):885-891.

Collins PL and Crowe JEJ (2007). Respiratory syncytial virus and metapneumovirus.1601-1646. In Knipe DM, Howley PM, Griffin DE, Lamb RA, Martin MA, Roizman B, and Straus SE. Fields virology. 5th ed. Lippincott Williams & Wilkins, Philadelphia, PA.

Collins PL and Graham BS. (2008) Viral and host factors in human respiratory syncytial virus pathogenesis. J Virol.82(5):2040-2055.

Collins PL and Melero JA. (2011) Progress in understanding and controlling respiratory syncytial virus: still crazy after all these years. Virus Res. 162(1-

2):80-99.

Collins PL and Mottet G. (1993) Membrane orientation and oligomerization of the small hydrophobic protein of human respiratory syncytial virus. J Gen Virol. 74(Pt 7):1445-1450

Collins PL, Fearns R, Graham BS. (2013) Respiratory syncytial virus: virology, reverse genetics, and pathogenesis of disease. Curr Top Microbiol Immunol. 372:3-38.

Collins PL, Huang YT, Wertz GW. (1984) Identification of a tenth mRNA of respiratory syncytial virus and assignment of polypeptides to the 10 viral genes. J Virol. 49(2): 572-578.

Collins PL and Wertz GW. (1983) cDNA cloning and transcriptional mapping of nine polyadenylylated RNAs encoded by the genome of human respiratory syncytial virus. Proc Natl Acad Sci USA. 80(11):3208-3212.

Crapo JD, Barry BE, Gehr P, Bachofen M, Weibel ER (1982). Cell number and cell characteristics of the normal human lung. Am Rev Respir Dis. 125(6):740-745.

Dagenais TR and Keller NP (2009). Pathogenesis of Aspergillus fumigatus in Invasive Aspergillosis. Clin Microbiol Rev. 22(3):447-465.

Dahlberg M (2007). Polymorphic phase behavior of cardiolipin derivatives studied by coarse-grained molecular dynamics. J Phys Chem B. 111(25):7194-200.

Dasaraju PV and Liu C (1996). Infections of the Respiratory System. In Medical Microbiology, 4th ed. S Baron, ed, Galveston (TX).

Daum G. (1985) Lipids of mitochondria. Biochim Biophys Acta. 822(1):1-42.

de Kroon AI, Dolis D, Mayer A, Lill R, de Kruijff B. (1997) Phospholipid composition of highly purified mitochondrial outer membranes of rat liver and Neurospora crassa. Is cardiolipin present in the mitochondrial outer membrane? Biochim Biophys Acta. 1325(1):108-116.

DiCarlo FJ, Fiore JV. (1958) On the composition of zymosan. Science. 127(3301):756-757.

Dixon PM, McGorum BC, Marley C, Halliwell RE, Matthews AG, Morris JR. (1996) Effects of equine influenza and tetanus vaccination on pulmonary function in normal and chronic obstructive pulmonary disease affected horses. Equine Vet J. 28(2):157-160.

Dochow M, Krumm SA, Crowe JE, Jr, Moore ML, Plemper RK. (2012) Independent structural domains in paramyxovirus polymerase protein. J Biol Chem. 287(9):6878-6891.

Duell BL, Su YC, Riesbeck K. (2016) Host-pathogen interactions of nontypeable *Haemophilus influenzae*: from commensal to pathogen. FEBS Lett. 590(21):3840-3853.

Dupuy LC, Dobson S, Bitko V, and Barik S. (1999) Casein kinase 2-mediated phosphorylation of respiratory syncytial virus phosphoprotein P is essential for the transcription elongation activity of the viral polymerase; phosphorylation by casein kinase 1 occurs mainly at Ser215 and is without effect. J Virol. 73 (10):8384-8392.

Elliott J, Lynch OT, Suessmuth Y, Qian P, Boyd CR, Burrows JF, Buick R, Stevenson NJ, Touzelet O, Gadina M, Power UF, Johnston JA. (2007) Respiratory syncytial virus NS1 protein degrades STAT2 by using the Elongin-Cullin E3 ligase. J Virol. 81(7):3428-3436.

Evans MJ and Hackney JD. (1972) Cell proliferation in lungs of mice exposed to elevated concentrations of oxygen. Aerosp Med. 43(6):620-622.

Farhat K, Riekenberg S, Heine H, Debarry J, Lang R, Mages J, Buwitt-Beckmann U, Roschmann K, Jung G, Wiesmuller KH, Ulmer AJ. (2008) Heterodimerization of TLR2 with TLR1 or TLR6 expands the ligand spectrum but does not lead to differential signaling. J Leukoc Biol. 83(3):692-701.

Fearns R and Collins PL. (1999) Role of the M2-1 transcription antitermination protein of respiratory syncytial virus in sequential transcription. J Virol. 73(7):5852-5864.

Fearns R and Deval J. (2016) New antiviral approaches for respiratory syncytial virus and other mononegaviruses: Inhibiting the RNA polymerase. Antiviral Res. 134(1):63-76.

Feldman SA, Audet S, Beeler JA. (2000) The fusion glycoprotein of human respiratory syncytial virus facilitates virus attachment and infectivity via an interaction with cellular heparan sulfate. J. Virol. 74(14): 6442-6447.

Few AV, Gilby AR, Seaman GV. (1960) An electrophoretic study on structural components of Micrococcus lysodeikticus. Biochim Biophys Acta. 38(1):130-136.

Finberg RW and Kurt-Jones EA. (2006) CD14: chaperone or matchmaker? Immunity. 24(2):127-129.

Flint SJ, Enquist LW; Krug RM, Racaniello VR, Skalka AM. (2000) Principles of Virology: Molecular Biology, Pathogenesis and Control. A S M

Press. Washington D C. 663-713.

Fong AM, Robinson LA, Steeber DA, Tedder TF, Yoshie O, Imai T, Patel DD. (1998) Fractalkine and CX3CR1 mediate a novel mechanism of leukocyte capture, firm adhesion, and activation under physiologic flow. J Exp Med. 188(8):1413-1419.

Gan, SW, Ng L, Lin X, Gong X, Torres J. (2008) Structure and ion channel activity of the human respiratory syncytial virus (hRSV) small hydrophobic protein transmembrane domain. Protein Sci. 17(5):813-820

Ganesan S, Comstock AT, and Sajjan US. (2013) Barrier function of airway tract epithelium. Tissue barriers. 1(4): e24997.

Gantner BN, Simmons RM, Canavera SJ, Akira S, Underhill DM (2003). Collaborative induction of inflammatory responses by dectin-1 and Toll-like receptor 2. J Exp Med ;197(9):1107-1117.

Garcia J, Garcia-Barreno B, Vivo A, Melero JA. (1993) Cytoplasmic inclusions of respiratory syncytial virus-infected cells: formation of inclusion bodies in transfected cells that coexpress the nucleoprotein, the phosphoprotein, and the 22K protein. Virology. 195(1): 243-247.

Geertsma MF, Nibbering PH, Haagsman HP, Daha MR, van Furth R. (1994) Binding of surfactant protein A to C1q receptors mediates phagocytosis of *Staphylococcus aureus* by monocytes. Am J Physiol. 267(5 Pt 1): L578-584.

Ghildyal R, Mills J, Murray M, Vardaxis N, Meanger J. (2002) Respiratory syncytial virus matrix protein associates with nucleocapsids in infected cells. J Gen Virol. 83(Pt 4):753-757.

Giard DJ, Aaronson SA, Todaro GJ, Arnstein P, Kersey JH, Dosik H, Parks WP. (1973) *In vitro* cultivation of human tumors: establishment of cell lines derived from a series of solid tumors. J Natl Cancer Inst. 51(5):1417-1423.

Glass CK and Ogawa S. (2006) Combinatorial roles of nuclear receptors in inflammation and immunity. Nat Rev Immunol. 6(1):44-55.

Glasser SW, Senft AP, Whitsett JA, Maxfield MD, Ross GF, Richardson TR, Prows DR, Xu Y, Korfhagen TR. (2008) Macrophage dysfunction and susceptibility to pulmonary *Pseudomonas aeruginosa* infection in surfactant protein C-deficient mice. J Immunol. 181(1):621-628.

Glasser SW, Witt TL, Senft AP, Baatz JE, Folger D, Maxfield MD, Akinbi HT, Newton DA, Prows DR, Korfhagen TR. (2009) Surfactant protein C-deficient mice are susceptible to respiratory syncytial virus infection. Am J Physiol Lung Cell Mol Physiol. 297(1): L64-72.

Goerke J. (1998) Pulmonary surfactant: functions and molecular composition. Biochim Biophys Acta. 1408 (2-3): 79-89.

Goodridge HS and Underhill DM. (2008) Fungal Recognition by TLR2 and Dectin-1. Handb Exp Pharmacol. 183(1):87-109.

Gordon SB and Read RC (2002). Macrophage defences against respiratory tract infections. Br Med Bull. 61(1):45-61.

Gower WA and Nogee LM. (2011) Surfactant dysfunction. Paediatr Respir Rev. 12(4):223-229.

Groskreutz DJ, Monick MM, Powers LS, arovinsky TO, Look DC, Hunninghake GW. (2006) Respiratory syncytial virus induces TLR3 protein and protein kinase R, leading to increased double-stranded RNA responsiveness in airway epithelial cells. J Immunol. 176(3):1733-1740.

Guan Z, Katzianer D, Zhu J, Goldfine H. (2014) *Clostridium difficile* contains plasmalogen species of phospholipids and glycolipids. Biochim Biophys Acta. 1842(10): 1353-1359.

Gunasekara L, Schoel WM, Schürch S, Amrein MW. (2008) A comparative study of mechanisms of surfactant inhibition. Biochim Biophys Acta. 1778(2):433-444.

Guth AM, Janssen WJ, Bosio CM, Crouch EC, Henson PM, Dow SW. (2009) Lung environment determines unique phenotype of alveolar macrophages. Am J Physiol Lung Cell Mol Physiol. 296(6): L936-946.

Haines TH. (2009) A new look at Cardiolipin. Biochim Biophys Acta. 1788(10):1997-2002.

Hallak LK, Kwilas SA, Peeples ME. (2007) Interaction between respiratory syncytial virus and glycosaminoglycans, including heparan sulfate. Methods Mol Biol. 379(1):15-34.

Hamelin ME, Abed Y, Boivin G. (2004) Human metapneumovirus: a new player among respiratory viruses. Clin Infect Dis. 38(7):983-990.

Hardaway RM. (2000) A review of septic shock. Am Surg. 66(1):22-29.

Hashimoto M, Asai Y, Ogawa T. (2003) Treponemal phospholipids inhibit innate immune responses induced by pathogen-associated molecular patterns. J Biol Chem. 278(45):44205-44213.

Haynes LM, Moore DD, Kurt-Jones EA, Finberg RW, Anderson LJ, Tripp RA. (2001) Involvement of Toll-Like Receptor 4 in Innate Immunity to Respiratory Syncytial Virus. J Virol. 75(22): 10730-10737.

Hendricks DA, McIntosh K, Patterson JL. (1988) Further characterization of the soluble form of the G glycoprotein of respiratory syncytial virus J Virol. 62(7):2228-2233.

Hickling TP, Malhotra R, Bright H, McDowell W, Blair ED, Sim RB. (2000) Lung surfactant protein A provides a route of entry for respiratory syncytial virus into host cells. Viral Immunol. 13(1):125-135.

Hoebe K, Janssen E, Beutler B. (2004) The interface between innate and adaptive immunity. Nat Immunol. 5(10):971-974.

Hogenkamp A, van Eijk M, Haagsman HP (2007). Collectins-interaction with pathogens. In: Kilpatrick D, editor. *Collargen-Related Lectins in Innate Immunity*. Kerala, India: Research Signpost, 119-177.

Hollifield M, Bou Ghanem E, de Villiers WJ, Garvy BA. (2007) Scavenger receptor A dampens induction of inflammation in response to the fungal pathogen Pneumocystis carinii. Infect Immun. 75(8):3999-4005.

Holt PG, Oliver J, Bilyk N, McMenamin C, McMenamin PG, Kraal G, Thepen T. (1993) Downregulation of the antigen presenting cell function(s) of pulmonary dendritic cells *in vivo* by resident alveolar macrophages. J Exp Med. 177(2):397-407.

Holtzman MJ. (1992) Arachidonic acid metabolism in airway epithelial cells. Annu Rev Physiol. 54(1):303-329.

Horvath CM, Stark GR, Kerr IM, Darnell JE Jr (1996). Interactions between STAT and non-STAT proteins in the interferon-stimulated gene factor 3 transcription complex. Mol Cell Biol. 16(12):6957-6964.

Hsu P, Shi Y. (2017) Regulation of autophagy by mitochondrial phospholipids in health and diseases, Biochimica Biophysica Acta. 1862(1):114-129.

Husebye H, Halaas Ø, Stenmark H, Tunheim G, Sandanger Ø, Bogen B, Brech A, Latz E, Espevik T. (2006) Endocytic pathways regulate Toll-like receptor 4 signaling and link innate and adaptive immunity. EMBO J. 25(4):683-692.

Hussell T and Bell TJ (2014). Alveolar macrophages: plasticity in a tissue-specific context. Nat Rev Immunol. 14(2): 81-93.

Huveneers S and Danen EH. (2009) Adhesion signaling - crosstalk between integrins, Src and Rho. J Cell Sci. 122(Pt 8):1059-1069.

IJpenberg A, Jeannin E, Wahli W, Desvergne B. (1997) Polarity and specific sequence requirements of peroxisome proliferator-activated receptor (PPAR)/retinoid X receptor heterodimer binding to DNA. A functional analysis of the malic enzyme gene PPAR response element. J Biol Chem. 272(32):20108-

20117.

Ikegami M, Whitsett JA, Martis PC, Weaver TE. (2005) Reversibility of lung inflammation caused by SP-B deficiency. Am J Physiol Lung Cell Mol Physiol. 289(6): L962-970.

Jeon YJ, Yoo HM, Chung CH. (2010) ISG15 and immune diseases. Biochim Biophys Acta. 1802(5):485-496.

Jiang C, Ting AT, Seed B. (1998) PPARα agonists inhibit production of monocyte inflammatory cytokines. Nature. 391(6662):82-86.

Jobe AH. (2006) Mechanisms to explain surfactant responses. Biol Neonate, 89(4):298-302.

Johnson SM, McNally BA, Ioannidis I, Flano E, Teng MN, Oomens AG, Walsh EE, Peeples ME. (2015) Respiratory Syncytial Virus Uses CX3CR1 as a Receptor on Primary Human Airway Epithelial Cultures. PLoS Pathog. 11(12): e1005318.

Jorens PG, Matthys KE, Bult H. (1995) Modulation of nitric oxide synthase activity in macrophages. 4(2):75-89.

Kagan JC, Su T, Horng T, Chow A, Akira S, Medzhitov R (2008). TRAM couples endocytosis of Toll-like receptor 4 to the induction of interferon-beta. Nat Immunol. 9(4):361-368.

Kandasamy P, Zarini S, Chan ED, Leslie CC, Murphy RC, Voelker DR. (2011) Pulmonary surfactant phosphatidylglycerol inhibits *Mycoplasma pneumoniae*-stimulated eicosanoid production from human and mouse macrophages. J Biol Chem. 286(10):7841-7853.

Kaser MR and Skouteris GG. (1997) Inhibition of bacterial growth by synthetic SP-B1-78 peptides. Peptides. 18(9):1441-1444.

Katoh Y and Katoh M. (2004) Identification and characterization of CDC50A, CDC50B and CDC50C genes in silico. Oncol Rep. 12(4):939-943.

Katze MG, He Y, Gale MJ (2002). Viruses and interferon: a fight for supremacy. Nat Rev Immunol. 2(9):675-687.

Kawai T and Akira S. (2005) Pathogen recognition with Toll-like receptors. Curr Opin Immunol.17(4):338-44.

Ketterer MR, Shao JQ, Hornick DB, Buscher B, Bandi VK, Apicella MA. (1999) Infection of primary human bronchial epithelial cells by *Haemophilus influenzae*: macropinocytosis as a mechanism of airway epithelial cell entry. Infect Immun. 67(8):4161-4170.

Knowles MR and Boucher RC. (2002) Mucus clearance as a primary innate defense mechanism for mammalian airways. The Journal of clinical investigation. 109(5): 571-577.

Knutsen AP, Bush RK, Demain JG, Denning DW, Dixit A,……..,Slavin RG, Vijay HM, Wardlaw AJ (2012). Fungi and allergic lower respiratory tract diseases. J Allergy Clin Immunol. 129(2):280-291.

Kong X, San Juan H, Kumar M, Behera AK, Mohapatra A, Hellermann GR, Mane S, Lockey RF, Mohapatra SS. (2003) Respiratory syncytial virus infection activates STAT signaling in human epithelial cells. Biochem Biophys Res Commun. 306(2):616-622.

Krebs JJ, Hauser H, Carafoli E. (1979) Asymmetric distribution of phospholipids in the inner membrane of beef heart mitochondria. J Biol Chem. 254(12):5308-5316.

Krusat T and Streckert HJ. (1997) Heparin-dependent attachment of respiratory syncytial virus (RSV) to host cells. Arch Virol. 142(6):1247-1254.

Kubota T, Matsuoka M, Chang TH, Tailor P, Sasaki T, Tashiro M, Kato A, Ozato K. (2008) Virus infection triggers SUMOylation of IRF3 and IRF7, leading to the negative regulation of type I interferon gene expression. J Biol Chem. 283(37):25660-25670.

Kudo K, Sano H, Takahashi H, Kuronuma K, Yokota S, Fujii N, Shimada K, Yano I, Kumazawa Y, Voelker DR, Abe S, Kuroki Y. (2004) Pulmonary collectins enhance phagocytosis of Mycobacterium avium through increased activity of mannose receptor. J Immunol. 172(12):7592-7602.

Kunzi MS and Pitha PM. (2003) Interferon targeted genes in host defense. Autoimmunity. 36(8):457-461.

Kuronuma K, Mitsuzawa H, Takeda K, Nishitani C, Chan ED, Kuroki Y, Nakamura M, Voelker DR. (2009) Anionic pulmonary surfactant phospholipids inhibit inflammatory responses from alveolar macrophages and U937 cells by binding the lipopolysaccharide-interacting proteins CD14 and MD-2. J Biol Chem. 284(38):25488-24500.

Kuronuma K, Sano H, Kato K, Kudo K, Hyakushima N, Yokota S, Takahashi H, Fujii N, Suzuki H, Kodama T, Abe S, Kuroki Y. (2004) Pulmonary surfactant protein A augments the phagocytosis of *Streptococcus* pneumoniae by alveolar macrophages through a casein kinase 2-dependent increase of cell surface localization of scavenger receptor A. J Biol Chem. 279(20):21421-21430.

Kuwana T, Mackey MR, Perkins G, Ellisman MH, Latterich M, Schneiter R, Green DR., Newmeyer DD. (2002) Bid, Bax, and lipids cooperate to formsupramolecular openings in the outer mitochondrial membrane. Cell.

111(3):331-342.

Lambrecht BN. (2006) Alveolar macrophage in the driver's seat. Immunity. 24(4):366-368.

Lamping N, Hoess A, Yu B, Park TC, Kirschning CJ, Pfeil D, Reuter D, Wright SD, Herrmann F, Schumann RR. (1996) Effects of site-directed mutagenesis of basic residues (Arg 94, Lys 95, Lys 99) of lipopolysaccharide (LPS)-binding protein on binding and transfer of LPS and subsequent immune cell activation. J Immunol. 157(10):4648-4656.

Laskin DL, Weinberger B, Laskin JD. (2001) Functional heterogeneity in liver and lung macrophages. J Leukoc Biol. 70(2):163-170.

Le Bon and Tough DF. (2002) Links between innate and adaptive immunity via type I interferon. Curr Opin Immunol. 14(4):432-436.

Lecocq J and Ballou CE. (1964) On the structure of cardiolipin. Biochem. 3(1): 976-980.

Lee CC, Avalos AM, Ploegh HL. (2012) Accessory molecules for Toll-like receptors and their function. Nat Rev Immunol. 12(3):168-179.

Lehrnbecher T, Frank C, Engels K, Kriener S, Groll AH, Schwabe D. (2010) Trends in the postmortem epidemiology of invasive fungal infections at a university hospital. J Infect. 61(3):259-265.

LeVine AM, Elliott J, Whitsett JA, Srikiatkhachorn A, Crouch E, DeSilva N, Korfhagen T. (2004) Surfactant protein-d enhances phagocytosis and pulmonary clearance of respiratory syncytial virus. Am J Respir Cell Mol Biol. 31(2):193-199.

LeVine AM, Gwozdz J, Stark J, Bruno M, Whitsett J, Korfhagen T. (1999) Surfactant protein-A enhances respiratory syncytial virus clearance *in vivo*. J Clin Invest. 103(7):1015-1021.

LeVine AM, Whitsett JA, Gwozdz JA, Richardson TR, Fisher JH, Burhans MS, Korfhagen TR. (2000) Distinct effects of surfactant protein A or D deficiency during bacterial infection on the lung. J Immunol. 165(7):3934-3940.

Lewis JF and Veldhuizen R. (2003) The role of exogenous surfactant in the treatment of acute lung injury. Annu Rev Physiol. 65(1):613-642.

Lewis RN and McElhaney RN. (2009) The physicochemical properties of cardiolipin bilayers and cardiolipin-containing lipid membranes. Biochim Biophys Acta. 1788(10):2069-2079.

Li D, Jans DA, Bardin PG, Meanger J, Mills J, Ghildyal R. (2008) Association

of Respiratory Syncytial Virus M Protein with Viral Nucleocapsids Is Mediated by the M2-1 Protein. J Virol. 82(17):8863-8870.

Lian X, Yan C, Qin Y, Knox L, Li T, Du H. (2005) Neutral Lipids and Peroxisome Proliferator-Activated Receptor-γ Control Pulmonary Gene Expression and Inflammation-Triggered Pathogenesis in Lysosomal Acid Lipase Knockout Mice. Am J Pathol.167(3):813-21.

Lin SM, Frevert CW, Kajikawa O, Wurfel MM, Ballman K, Mongovin S, Wong VA, Selk A. Martin TR. (2004) Differential regulation of membrane CD14 expression and endotoxin-tolerance in alveolar macrophages. Am J Respir Cell Mol Biol. 31(2):162-170.

Lin WJ and Yeh WC. (2005) Implication of Toll-Like receptor and tumor necrosis factor signaling in septic shock. Shock. 24(3): 206-209.

Lin Y, Zhang M, Barnes PF (1998). Chemokine production by a human alveolar epithelial cell line in response to Mycobacterium tuberculosis. Infect Immun. 66(3):1121-1126.

Liu P, Jamaluddin M, Li K, Garofalo RP, Casola A, Brasier AR. (2007) Retinoic acid-inducible gene I mediates early antiviral response and Toll-like receptor 3 expression in respiratory syncytial virus-infected airway epithelial cells. J Virol. 81(3):1401-1411.

Liu M, Guo S, Stiles JK. (2011) The emerging role of CXCL10 in cancer. Oncol Lett. 2(4):583-589.

Livak KJ and Schmittgen TD. (2001) Analysis of relative gene expression data using real-time quantitative PCR and the 2(-Delta Delta C(T)) Method. Methods. 25(4):402-408.

López-Gómez A, Cano V, Moranta D, Morey P, García del Portillo F, Bengoechea JA, Garmendia J. (2012) Host cell kinases, α5 and β1 integrins, and Rac1 signalling on the microtubule cytoskeleton are important for non-typable *Haemophilus influenzae* invasion of respiratory epithelial cells. Microbiology. 158(Pt 9):2384-2398.

Lopez-Marques RL, Theorin L, Palmgren MG, Pomorski TG. (2014) P4-ATPases: lipid flippases in cell membranes. Pflugers Arch. 466 (7):1227-1240.

Lotz MT and Peebles RS Jr. (2012) Mechanisms of respiratory syncytial virus modulation of airway immune responses. Curr Allergy Asthma Rep. 12(5):380-387.

Lu YW, Galbraith L, Herndon JD, Lu YL, Pras-Raves M, Vervaart M, Van Kampen A, Luyf A, Koehler CM, McCaffery JM, Gottlieb E, Vaz FM, SM. Claypool (2016) Defining functional classes of Barth syndrome mutation in humans. Hum

Mol Genet. 25(9):1754-1770.

Lüderitz O, Galanos C, Lehmann V, Mayer H, Rietschel ET, Weckesser J. (1978) Chemical structure and biological activities of lipid A's from various bacterial families. Naturwissenschaften. 65(11):578-585.

Lukacs NW, Smit JJ, Mukherjee S, Morris SB, Nunez G, Lindell DM. (2010) Respiratory virus-induced TLR7 activation controls IL-17-associated increased mucus via IL-23 regulation. J Immunol. 185(4):2231-2239

Maclellan K, Loney C, Yeo RP, Bhella D (2007). The 24-angstrom structure of respiratory syncytial virus nucleocapsid protein-RNA decameric rings. J Virol. 81(17): 9519-9524.

Maguire JJ, Tyurina YY, Mohammadyani D, Kapralov AA, Anthonymuthu TS, Qu F, Amoscato AA, Bayır H, Kagan VE. (2017) Known unknowns of cardiolipin signaling: The best is yet to come. Biochim Biophys Acta.1862(1):8-24.

Malhotra R, Ward M, Bright H, Priest R, Foster MR, Hurle M, Blair E, Bird M. (2003) Isolation and characterisation of potential respiratory syncytial virus receptor(s) on epithelial cells. Microbes Infect. 5(2):123-133.

Margalit A and Kavanagh K. (2015) The innate immune response to Aspergillus fumigatus at the alveolar surface. FEMS Microbiol Rev. 39(5):670-687.

Marsh D. (1996) Lateral pressure in membranes. Biochim Biophys Acta.1286(3): 183-223.

Martin TR and Frevert CW. (2005) Innate immunity in the lungs. Proc Am Thorac Soc. 2(5):403-411.

Martínez I and Melero JA. (2000) Binding of human respiratory syncytial virus to cells: implication of sulfated cell surface proteoglycans. J Gen Virol. 81(Pt 11):2715-2722.

Martinez I, Dopazo J, Melero JA. (1997) Antigenic structure of the human respiratory syncytial virus G glycoprotein and relevance of hypermutation events for the generation of antigenic variants. J Gen Virol. 78(Pt 10):2419-2429.

Mason RJ. (2006) Biology of alveolar type II cells. Respirology. 11: S12-15.

Matute-Bello G, Frevert CW, Martin TR. (2008) Animal models of acute lung injury. Am J Physiol Lung Cell Mol Physiol. 295(3): L379-399.

Mayr JA. (2015) Lipid metabolism in mitochondrial membranes. J Inherit

Metab Dis, 38(1):137-144.

Mbawuike IN and Hercowitz HB. (1989) MH-S, a murine alveolar macrophage cell line: morphological, cytochemical, and functional characteristics. J Leukoc Biol. 46(2):119-127.

Mbiguino A and Menezes J. (1991) Purification of human respiratory syncytial virus: superiority of sucrose gradient over percoll, renografin, and metrizamide gradients. J Virol Methods. 31(2-3):161-170.

McCormack FX and Whitsett JA. (2002) The pulmonary collectins, SP-A and SP-D, orchestrate innate immunity in the lung. J Clin Invest. 109(6):707-712.

McCormack FX, Gibbons R, Ward SR, Kuzmenko A, Wu H, Deepe GS Jr. (2003) Macrophage-independent fungicidal action of the pulmonary collectins. J Biol Chem. 278(38):36250-36256.

Medzhitov R and Janeway C Jr. (2000) Innate immune recognition: mechanisms and pathways. Immunol Rev. 173(1):89-97.

Meng F and Lowell CA. (1997) Lipopolysaccharide (LPS)-induced macrophage activation and signal transduction in the absence of Src-family kinases Hck, Fgr, and Lyn. J Exp Med. 185(9):1661-1670.

Mejia EM, Cole LK, Hatch GM. (2014) Cardiolipin metabolism and the role it plays in heart failure and mitochondrial supercomplex formation. Cardiovasc Hematol Disord. Drug Targets. 14(2):98-106.

Michael DR, Davies TS, Laubertová L, Gallagher H, Ramji DP. (2015) The phosphoinositide 3-kinase signaling pathway is involved in the control of modified low-density lipoprotein uptake by human macrophages. Lipids. 50(3):253-260.

Miles PR, Bowman L, Rao KM, Baatz JE, Huffman L. (1999) Pulmonary surfactant inhibits LPS-induced nitric oxide production by alveolar macrophages. Am J Physiol. 276(1 Pt 1): L186- 196.

Mitra R, Baviskar P, Duncan-Decocq RR, Patel D, Oomens AGP. (2012) The human respiratory syncytial virus matrix protein is required for maturation of viral filaments. J Virol. 86(8):4432-4443.

Mizgerd JP. (2008) Acute lower respiratory tract infection. N Engl J Med. 358(7): 716-727.

Moghaddam SJ, Ochoa C, Sethi S, Dickey BF. (2011) Nontypeable *Haemophilus influenzae* in chronic obstructive pulmonary disease and lung cancer. Int J Chron Obstruct Pulmon Dis. 6(1): 113-123.

Moore AE, Sabachewsky L, Toolan HW. (1955) Culture characteristics of four permanent lines of human cancer cells. Cancer Res. 15(9):598-602.

Moore EC, Barber J, Tripp RA. (2008) Respiratory syncytial virus (RSV) attachment and nonstructural proteins modify the type I interferon response associated with suppressor of cytokine signaling (SOCS) proteins and IFN-stimulated gene-15 (ISG15). Virol J. 5(1):116.

Morey P, Cano V, Martí-Lliteras P, López-Gómez A, Regueiro V, Saus C, Bengoechea JA, Garmendia J. (2011) Evidence for a non-replicative intracellular stage of nontypable *Haemophilus influenzae* in epithelial cells. Microbiol. 157(Pt 1): 234-250.

Morin B, Rahmeh AA, Whelan SP. (2012) Mechanism of RNA synthesis initiation by the vesicular stomatitis virus polymerase. EMBO J. 31(5):1320-1329.

Morris JA, Blount RE Jr, Savage RE. (1956) Recovery of Cytopathogenic Agent from Chimpanzees with Coryza. Proc Soc Exper Biol & Med. 92(3):544-549.

Morris RH, Tonks AJ, Jones KP, Ahluwalia MK, Thomas AW, Tonks A, Jackson SK. (2008) DPPC regulates COX-2 expression in monocytes via phosphorylation of CREB. Biochem Biophys Res Commun. 370(1):174-178.

Mueller M, Brandenburg K, Dedrick R, Schromm AB, Seydel U. (2005) Phospholipids inhibit lipopolysaccharide (LPS)-induced cell activation: a role for LPS-binding protein. J Immunol. 174(2):1091-1096.

Mukhopadhyay S and Gordon S. (2004) The role of scavenger receptors in pathogen recognition and innate immunity. Immunobiol. 209 (1-2):39-49.

Murawski MR, Bowen GN, Cerny AM, Anderson LJ, Haynes LM, Tripp RA, Kurt-Jones EA, Finberg RW. (2009) Respiratory syncytial virus activates innate immunity through Toll-like receptor 2. J Virol. 83(3):1492-1500.

Murphy TF. (2003) Respiratory infections caused by non-typeable *Haemophilus influenzae*. Curr Opin Infect Dis. 16(2):129-134.

Murphy TF, Brauer AL, Schiffmacher AT, Sethi S. (2004) Persistent colonization by *Haemophilus influenzae* in chronic obstructive pulmonary disease. Am J Respir Crit Care Med. 170(3):266-272.

Newton K and Dixit VM. (2012) Signaling in innate immunity and inflammation. Cold Spring Harb Perspect Biol. 4(3).

Nishino T. (2000) Physiological and pathophysiological implications of upper airway reflexes in humans. Jpn J Physiol. 50(1): 3-14.

Noah TL, Ivins SS, Murphy P, Kazachkova I, Moats-Staats B, Henderson FW. (2002) Chemokines and inflammation in the nasal passages of infants with respiratory syncytial virus bronchiolitis. Clin Immunol. 104(1):86-95.

Nogee LM, Garnier G, Dietz HC, Singer L, Murphy AM, deMello DE, Colten HR. (1994) A mutation in the surfactant protein B gene responsible for fatal neonatal respiratory disease in multiple kindreds. J Clin Invest. 93(4):1860-1863.

Numata M, Chu HW, Dakhama A, Voelker DR. (2010) Pulmonary surfactant phosphatidylglycerol inhibits respiratory syncytial virus-induced inflammation and infection. Proc Natl Acad Sci USA. 107(1):320-325.

Numata M, Grinkova YV, Mitchell JR, Chu HW, Sligar SG, Voelker DR. (2013a) Nanodiscs as a therapeutic delivery agent: inhibition of respiratory syncytial virus infection in the lung. Int J Nanomedicine. 8:1417-1427.

Numata M, Kandasamy P, Nagashima Y, Fickes R, Murphy RC, Voelker DR (2015). Phosphatidylinositol inhibits respiratory syncytial virus infection. J Lipid Res, 56(3):578-587.

Numata M, Kandasamy P, Nagashima Y, Posey J, Hartshorn K, Woodland D, Voelker DR. (2012) Phosphatidylglycerol suppresses influenza A virus infection. Am J Respir Cell Mol Biol. 46(4):479-487.

Numata M, Nagashima Y, Moore ML, Berry KZ, Chan M, Kandasamy P, Peebles RS Jr, Murphy RC, Voelker DR. (2013b) Phosphatidylglycerol provides short-term prophylaxis against respiratory syncytial virus infection. J Lipid Res. 54(8):2133-2143.

O'Brien AD, Rosenstreich DL, Scher I, Campbell GH, MacDermott RP, Formal SB. (1980) Genetic control of susceptibility to Salmonella typhimurium in mice: role of the LPS gene. J Immunol. 124(1): 20-24

Olmsted, RA and Collins PL. (1989) The 1A protein of respiratory syncytial virus is an integral membrane protein present as multiple, structurally distinct species. J Virol. 63(5): 2019-2029.

Olsson S and Sundler R. (2006) The role of lipid rafts in LPS-induced signaling in a macrophage cell line. Mol Immunol. 43(6):607-612.

Ortiz A, Killian JA, Verkleij AJ, Wilschut J. (1999) Membrane fusion and the lamellar-to-inverted-hexagonal phase transition in cardiolipin vesicle systems induced by divalent cations. Biophys J. 77(4):2003-2014.

Ozinsky A, Underhill DM, Fontenot JD, Hajjar AM, Smith KD, Wilson CB, Schroeder L, Aderem A. (2000) The repertoire for pattern recognition of pathogens by the innate immune system is defined by cooperation between

toll-like receptors. Proc Natl Acad Sci USA. 97(25):13766-13771.

Paradies G, Paradies V, De Benedictis V, Ruggiero FM, Petrosillo G. (2014) Functional role of cardiolipin in mitochondrial bioenergetics. Biochim Biophys Acta. 1837(4):408-417.

Park WY, Goodman RB, Steinberg KP, Ruzinski JT, Radella F, Park DR, Pugin J, Skerrett SJ, Hudson LD, Martin TR. (2001) Cytokine balance in the lungs of patients with acute respiratory distress syndrome. Am J Respir Crit Care Med. 164(10 Pt 1):1896-1903.

Paulusma CC, Folmer DE, Ho-Mok KS, de Waart DR, Hilarius PM, Verhoeven AJ, Oude Elferink RP. (2008) ATP8B1 requires an accessory protein for endoplasmic reticulum exit and plasma membrane lipid flippase activity. Hepatology. 47(1):268-278.

Pérez-Gil J. (2008) Structure of pulmonary surfactant membranes and films: the role of proteins and lipid-protein interactions. Biochim Biophys Acta. 1778(7-8):1676-1695.

Piantadosi CA and Schwartz DA. (2004) The acute respiratory distress syndrome. Ann Intern Med. 141(6):460-470.

Pillemer L and Ecker EE. (1941) Anticomplementary factor in fresh yeast. J Biol. Chem. 137:139-142.

Pitha-Rowe IF and Pitha PM. (2007) Viral defense, carcinogenesis and ISG15: novel roles for an old ISG. Cytokine Growth Factor Rev. 8 (5-6):409-417.

Possmayer F. (1988) A proposed nomenclature for pulmonary surfactant-associated proteins. Am Rev Respir Dis. 138(4):990-998.

Pugin J, Kravchenko VV, Lee JD, Kline L, Ulevitch RJ, Tobias PS. (1998) Cell activation mediated by glycosylphosphatidylinositol-anchored or transmembrane forms of CD14. Infect. Immun. 66(3):1175-1180.

Ramaswamy M, Shi L, Monick MM, Hunninghake GW, Look DC. (2004) Specific inhibition of type I interferon signal transduction by respiratory syncytial virus. Am J Respir Cell Mol Biol. 30(6):893-900.

Ray NB, Durairaj L, Chen BB, McVerry BJ, Ryan AJ, Donahoe M, Waltenbaugh AK ,…….,and Mallampalli RK. (2010) Dinamic regulation of cardiolipin by the lipid pump Atp8b1 determines the severity of lung injury in experimental pneumonia. Nat Med. 16(10):1120-1127.

Recht M, Borden EC, Knight E Jr. (1991) A human 15-kDa IFN-induced protein induces the secretion of IFN-gamma. J Immunol. 147(8):2617-2623.

Ricote M and Glass CK. (2007) PPARs and molecular mechanisms of transrepression. Biochim Biophys Acta. 1771(8):926-935.

Ricote M, Li AC, Willson TM, Kelly CJ, Glass CK. (1998) The peroxisome proliferator-activated receptor-gamma is a negative regulator of macrophage activation. Nature. 391(6662):79-82.

Rixon HW, Brown G, Aitken J, McDonald T, Graham S, Sugrue RJ. (2004) The small hydrophobic (SH) protein accumulates within lipid-raft structures of the Golgi complex during respiratory syncytial virus infection. J Gen Virol. 85 (Pt 5):1153-1165

Robertson B and Halliday HL. (1998) Principles of surfactant replacement. Biochim Biophys Acta. 1408(2-3):346-361.

Roth MD and Golub SH. (1993) Human pulmonary macrophages utilize prostaglandins and transforming growth factor beta 1 to suppress lymphocyte activation. J Leukoc Biol. 53(4):366-371.

Rouser G, Siakotos AN, Fleischer S. (1966) Quantitative analysis of phospholipids by thin-layer chromatography and phosphorus analysis of spots. Lipids. 1(1): 85-86.

Rudd BD, Burstein E, Duckett CS, Li X, Lukacs NW. (2005) Differential role for TLR3 in respiratory syncytial virus-induced chemokine expression. J Virol. 79(6):3350-3357.

Rutigliano JA and Graham BS. (2004) Prolonged production of TNF-alpha exacerbates illness during respiratory syncytial virus infection. J Immunol. 173(5):3408-3417.

Ruysschaert JM and Lonez C. (2015) Role of lipid microdomains in TLR-mediated signalling. Biochim Biophys Acta. 1848(9):1860-1867.

Ryan MA, Akinbi HT, Serrano AG, Perez-Gil J, Wu H, McCormack FX, Weaver TE. (2006) Antimicrobial activity of native and synthetic surfactant protein B peptides. J Immunol. 176(1):416-425.

Saenz A, Lopez-Sanchez A Mojica-Lazaro J, Martinez-Caro L, Nin N, Bagatolli LA, Casals C. (2010) Fluidizing effects of C-reactive protein on lung surfactant membranes: protective role of surfactant protein A. Faseb J. 24(10):3662-3673.

Saenz A, Canadas O, Bagatolli LA, Sanchez-Barbero F, Johnson M, Casals C. (2007) Effect of surfactant protein A on the physical properties and surface activity of KL4-surfactant. Biophys J. 92(2):482-492.

Sano H and Kuroki Y. (2005) The lung collectins, SP-A and SP-D, modulate

pulmonary innate immunity. Mol Immunol. 42(3):279-287.

Sano H, Chiba H, Iwaki D, Sohma H, Voelker DR, Kuroki Y. (2000) Surfactant proteins A and D bind CD14 by different mechanisms. J Biol Chem. 275(29):22442-22451

Sano H, Sohma H, Muta T, Nomura S, Voelker DR, Kuroki Y. (1999) Pulmonary surfactant protein A modulates the cellular response to smooth and rough lipopolysaccharides by interaction with CD14. J Immunol. 163(1):387-395.

Sato M, Sano H, Iwaki D, Kudo K, Konishi M, Takahashi H, Takahashi T, Imaizumi H, Asai Y, Kuroki Y. (2003) Direct binding of Toll-like receptor 2 to zymosan, and zymosan-induced NF-kappa B activation and TNF-alpha secretion are down-regulated by lung collectin surfactant protein A. J Immunol. 171(1):417-425.

Schlame M. (2008) Cardiolipin synthesis for the assembly of bacterial and mitochondrial membranes. J Lipid Res. 49(8):1607-1620.

Schlame M, Ren M, Xu Y, Greenberg ML, Haller I. (2005) Molecular symmetry in mitochondrial cardiolipins. Chem. Phys. Lipids. 138(1-2):38-49.

Schürch S, Possmayer F, Cheng S, Cockshutt AM. (1992) Pulmonary SP-A enhances adsorption and appears to induce surface sorting of lipid extract surfactant. Am J Physiol. 263(2 Pt 1): L210-218.

Sennato S, Bordi F, Cametti C, Coluzza C, Desideri A, Rufini S. Evidence of domain formation in cardiolipin-glycerophospholipid mixed monolayers. (2005) A thermodynamic and AFM study. J Phys Chem B. 109 (33):15950-15957.

Sethi S and Murphy TF. (2008) Infection in the pathogenesis and course of chronic obstructive pulmonary disease. N Engl J Med. 359(22):2355-2365.

Sever-Chroneos Z, Krupa A, Davis J, Hasan M, Yang CH, Szeliga J, Herrmann M, Hussain M, Geisbrecht BV, Kobzik L, Chroneos ZC. (2011) Surfactant protein A (SP-A)-mediated clearance of *Staphylococcus aureus* involves binding of SP-A to the staphylococcal adhesin eap and the macrophage receptors SP-A receptor 210 and scavenger receptor class A. J Biol Chem. 286(6):4854-4870.

Shaikh FY and Crowe JE Jr. (2013) Molecular mechanisms driving respiratory syncytial virus assembly. Future Microbiol. 8(1):123-131.

Silverstein RL, Li W, Park YM, Rahaman SO. (2010) Mechanisms of cell signaling by the scavenger receptor CD36: implications in atherosclerosis and thrombosis. Trans Am Clin Climatol Assoc. 121(1): 206-220.

Simionescu M. (1997) Lung endothelium: structure-function correlates. In: Crystal RG WJB, editor. The Lung: Scientific Foundations. 2d ed. Philadelphia: LippincotRaven, 615-628.

Skelton R, Holland P, Darowski M, Chetcuti PA, Morgan LW, Harwood JL (1999). Abnormal surfactant composition and activity in severe bronchiolitis. Acta Paediatr. 88(9):942-946.

Smith PK, Krohn RI, Hermanson GT, Mallia AK, Gartner FH, Provenzano MD, Fujimoto EK, Goeke NM, Olson BJ, Klenk DC. (1985) Measurement of protein using bicinchoninic acid. Anal Biochem. 150(1):76-85.

Stamme C, Müller M, Hamann L, Gutsmann T, Seydel U. (2002) Surfactant protein a inhibits lipopolysaccharide-induced immune cell activation by preventing the interaction of lipopolysaccharide with lipopolysaccharide-binding protein. Am J Respir Cell Mol Biol. 27(3):353-360.

Swords WE, Buscher BA, Ver Steeg Ii K, Preston A, Nichols WA, Weiser JN, Gibson BW, Apicella MA. (2000) Non-typeable *Haemophilus influenzae* adhere to and invade human bronchial epithelial cells via an interaction of lipooligosaccharide with the PAF receptor. Mol Microbiol. 37(1):13-27.

Taeusch HW, Bernardino de la Serna J, Perez-Gil J, Alonso C, Zasadzinski JA. (2005) Inactivation of pulmonary surfactant due to serum-inhibited adsorption and reversal by hydrophilic polymers: experimental. Biophys J. 89(3):1769-1779.

Takatsu H, Tanaka G, Segawa K, Suzuki J, Nagata S, Nakayama K, Shin HW (2014). Phospholipid flippase activities and substrate specificities of human type IV P-type ATPases localized to the plasma membrane. J Biol Chem. 289(48):33543-33556.

Takeda K and Akira S (2015). Toll-like receptors. Curr Protoc Immunol. 109(14):1-10.

Tawar RG, Duquerroy S, Vonrhein C, Varela PF, Damier-Piolle L, Castagné N, MacLellan K, Bedouelle H, Bricogne G, Bhella D; Eléouët JF, Rey FA (2009). Crystal structure of a nucleocapsid-like nucleoprotein-RNA complex of respiratory syncytial virus. Science. 326(5957):1279-1283.

Techaarpornkul S, Collins PL, Peeples ME. (2002) Respiratory syncytial virus with the fusion protein as its only viral glycoprotein is less dependent on cellular glycosaminoglycans for attachment than complete virus. Virology. 294(2):296-304.

Teng MN and Collins PL. (1998) Identification of the respiratory syncytial virus proteins required for formation and passage of helper-dependent infectious particles. J Virol. 72(7):5707-5716.

Thorne RF, Mhaidat NM, Ralston KJ, Burns GF. (2007) CD36 is a receptor for oxidized high density lipoprotein: implications for the development of atherosclerosis. FEBS Lett. 581(6):1227-1232.

Tian B, Y. Zhang BA, Luxon RP, Garofalo A, Casola MS, Brasier AR. (2002) Identification of NFkB-dependent gene networks in respiratory syncytial virus-infected cells. J Virol. 76(13):6800-6814.

Tian HF, Feng JM, Wen JF. (2012) The evolution of cardiolipin biosynthesis and maturation pathways and its implications for the evolution of eukaryotes. BMC Evol Biol. 12(1):32.

Tobias PS, Soldau K, Kline L, Lee JD, Kato K, Martin TP, Ulevitch RJ. (1993) Cross-linking of lipopolysaccharide (LPS) to CD14 on THP-1 cells mediated by LPS-binding protein. J Immunol. 150(7): 3011-3021.

Tobias PS, Soldau K, Ulevitch RJ. (1986) Isolation of a lipopolysaccharide-binding acute phase reactant from rabbit serum. J Exp Med, 164(3):777-793.

Tonks A, Parton J, Tonks AJ, Morris RH, Finall A, Jones KP, Jackson SK. (2005) Surfactant phospholipid DPPC downregulates monocyte respiratory burst via modulation of PKC. Am J Physiol Lung Cell Mol Physiol. 288(6): L1070-1080.

Tonks AJ, Tonks A, Morris RH, Jones KP, Jackson SK. (2003) Regulation of platelet-activating factor synthesis in human monocytes by dipalmitoyl phosphatidylcholine. J Leukoc Biol. 74(1):95-101.

Trapnell BC and Whitsett JA. (2002) Gm-CSF regulates pulmonary surfactant homeostasis and alveolar macrophage-mediated innate host defense. Annu Rev Physiol. 64(1):775-802.

Triantafilou M, Miyake K, Golenbock DT, Triantafilou K. (2002) Mediators of innate immune recognition of bacteria concentrate in lipid rafts and facilitate lipopolysaccharide-induced cell activation. J Cell Sci. 115(12):2603-2611.

Tripp RA, Jones LP, Haynes LM, Zheng H, Murphy PM, Anderson LJ. (2001) CX3C chemokine mimicry by respiratory syncytial virus G glycoprotein. Nat Immunol. 2(8):732-738.

Ulevitch RJ and Tobias PS. (1995) Receptor-dependent mechanisms of cell stimulation by bacterial endotoxin. Annu Rev Immunol. 13(1):437-457.

Unsay JD, Cosentino K, Subburaj Y, García-Sáez AJ (2013). Cardiolipin effects on membrane structure and dynamics. Langmuir. 29(51):15878-15887.

van der Mark VA, Elferink RP, Paulusma CC. (2013) P4 ATPases: flippases in health and disease. Int J Mol Sci. 14(4):7897-7922.

van der Mark VA, Ghiboub M, Marsman C, Zhao J, van Dijk R, Hiralall JK, Ho-Mok KS, Castricum Z, de Jonge WJ, Oude Elferink RP, Paulusma CC. (2017) Phospholipid flippases attenuate LPS-induced TLR4 signaling by mediating endocytic retrieval of Toll-like receptor 4. Cell Mol Life Sci. 74(4):715-730.

Vareille M, Kieninger E, Edwards MR, Regamey N. (2011) The airway epithelium: soldier in the fight against respiratory viruses. Clin Microbiol Rev. 24(1):210-229.

Varga T, Czimmerer Z, Nagy L (2011). PPARs are a unique set of fatty acid regulated transcription factors controlling both lipid metabolism and inflammation. Biochim Biophys Acta. 1812(8):1007-1022.

Veldhuizen R, Nag K, Orgeig S, Possmayer F. (1998) The role of lipids in pulmonary surfactant. Biochim Biophys Acta. 1408(2-3):90-108.

Virji M, Kayhty H, Ferguson DJ, Alexandrescu C, Moxon ER. (1991) Interactions of *Haemophilus influenzae* with cultured human endothelial cells. Microb Pathog, 10(3):231-245.

Walsh EE and Hruska J. (1983) Monoclonal antibodies to respiratory syncytial virus proteins: identification of the fusion protein. J Virol. 47(1):171-177.

Wang Z and Notter RH. (1998) Additivity of protein and nonprotein inhibitors of lung surfactant activity. Am J Respir Crit Care Med. 158(1):28-35.

Weibel ER. (1984) The pathway for oxygen: structure and function in the mammalian respiratory system. Cambridge: Harvard University press.

Weikert LF, Edwards K, Chroneos ZC, Hager C, Hoffman L, Shepherd VL. (1997) SP-A enhances uptake of bacillus Calmette-Guérin by macrophages through a specific SP-A receptor. Am J Physiol. 272(5 Pt 1): L989-995.

Welch JS, Ricote M, Akiyama TE, Gonzalez FJ, Glass CK. (2003) PPARγ and PPARα negatively regulate specific subsets of lipopolysaccharide and IFNγ target genes in macrophages. Proc Natl Acad Sci USA. 100(11):6712-6717.

Whitsett JA, Ross G, Weaver T, Rice W, Dion C, Hull W. (1985) Glycosylation and secretion of surfactant-associated glycoprotein A. J Biol Chem. 260(28):15273-15279.

Whitsett JA and Weaver TE (2002). Hydrophobic surfactant proteins in lung function and disease. N Engl J Med. 347(26):2141-2148.

Wiechelman KJ, Braun RD, Fitzpatrick JD. (1988) Investigation of the bicinchoninic acid protein assay: identification of the groups responsible for color formation. Anal Biochem. 175(1):231-237.

Wikenheiser KA, Vorbroker DK, Rice WR, Clark JC, Bachurski CJ, Oie HK, Whitsett JA. (1993) Production of immortalized distal respiratory epithelial cell lines from surfactant protein C/simian virus 40 large tumor antigen transgenic mice. Proc Natl Acad Sci USA. 90(23):11029-11033.

Winther MP, van Dijk KW, Havekes LM, Hofker MH. (2000) Macrophage scavenger receptor class A: A multifunctional receptor in atherosclerosis. Arterioscler Thromb Vasc Biol. 20(2):290-297.

Woodhead MF, Blasi S, Ewig J, Garau G, Huchon M, Ieven A, Ortqvist T, Schaberg A, Torres G, van der Heijden R, Read TJ, Verheij S. (2011) Joint Taskforce of the European Respiratory, M. European Society for Clinical, and D. Infectious. Guidelines for the management of adult lower respiratory tract infections-full version. Clinical microbiology and infection: the official publication of the European Society of Clinical Microbiology and Infectious Diseases. 17 Suppl 6: E1-59.

Wright JR. (2005) Immunoregulatory functions of surfactant proteins. Nat Rev Immunol. 5(1):58-68.

Wright SD, Ramos RA, Tobias PS, Ulevitch RJ, Mathison JC (1990).CD14, a receptor for complexes of lipopolysaccharide (LPS) and LPS binding protein. Science. 249(4975):1431-1433.

Wu H, Kuzmenko A, Wan S, Schaffer L, Weiss A, Fisher JH, Kim KS, McCormack FX. (2003) Surfactant proteins A and D inhibit the growth of Gram-negative bacteria by increasing membrane permeability. Journal of Clinical Investigation. 111(10):1589-1602.

Wydro P. (2013) The influence of cardiolipin on phosphatidylglycerol/phosphatidylethanolamine monolayers-studies on ternary films imitating bacterial membranes. Colloids Surf B Biointerfaces; 106:217-223.

Yamada T and Kawasaki T. (2005) Microbial synthesis of hyaluronan and chitin: new approaches. J Biosci Bioeng. 99(6):521-528.

Yamamoto M, Sato S, Hemmi H, Hoshino K, Kaisho T, Sanjo H, Takeuchi O, Sugiyama M, Okabe M, Takeda K, Akira S. (2003) Role of adaptor TRIF in the MyD88-independent toll-like receptor signaling pathway. Science. 301(5633):640-643.

Yamazoe M, Nishitani C, Takahashi M, Katoh T, Ariki S, Shimizu T, Mitsuzawa H, Sawada K, Voelker DR, Takahashi H, Kuroki Y (2008). Pulmonary surfactant protein D inhibits lipopolysaccharide (LPS)-induced inflammatory cell responses by altering LPS binding to its receptors. J Biol Chem. 283(51):35878-35888.

Yu H, Ha T, Liu L, Wang X, Gao M, Kelley J, Kao R, Williams D, Li C. (2012)

Scavenger receptor A (SR-A) is required for LPS-induced TLR4 mediated NF-κB activation in macrophages. Biochim Biophys Acta. 1823(7):1192-1198.

Yu M and Levine SJ. (2011) Toll-like receptor, RIG-I-like receptors and the NLRP3 inflammasome: key modulators of innate immune responses to double-stranded RNA viruses. Cytokine Growth Factor Rev. 22(2):63-72.

Yui S and Yamazaki M. (1991) Augmentation and suppression of release of tumor necrosis factor from macrophages by negatively charged phospholipids. Jpn J Cancer Res. 82(9):1028-1034.

Zanoni I, Ostuni R, Marek LR, Barresi S, Barbalat R, Barton GM, Granucci F, Kagan JC. (2011) CD14 controls the LPS-induced endocytosis of Toll-like receptor 4. Cell. 147(4):868-880.

Zasadzinski JA, Alig TF, Alonso C, Bernardino de la Serna J, Perez-Gil J, Taeusch HW (2005). Inhibition of pulmonary surfactant adsorption by serum and the mechanisms of reversal by hydrophilic polymers: theory. Biophys J. 89(3):1621-1629.

Zhao MQ, Stoler MH, Liu AN, Wei B, Soguero C, Hahn YS, Enelow RI (2000). Alveolar epithelial cell chemokine expression triggered by antigen-specific cytolytic T cell recognition. J Clin Invest. 106(6):49-45.

Zhao Y, Chen YQ, Li S, Konrad RJ, Cao G. (2009) The microsomal cardiolipin remodeling enzyme acyl-CoA lysocardiolipin acyltransferase is an acyltransferase of multiple anionic lysophospholipids. J Lipid Res. 50(5):945-956.

Zinser E, Sperka-Gottlieb CD, Fasch EV, Kohlwein SD, Paltauf F, Daum G. (1991) Phospholipid synthesis and lipid composition of subcellular membranes in the unicellular eukaryote *Saccharomyces cerevisiae*. J Bacteriol.173(6):2026-2034.

Zuo YY, Veldhuizen RA, Neumann AW, Petersen NO, Possmayer F. (2008) Current perspectives in pulmonary surfactant inhibition, enhancement and evaluation. Biochim Biophys Acta. 1778(10):1947-1977.